Radar Sounding of the Auroral Plasma

by

Cesar La Hoz

cesar.la.hoz@uit.no

with contributions by my friends

Brett Isham, Mike Kosch and Mike Rietveld

The Arctic University of Norway

Cornell University

OUTLINE

1. Background on Radar Incoherent Scattering theory
2. Natural Enhanced Ion Acoustic Lines, NEIAL
3. Polar Mesospheric Summer Echoes, PMSE
4. Langmuir turbulence: decay and cavitating instability

disclaimer: time constraint and personal participation have defined this work

EISCAT

near Tromsø
Northern Norway

VHF radar

UHF radar

HF Heater

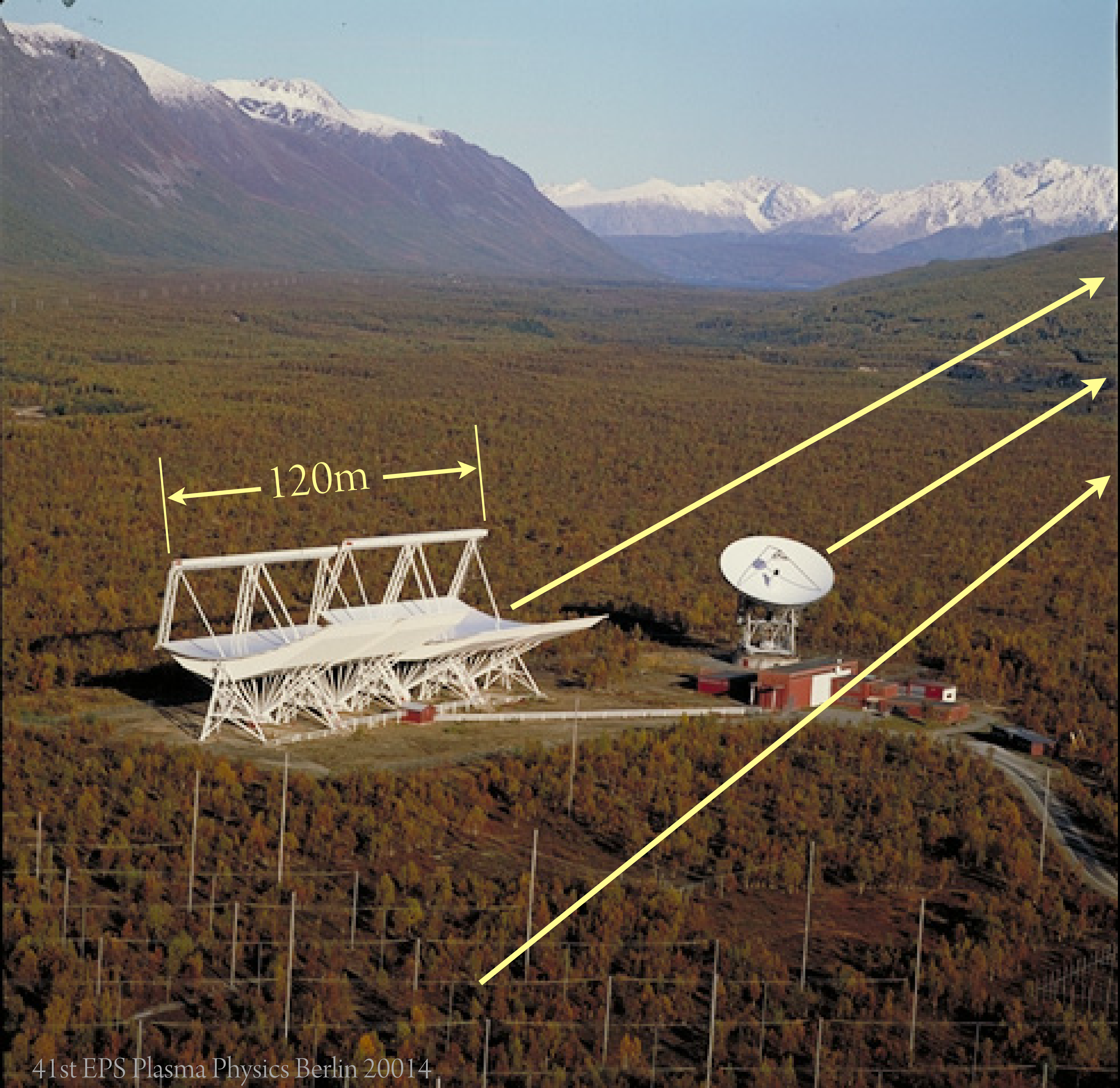

EISCAT

near Tromsø
Northern Norway

VHF radar

UHF radar

HF Heater

Thomson Scattering

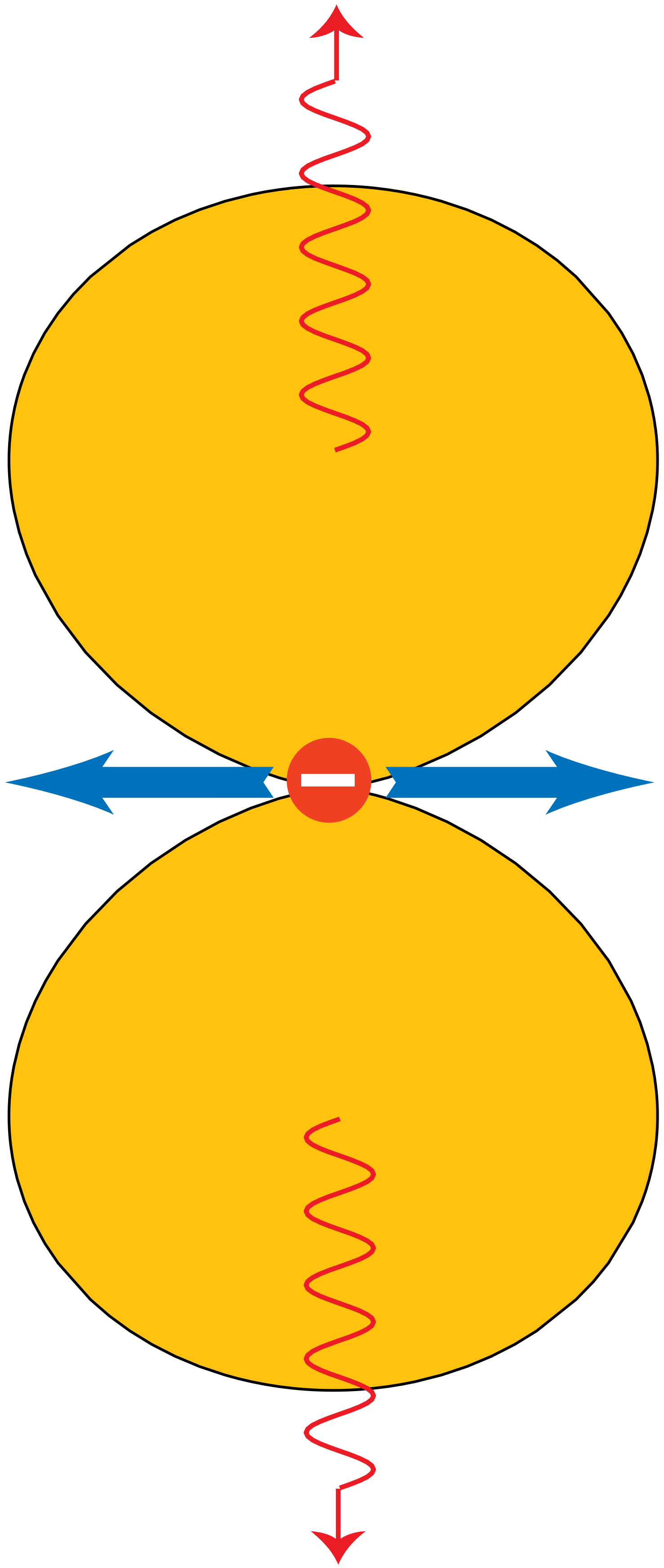

electron

$$\sigma_{ele} = 10^{-28}\ \mathrm{m}^2$$

scattering x-section

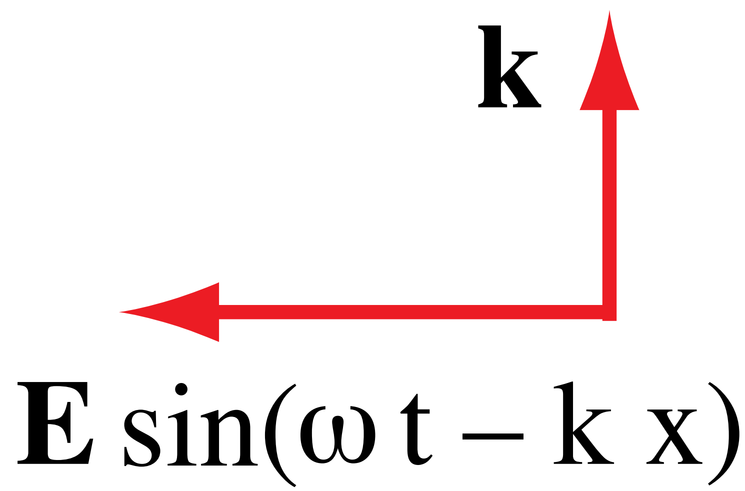

e+i_RadiationPattern.ai6

Thomson Scattering

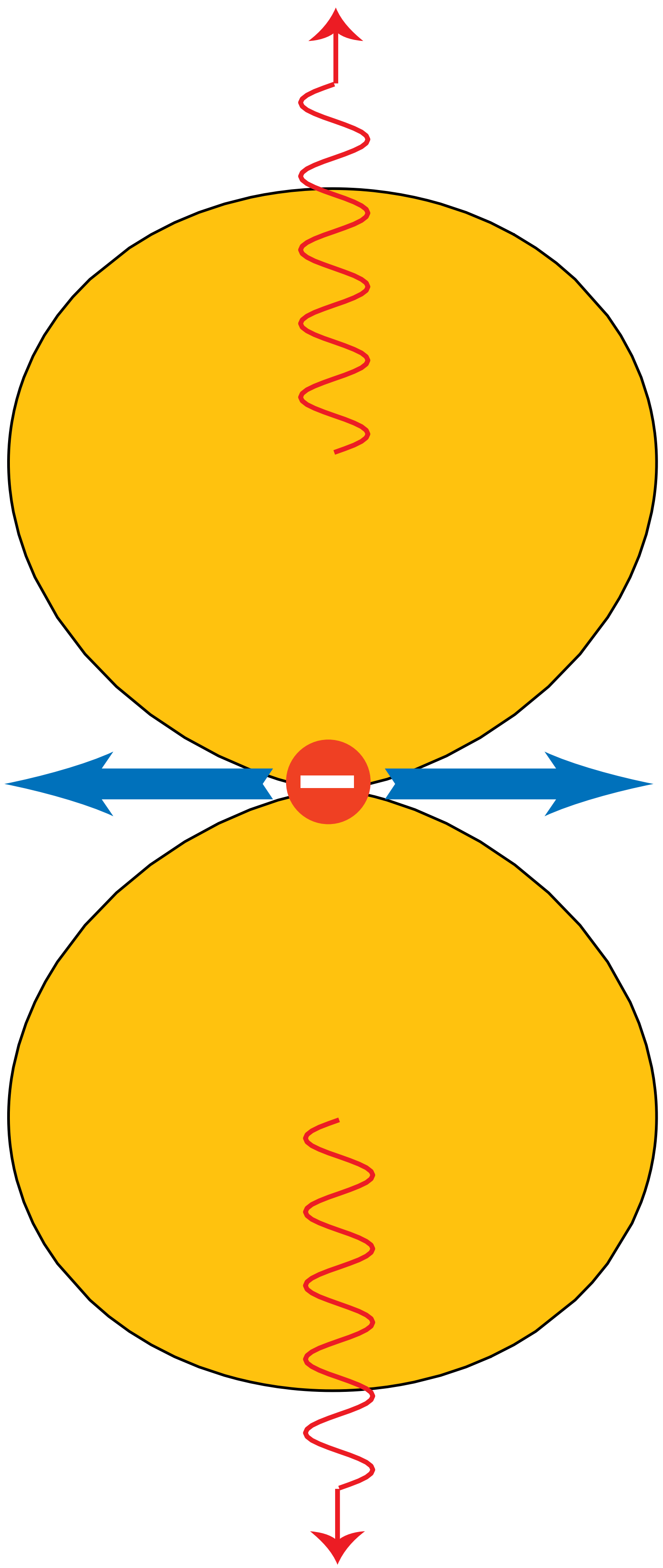

electron

$$\sigma_{ele} = 10^{-28}\ \mathrm{m}^2$$

scattering x-section

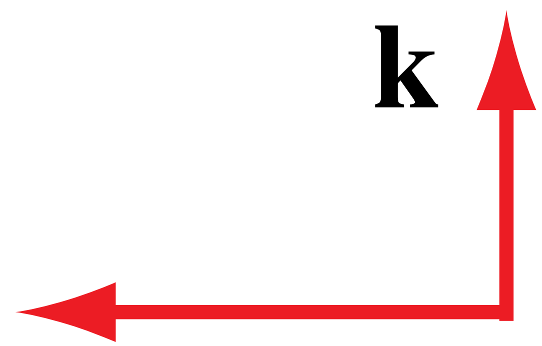

$$\mathbf{E}\,\sin(\omega\, t - k\, x)$$

ion

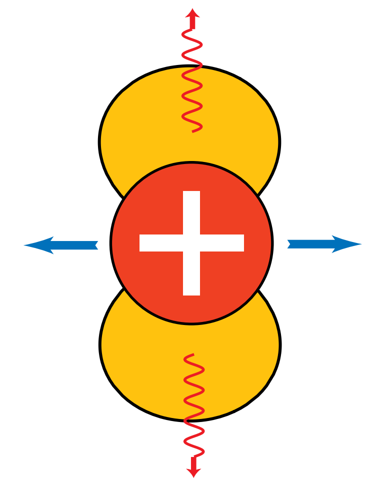

$$\frac{\sigma_{ion}}{\sigma_{ele}} = \left(\frac{m_{ele}}{m_{ion}}\right)^2 \approx 10^{-6} - 10^{-8}$$

e+i_RadiationPattern.ai6

Incoherent Scattering from ionised media

arises from fluctuations of electron density

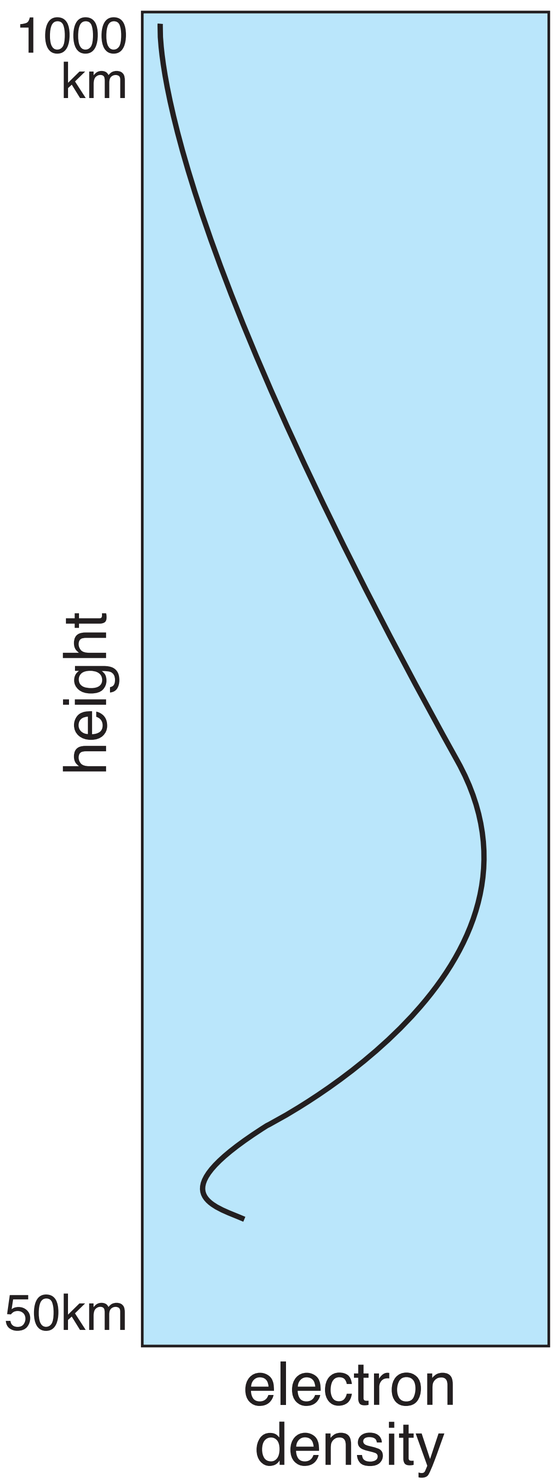

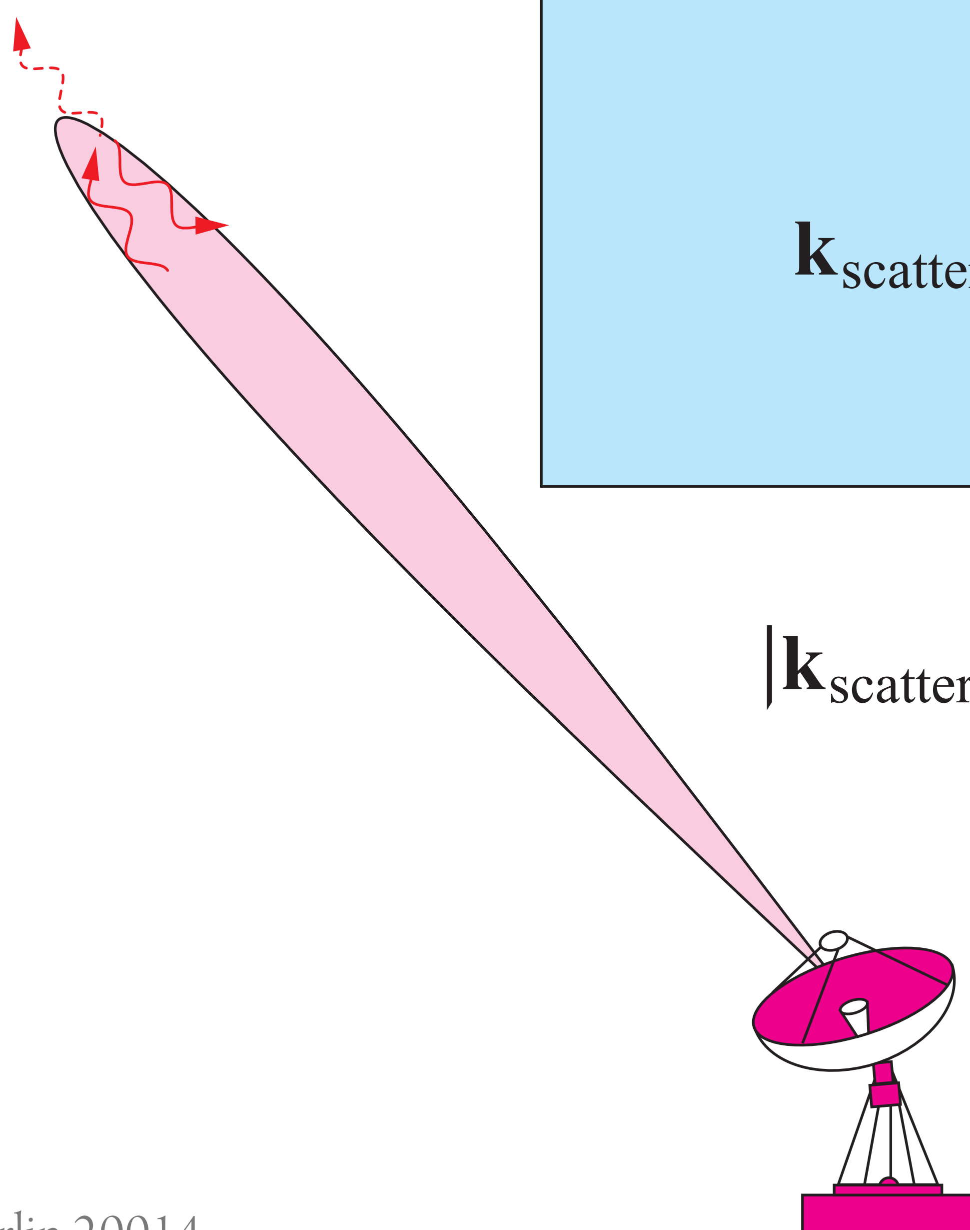

momentum conservation

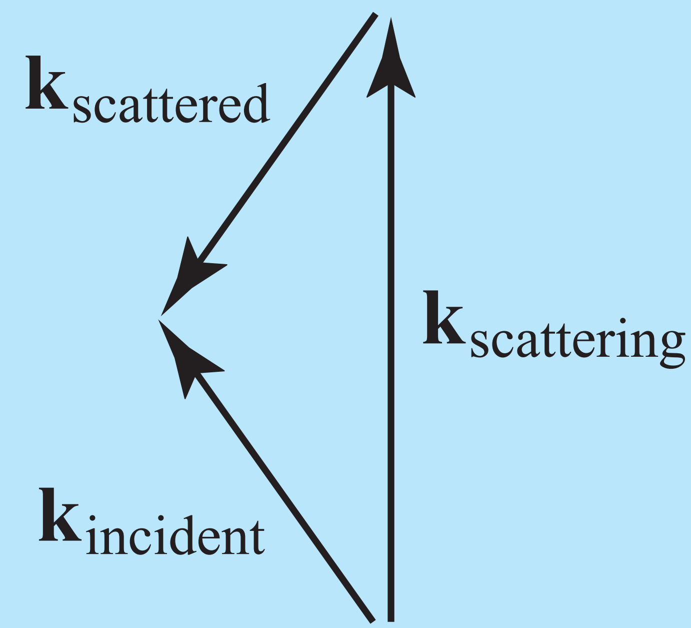

$$\mathbf{k}_{\text{scattered}} = \mathbf{k}_{\text{scattering}} - \mathbf{k}_{\text{incident}}$$

Bragg condition

$$|\mathbf{k}_{\text{scattered}}| = |\mathbf{k}_{\text{incident}}| \left\{ \begin{array}{l} \text{e.m. wave} \\ \text{photon} \end{array} \right.$$

Incoherent Scattering from ionised media

arises from fluctuations of electron density

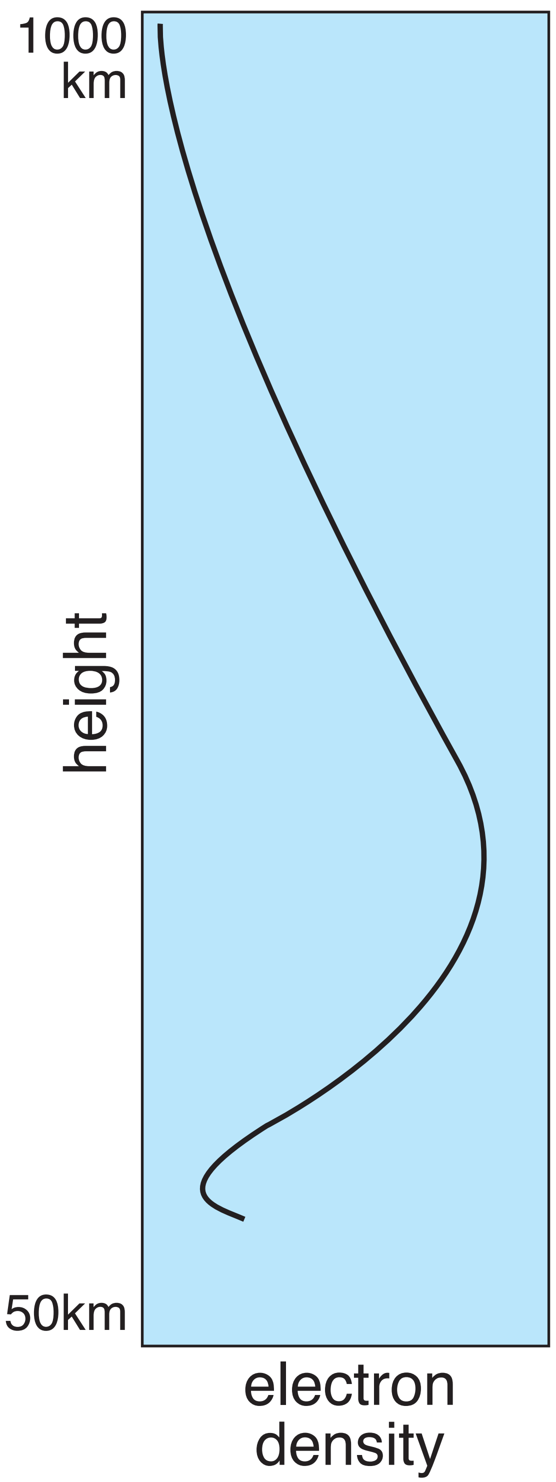

Backscatter

$$\mathbf{k}_{scattered} = -\,\mathbf{k}_{incident}$$

$$\mathbf{k}_{scattering} = 2\,\mathbf{k}_{incident}$$

$$\boxed{\lambda_{medium} = \frac{1}{2}\lambda_{radar}}$$

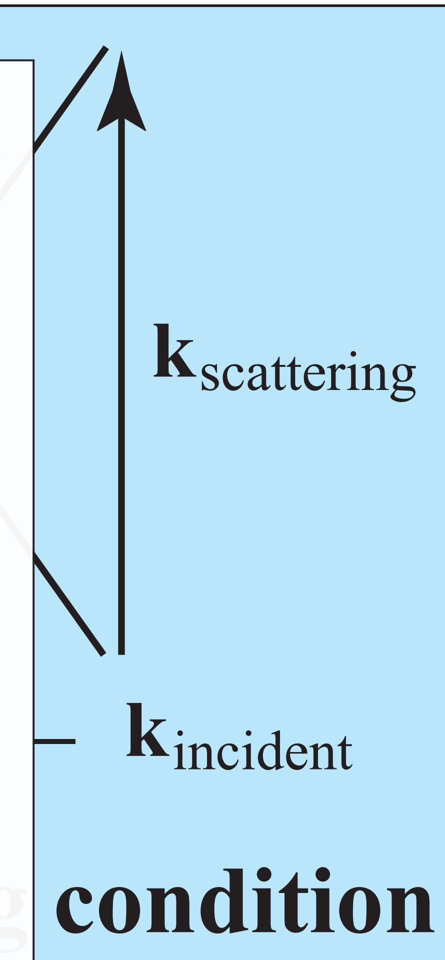

$$\lambda_{medium} \begin{cases} \text{ion acoustic wave (phonon)} \\ \text{Langmuir wave (plasmon)} \\ \text{Turbulence scale} \end{cases}$$

e.m. wave
photon

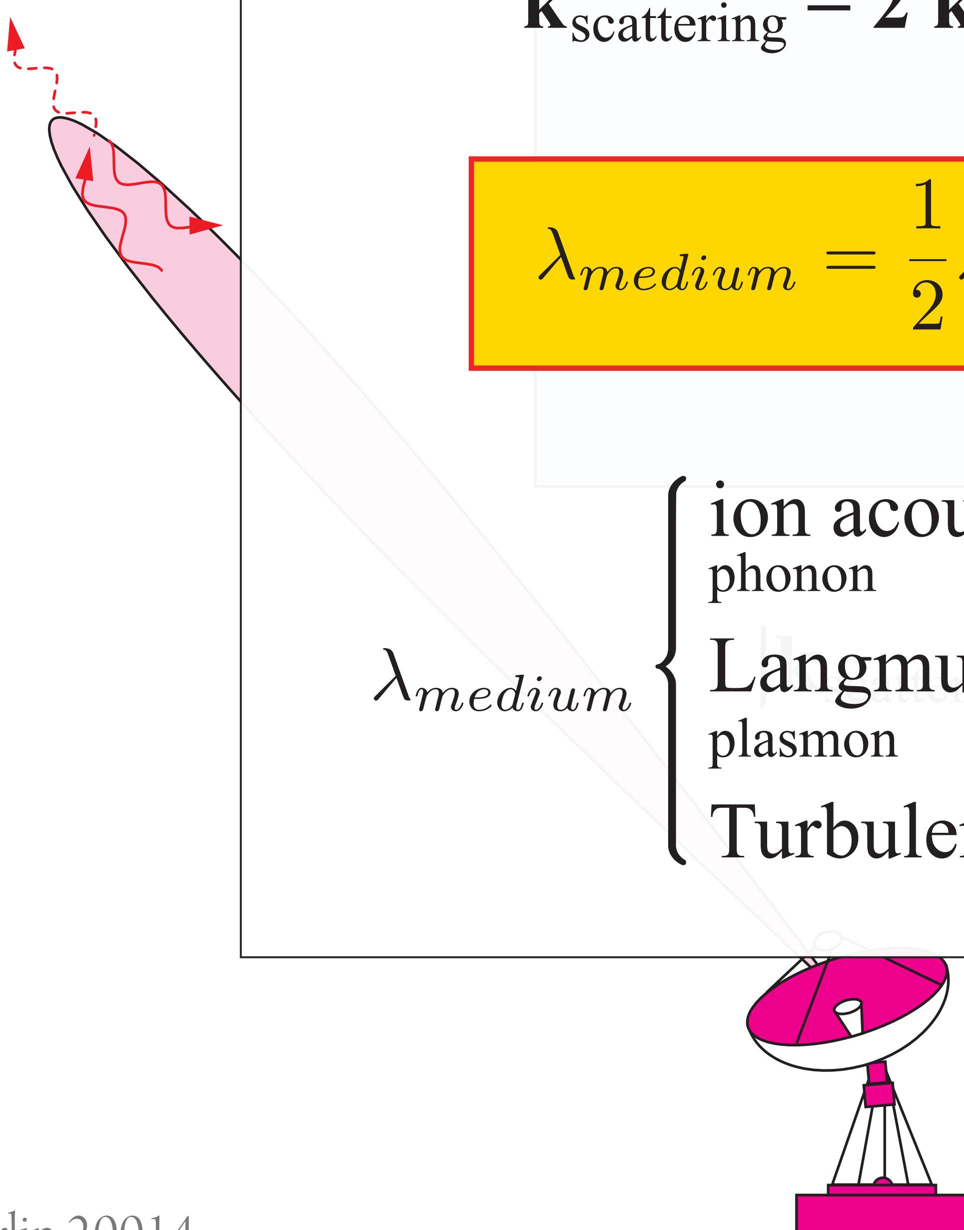

How does it work?

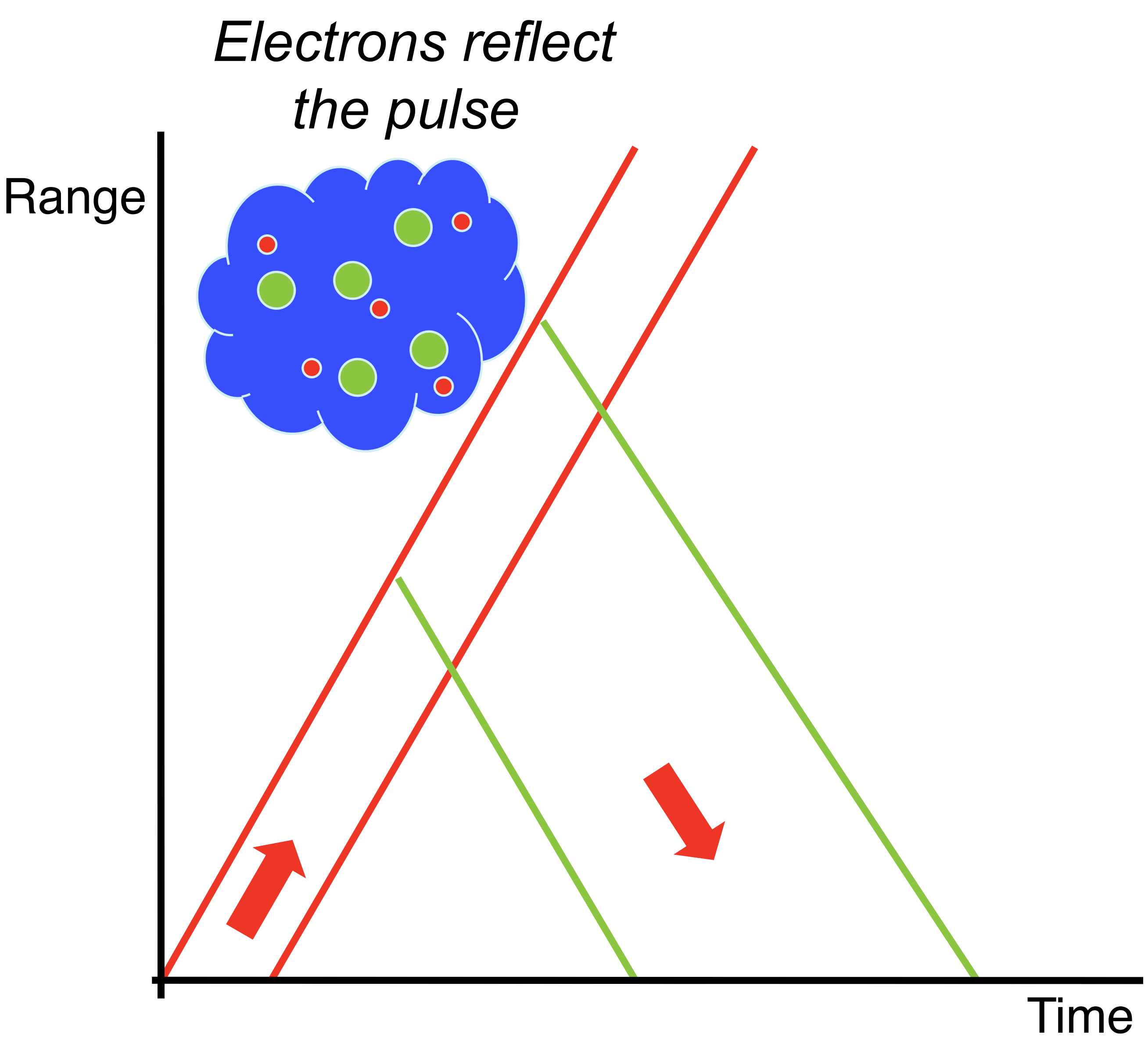

High power pulse Very sensitive receiver

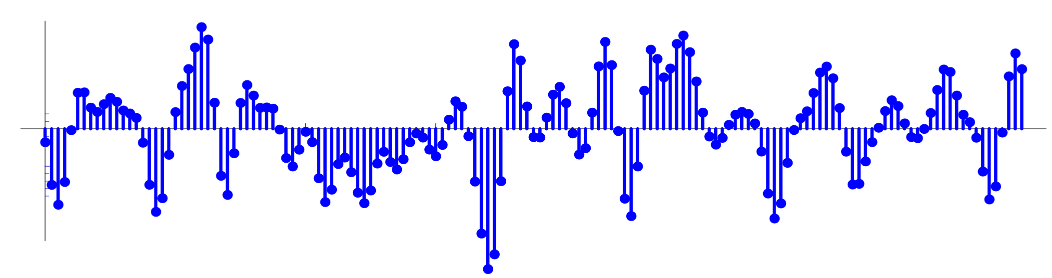

*produces a **stochastic** signal much smaller than the noise*

How does it work?

Typical: 1 Mega Watt tansmitted (10^6 W)
1 femto Watt received (10^{-15} W)

Electrons reflect the pulse

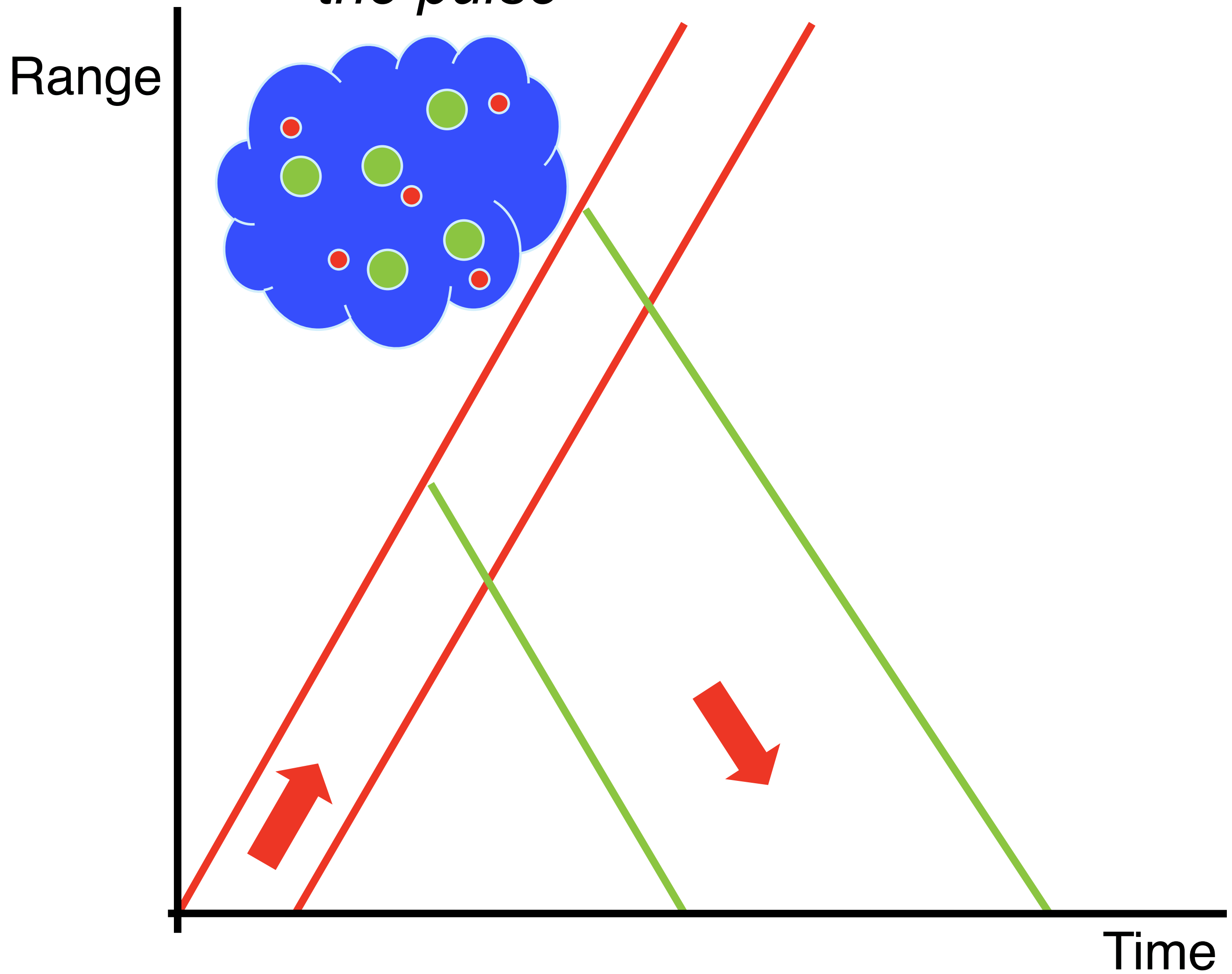

High power pulse Very sensitive receiver

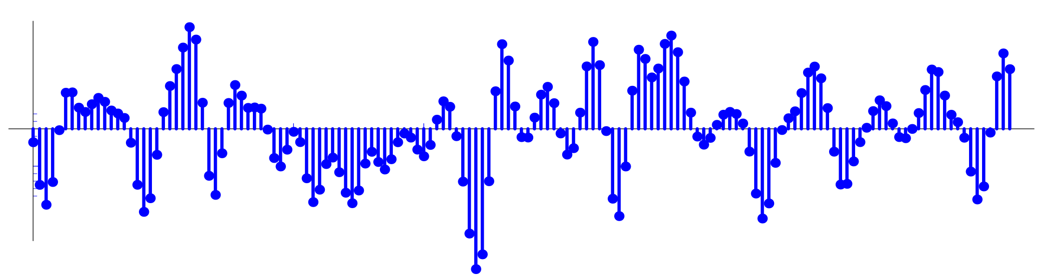

*produces a **stochastic** signal much smaller than the noise*

How does it work?

Typical: 1 Mega Watt tansmitted (10^6 W)
1 femto Watt received (10^{-15} W)

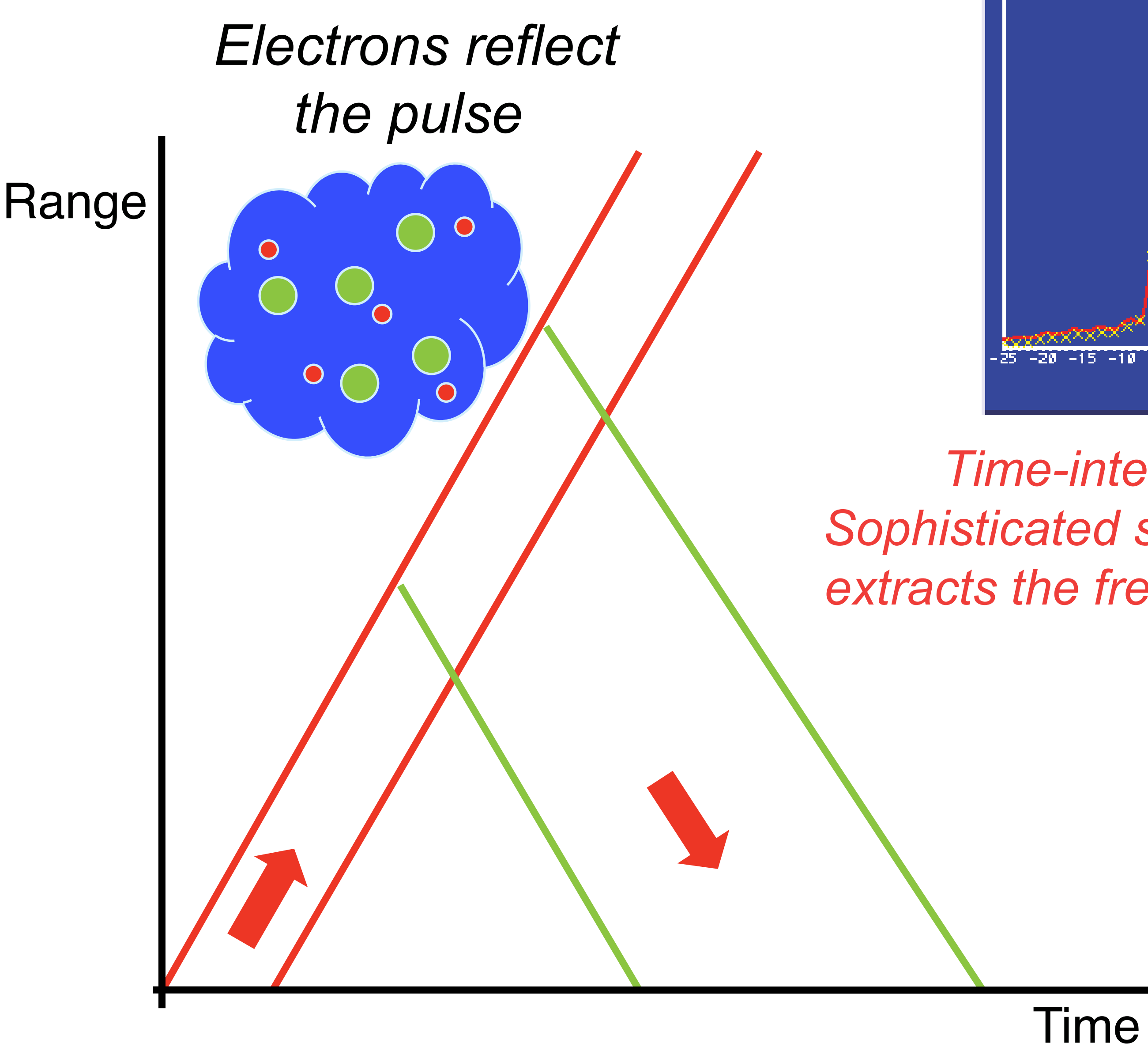

High power pulse Very sensitive receiver

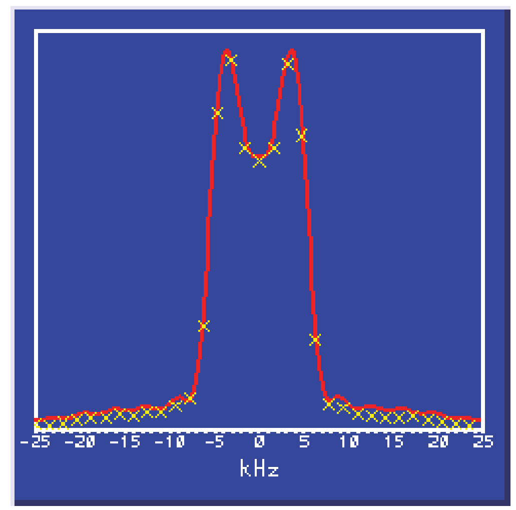

Time-integration and Sophisticated signal processing extracts the frequency spectrum

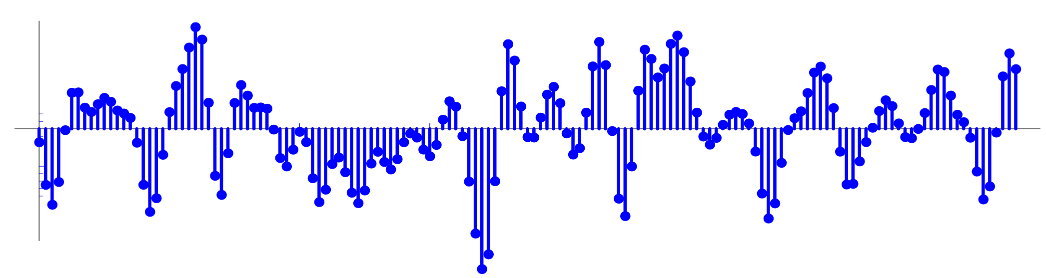

produces a ***stochastic*** *signal much smaller than the noise*

How does it work?

Typical: 1 Mega Watt tansmitted (10^6 W)
1 femto Watt received (10^{-15} W)

Least squares fitting produces ionospheric plasma parameters

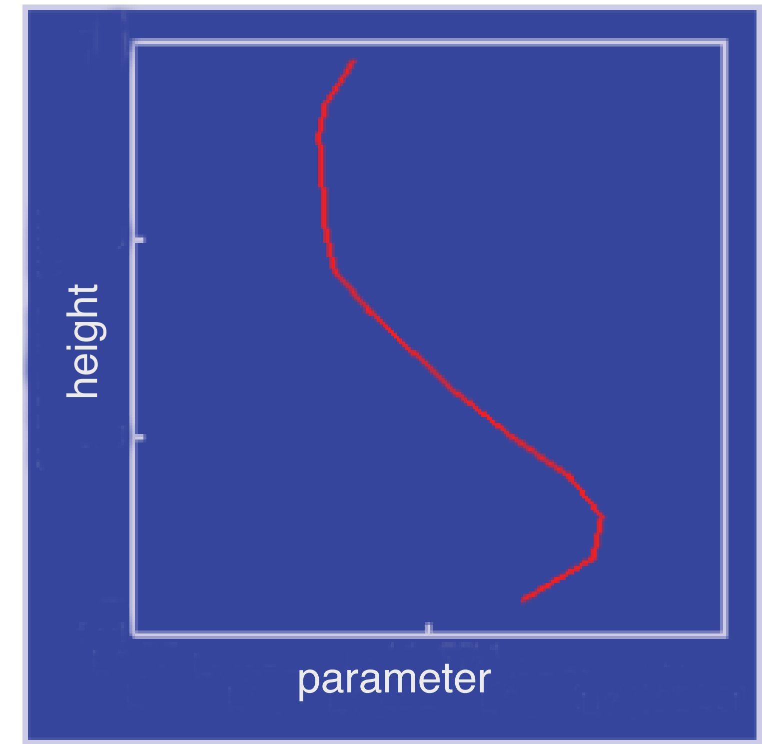

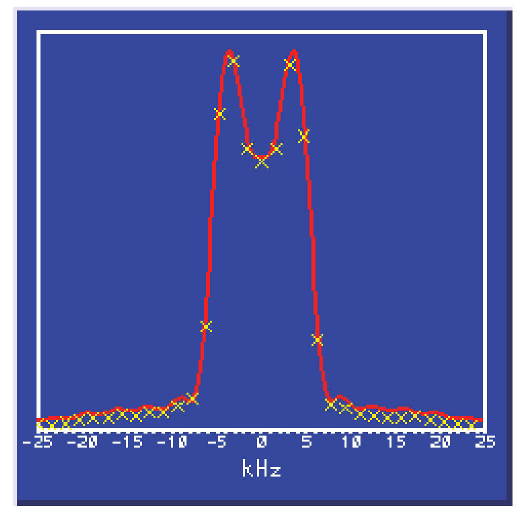

Time-integration and Sophisticated signal processing extracts the frequency spectrum

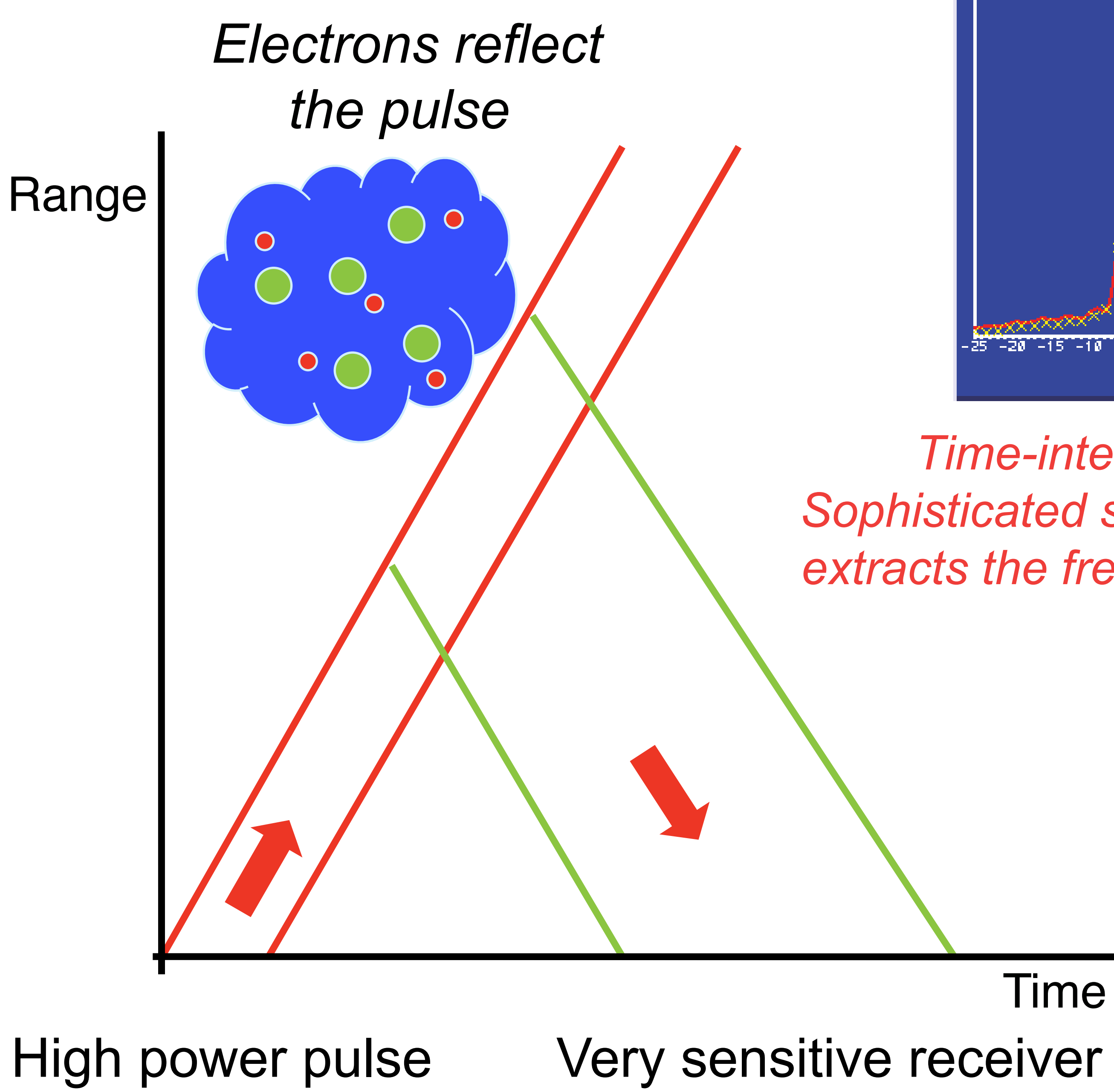

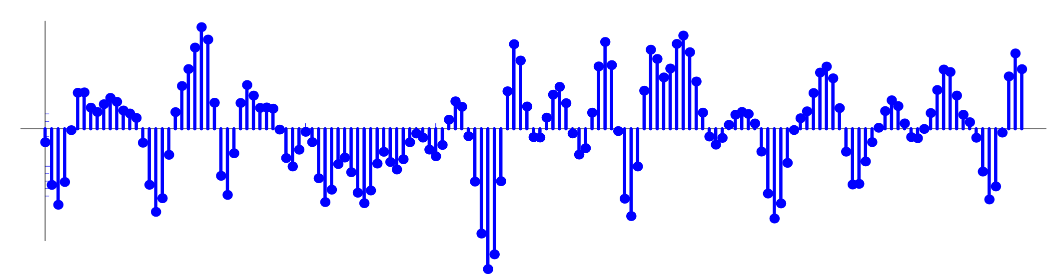

*produces a **stochastic** signal much smaller than the noise*

4-days of Incoherent Scatter Above Tromsø, Norway

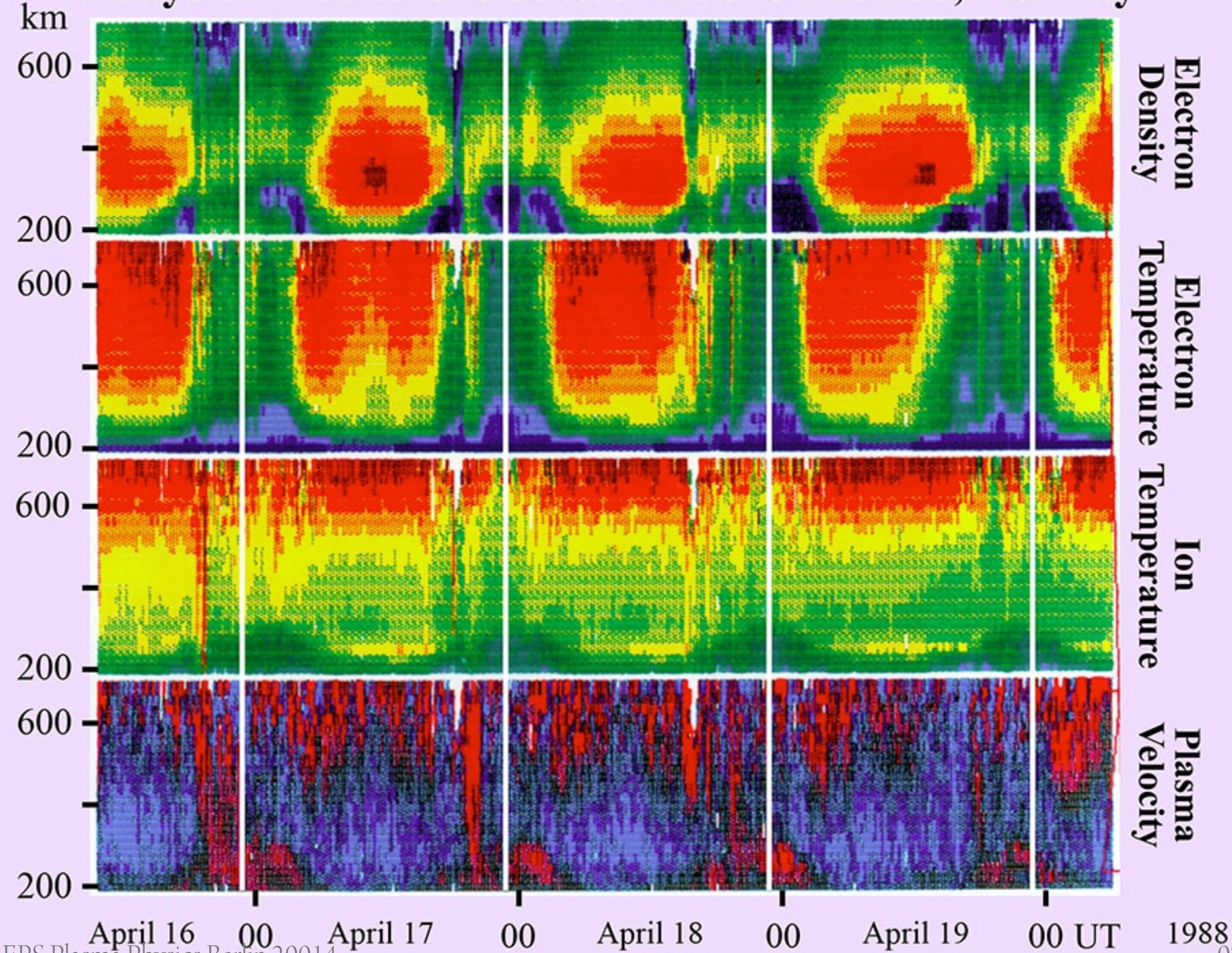

4-days of Incoherent Scatter Above Tromsø, Norway

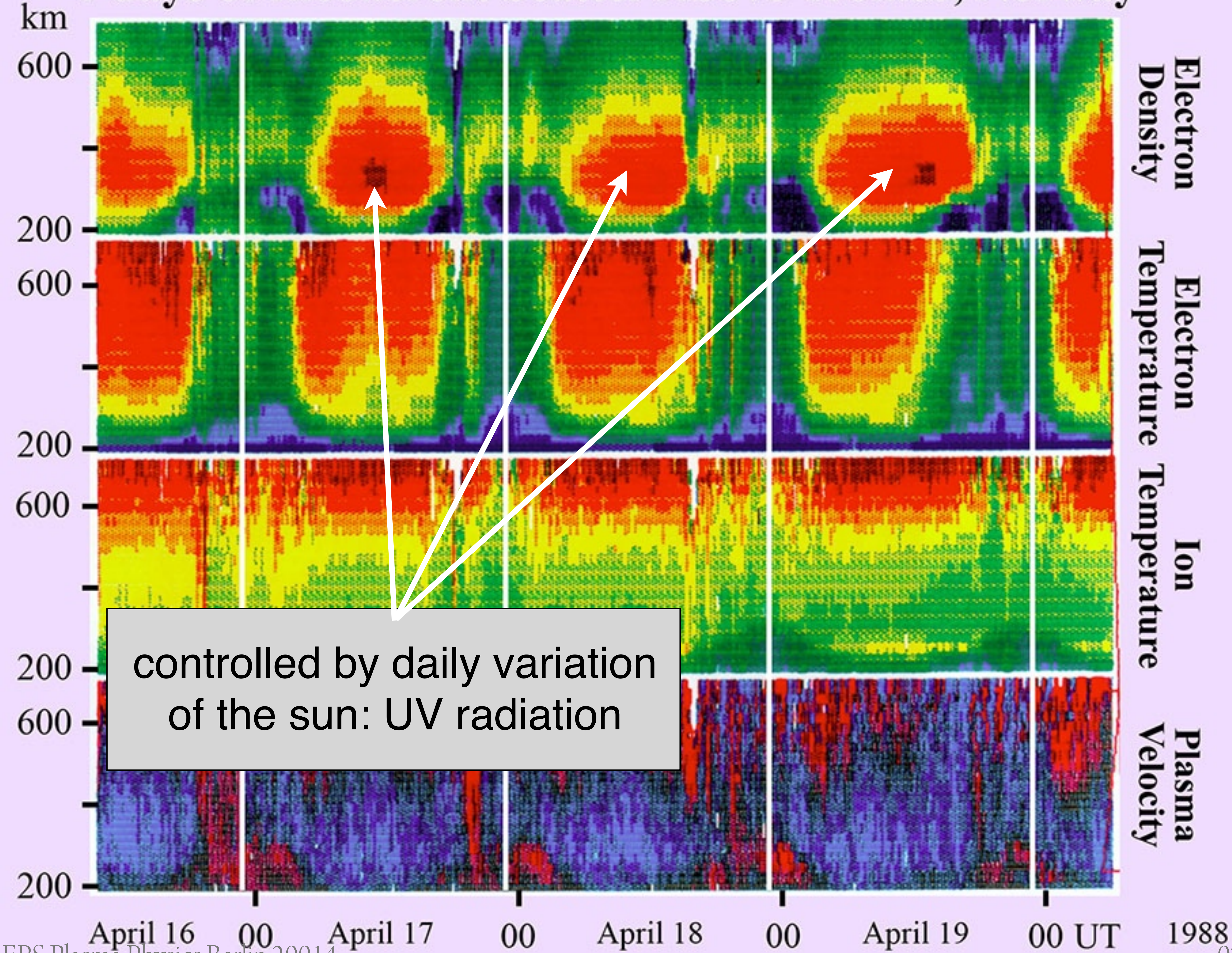

4-days of Incoherent Scatter Above Tromsø, Norway

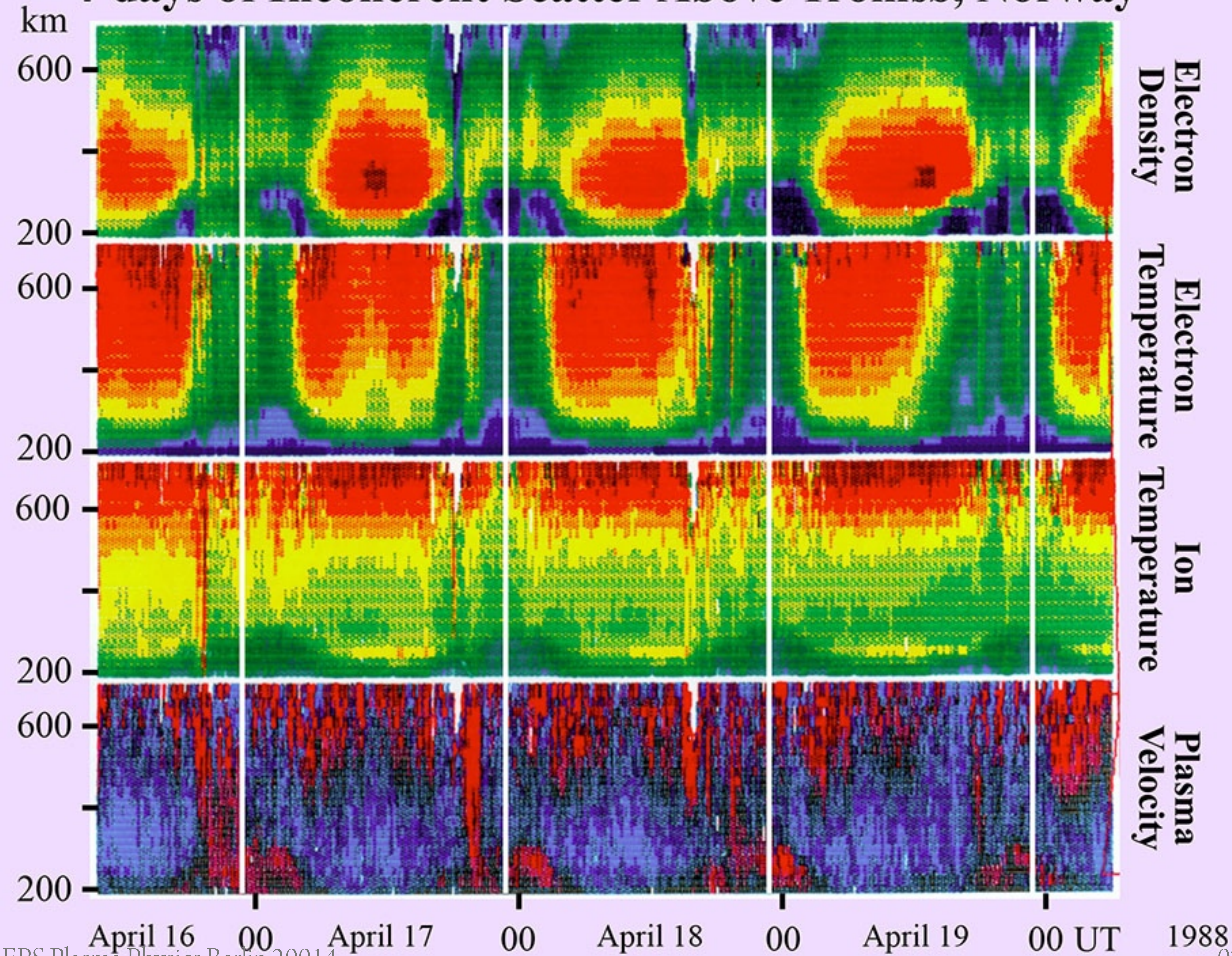

4-days of Incoherent Scatter Above Tromsø, Norway

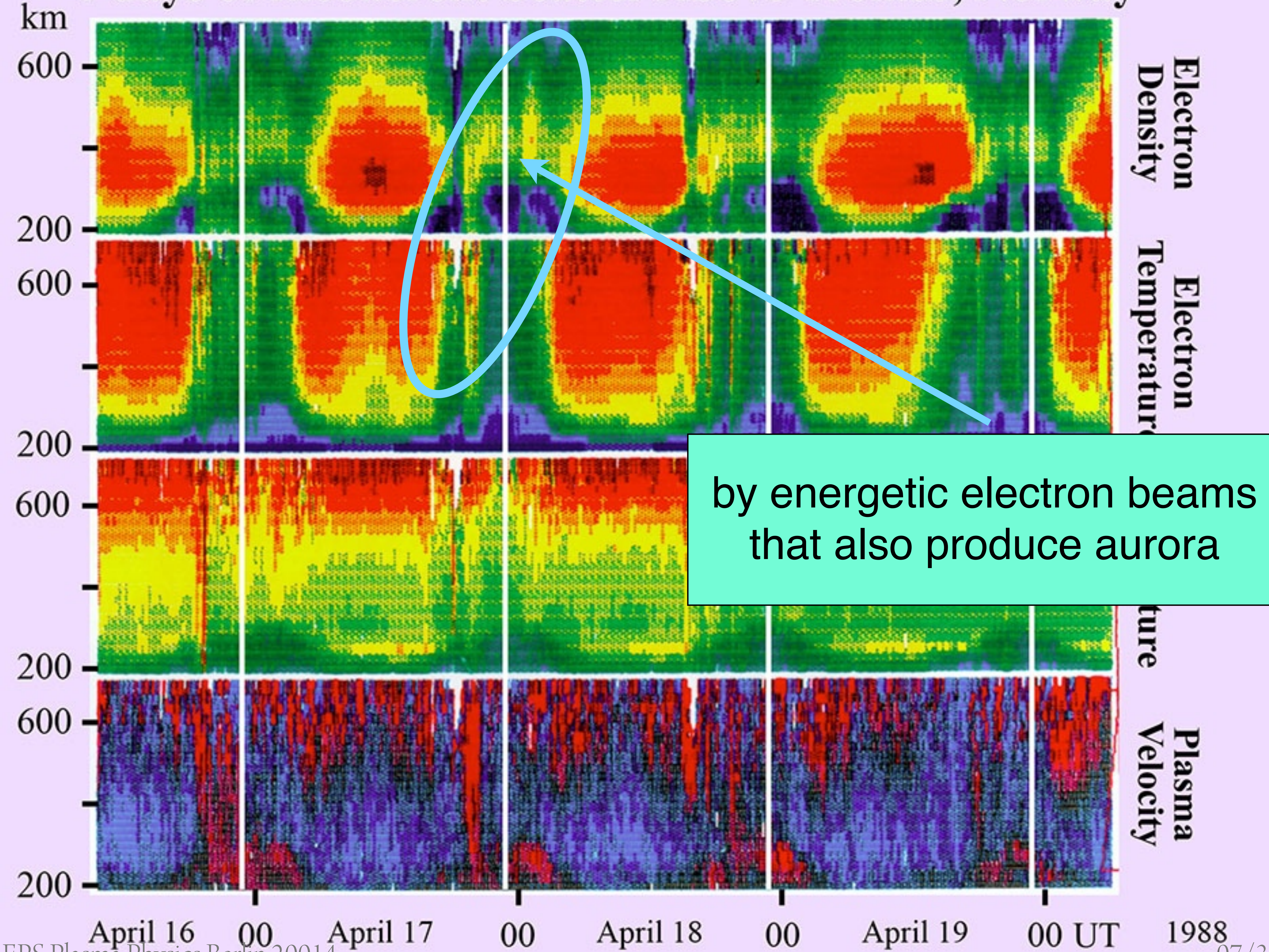

The Incoherent Scattering Spectrum

$$S_e(\mathbf{k},\omega) = N_e\left|1-\frac{\chi_e(\mathbf{k},\omega)}{\epsilon(\mathbf{k},\omega)}\right|^2\int f_e(\mathbf{v})\delta(\omega-\mathbf{k}\cdot\mathbf{v})d^3\mathbf{v}+\sum_i N_i\left|\frac{\chi_e(\mathbf{k},\omega)}{\epsilon(\mathbf{k},\omega)}\right|^2\int f_i(\mathbf{v})\delta(\omega-\mathbf{k}\cdot\mathbf{v})d^3\mathbf{v}$$

The Incoherent Scattering Spectrum

$$S_e(\mathbf{k},\omega) = N_e\left|1-\frac{\chi_e(\mathbf{k},\omega)}{\epsilon(\mathbf{k},\omega)}\right|^2\int f_e(\mathbf{v})\delta(\omega-\mathbf{k}\cdot\mathbf{v})d^3\mathbf{v}+\sum_i N_i\left|\frac{\chi_e(\mathbf{k},\omega)}{\epsilon(\mathbf{k},\omega)}\right|^2\int f_i(\mathbf{v})\delta(\omega-\mathbf{k}\cdot\mathbf{v})d^3\mathbf{v}$$

dielectric function

$$\epsilon(\mathbf{k},\omega) = 1+\textstyle\sum_\alpha \chi_\alpha(\mathbf{k},\omega)$$

electric susceptibility

$$\chi_\alpha(\mathbf{k},\omega) = \frac{\omega_{pe}^2}{k^2}\int_{\mathcal{L}}\frac{\mathbf{k}\cdot\partial_{\mathbf{v}}f_\alpha(\mathbf{v})}{\omega-\mathbf{k}\cdot\mathbf{v}}d\mathbf{v}$$

velocity distribution function

$$f_{e,i}(\mathbf{v};T_e,T_i,m_i,\nu_{in})$$

Charge densities

$$N_e = \sum_i N_i$$

$$S_e(\mathbf{k},\omega) = N_e \left| 1 - \frac{\chi_e(\mathbf{k},\omega)}{\epsilon(\mathbf{k},\omega)} \right|^2 \int f_e(\mathbf{v}) \delta(\omega - \mathbf{k}\cdot\mathbf{v}) d^3\mathbf{v} + \sum_i N_i \left| \frac{\chi_e(\mathbf{k},\omega)}{\epsilon(\mathbf{k},\omega)} \right|^2 \int f_i(\mathbf{v}) \delta(\omega - \mathbf{k}\cdot\mathbf{v}) d^3\mathbf{v}$$

$$S_e(\mathbf{k},\omega) = N_e\left|1-\frac{\chi_e(\mathbf{k},\omega)}{\epsilon(\mathbf{k},\omega)}\right|^2 \int f_e(\mathbf{v})\delta(\omega-\mathbf{k}\cdot\mathbf{v})d^3\mathbf{v} + \sum_i N_i\left|\frac{\chi_e(\mathbf{k},\omega)}{\epsilon(\mathbf{k},\omega)}\right|^2 \int f_i(\mathbf{v})\delta(\omega-\mathbf{k}\cdot\mathbf{v})d^3\mathbf{v}$$

Each charge in the plasma behaves as in vacuum but it polarises the rest of the plasma resulting in neutralising clouds around each charge:

the charge and its cloud is a **dressed** (quasi) **particle**

$$S_e(\mathbf{k},\omega) = N_e \left| 1 - \frac{\chi_e(\mathbf{k},\omega)}{\epsilon(\mathbf{k},\omega)} \right|^2 \int f_e(\mathbf{v})\delta(\omega - \mathbf{k}\cdot\mathbf{v})d^3\mathbf{v} + \sum_i N_i \left| \frac{\chi_e(\mathbf{k},\omega)}{\epsilon(\mathbf{k},\omega)} \right|^2 \int f_i(\mathbf{v})\delta(\omega - \mathbf{k}\cdot\mathbf{v})d^3\mathbf{v}$$

Plasma Line $S_{PL}(\mathbf{k},\omega)$

$$S_e(\mathbf{k},\omega) = N_e \left| 1 - \frac{\chi_e(\mathbf{k},\omega)}{\epsilon(\mathbf{k},\omega)} \right|^2 \int f_e(\mathbf{v})\delta(\omega - \mathbf{k}\cdot\mathbf{v})d^3\mathbf{v} + \sum_i N_i \left| \frac{\chi_e(\mathbf{k},\omega)}{\epsilon(\mathbf{k},\omega)} \right|^2 \int f_i(\mathbf{v})\delta(\omega - \mathbf{k}\cdot\mathbf{v})d^3\mathbf{v}$$

test electron with cloud

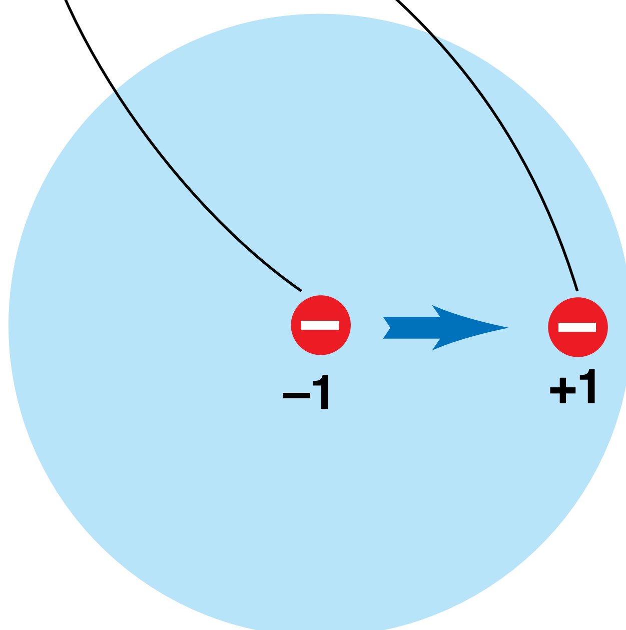

$$\omega_{pl}(k) \approx \omega_{pe}(1+3\ \lambda_D^2 k^2) \longleftarrow \epsilon(\mathbf{k},\omega) = \mathbf{0}$$

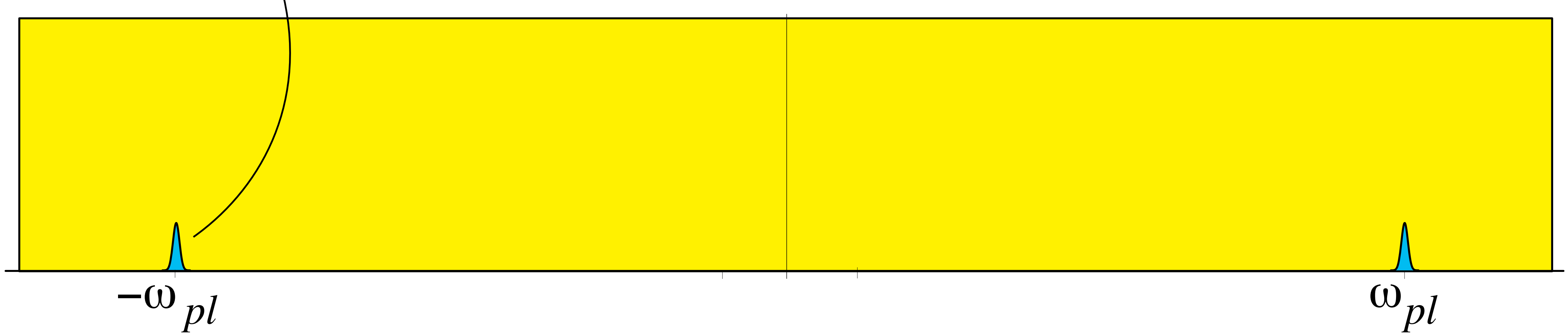

Plasma Line $S_{PL}(\mathbf{k},\omega)$ — Ion Line $S_{IL}(\mathbf{k},\omega)$

$$S_e(\mathbf{k},\omega) = N_e \left| 1 - \frac{\chi_e(\mathbf{k},\omega)}{\epsilon(\mathbf{k},\omega)} \right|^2 \int f_e(\mathbf{v})\delta(\omega - \mathbf{k}\cdot\mathbf{v})d^3\mathbf{v} + \sum_i N_i \left| \frac{\chi_e(\mathbf{k},\omega)}{\epsilon(\mathbf{k},\omega)} \right|^2 \int f_i(\mathbf{v})\delta(\omega - \mathbf{k}\cdot\mathbf{v})d^3\mathbf{v}$$

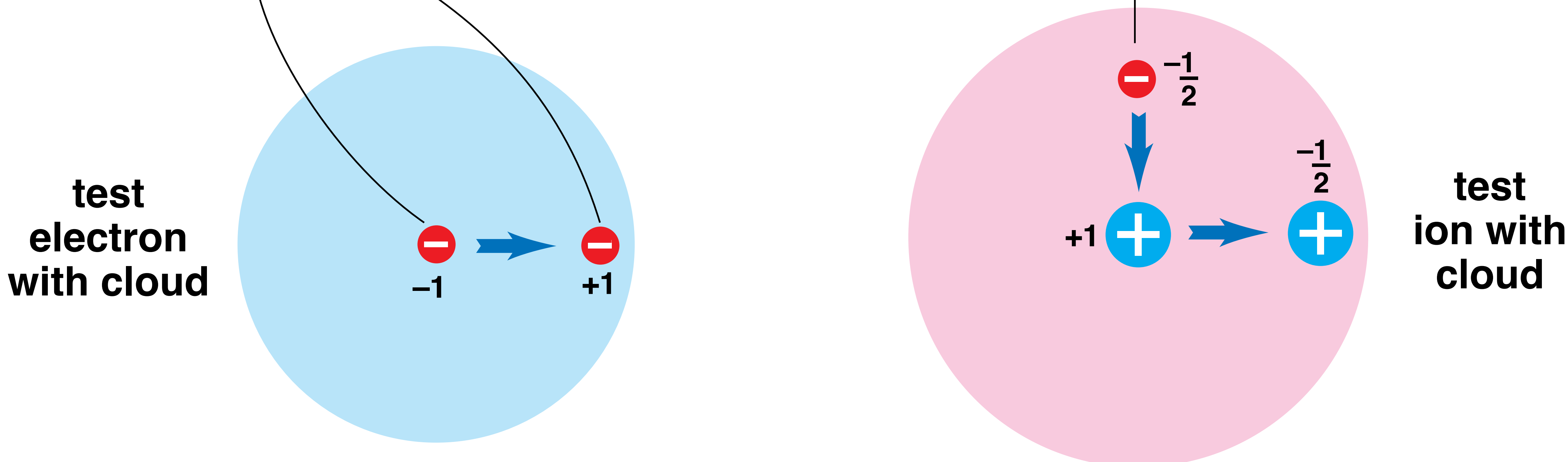

$$\omega_{pl}(k) \approx \omega_{pe}(1+3\ \lambda_D^2 k^2) \longleftarrow \epsilon(\mathbf{k},\omega) = \mathbf{0} \longrightarrow \omega_{ia}(k) \approx k\sqrt{\frac{T_e + 3\,T_i}{m_i}}$$

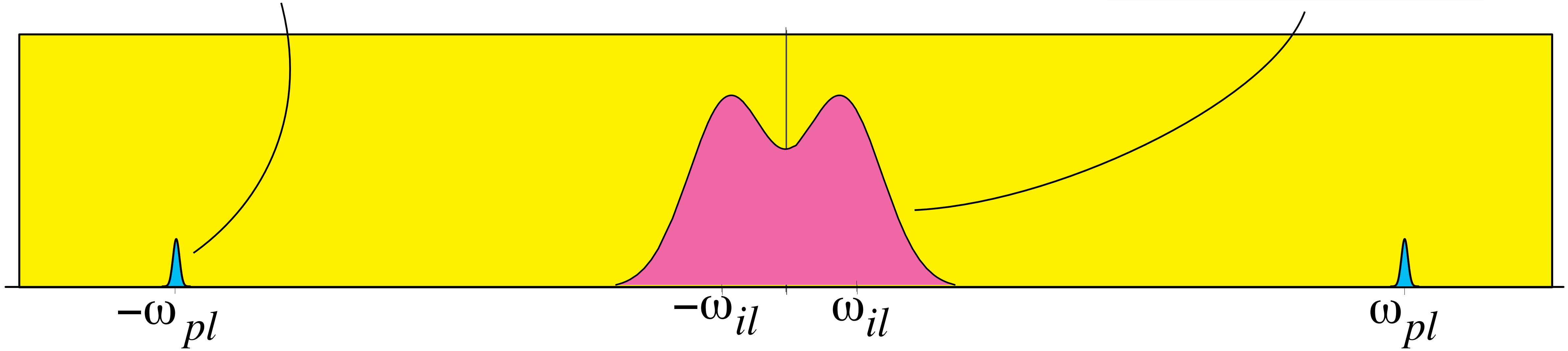

no collective interactions: no clouds: $\chi_e(\mathbf{k},\omega)=0$

$$S_e(\mathbf{k},\omega) = N_e\left|1-\cancel{\frac{\chi_e(\mathbf{k},\omega)}{\epsilon(\mathbf{k},\omega)}}\right|^2\int f_e(\mathbf{v})\delta(\omega-\mathbf{k}\cdot\mathbf{v})d^3\mathbf{v} + \sum_i N_i\left|\cancel{\frac{\chi_e(\mathbf{k},\omega)}{\epsilon(\mathbf{k},\omega)}}\right|^2\int f_i(\mathbf{v})\delta(\omega-\mathbf{k}\cdot\mathbf{v})d^3\mathbf{v}$$

no collective interactions: no clouds: $\chi_e(\mathbf{k},\omega)=0$

$$S_e(\mathbf{k},\omega) = N_e\left|1-\cancel{\frac{\chi_e(\mathbf{k},\omega)}{\epsilon(\mathbf{k},\omega)}}\right|^2\int f_e(\mathbf{v})\delta(\omega-\mathbf{k}\cdot\mathbf{v})d^3\mathbf{v} + \sum_i N_i\left|\cancel{\frac{\chi_e(\mathbf{k},\omega)}{\epsilon(\mathbf{k},\omega)}}\right|^2\int f_i(\mathbf{v})\delta(\omega-\mathbf{k}\cdot\mathbf{v})d^3\mathbf{v}$$

$$S_e(\mathbf{k},\omega) = N_e\int f_e(\mathbf{v})\delta(\omega-\mathbf{k}\cdot\mathbf{v})d^3\mathbf{v}$$

no collective interactions: no clouds: $\chi_e(\mathbf{k},\omega)=0$

$$S_e(\mathbf{k},\omega) = N_e\left|1-\cancel{\frac{\chi_e(\mathbf{k},\omega)}{\epsilon(\mathbf{k},\omega)}}\right|^2\int f_e(\mathbf{v})\delta(\omega-\mathbf{k}\cdot\mathbf{v})d^3\mathbf{v} + \sum_i N_i\left|\cancel{\frac{\chi_e(\mathbf{k},\omega)}{\epsilon(\mathbf{k},\omega)}}\right|^2\int f_i(\mathbf{v})\delta(\omega-\mathbf{k}\cdot\mathbf{v})d^3\mathbf{v}$$

$$S_e(\mathbf{k},\omega) = N_e\int f_e(\mathbf{v})\delta(\omega-\mathbf{k}\cdot\mathbf{v})d^3\mathbf{v}$$

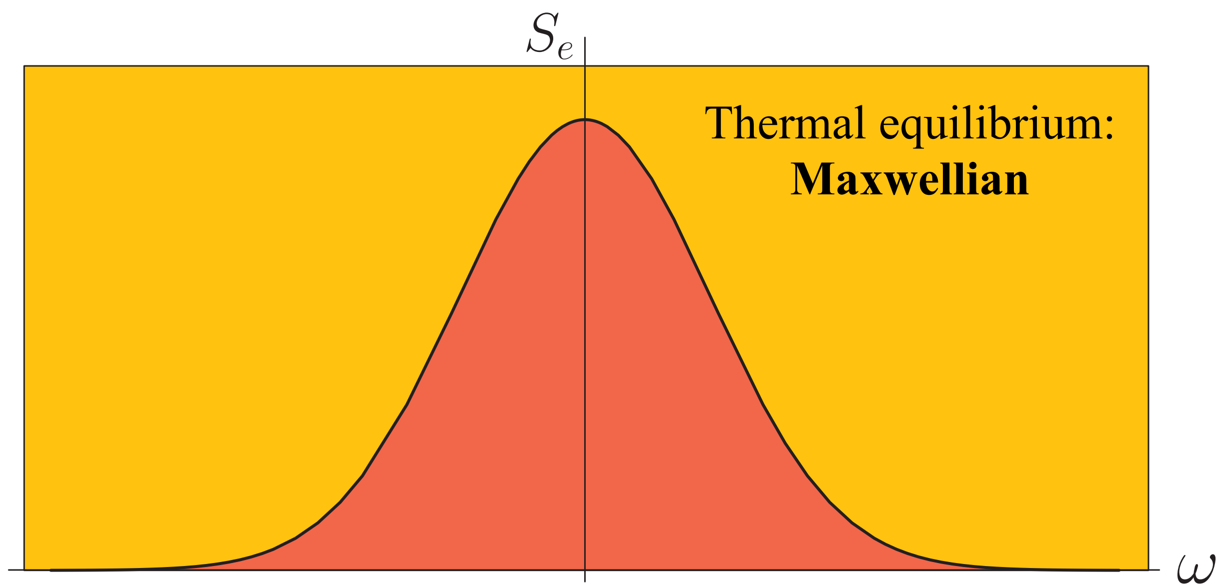

no collective interactions: no clouds: $\chi_e(\mathbf{k},\omega)=0$

$$S_e(\mathbf{k},\omega) = N_e\left|1-\cancel{\frac{\chi_e(\mathbf{k},\omega)}{\epsilon(\mathbf{k},\omega)}}\right|^2\int f_e(\mathbf{v})\delta(\omega-\mathbf{k}\cdot\mathbf{v})d^3\mathbf{v} + \sum_i N_i\left|\cancel{\frac{\chi_e(\mathbf{k},\omega)}{\epsilon(\mathbf{k},\omega)}}\right|^2\int f_i(\mathbf{v})\delta(\omega-\mathbf{k}\cdot\mathbf{v})d^3\mathbf{v}$$

$$S_e(\mathbf{k},\omega) = N_e\int f_e(\mathbf{v})\delta(\omega-\mathbf{k}\cdot\mathbf{v})d^3\mathbf{v}$$

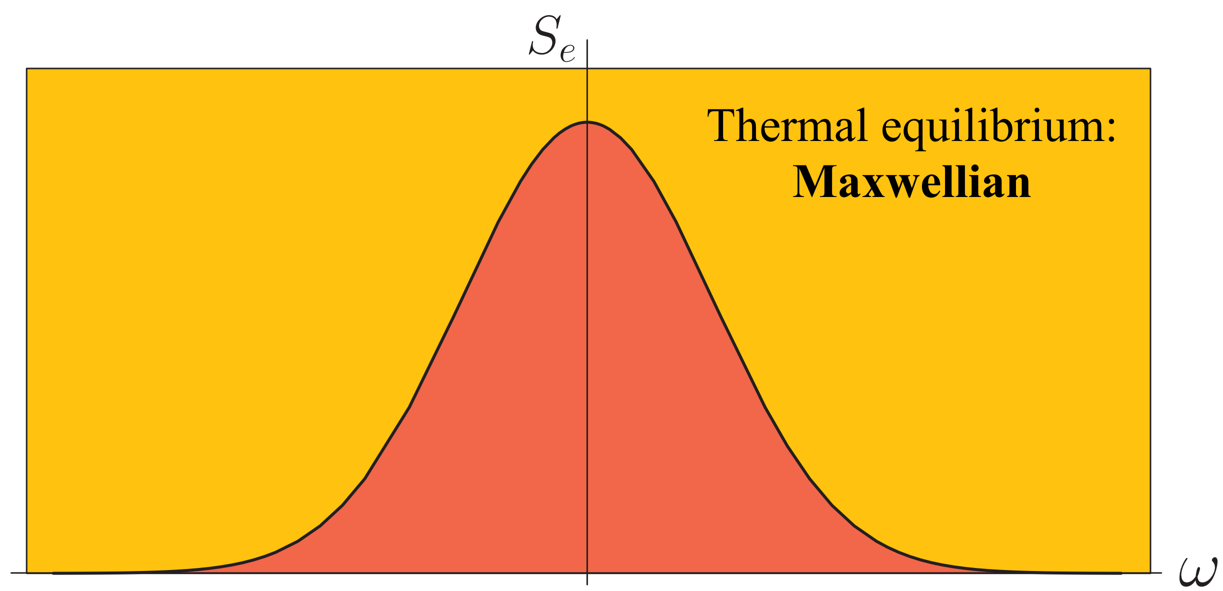

The Arecibo Observatory was designed and built under this premise.

SNR = 0.005

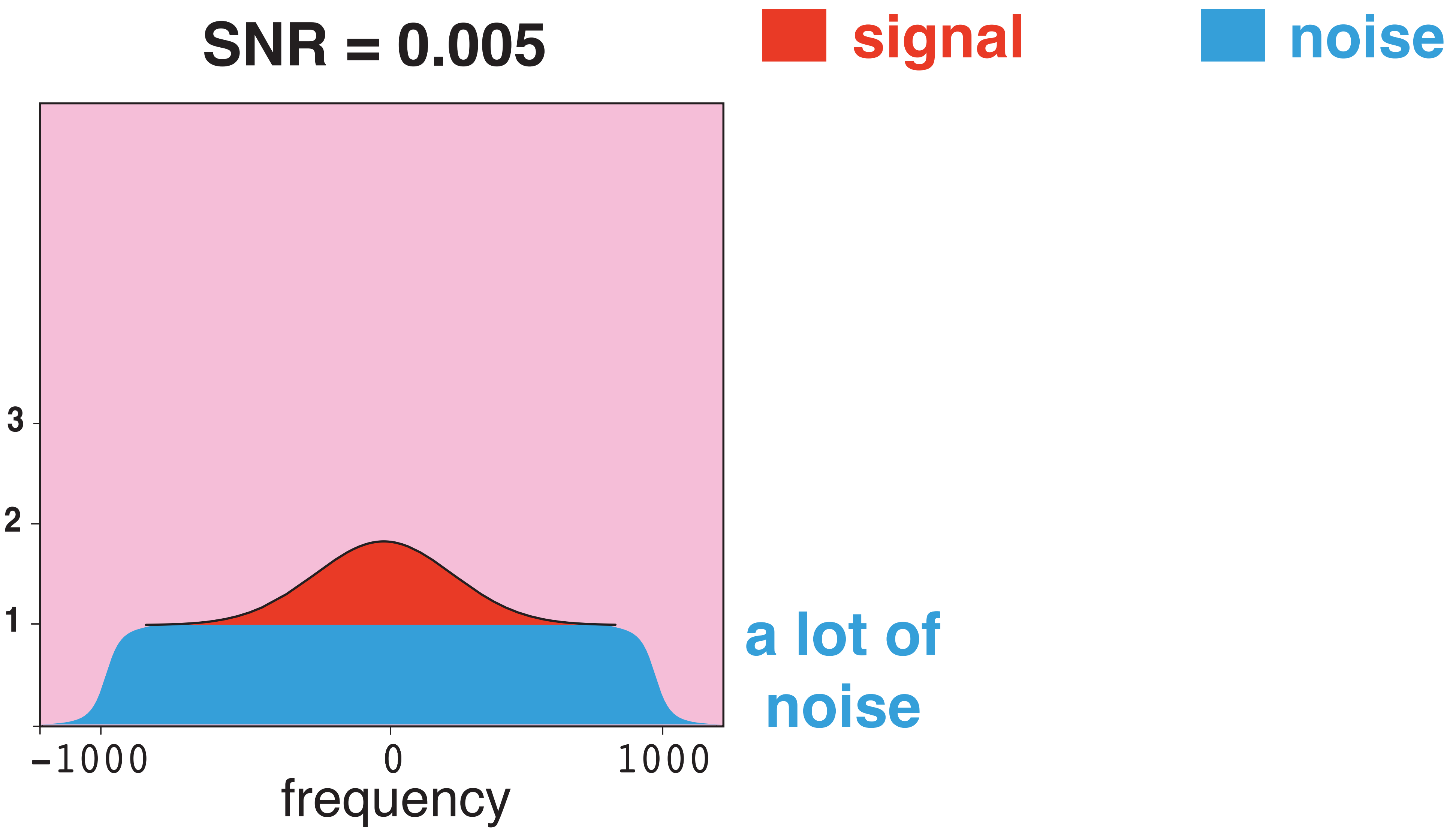

300 metre dish
Arecibo

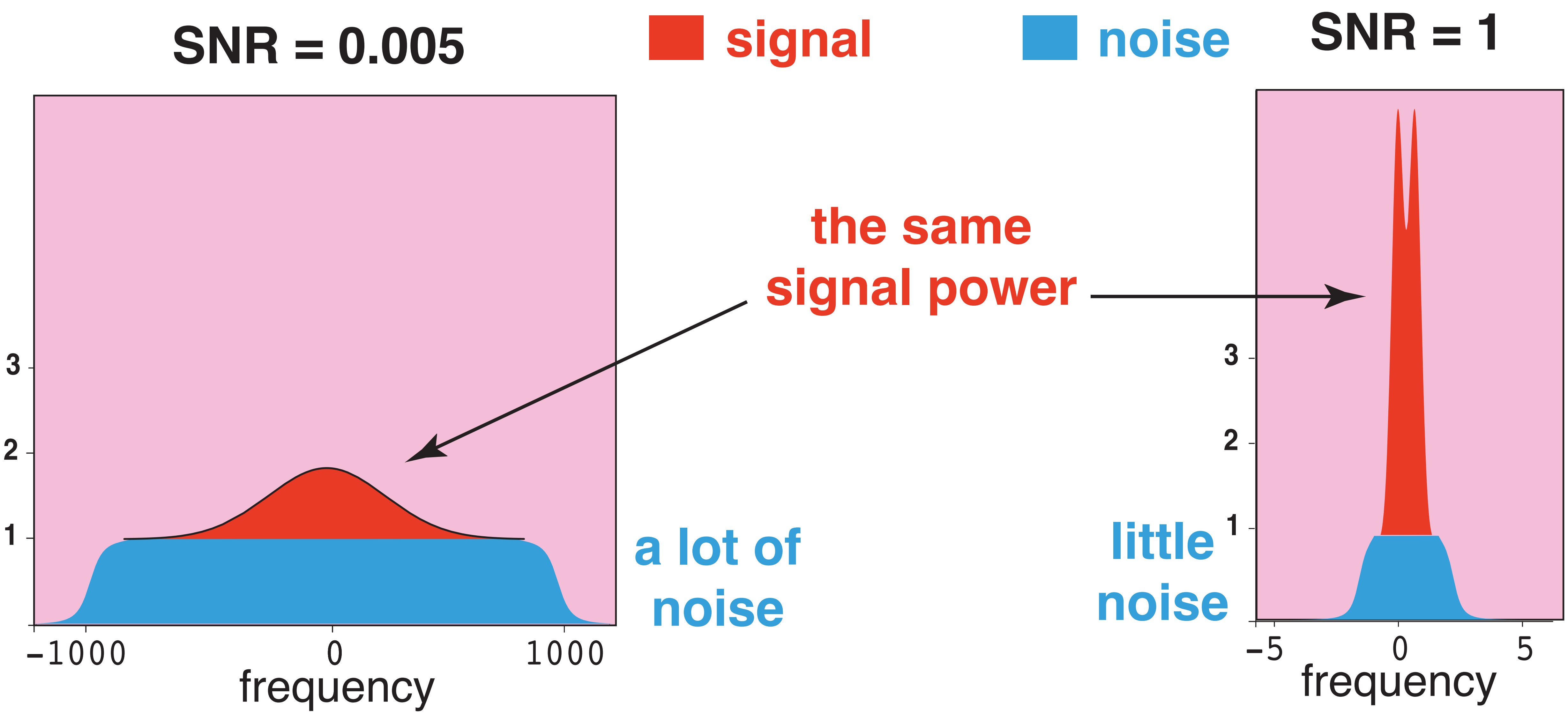

300 metre dish
Arecibo

antenna area ratio: 100

30 metre dish
EISCAT

SNR = 0.005 signal noise **SNR = 1**

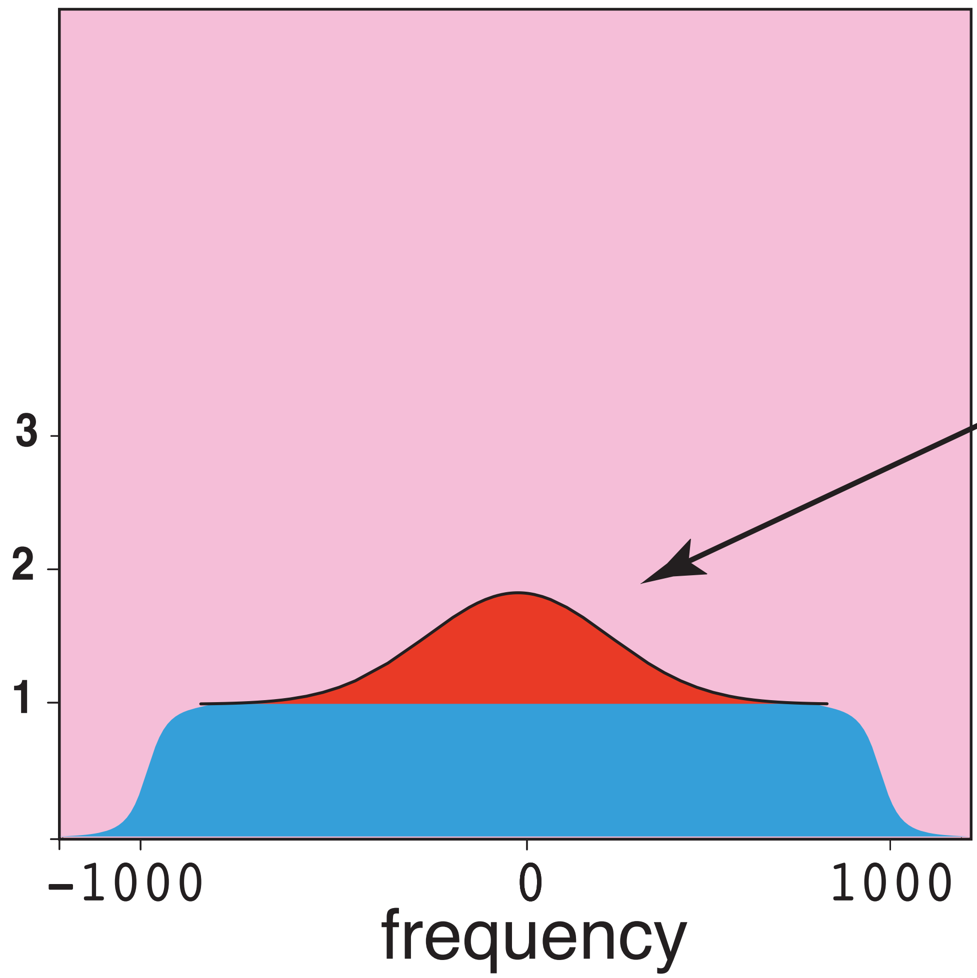

a lot of noise

the same signal power

little noise

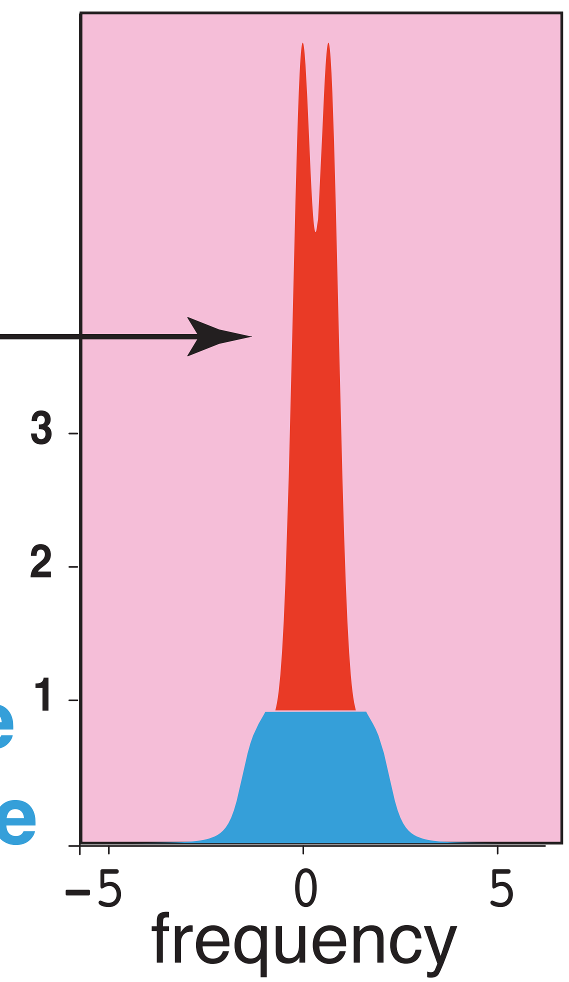

300 metre dish
Arecibo

antenna area ratio: 100

30 metre dish
EISCAT

extraordinary
radio telescope

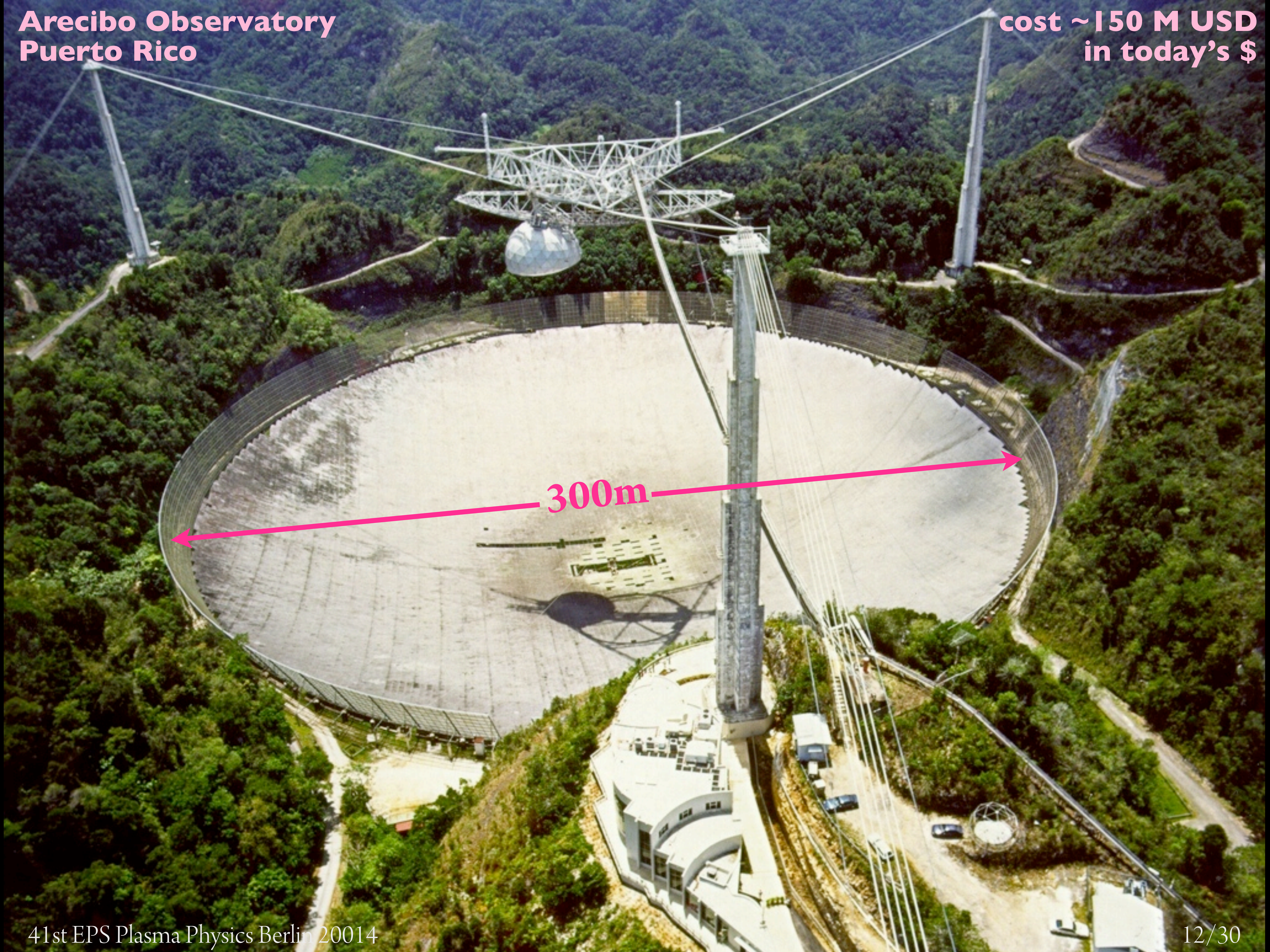
Arecibo Observatory
Puerto Rico
cost ~150 M USD
in today's $
300m

2. Natural Enhanced Ion Acoustic Lines, NEIAL

2. Natural Enhanced Ion Acoustic Lines, NEIAL

normal

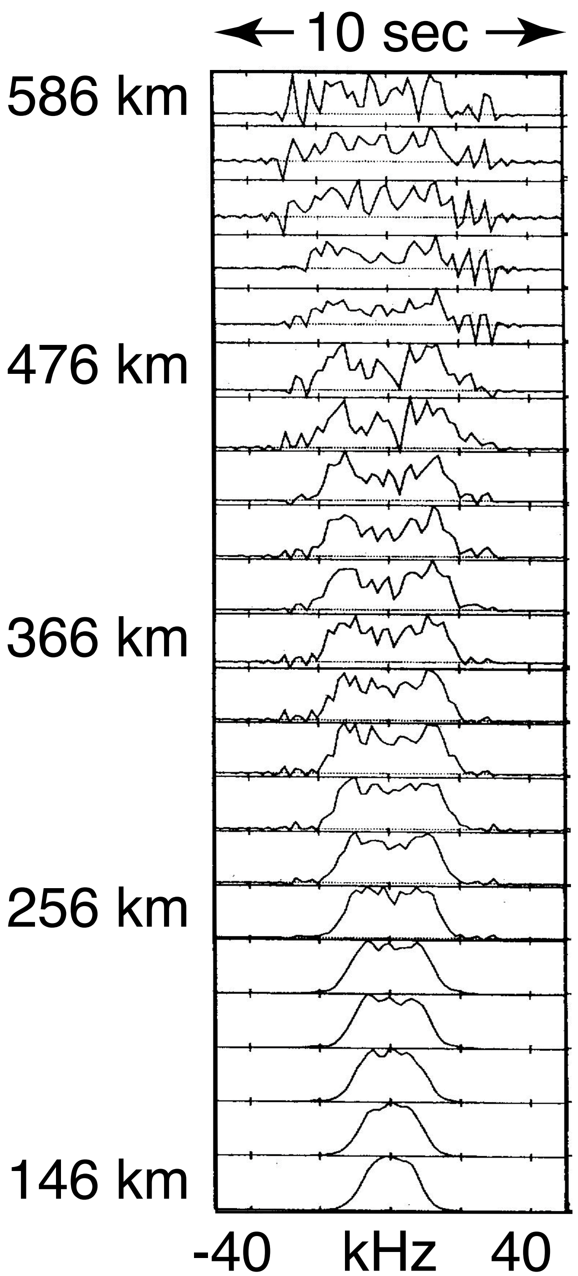

normal

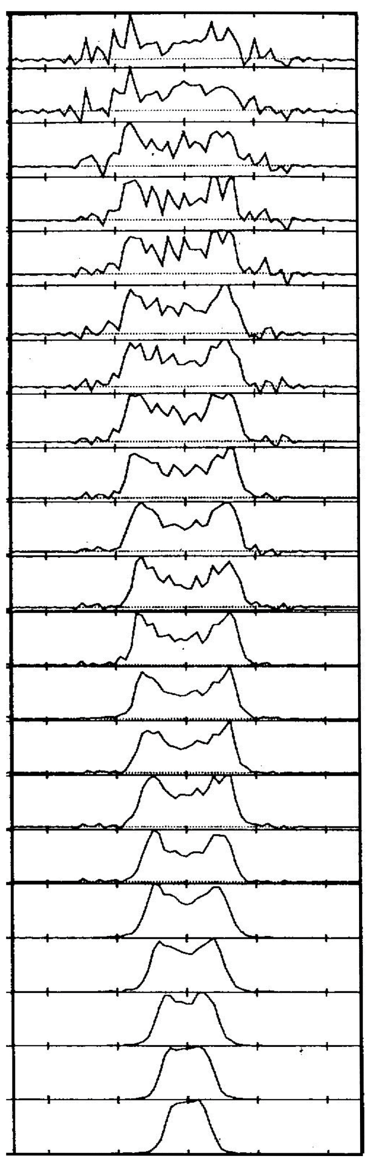

2. Natural Enhanced Ion Acoustic Lines, NEIAL

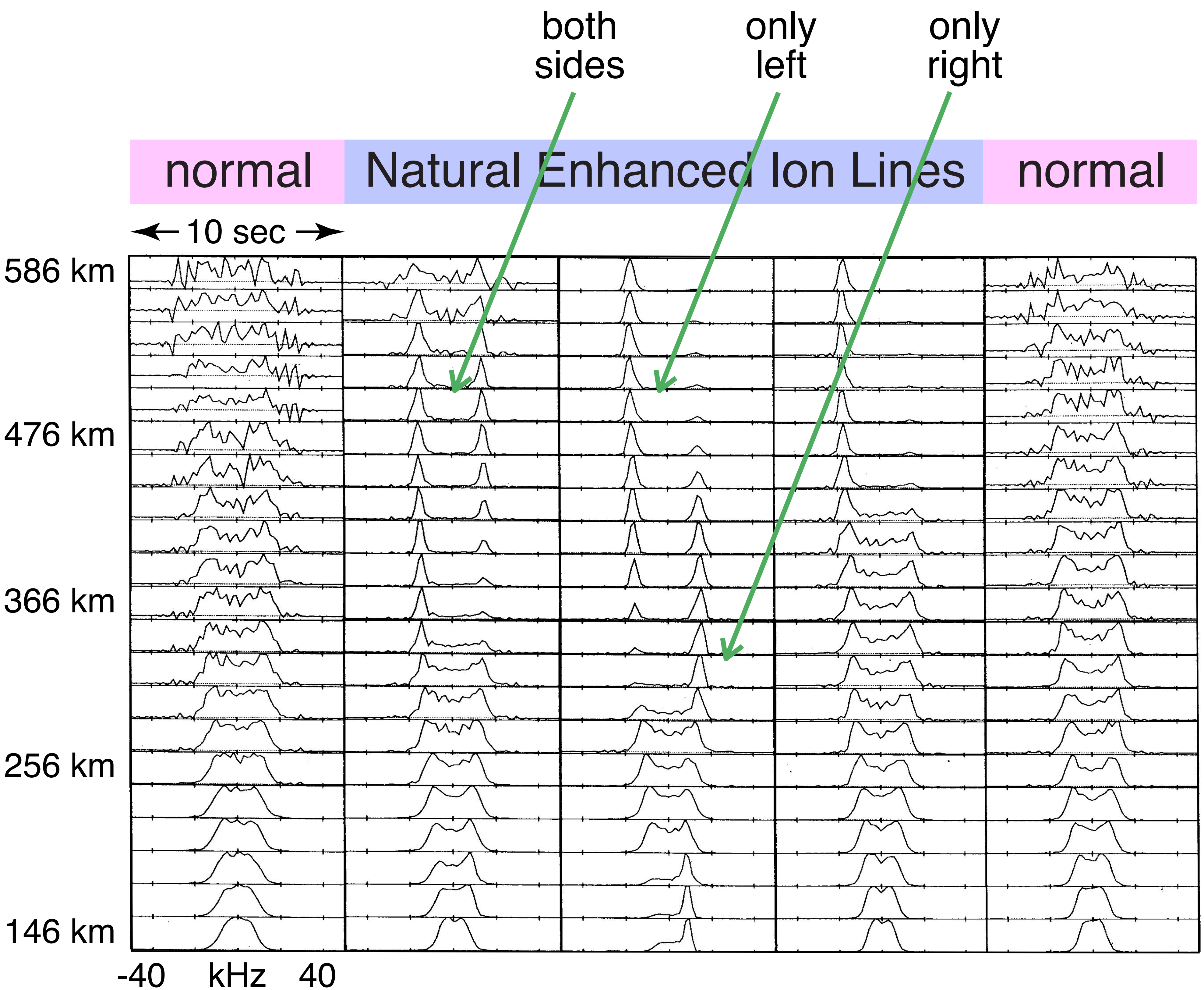

2. Natural Enhanced Ion Acoustic Lines, NEIAL

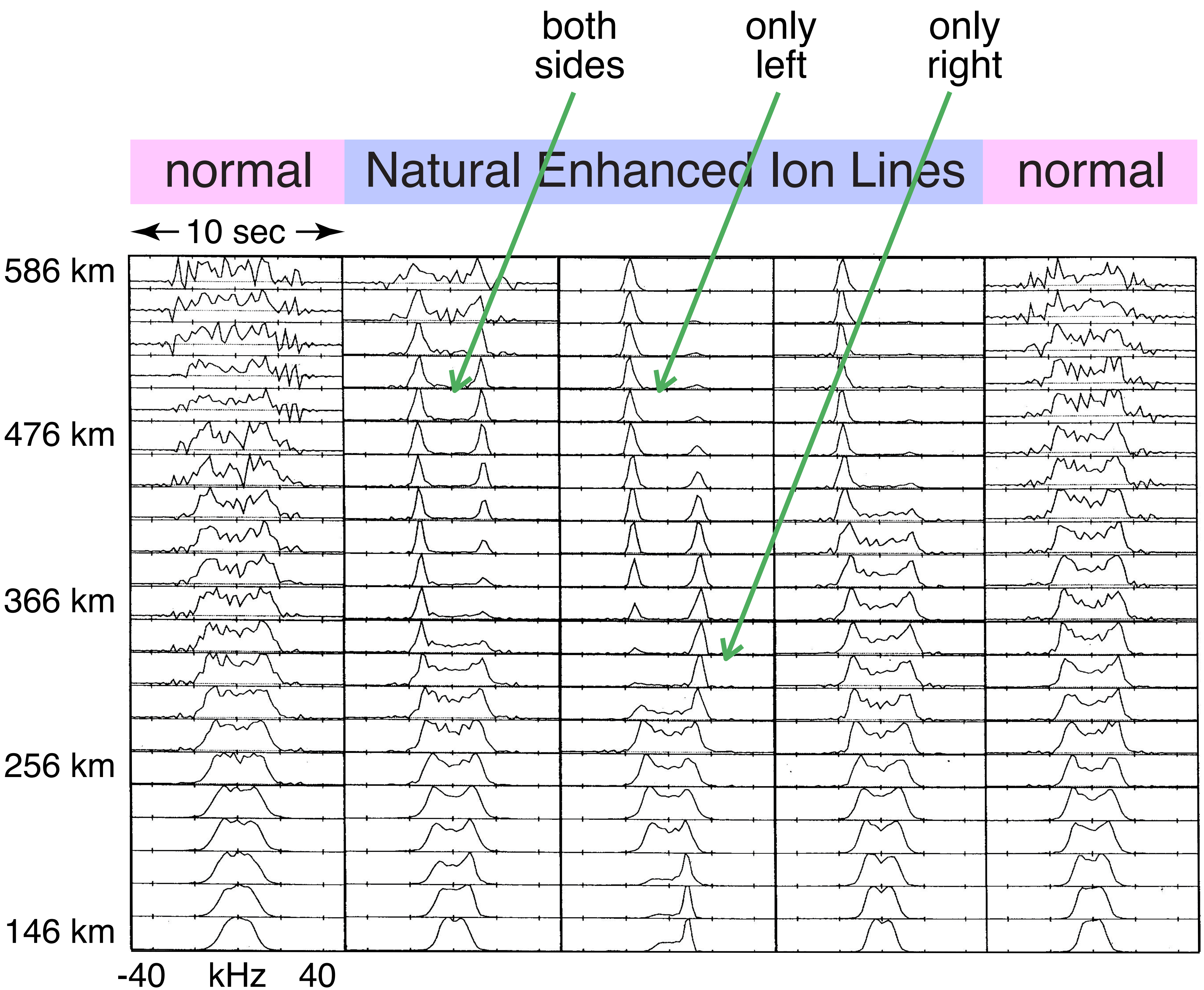

- Infrequent, short lifetime 100ms to ≥ 1min

2. Natural Enhanced Ion Acoustic Lines, NEIAL

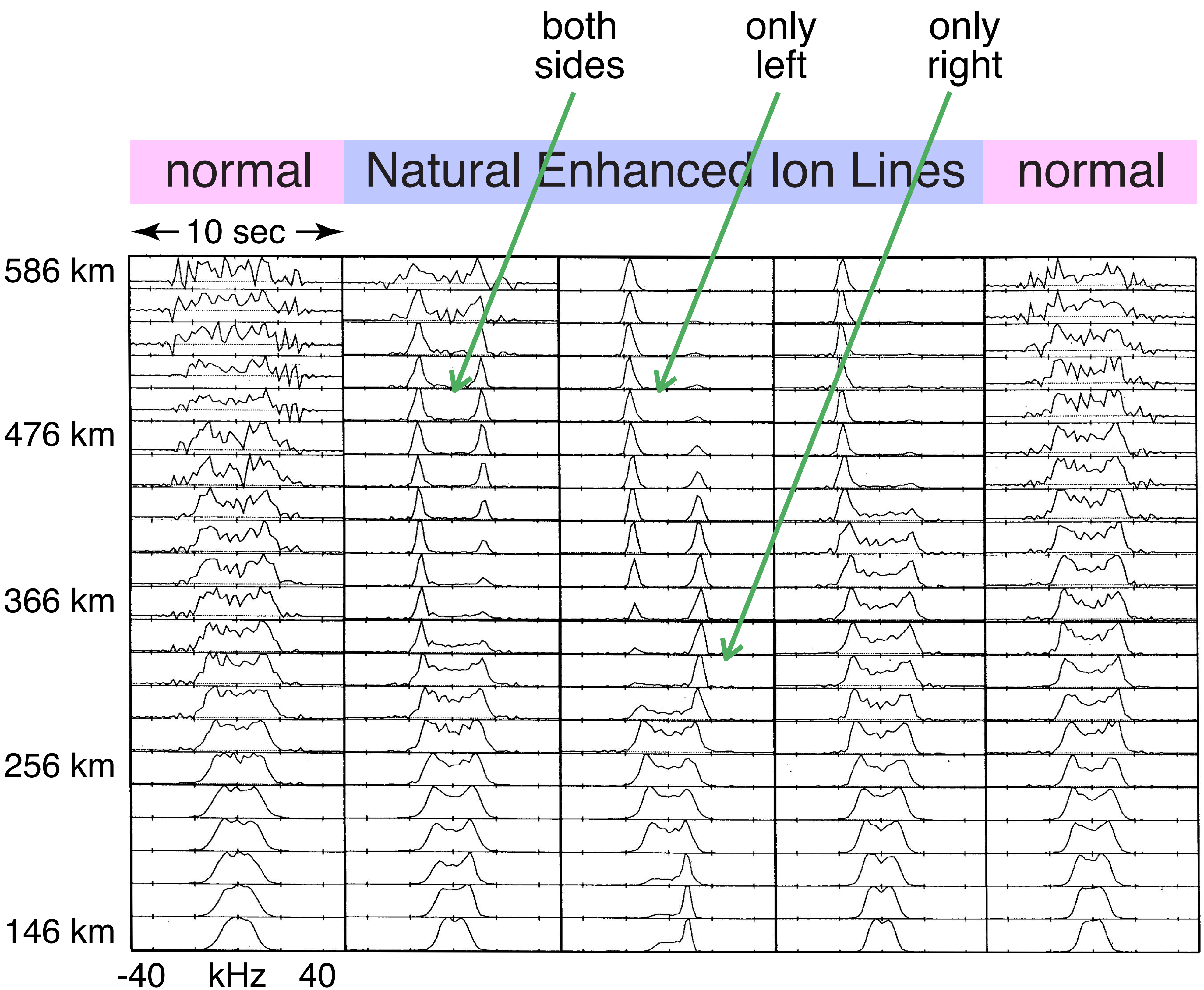

- Infrequent, short lifetime 100ms to ≥ 1min
- Enhanced up to 50 dB

2. Natural Enhanced Ion Acoustic Lines, NEIAL

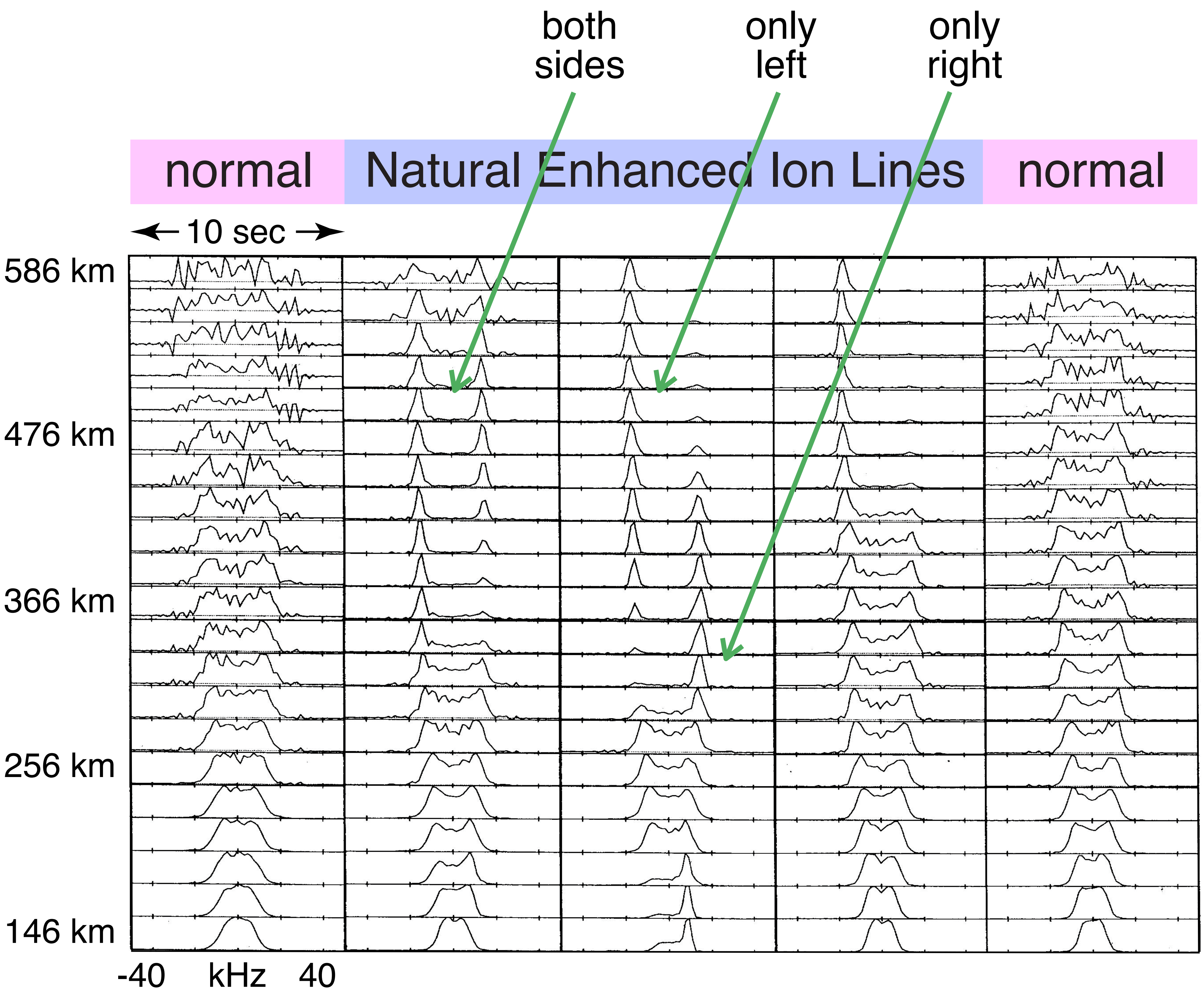

- Infrequent, short lifetime 100ms to ≥ 1min
- Enhanced up to 50 dB
- Long filaments aligned with geomagnetic field - from 150 to ≥ 1500 km long and 300 m thick

2. Natural Enhanced Ion Acoustic Lines, NEIAL

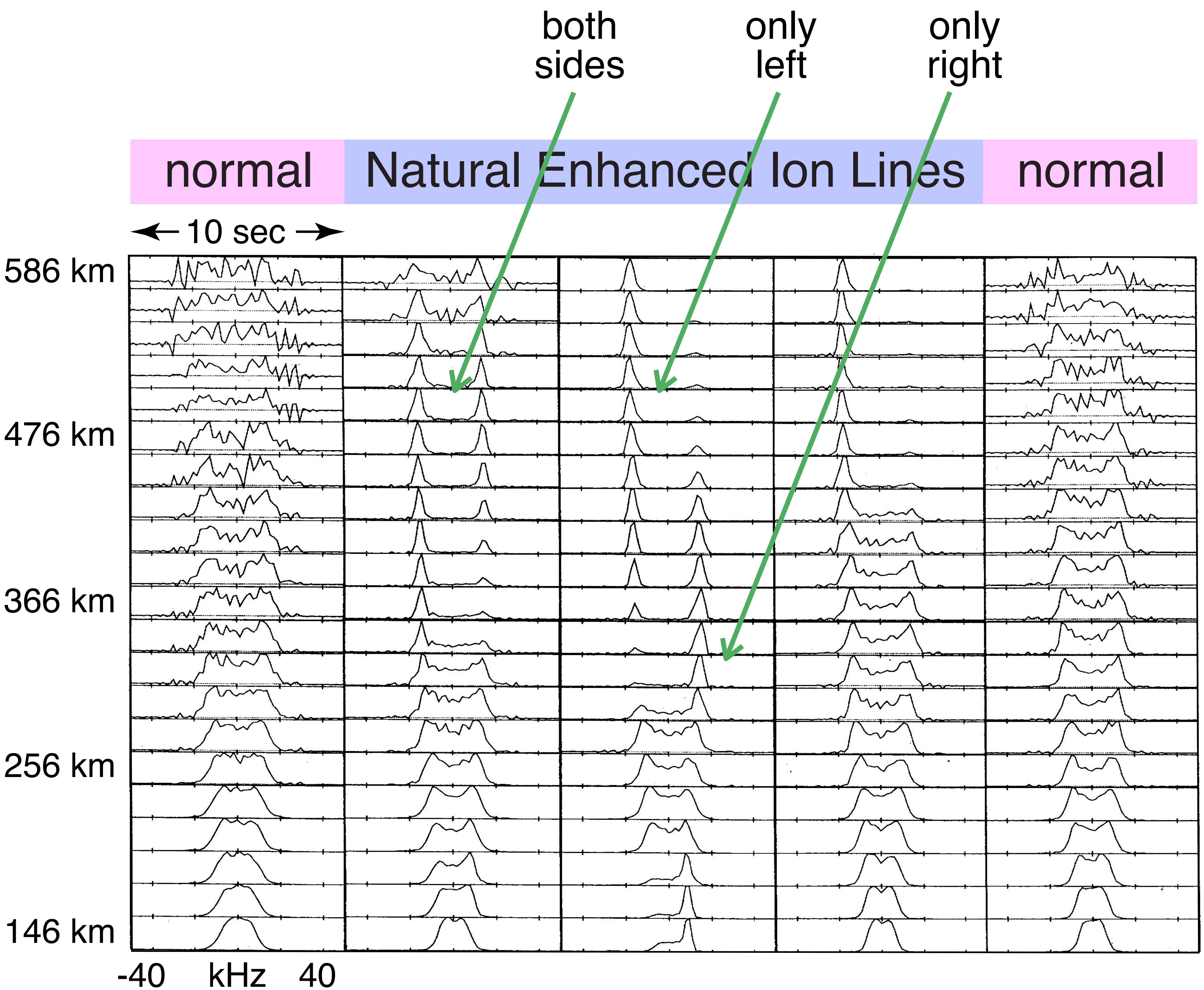

- Infrequent, short lifetime 100ms to ≥ 1min
- Enhanced up to 50 dB
- Long filaments aligned with geomagnetic field - from 150 to ≥ 1500 km long and 300 m thick
- Correlation with soft electron aurora ≤ 500 eV

thermal electron current

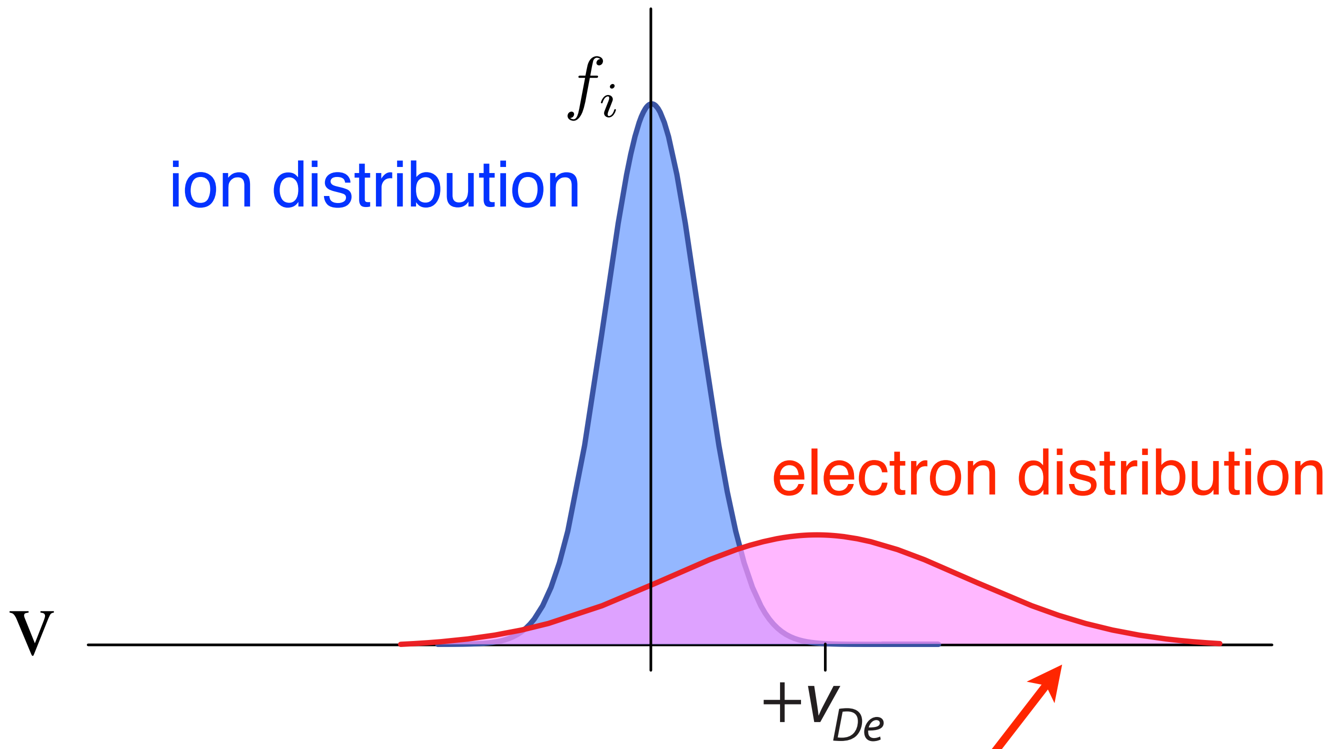

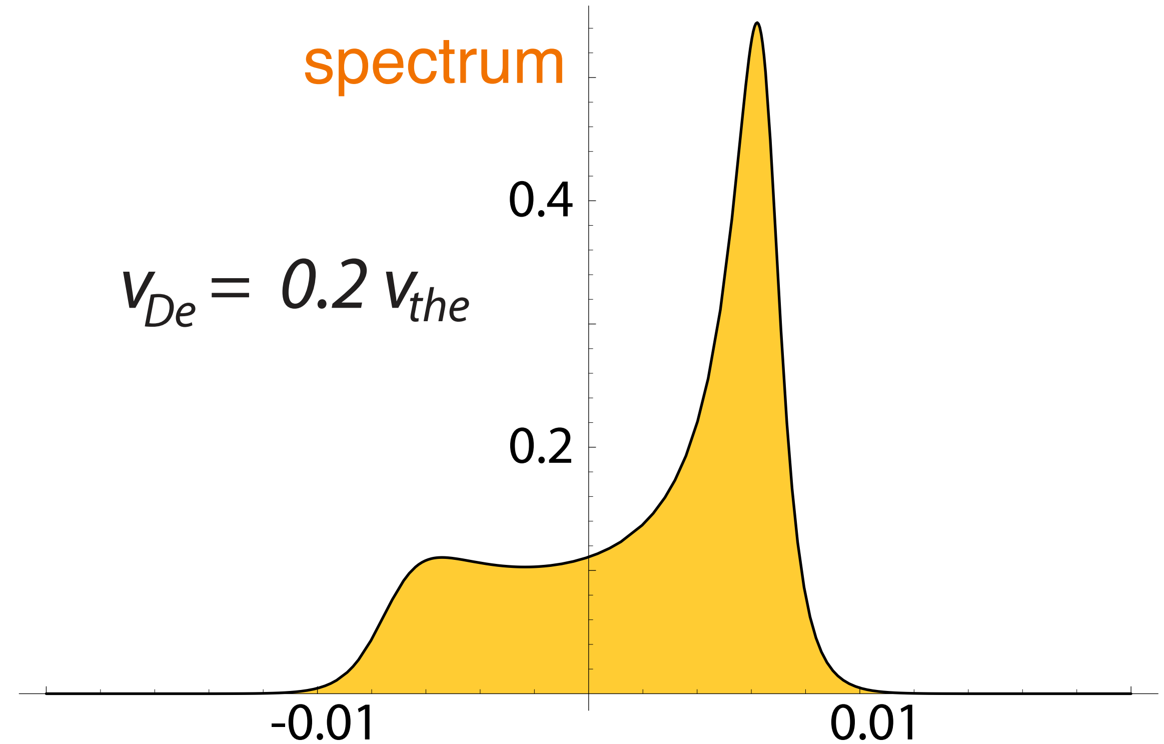

$$f_e(v) \propto \exp\left[-\frac{(v \pm v_{De})^2}{v_{e,ther}^2}\right]$$

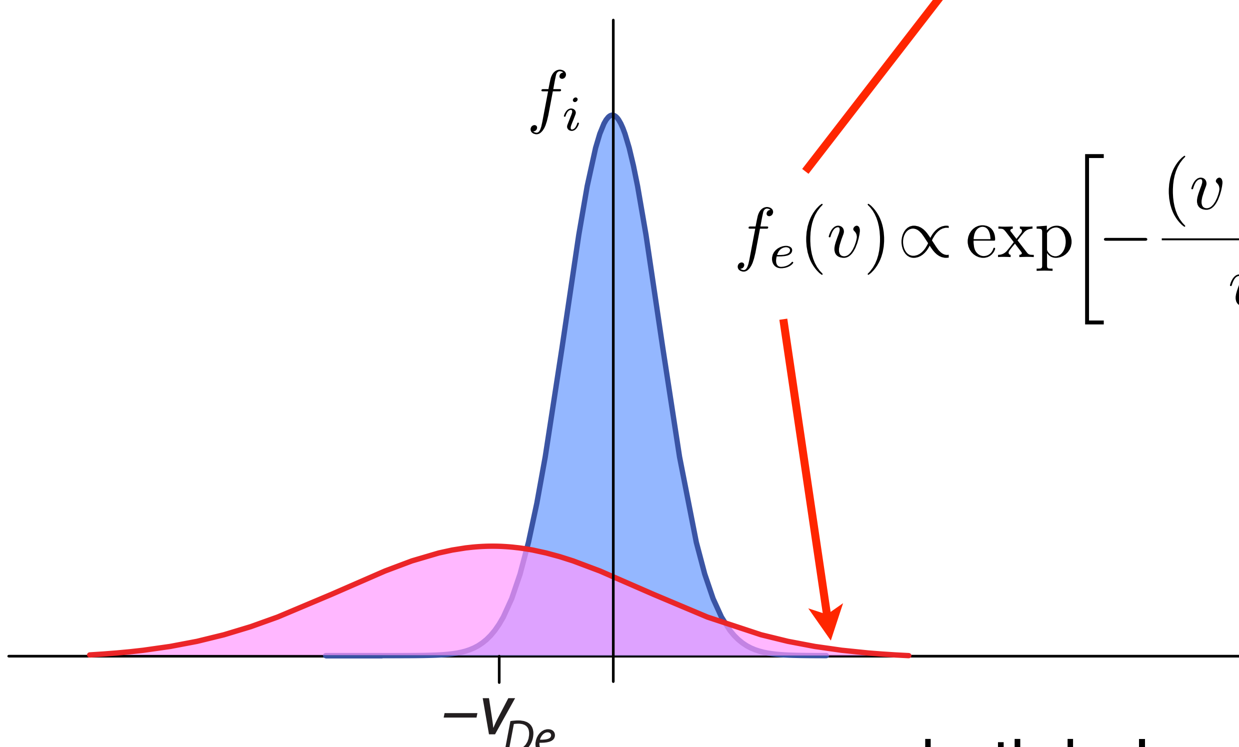

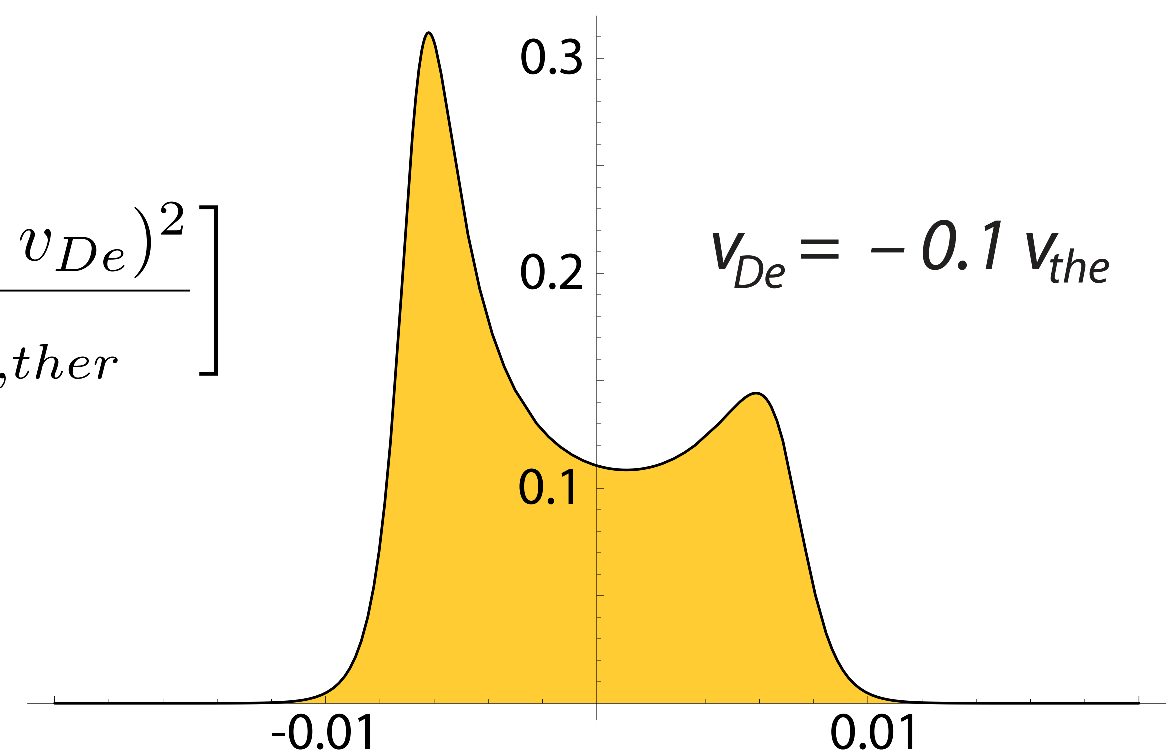

both below threshold
for instability

thermal electron current

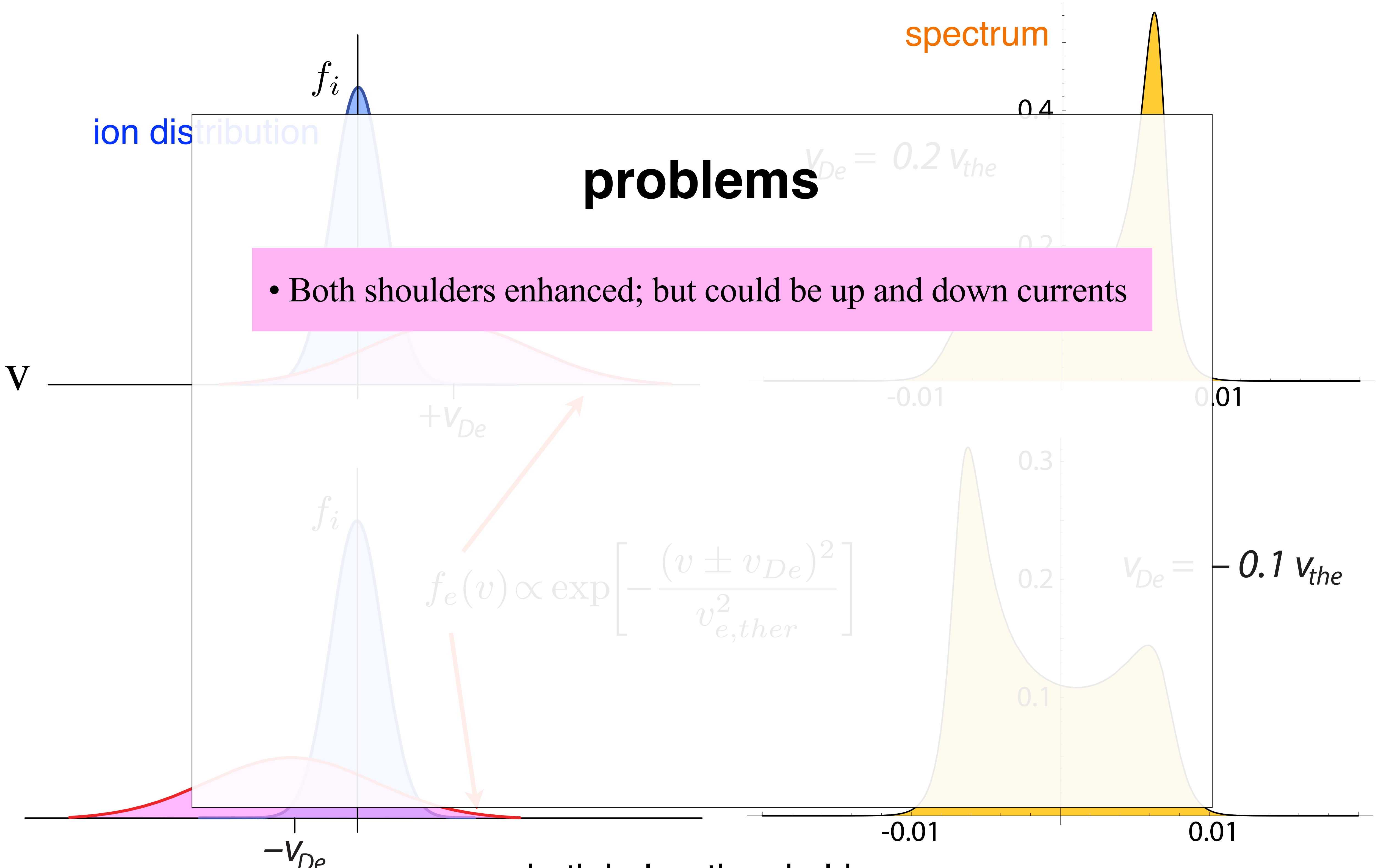

problems

- Both shoulders enhanced; but could be up and down currents

both below threshold
for instability

thermal electron current

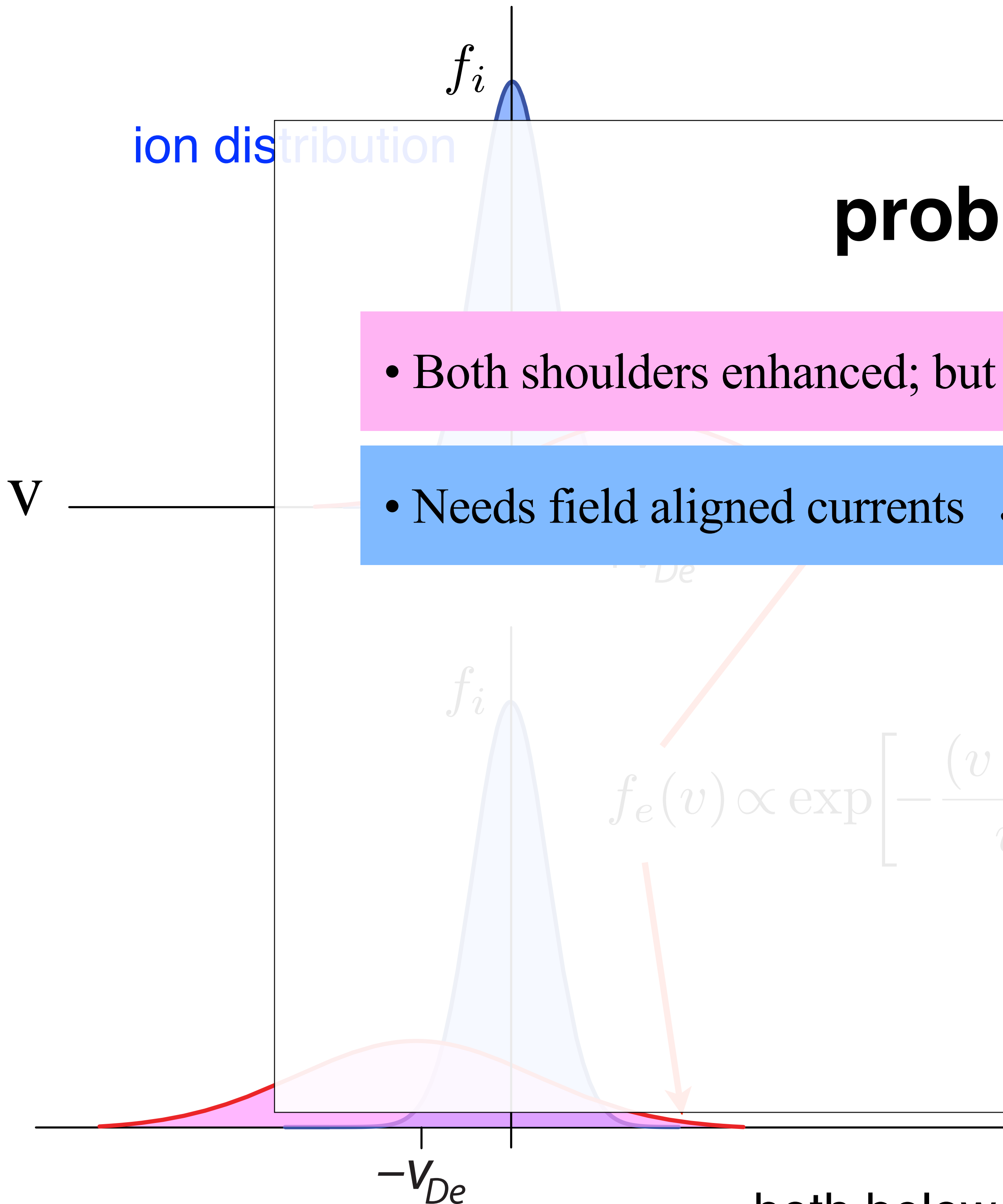

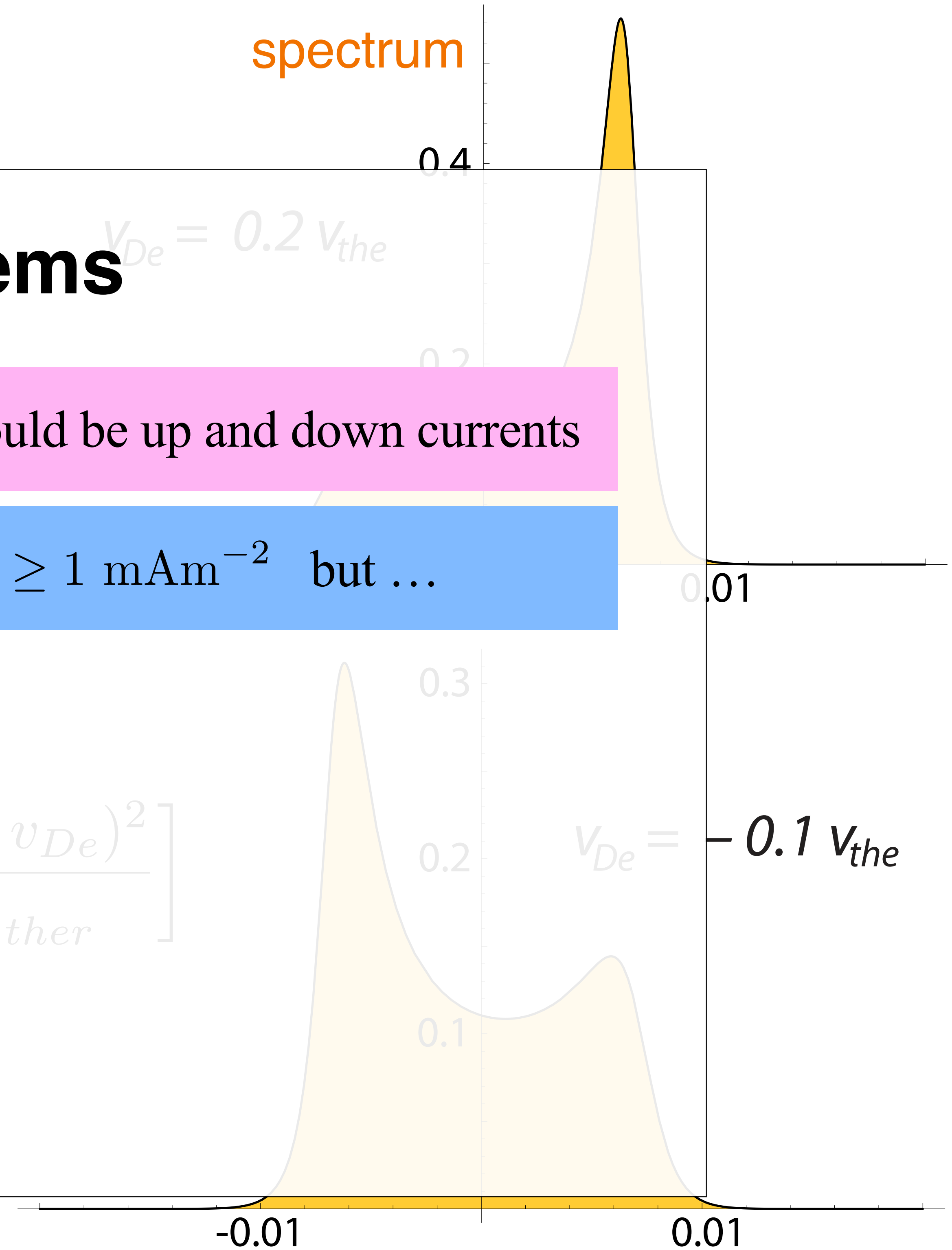

problems

- Both shoulders enhanced; but could be up and down currents
- Needs field aligned currents $\mathbf{J}_{\|} \geq 1\ \mathrm{mAm}^{-2}$ but …

both below threshold
for instability

thermal electron current

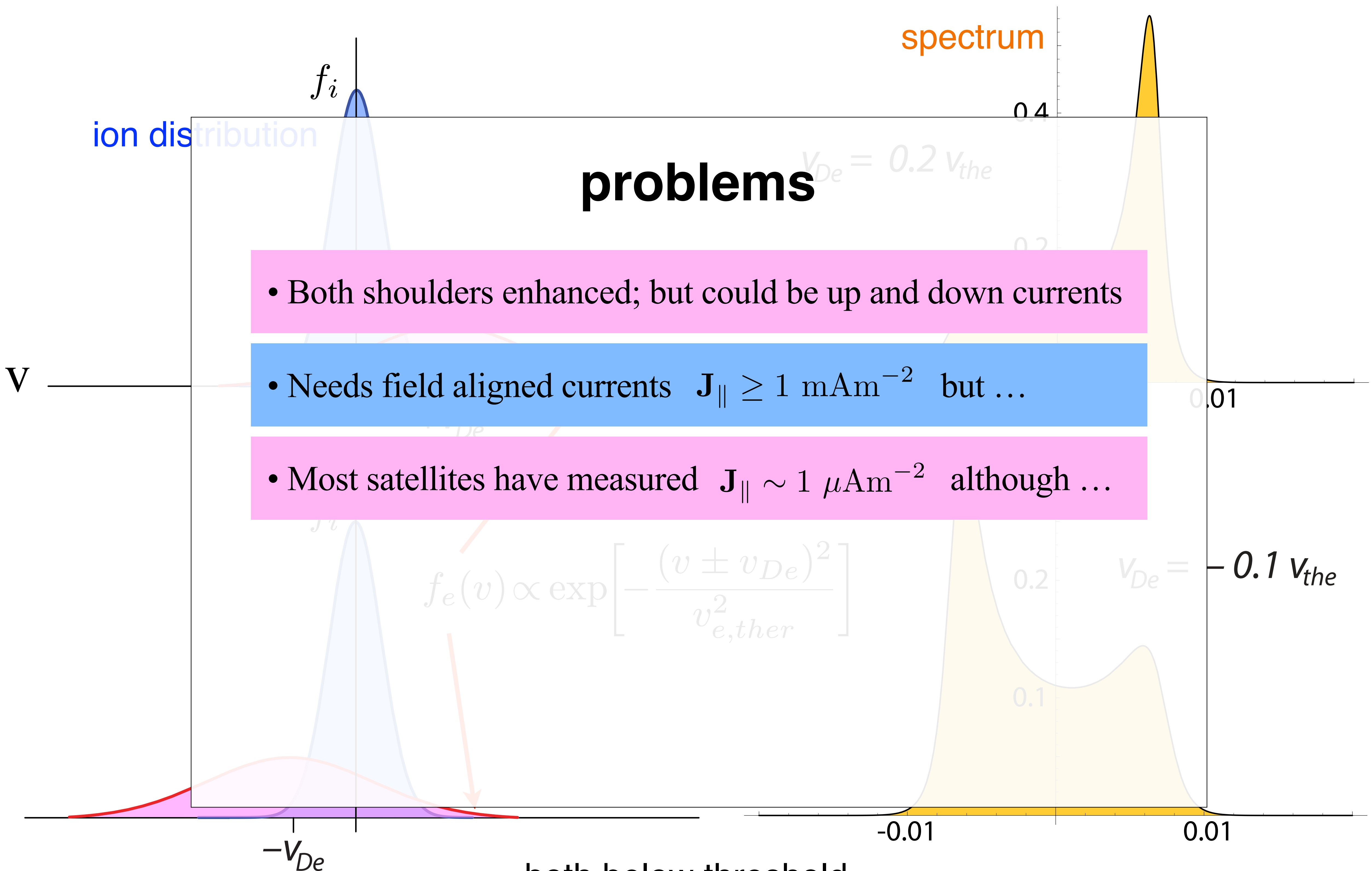

problems

- Both shoulders enhanced; but could be up and down currents
- Needs field aligned currents $\mathbf{J}_{\parallel} \geq 1\ \mathrm{mAm}^{-2}$ but …
- Most satellites have measured $\mathbf{J}_{\parallel} \sim 1\ \mu\mathrm{Am}^{-2}$ although …

both below threshold
for instability

thermal electron current

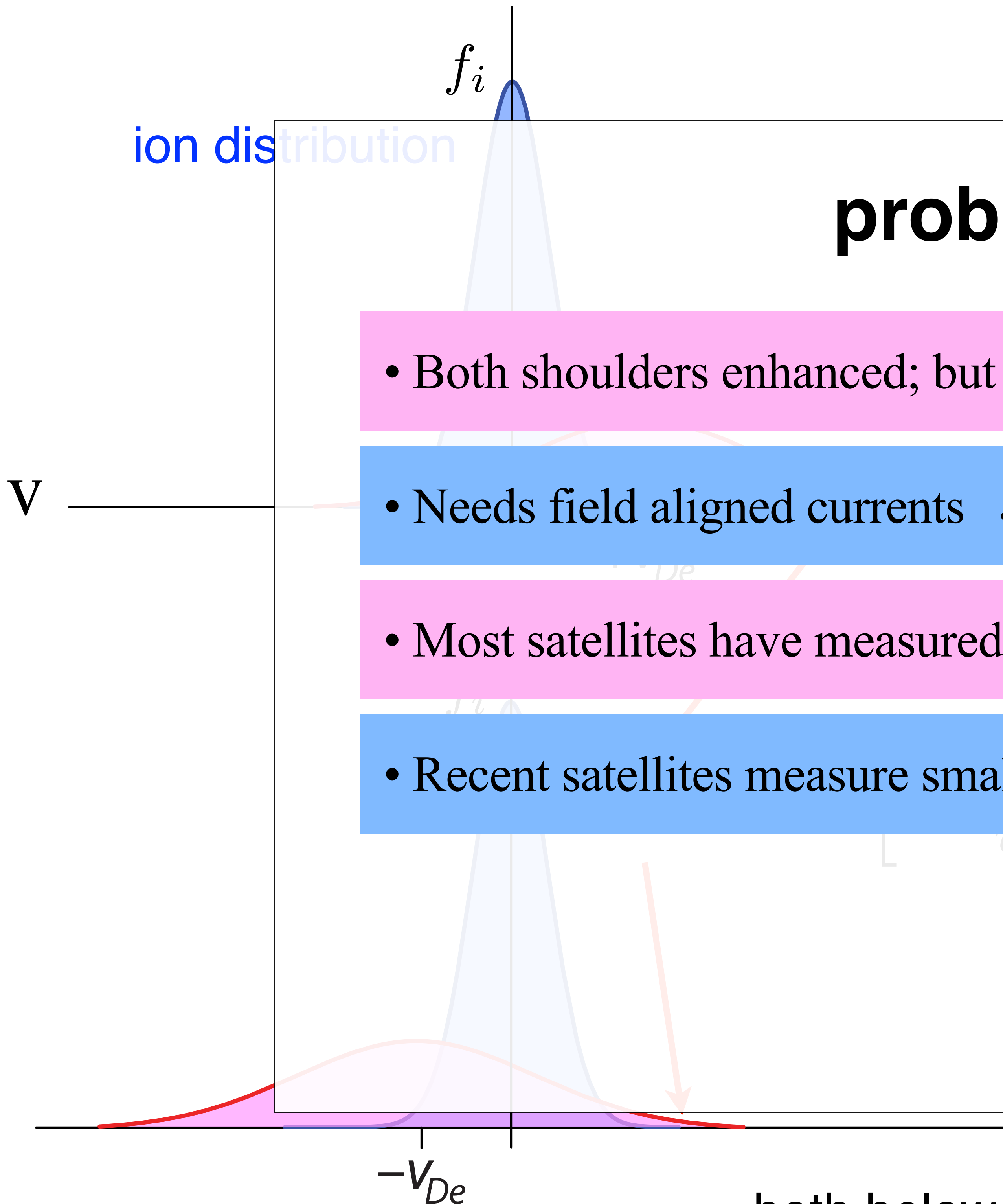

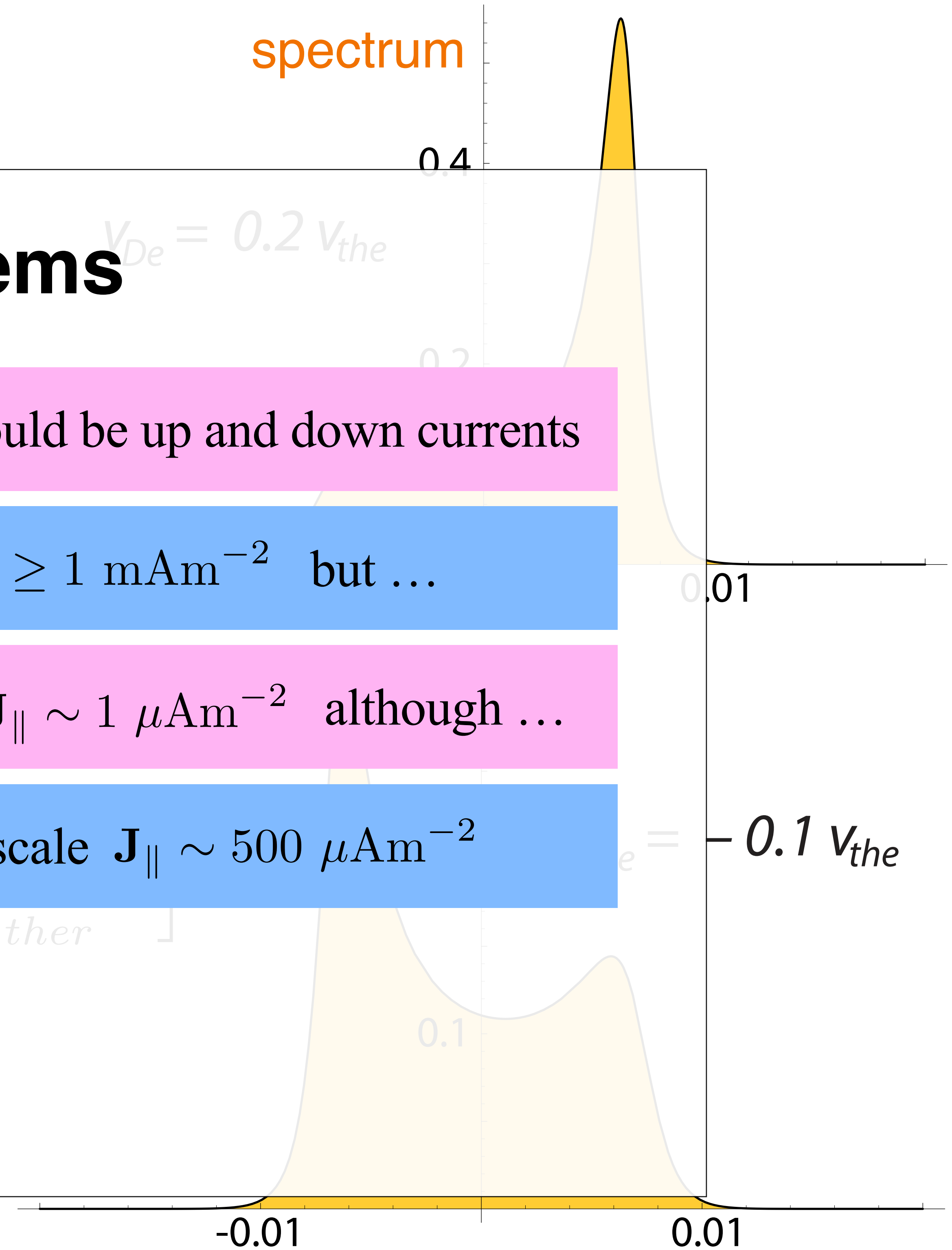

problems

- Both shoulders enhanced; but could be up and down currents
- Needs field aligned currents $\mathbf{J}_{\|} \geq 1\ \mathrm{mAm}^{-2}$ but …
- Most satellites have measured $\mathbf{J}_{\|} \sim 1\ \mu\mathrm{Am}^{-2}$ although …
- Recent satellites measure small scale $\mathbf{J}_{\|} \sim 500\ \mu\mathrm{Am}^{-2}$

both below threshold
for instability

thermal electron current

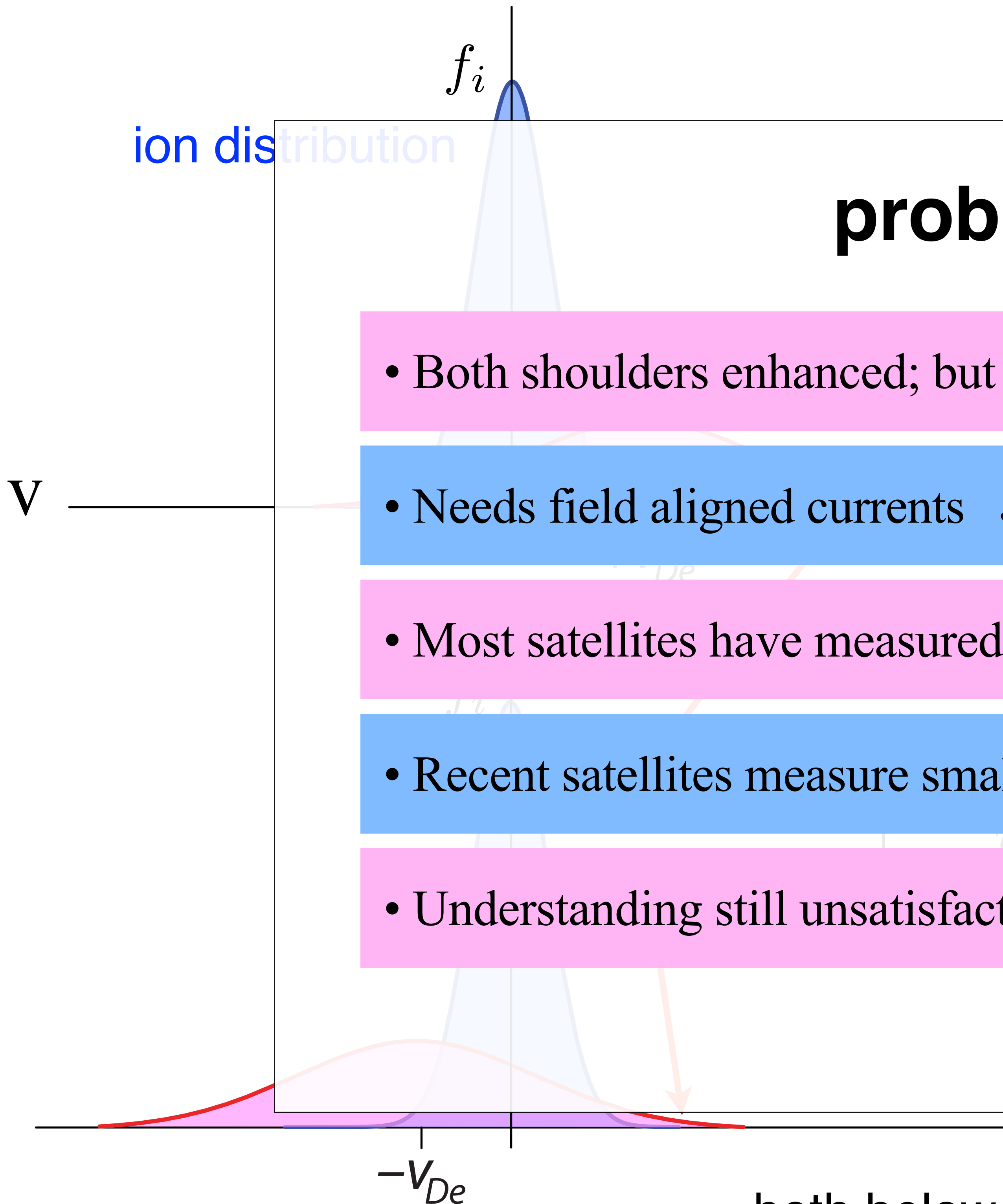

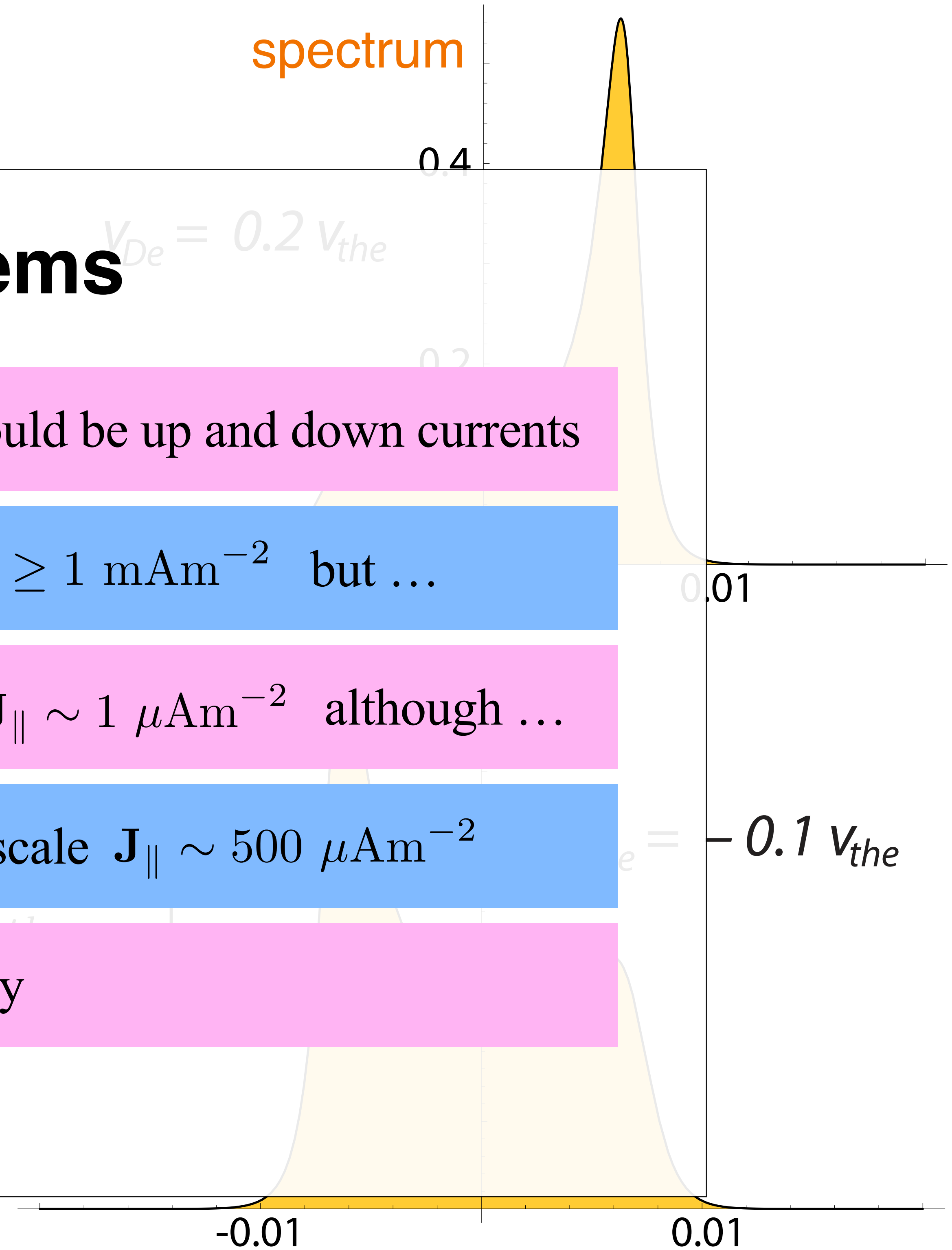

problems

- Both shoulders enhanced; but could be up and down currents
- Needs field aligned currents $\mathbf{J}_{\parallel} \geq 1\ \mathrm{mAm}^{-2}$ but …
- Most satellites have measured $\mathbf{J}_{\parallel} \sim 1\ \mu\mathrm{Am}^{-2}$ although …
- Recent satellites measure small scale $\mathbf{J}_{\parallel} \sim 500\ \mu\mathrm{Am}^{-2}$
- Understanding still unsatisfactory

both below threshold
for instability

total power measurements

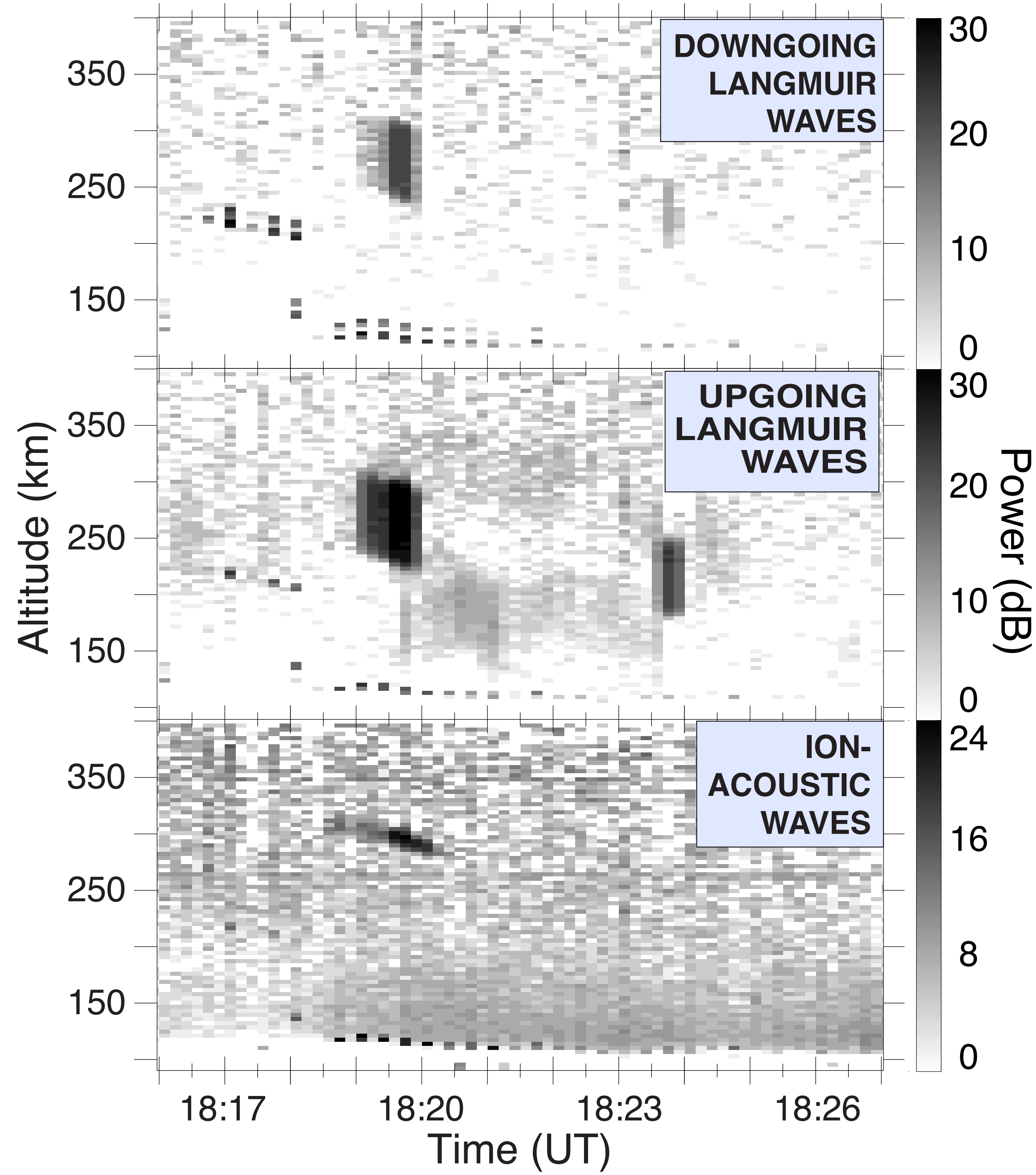

total power measurements

ion acoustic waves
enhanced x10^2
above thermal level

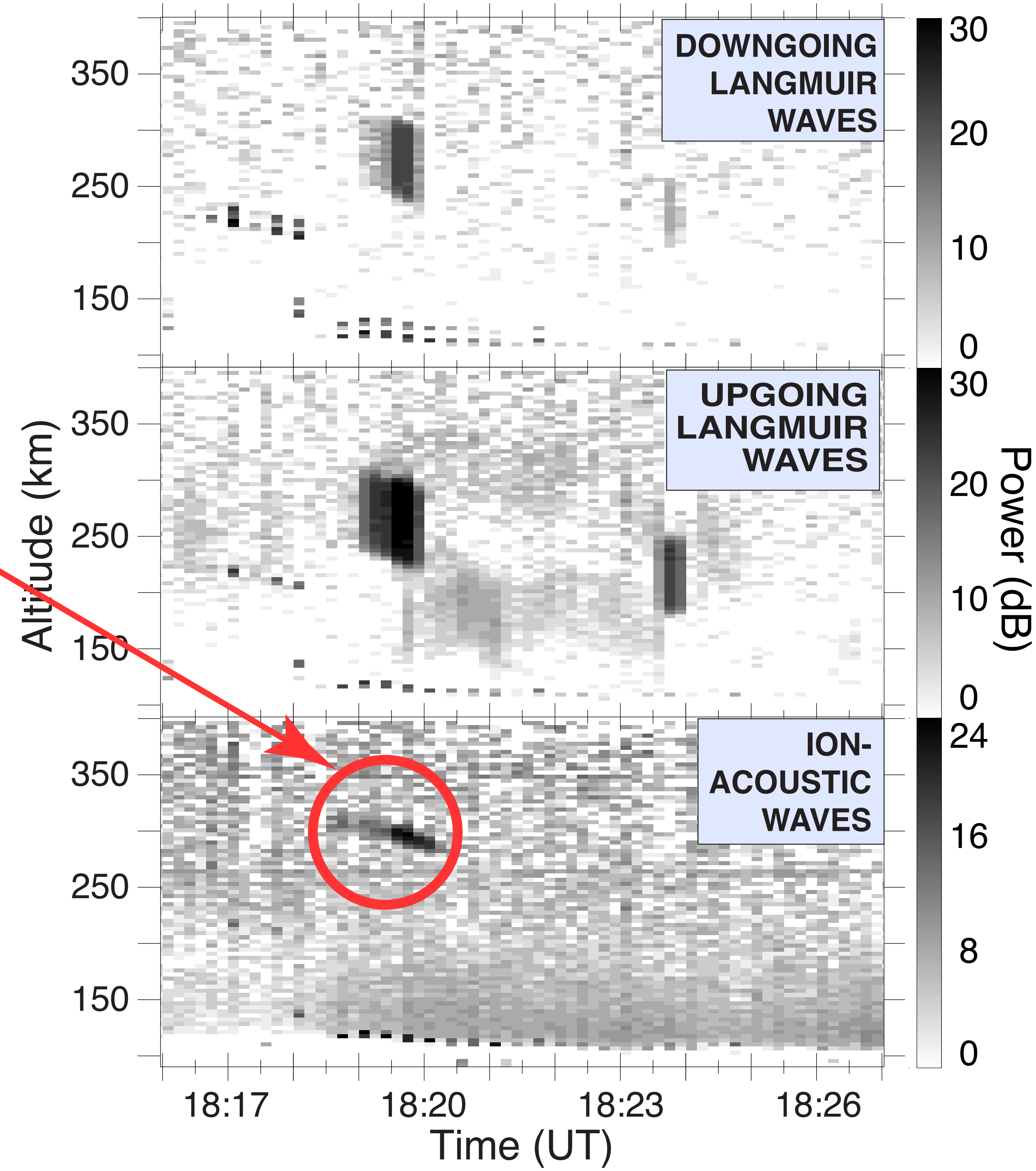

total power measurements

Langmuir waves down- and upgoing enhanced x10^2 and x10^3 above thermal level

ion acoustic waves enhanced x10^2 above thermal level

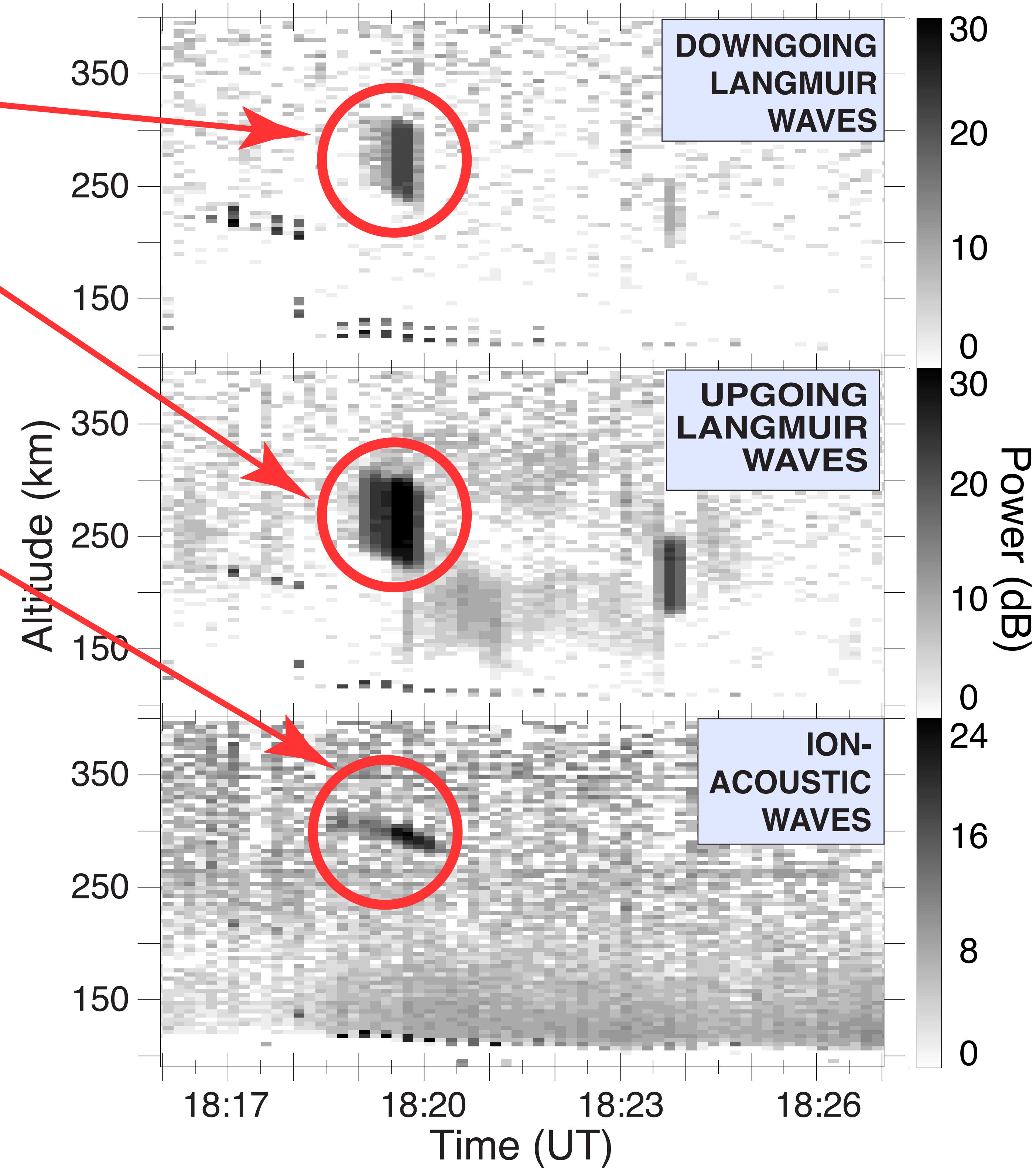

total power measurements

Langmuir waves down- and upgoing enhanced x10^2 and x10^3 above thermal level

ion acoustic waves enhanced x10^2 above thermal level

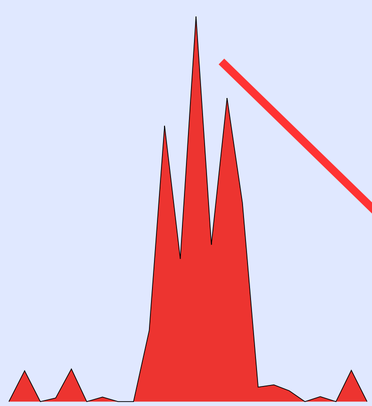

central peak: signature of strong Lagmuir turbulence

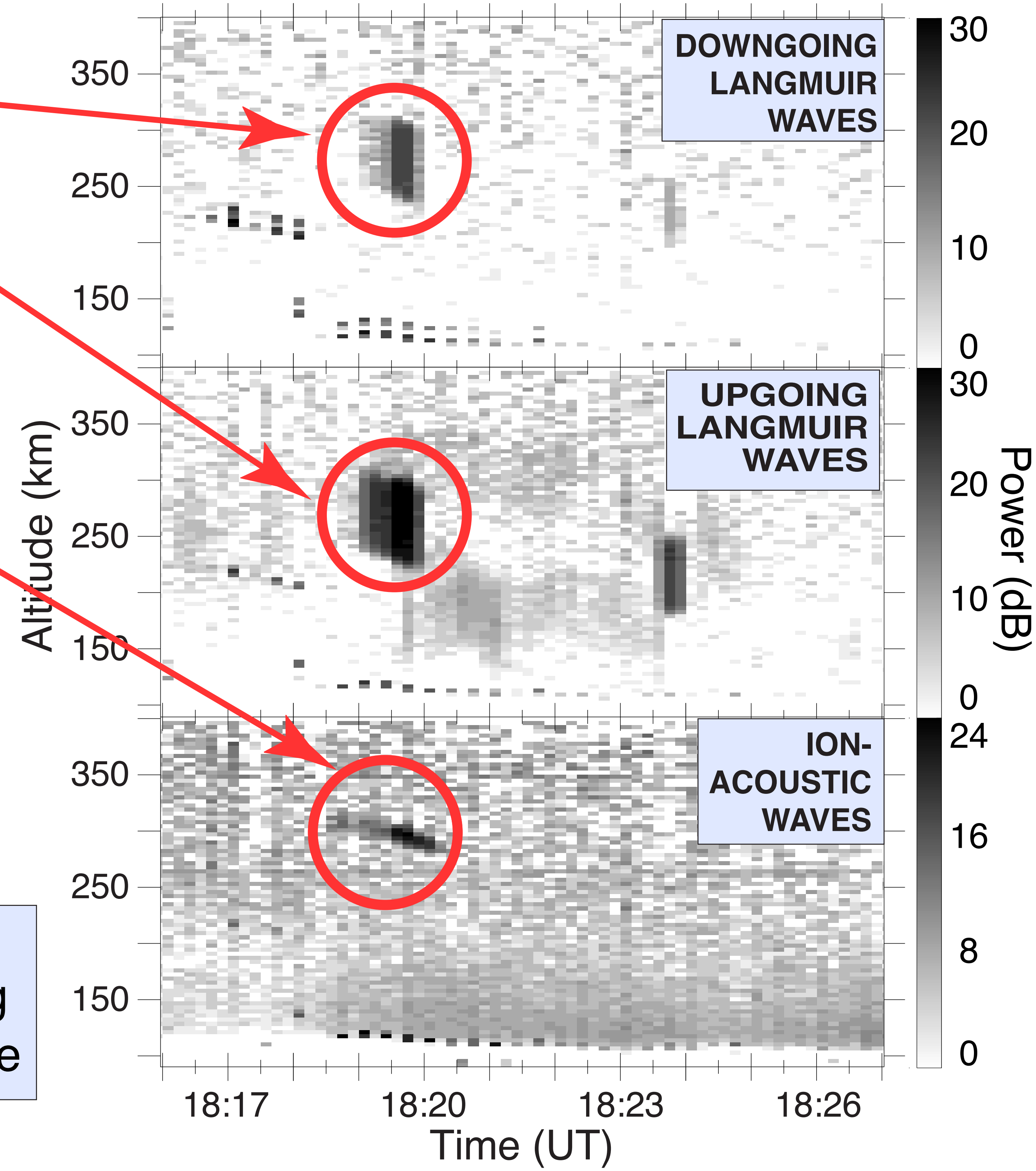

Zakharov equations 1-D

Langmuir waves	$i(\partial_t + \gamma^\ell)E + \partial^2_{xx}E = nE$
Ion sound waves	$(\partial^2_{tt} + \gamma^s \partial_t)n - \partial^2_{xx}n = \partial^2_{xx}|E|^2$

Zakharov equations 1-D

Langmuir waves	$i(\partial_t + \gamma^\ell)E + \partial^2_{xx}E = nE$
Ion sound waves	$(\partial^2_{tt} + \gamma^s \partial_t)n - \partial^2_{xx} n = \partial^2_{xx}\|E\|^2$
Damping and growth rates	$\gamma^\ell(k) = \frac{1}{2}\nu_e + \gamma_{Le}(k) - \gamma_b(k)$ $\gamma^s(k) = \gamma_{Li}(k)$
Bump-in-tail growth	$\gamma_b(k) = \frac{\chi}{\tau}\frac{\pi}{2n}\frac{\omega^3_{pe}}{k^2}\partial_v F_b(v)\Big\|_{v=\omega_{pe}/k}$

Zakharov equations 1-D

Langmuir waves	$i(\partial_t + \gamma^\ell)E + \partial^2_{xx}E = nE$
Ion sound waves	$(\partial^2_{tt} + \gamma^s\partial_t)n - \partial^2_{xx}n = \partial^2_{xx}\lvert E\rvert^2$
Damping and growth rates	$\gamma^\ell(k) = \frac{1}{2}\nu_e + \gamma_{Le}(k) - \gamma_b(k)$ $\gamma^s(k) = \gamma_{Li}(k)$
Bump-in-tail growth	$\gamma_b(k) = \frac{\chi}{\tau}\frac{\pi}{2n}\frac{\omega^3_{pe}}{k^2}\partial_v F_b(v)\Big\vert_{v=\omega_{pe}/k}$

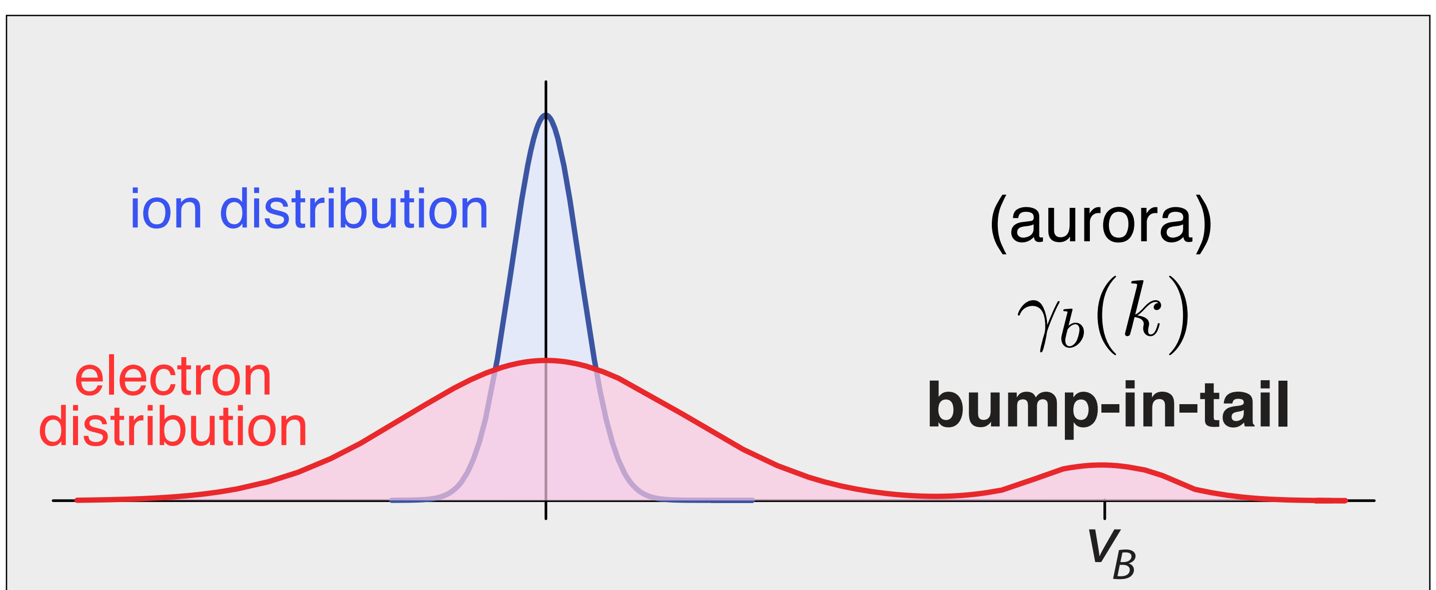

Zakharov equations 1-D

Langmuir waves	$i(\partial_t + \gamma^\ell)E + \partial^2_{xx}E = nE$
Ion sound waves	$(\partial^2_{tt} + \gamma^s\partial_t)n - \partial^2_{xx}n = \partial^2_{xx}\|E\|^2$
Damping and growth rates	$\gamma^\ell(k) = \frac{1}{2}\nu_e + \gamma_{Le}(k) - \gamma_b(k)$ $\gamma^s(k) = \gamma_{Li}(k)$
Bump-in-tail growth	$\gamma_b(k) = \frac{\chi}{\tau}\frac{\pi}{2n}\frac{\omega^3_{pe}}{k^2}\partial_v F_b(v)\Big\|_{v=\omega_{pe}/k}$

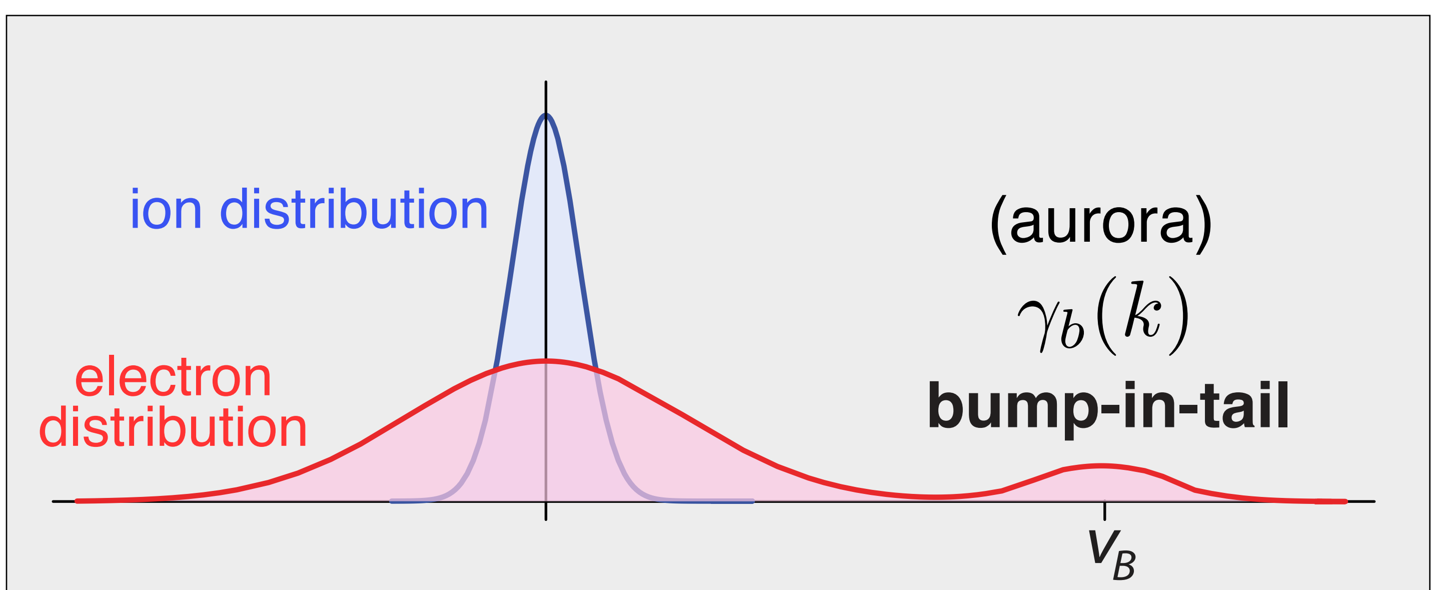

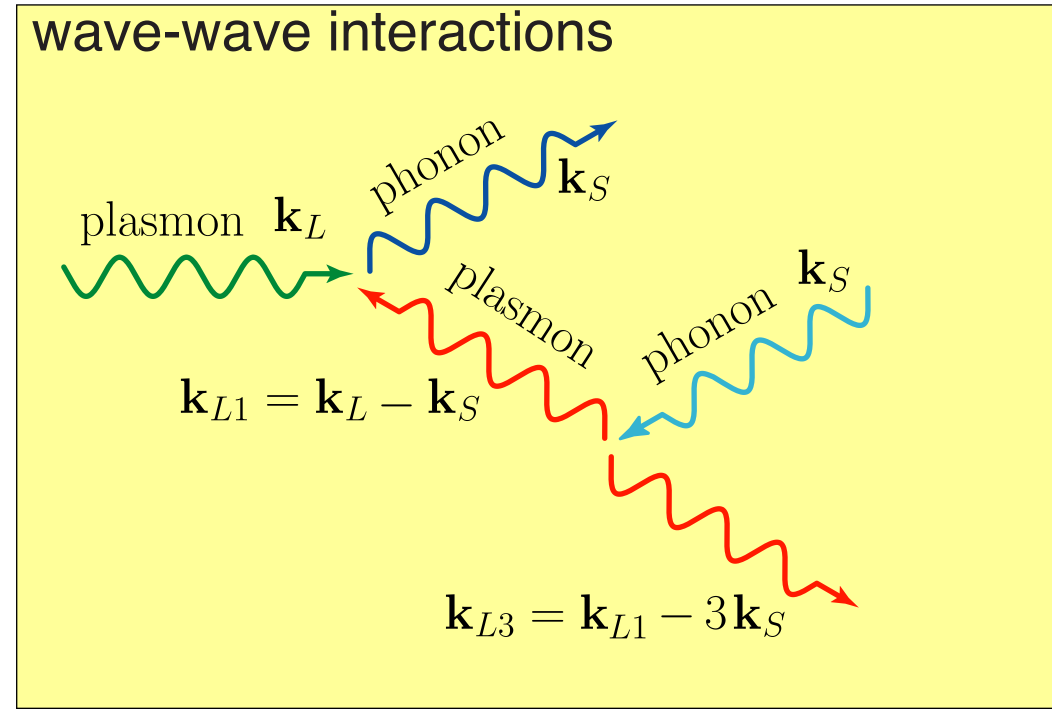

Zakharov equations 1-D

Langmuir waves	$i(\partial_t + \gamma^\ell)E + \partial^2_{xx}E = nE$
Ion sound waves	$(\partial^2_{tt} + \gamma^s\partial_t)n - \partial^2_{xx}n = \partial^2_{xx}\lvert E\rvert^2$
Damping and growth rates	$\gamma^\ell(k) = \frac{1}{2}\nu_e + \gamma_{Le}(k) - \gamma_b(k)$ $\gamma^s(k) = \gamma_{Li}(k)$
Bump-in-tail growth	$\gamma_b(k) = \frac{\chi}{\tau}\frac{\pi}{2n}\frac{\omega^3_{pe}}{k^2}\partial_v F_b(v)\Big\rvert_{v=\omega_{pe}/k}$

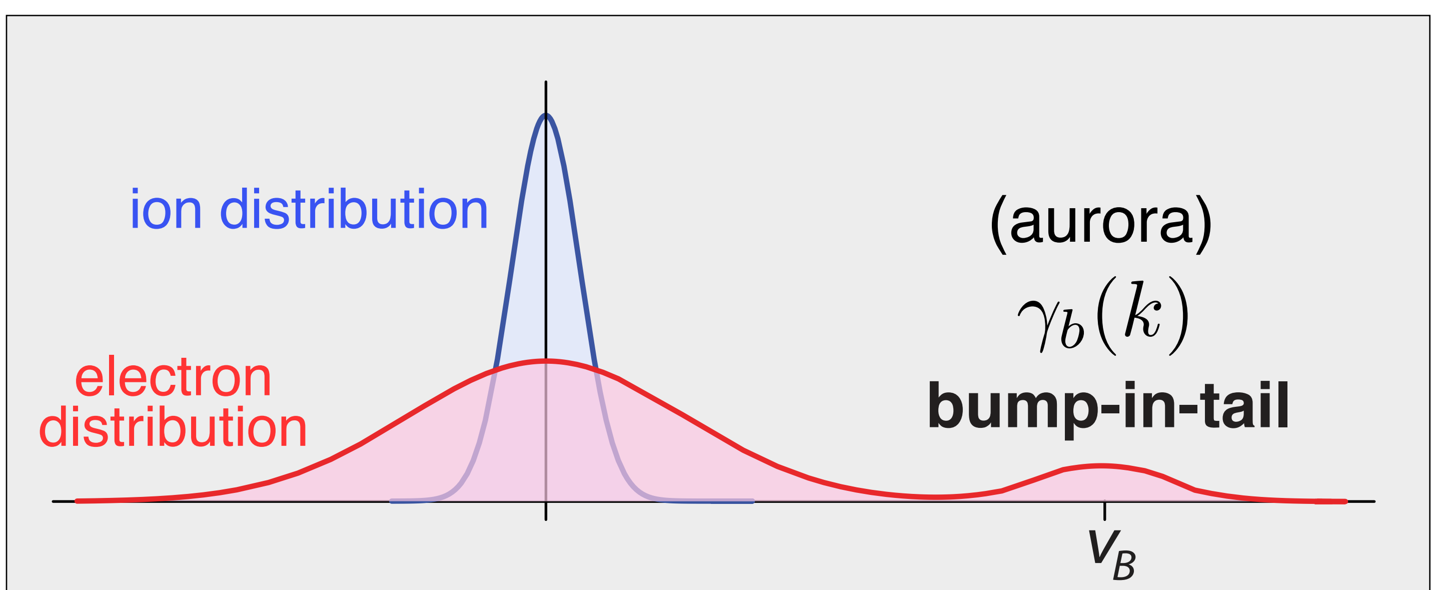

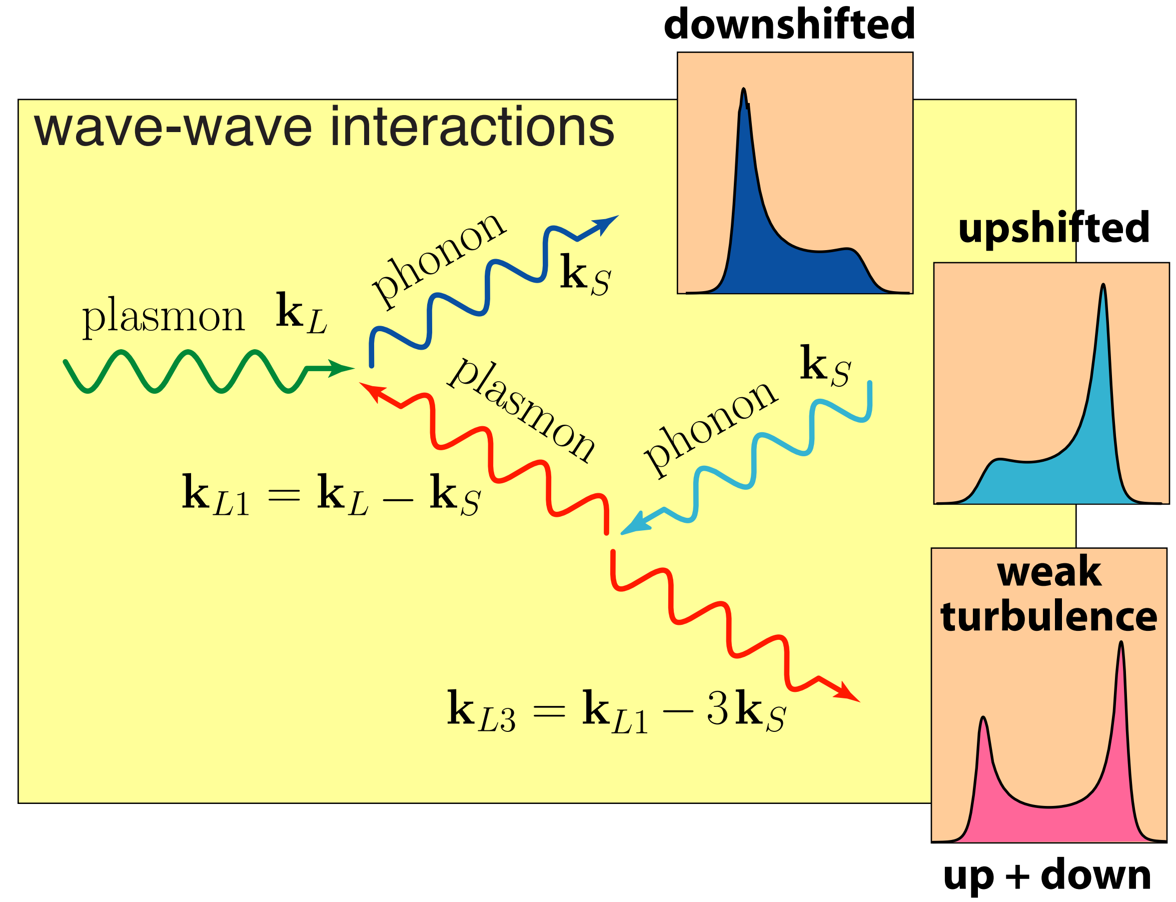

Zakharov equations 1-D

Langmuir waves	$i(\partial_t + \gamma^\ell)E + \partial^2_{xx}E = nE$
Ion sound waves	$(\partial^2_{tt} + \gamma^s\partial_t)n - \partial^2_{xx}n = \partial^2_{xx}\|E\|^2$
Damping and growth rates	$\gamma^\ell(k) = \frac{1}{2}\nu_e + \gamma_{Le}(k) - \gamma_b(k)$ $\gamma^s(k) = \gamma_{Li}(k)$
Bump-in-tail growth	$\gamma_b(k) = \frac{\chi}{\tau}\frac{\pi}{2n}\frac{\omega^3_{pe}}{k^2}\partial_v F_b(v)\Big\|_{v=\omega_{pe}/k}$

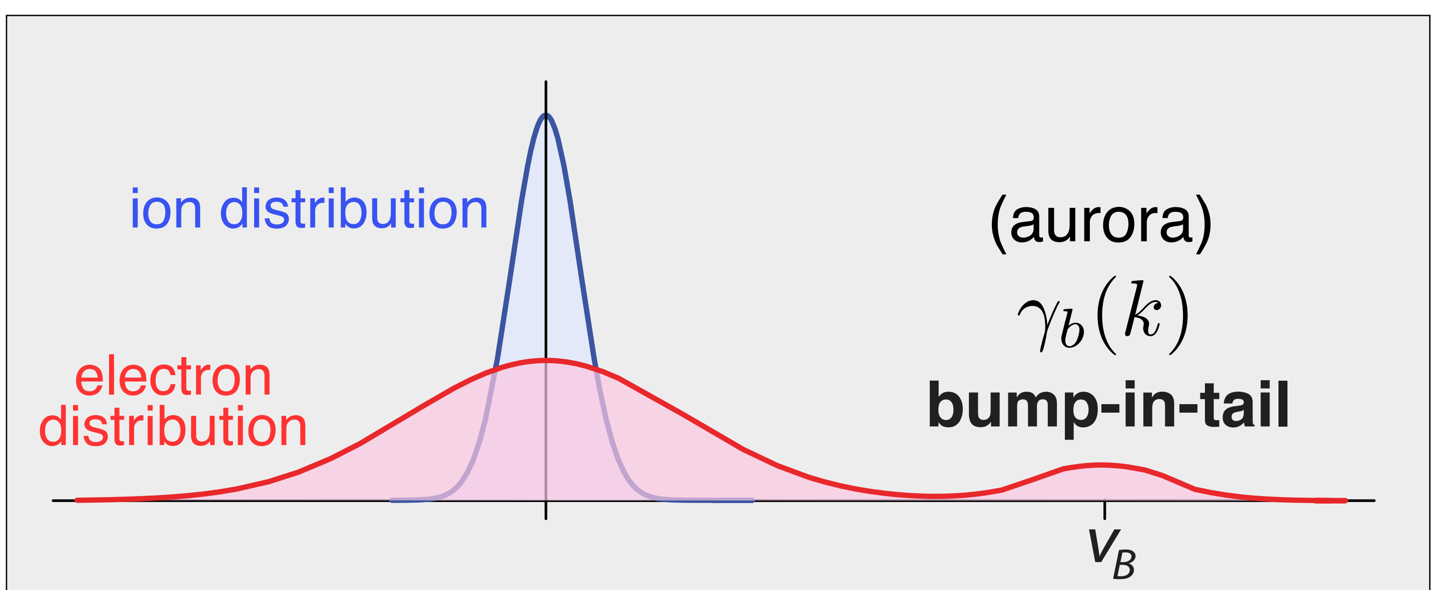

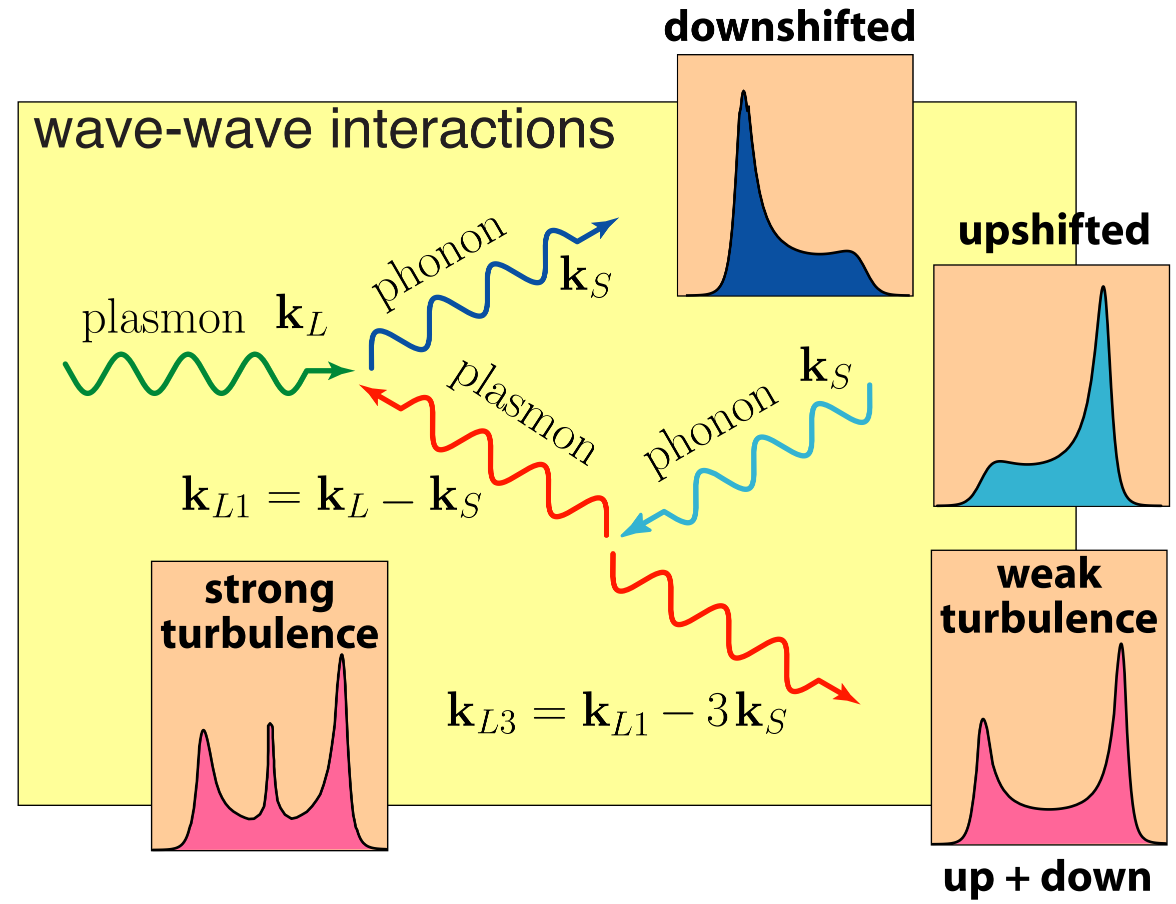

Zakharov equations 1-D

Langmuir waves
$$i(\partial_t + \gamma^\ell)E + \partial_{xx}^2 E = nE$$

Ion sound waves
$$(\partial_{tt}^2 + \gamma^s\partial_t)n - \partial_{xx}^2 n = \partial_{xx}^2 |E|^2$$

Damping and growth rates
$$\gamma^\ell(k) = \frac{1}{2}\nu_e + \gamma_{Le}(k) - \gamma_b(k)$$
$$\gamma^s(k) = \gamma_{Li}(k)$$

Bump-in-tail growth
$$\gamma_b(k) = \frac{\chi}{\tau}\frac{\pi}{2n}\frac{\omega_{pe}^3}{k^2}\partial_v F_b(v)\Big|_{v=\omega_{pe}/k}$$

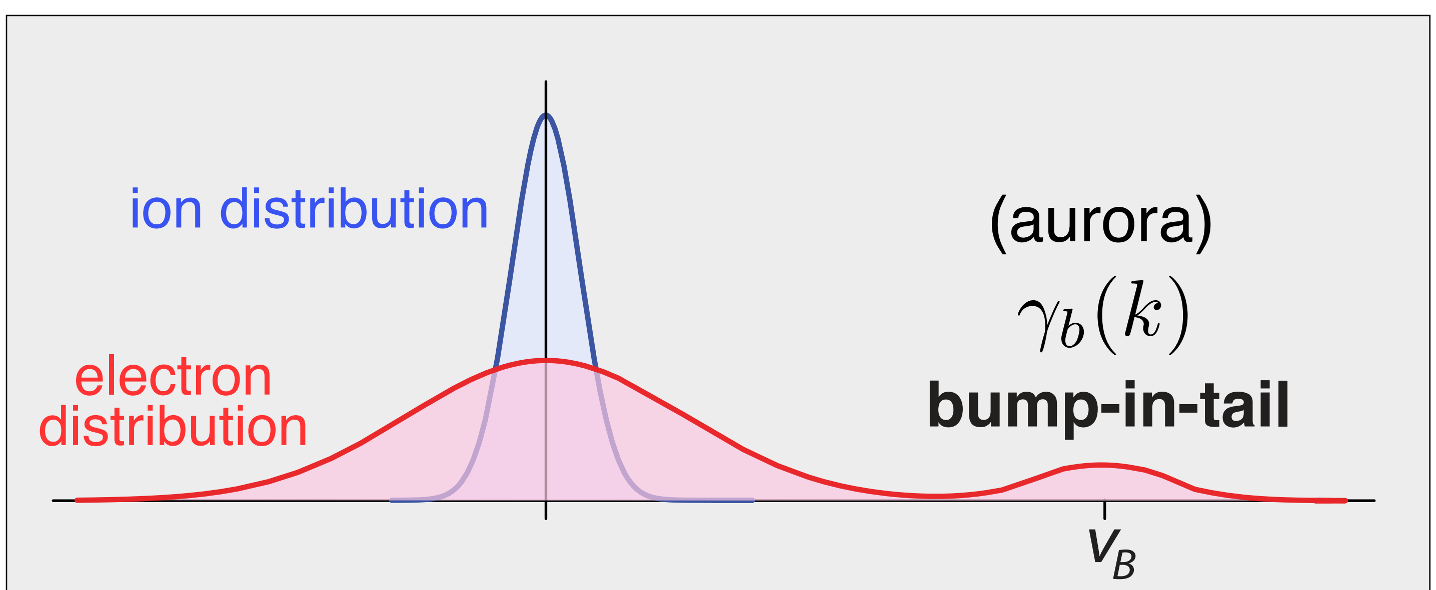

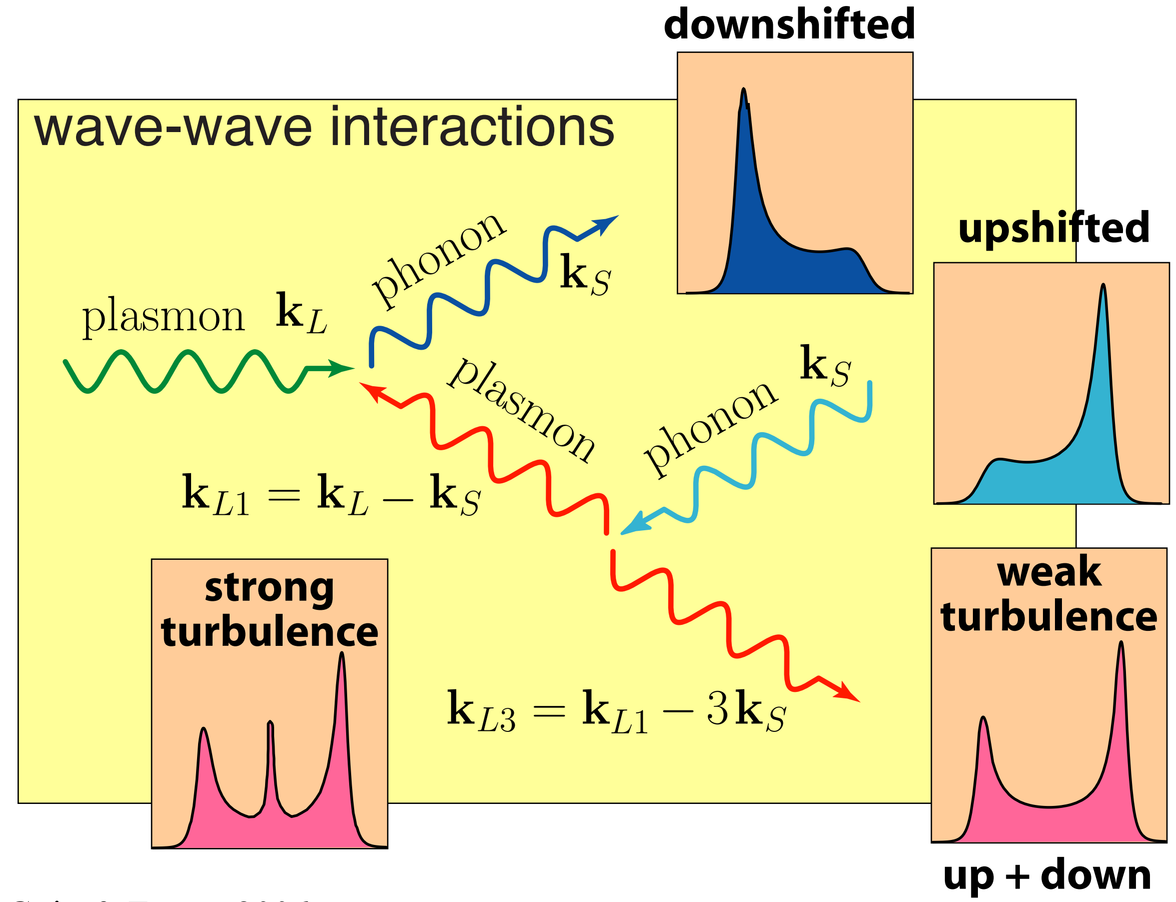

Guio & Forme 2006

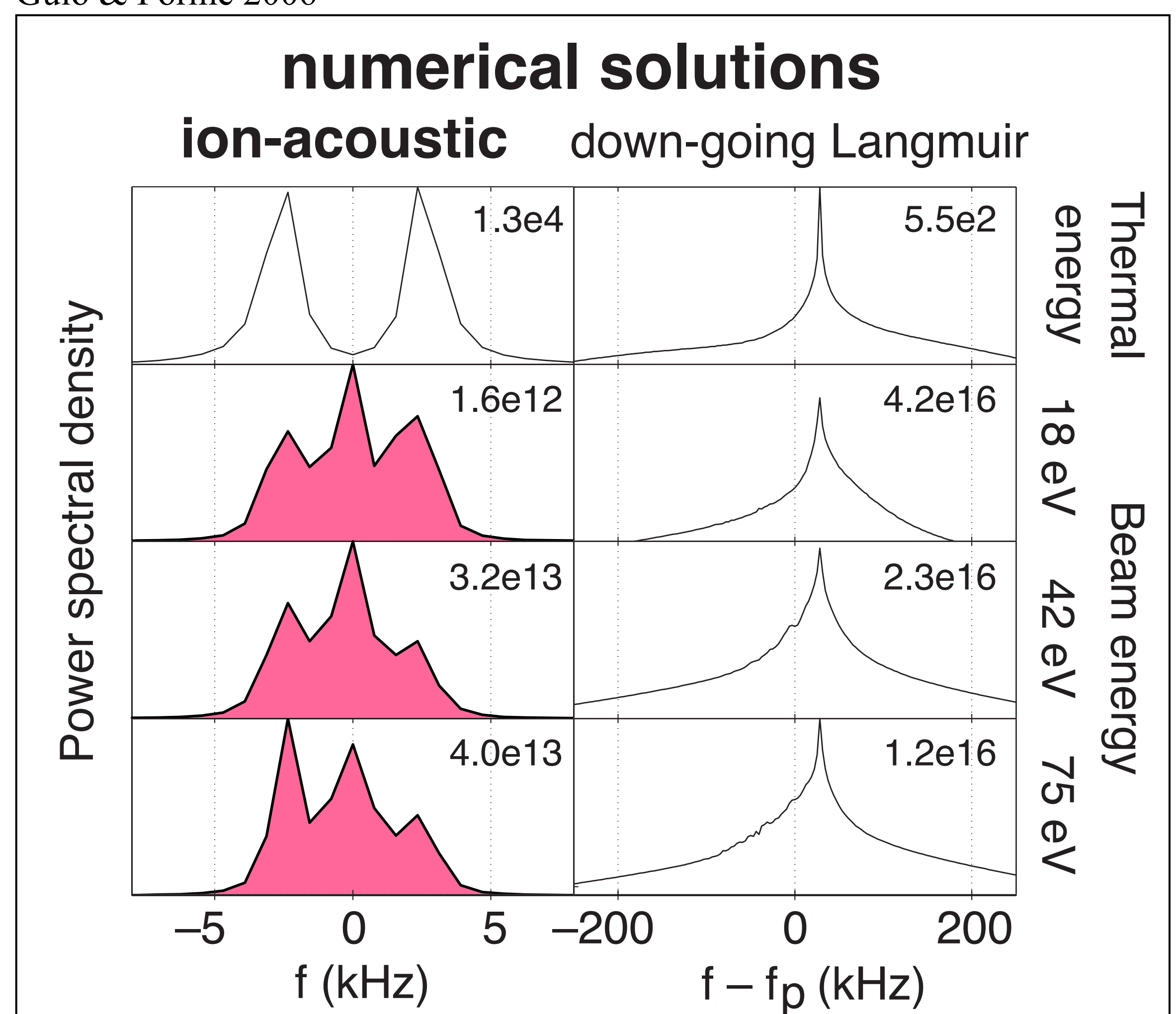

3. Polar Mesospheric Summer Echoes PMSE

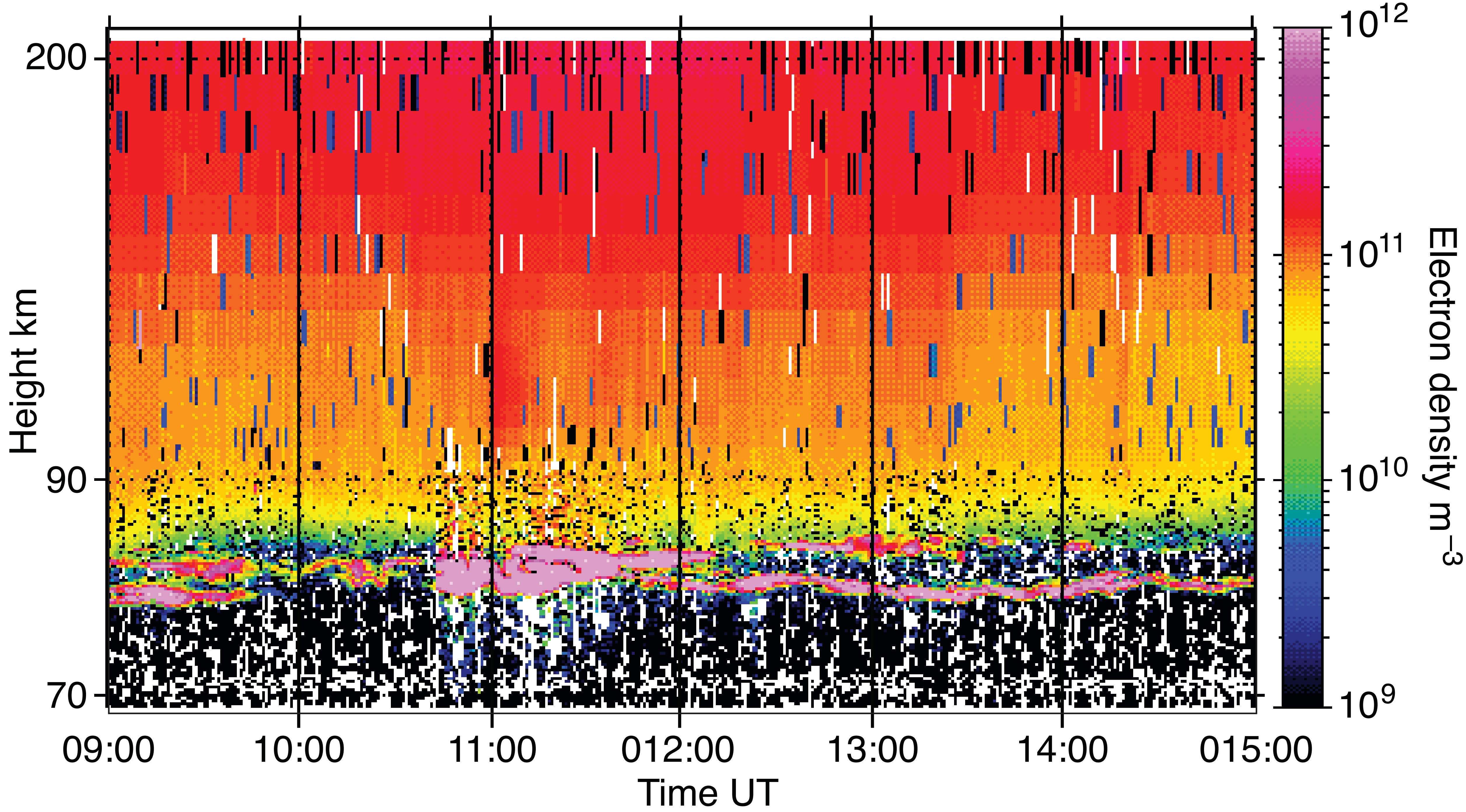

3. Polar Mesospheric Summer Echoes PMSE

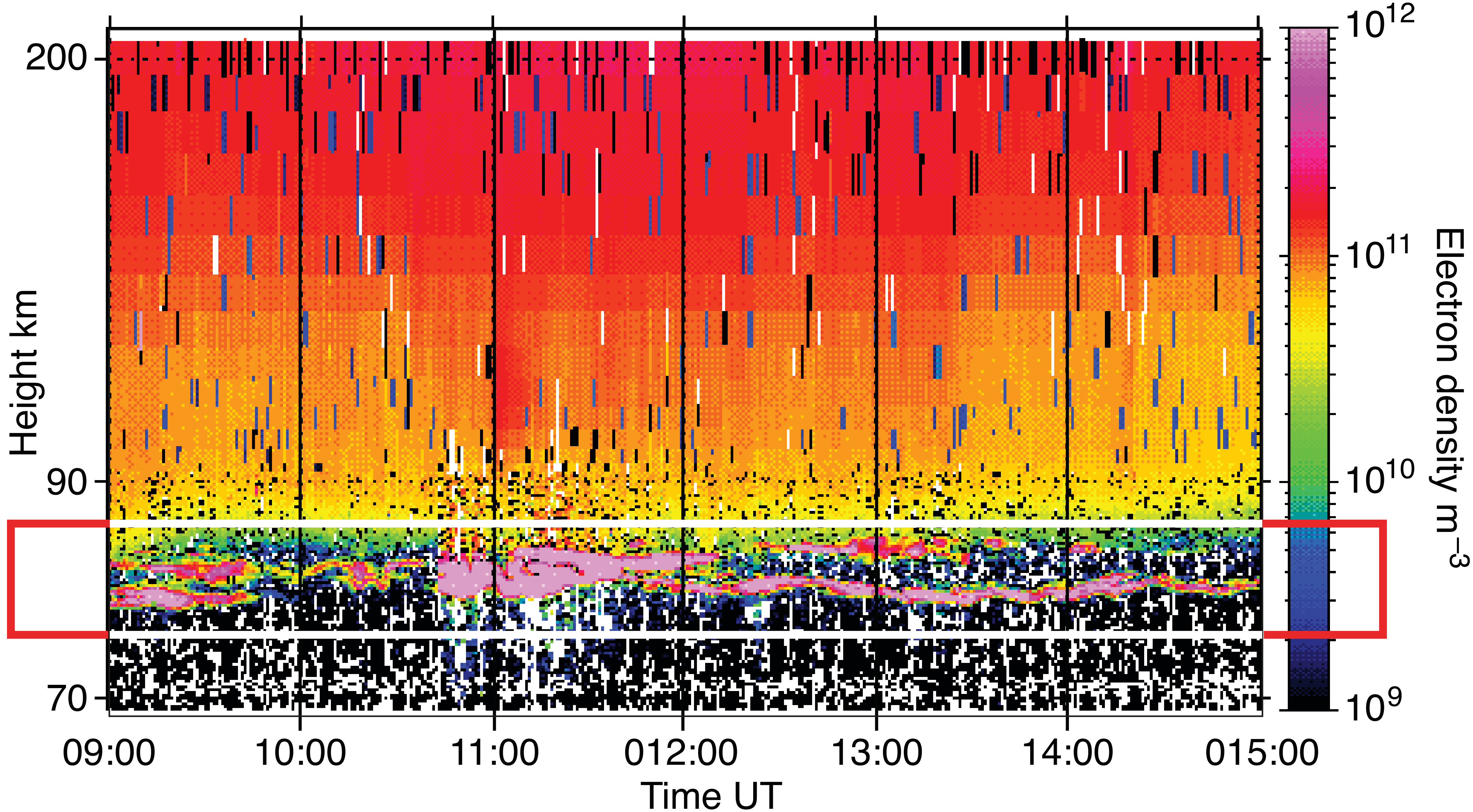

3. Polar Mesospheric Summer Echoes PMSE

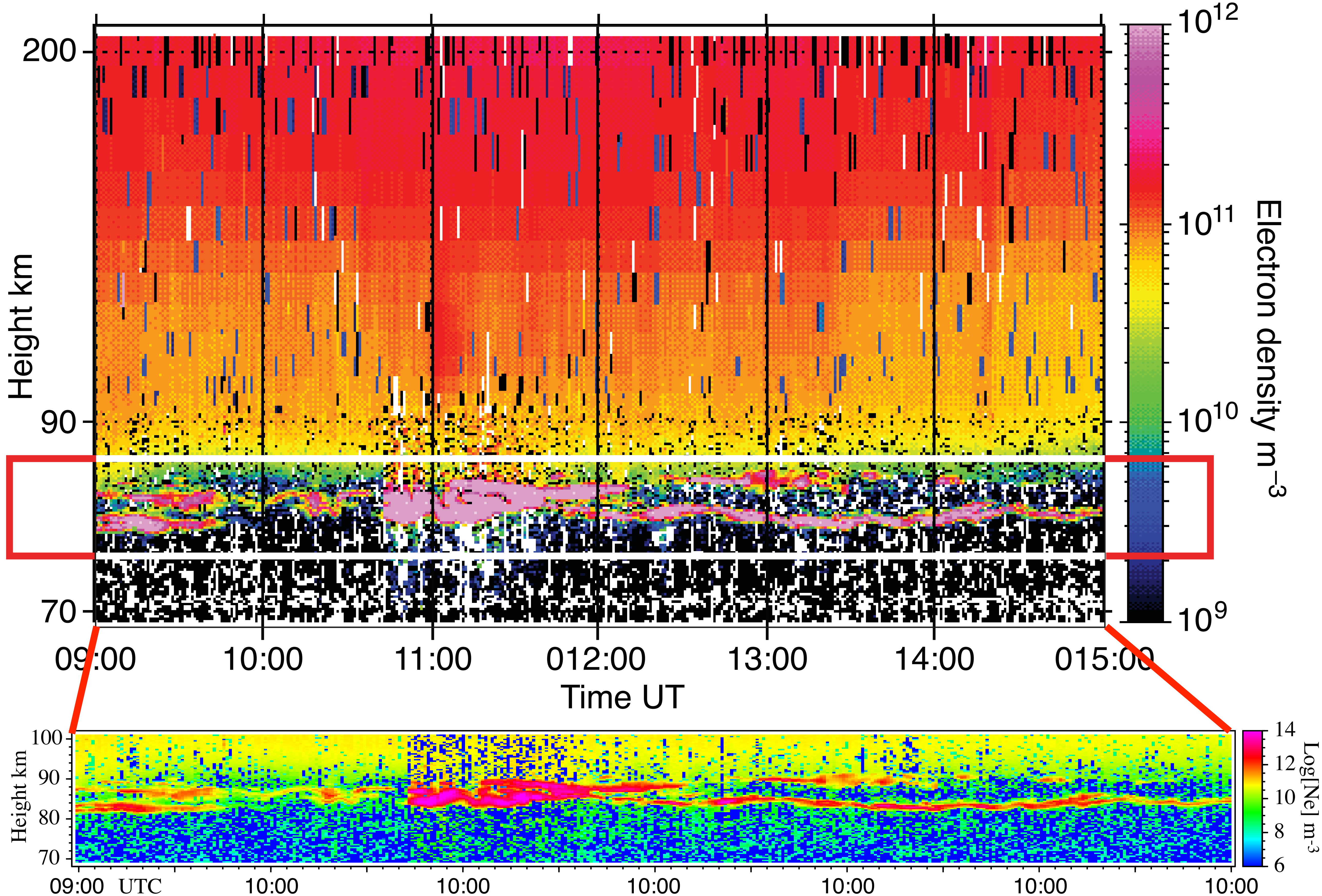

3. Polar Mesospheric Summer Echoes PMSE

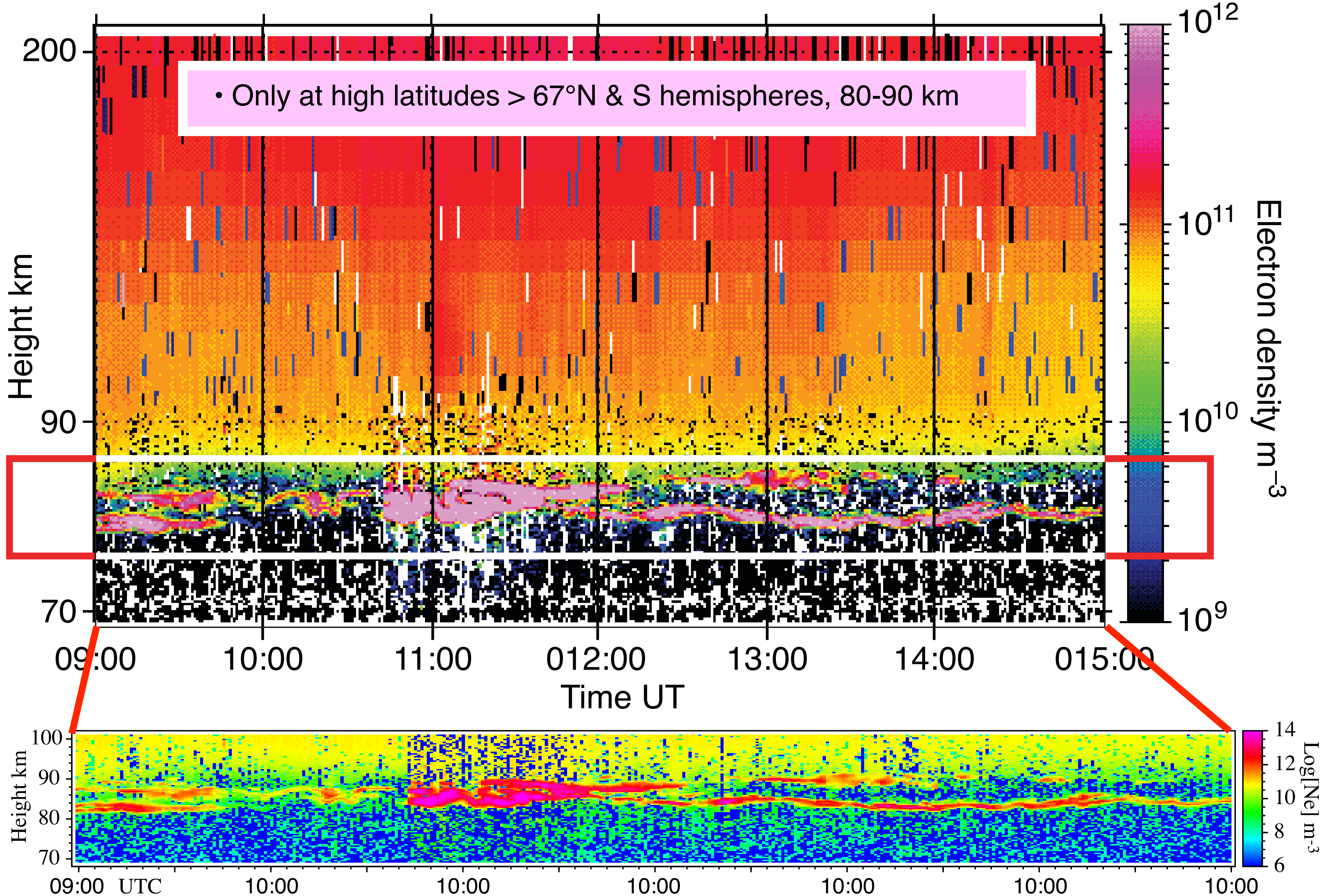

3. Polar Mesospheric Summer Echoes PMSE

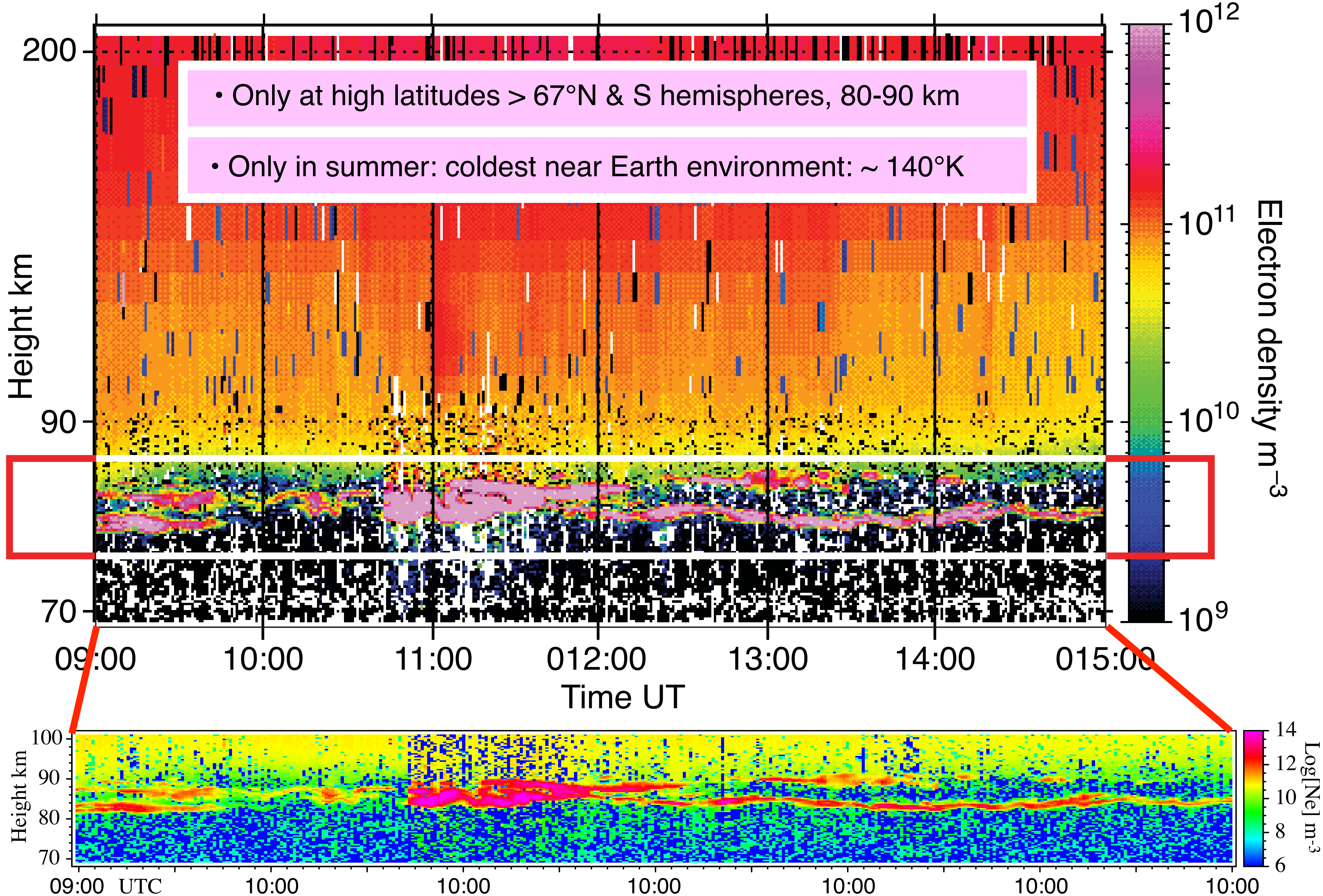

3. Polar Mesospheric Summer Echoes PMSE

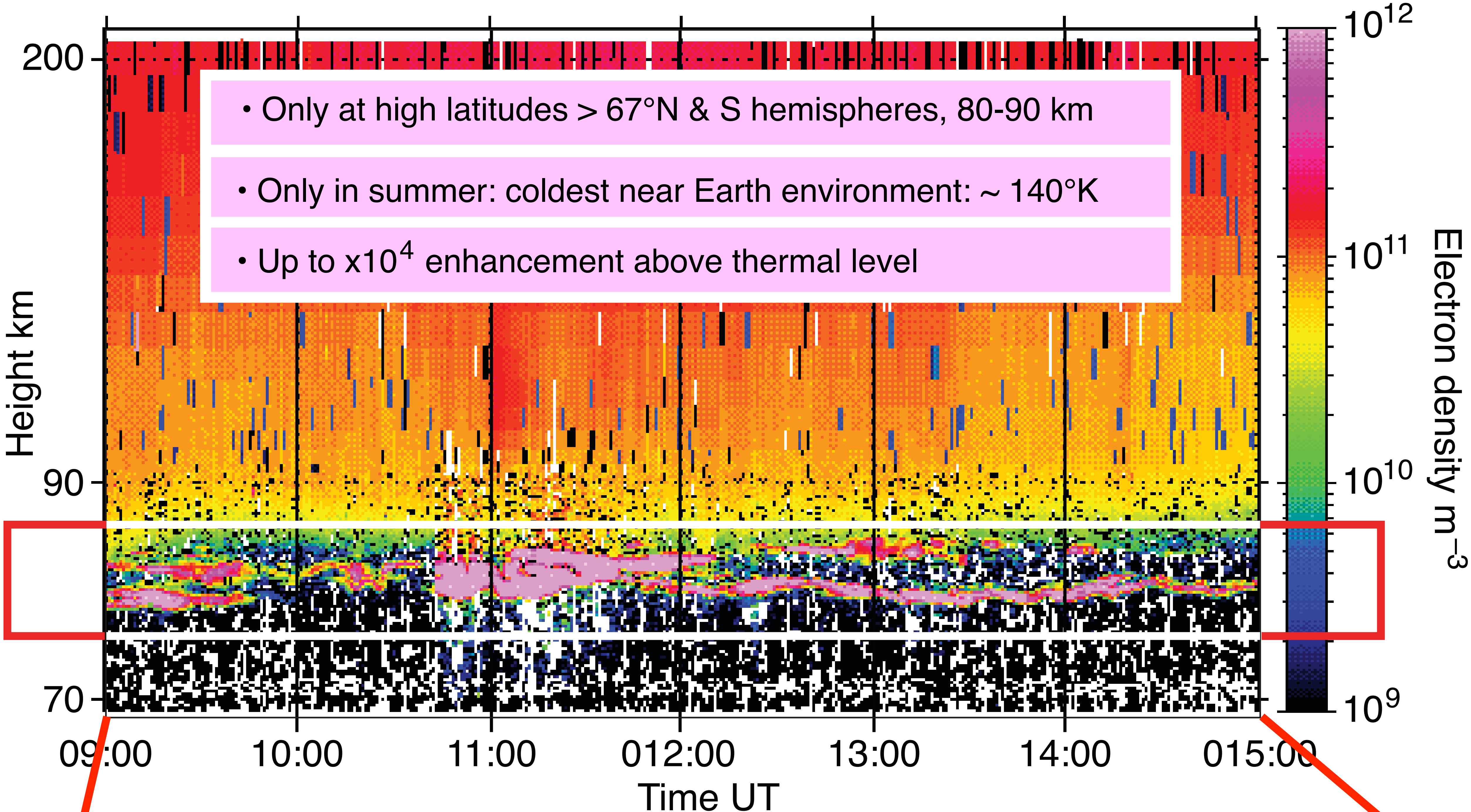

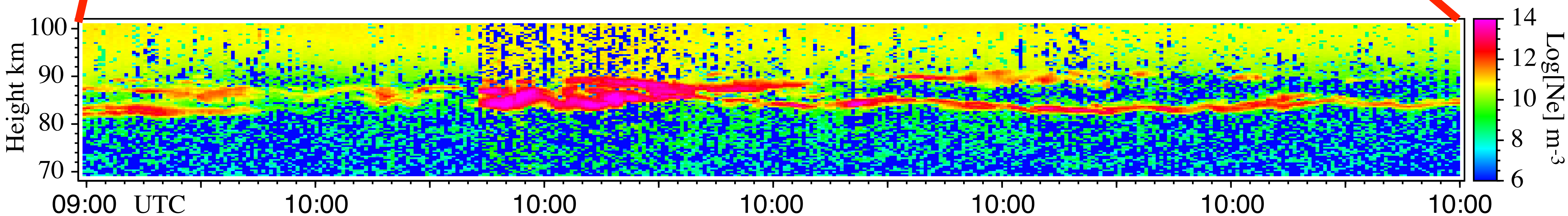

3. Polar Mesospheric Summer Echoes PMSE

- Only at high latitudes > 67°N & S hemispheres, 80-90 km
- Only in summer: coldest near Earth environment: ~ 140°K
- Up to x10^4 enhancement above thermal level
- Only possibility: Neutral air turbulence; Ne is passive scalar

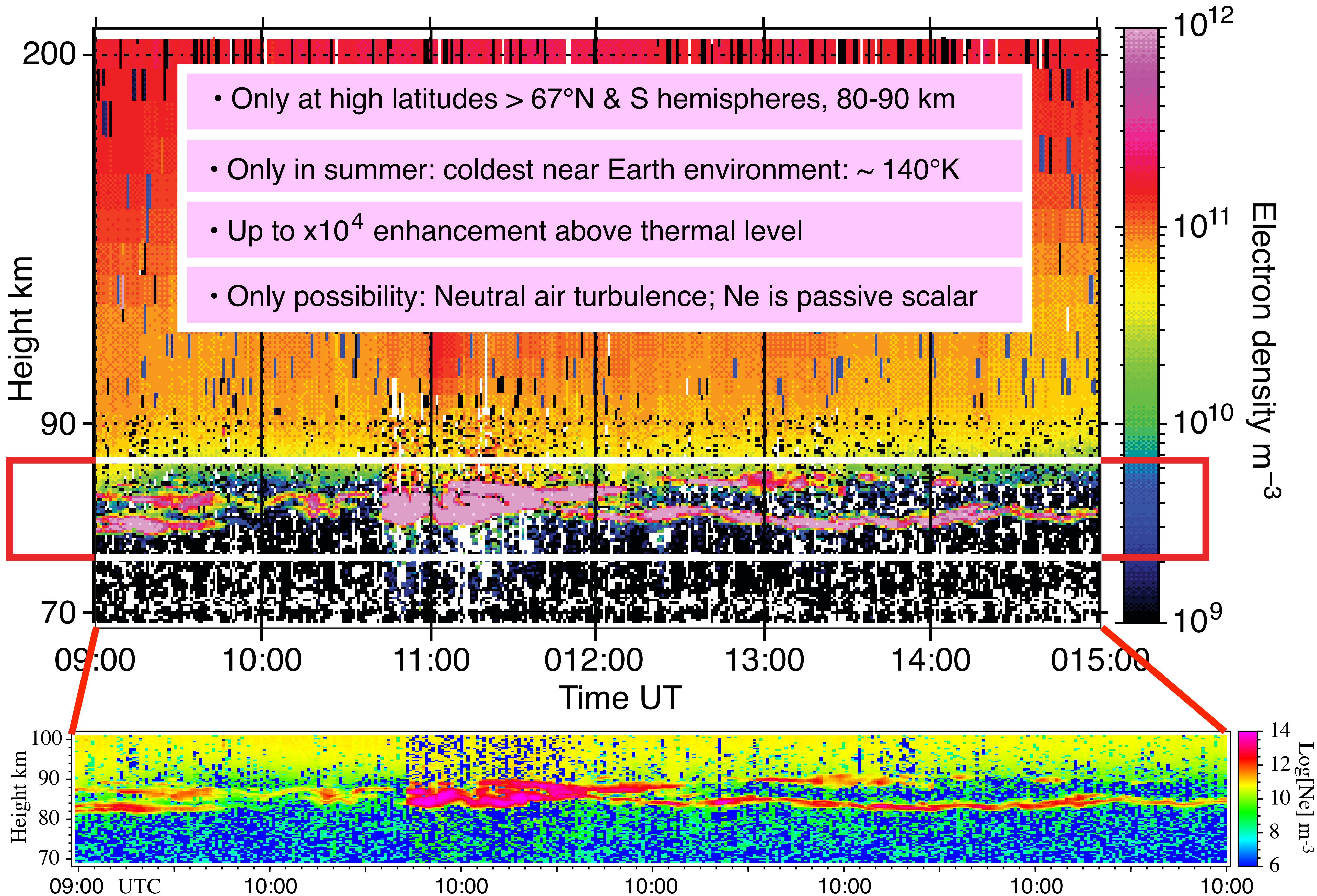

3. Polar Mesospheric Summer Echoes PMSE

- Only at high latitudes > 67°N & S hemispheres, 80-90 km
- Only in summer: coldest near Earth environment: ~ 140°K
- Up to x10^4 enhancement above thermal level
- Only possibility: Neutral air turbulence; Ne is passive scalar
- Problem: NO fluctuations at radar (Bragg) scale

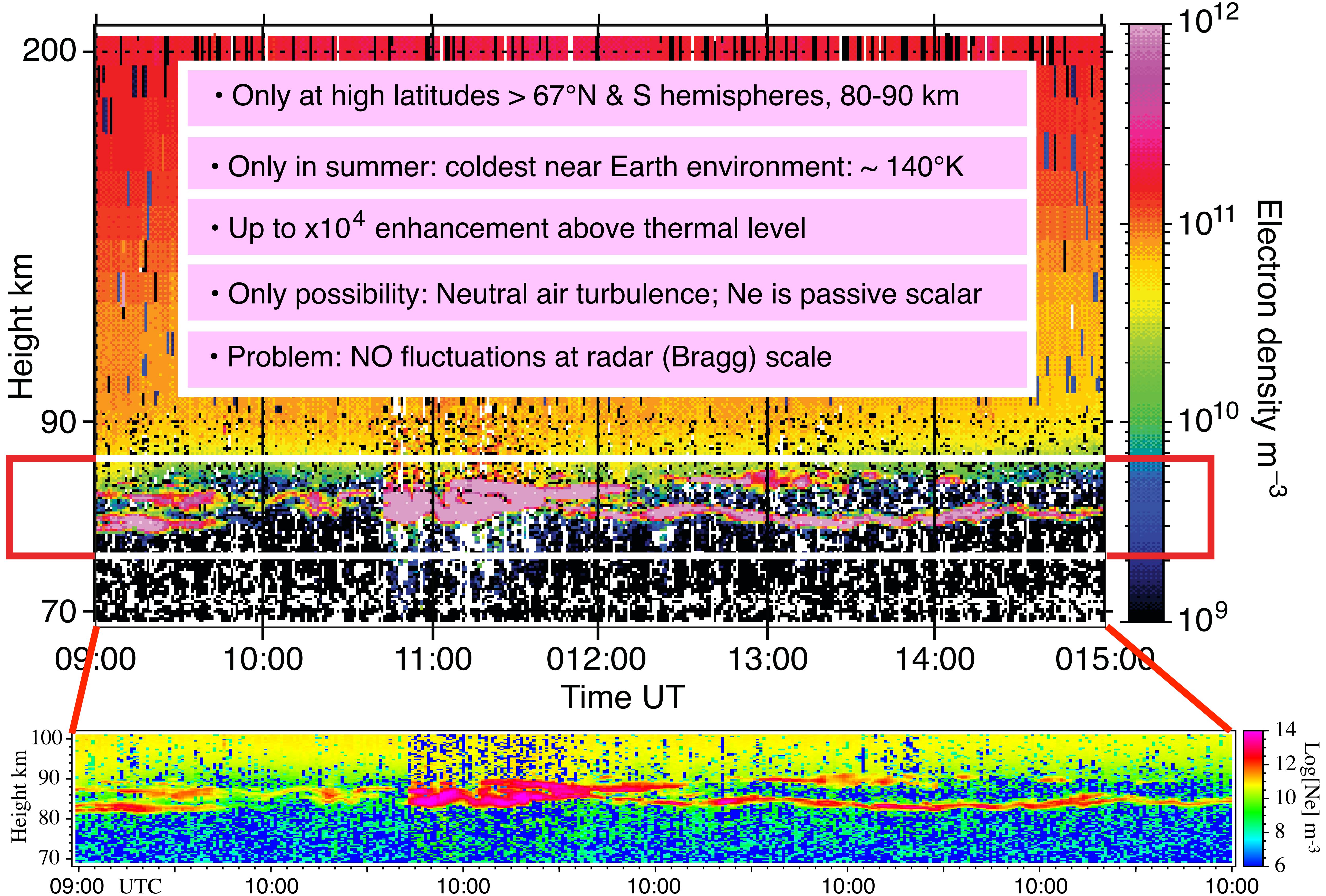

3. Polar Mesospheric Summer Echoes PMSE

- Only at high latitudes > 67°N & S hemispheres, 80-90 km
- Only in summer: coldest near Earth environment: ~ 140°K
- Up to x10^4 enhancement above thermal level
- Only possibility: Neutral air turbulence; Ne is passive scalar
- Problem: NO fluctuations at radar (Bragg) scale
- Solution: Charged ice extends electron scale: Sc number

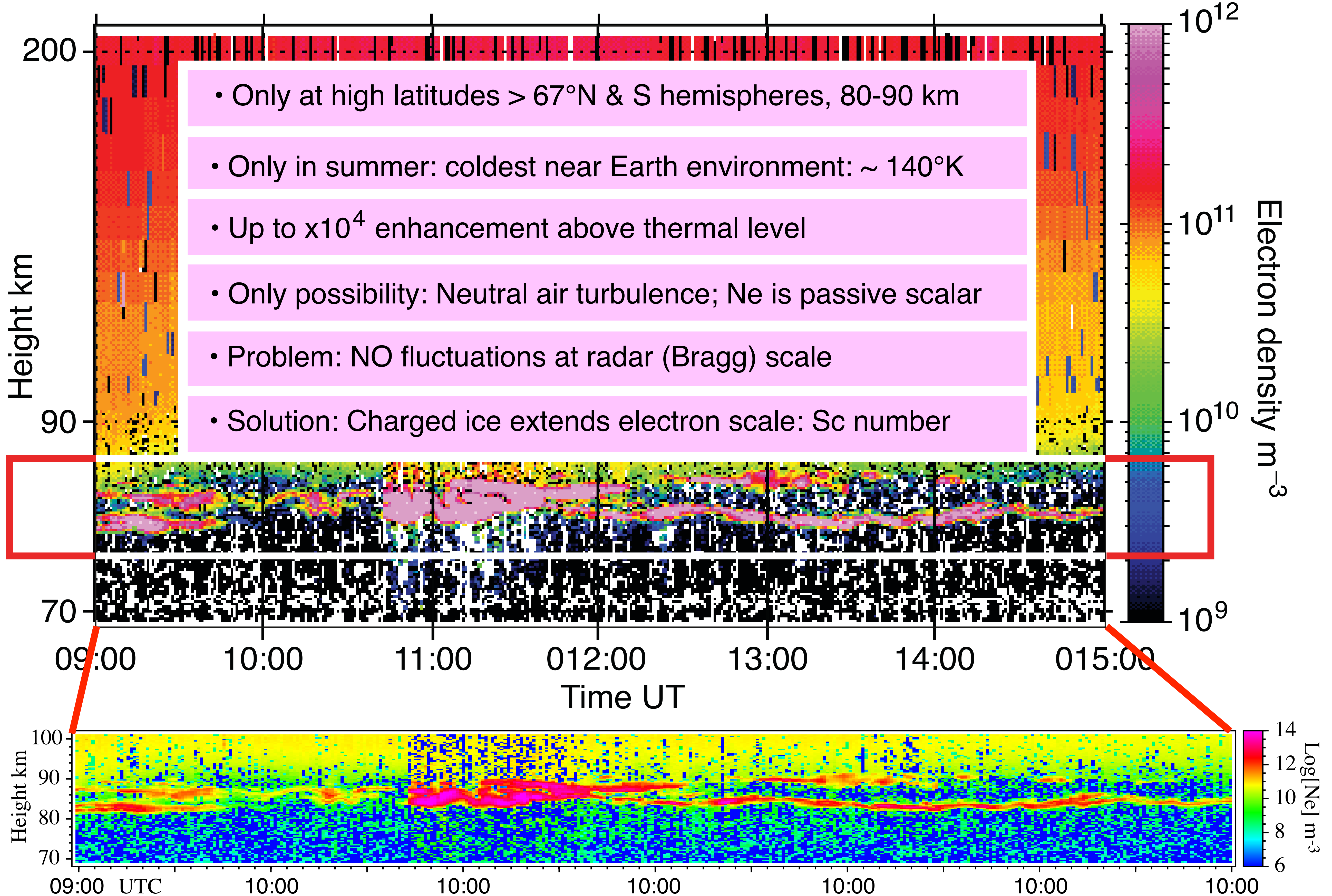

3. Polar Mesospheric Summer Echoes PMSE

- Only at high latitudes > 67°N & S hemispheres, 80-90 km
- Only in summer: coldest near Earth environment: ~ 140°K
- Up to x10^4 enhancement above thermal level
- Only possibility: Neutral air turbulence; Ne is passive scalar
- Problem: NO fluctuations at radar (Bragg) scale
- Solution: Charged ice extends electron scale: Sc number
- Gravity waves reverse GLOBAL wind circulation

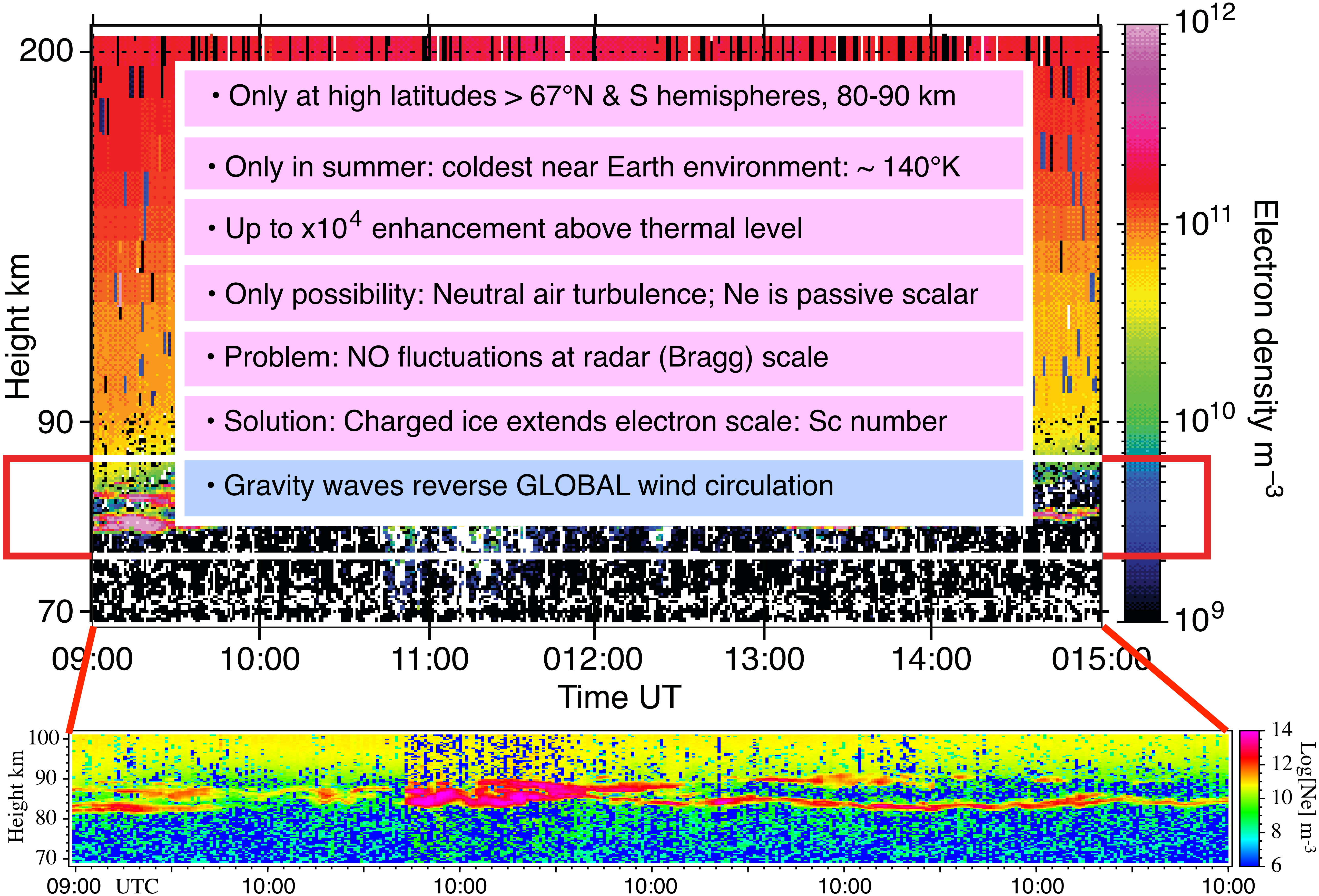

3. Polar Mesospheric Summer Echoes PMSE

- Only at high latitudes > 67°N & S hemispheres, 80-90 km
- Only in summer: coldest near Earth environment: ~ 140°K
- Up to x10^4 enhancement above thermal level
- Only possibility: Neutral air turbulence; Ne is passive scalar
- Problem: NO fluctuations at radar (Bragg) scale
- Solution: Charged ice extends electron scale: Sc number
- Gravity waves reverse GLOBAL wind circulation
- Polar mesosphere is a refrigerator due to adiabatic cooling

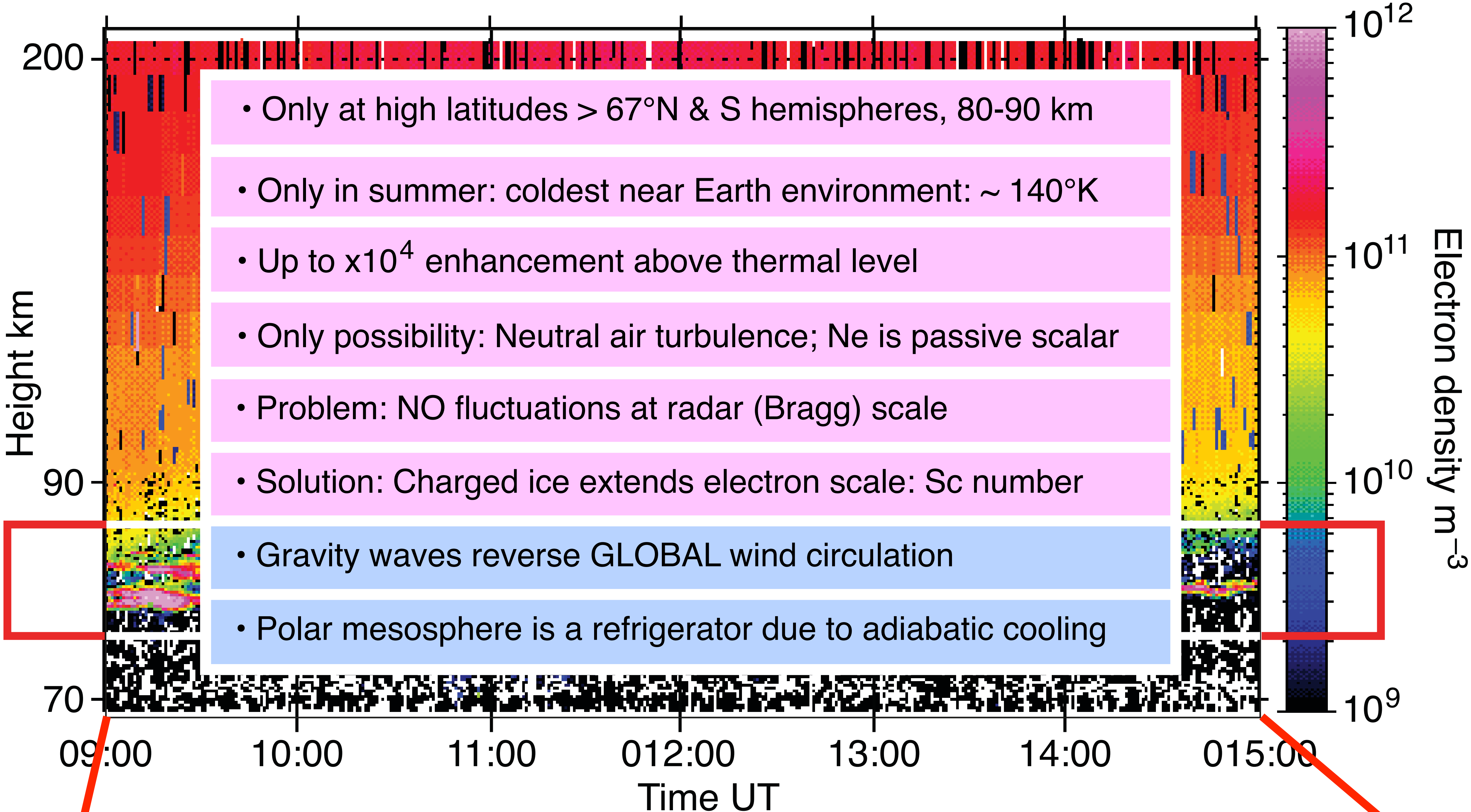

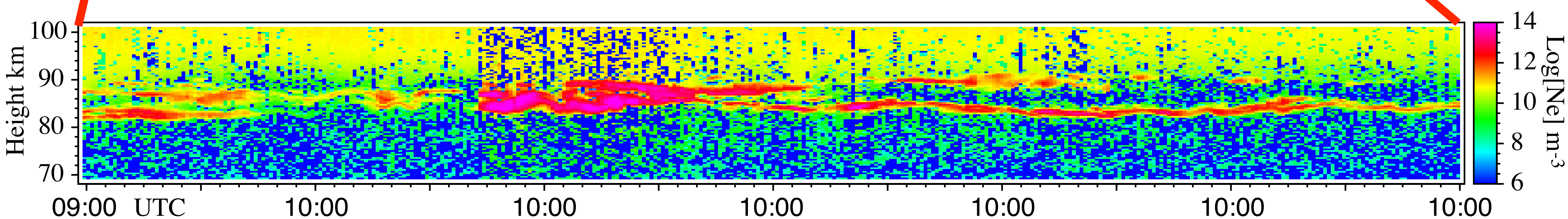

3. Polar Mesospheric Summer Echoes PMSE

- Only at high latitudes > 67°N & S hemispheres, 80-90 km
- Only in summer: coldest near Earth environment: ~ 140°K
- Up to x10^4 enhancement above thermal level
- Only possibility: Neutral air turbulence; Ne is passive scalar
- Problem: NO fluctuations at radar (Bragg) scale
- Solution: Charged ice extends electron scale: Sc number
- Gravity waves reverse GLOBAL wind circulation
- Polar mesosphere is a refrigerator due to adiabatic cooling
- 10-50 nm ice particles form: Noctilucent clouds

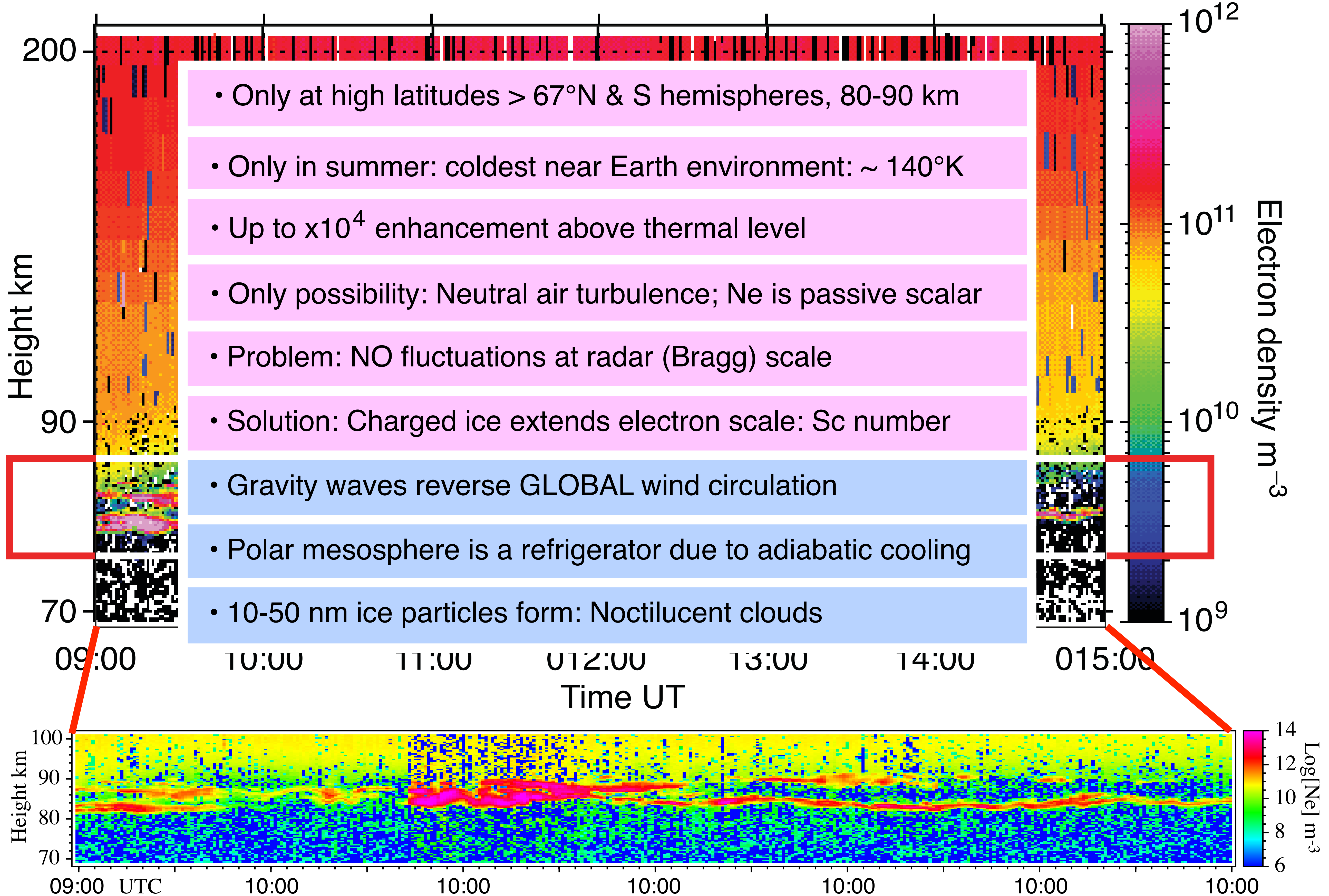

3. Polar Mesospheric Summer Echoes PMSE

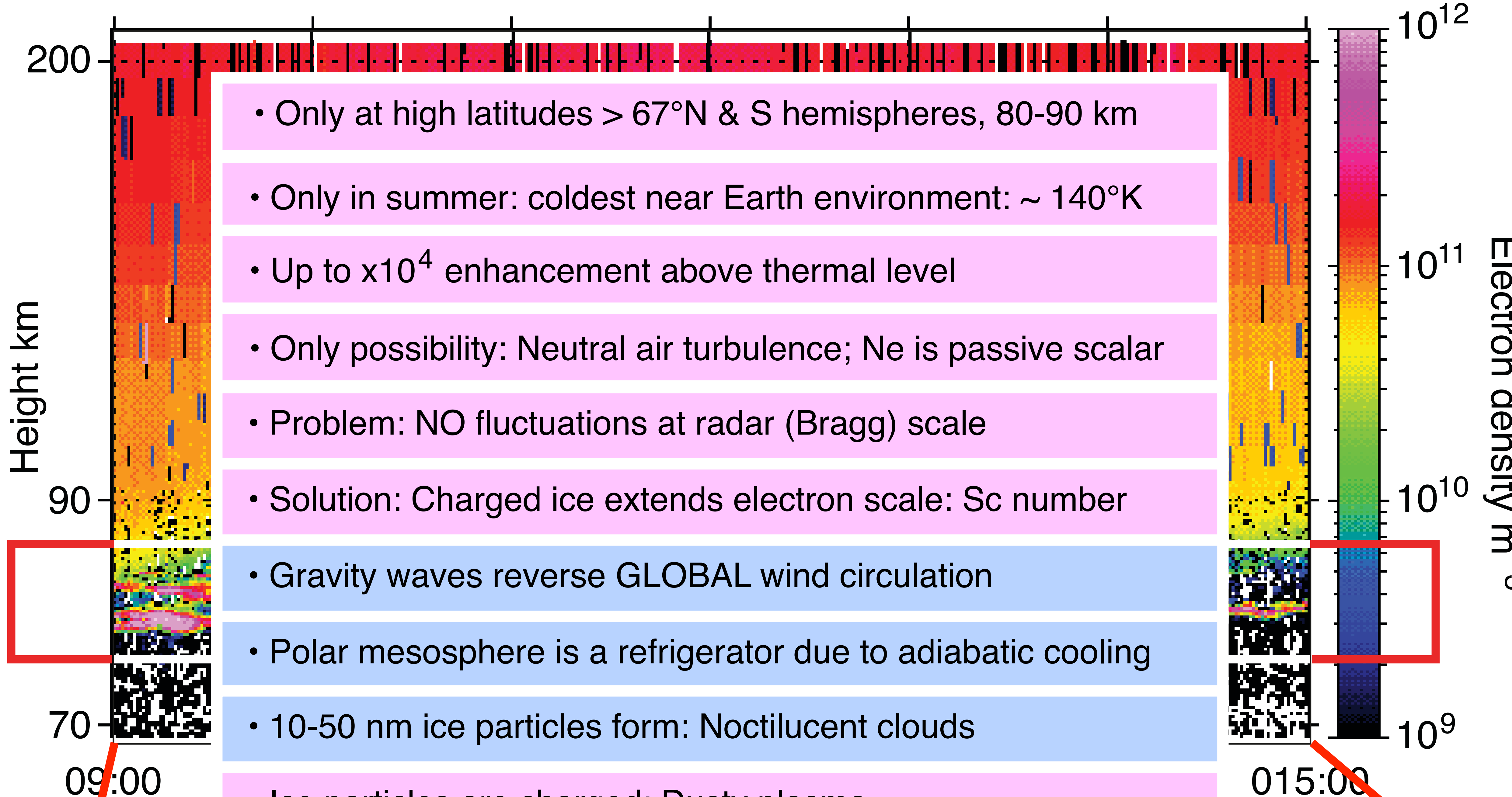

- Only at high latitudes > 67°N & S hemispheres, 80-90 km
- Only in summer: coldest near Earth environment: ~ 140°K
- Up to x10^4 enhancement above thermal level
- Only possibility: Neutral air turbulence; Ne is passive scalar
- Problem: NO fluctuations at radar (Bragg) scale
- Solution: Charged ice extends electron scale: Sc number
- Gravity waves reverse GLOBAL wind circulation
- Polar mesosphere is a refrigerator due to adiabatic cooling
- 10-50 nm ice particles form: Noctilucent clouds
- Ice particles are charged: Dusty plasma

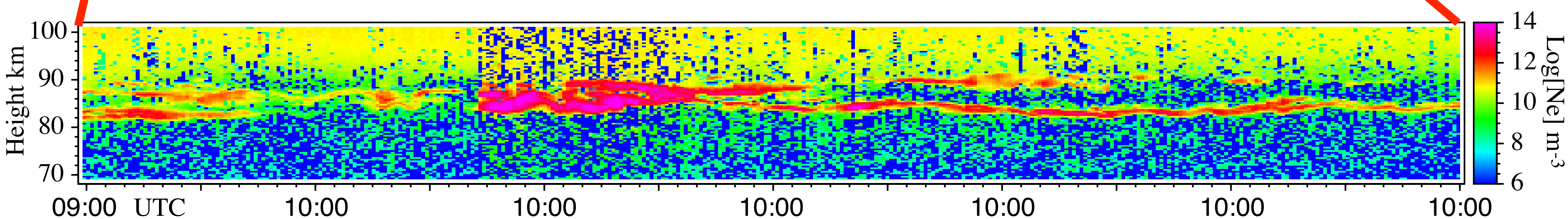

3. Polar Mesospheric Summer Echoes PMSE

- Only at high latitudes > 67°N & S hemispheres, 80-90 km
- Only in summer: coldest near Earth environment: ~ 140°K
- Up to x10^4 enhancement above thermal level
- Only possibility: Neutral air turbulence; Ne is passive scalar
- Problem: NO fluctuations at radar (Bragg) scale
- Solution: Charged ice extends electron scale: Sc number
- Gravity waves reverse GLOBAL wind circulation
- Polar mesosphere is a refrigerator due to adiabatic cooling
- 10-50 nm ice particles form: Noctilucent clouds
- Ice particles are charged: Dusty plasma
- Electron diffusion slowed down by heavy charged ice

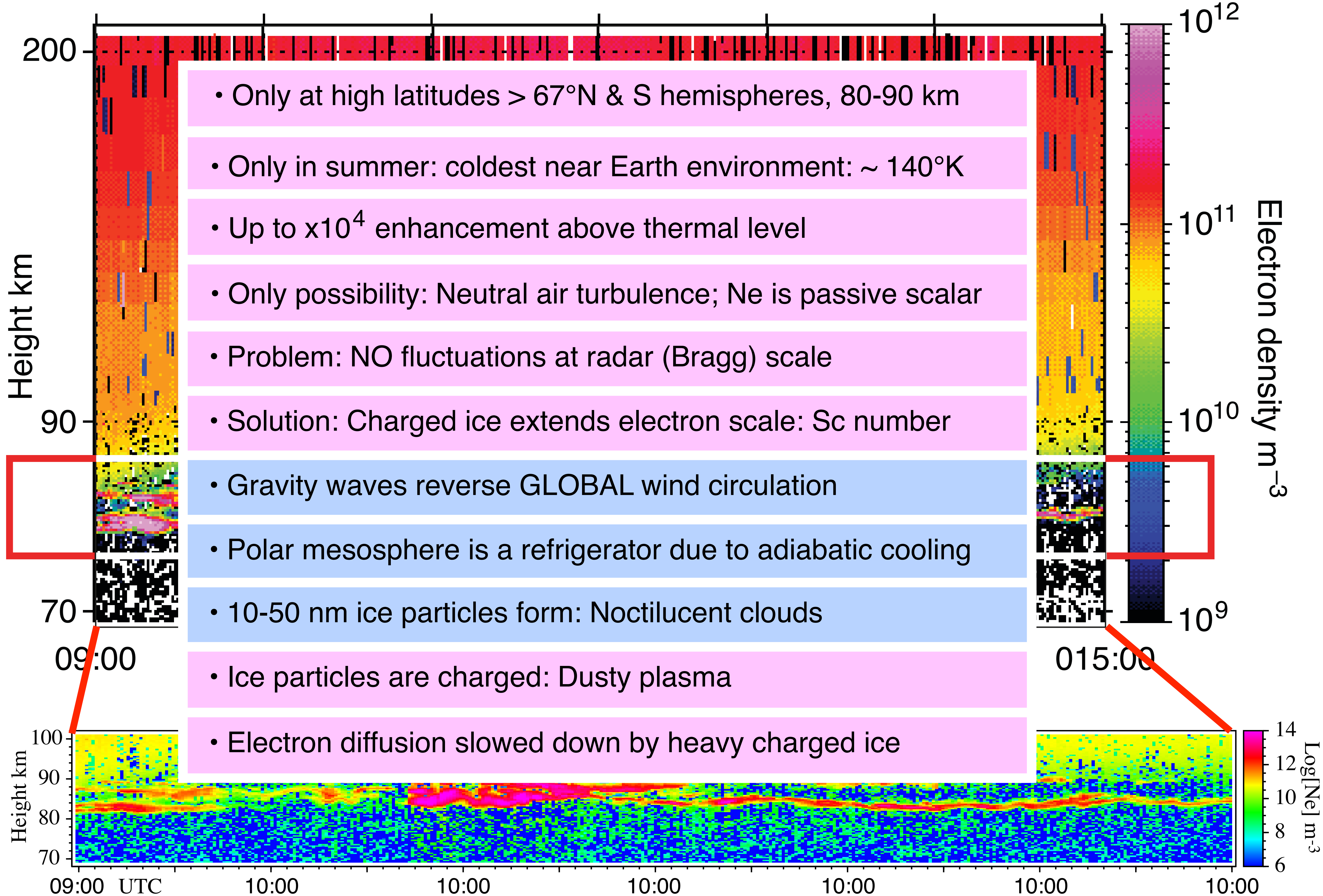

3. Polar Mesospheric Summer Echoes PMSE

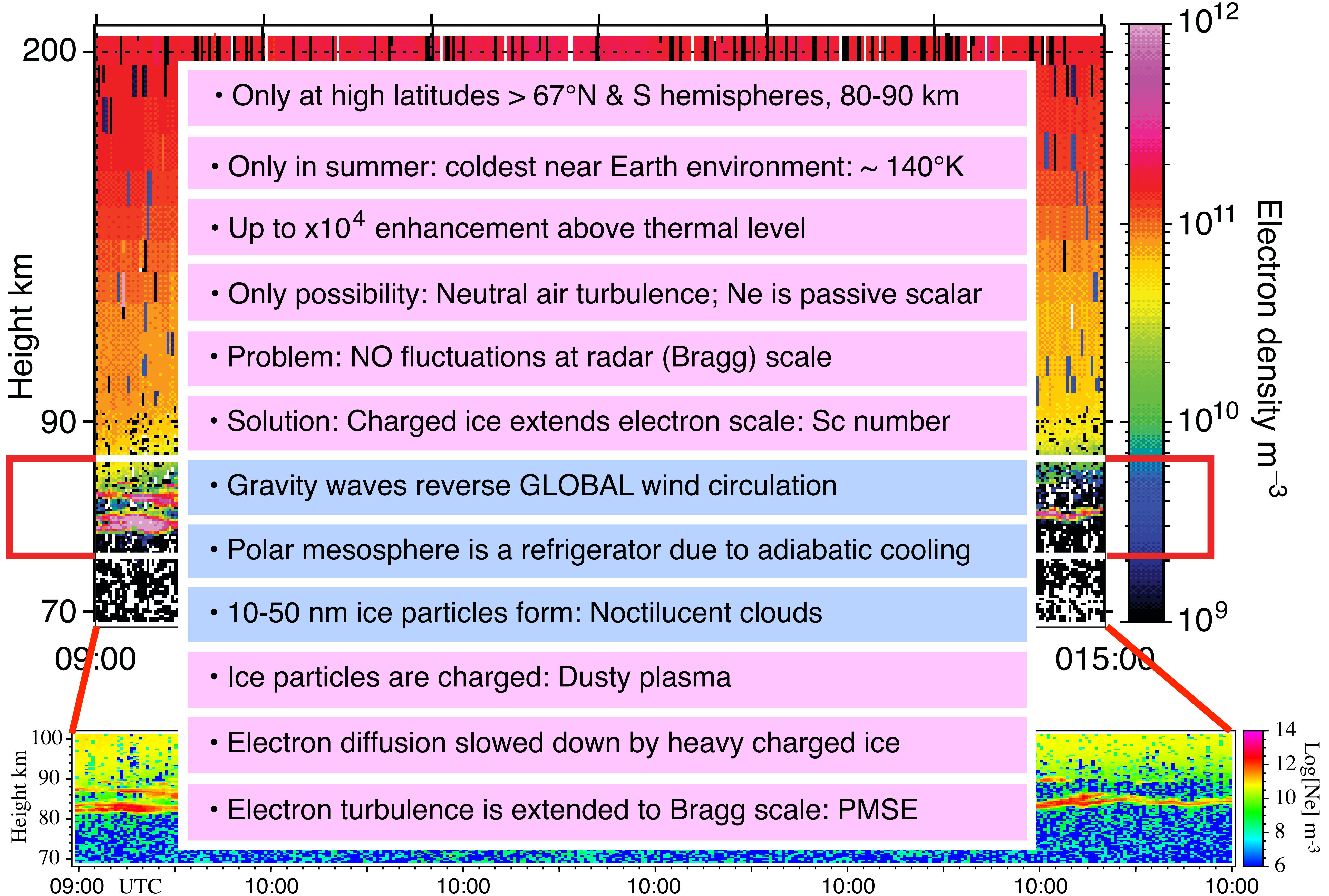

- Only at high latitudes > 67°N & S hemispheres, 80-90 km
- Only in summer: coldest near Earth environment: ~ 140°K
- Up to x10^4 enhancement above thermal level
- Only possibility: Neutral air turbulence; Ne is passive scalar
- Problem: NO fluctuations at radar (Bragg) scale
- Solution: Charged ice extends electron scale: Sc number
- Gravity waves reverse GLOBAL wind circulation
- Polar mesosphere is a refrigerator due to adiabatic cooling
- 10-50 nm ice particles form: Noctilucent clouds
- Ice particles are charged: Dusty plasma
- Electron diffusion slowed down by heavy charged ice
- Electron turbulence is extended to Bragg scale: PMSE

Seasonal Temperatures – Alaska, 71° N

Noctilucent Clouds & PMSE

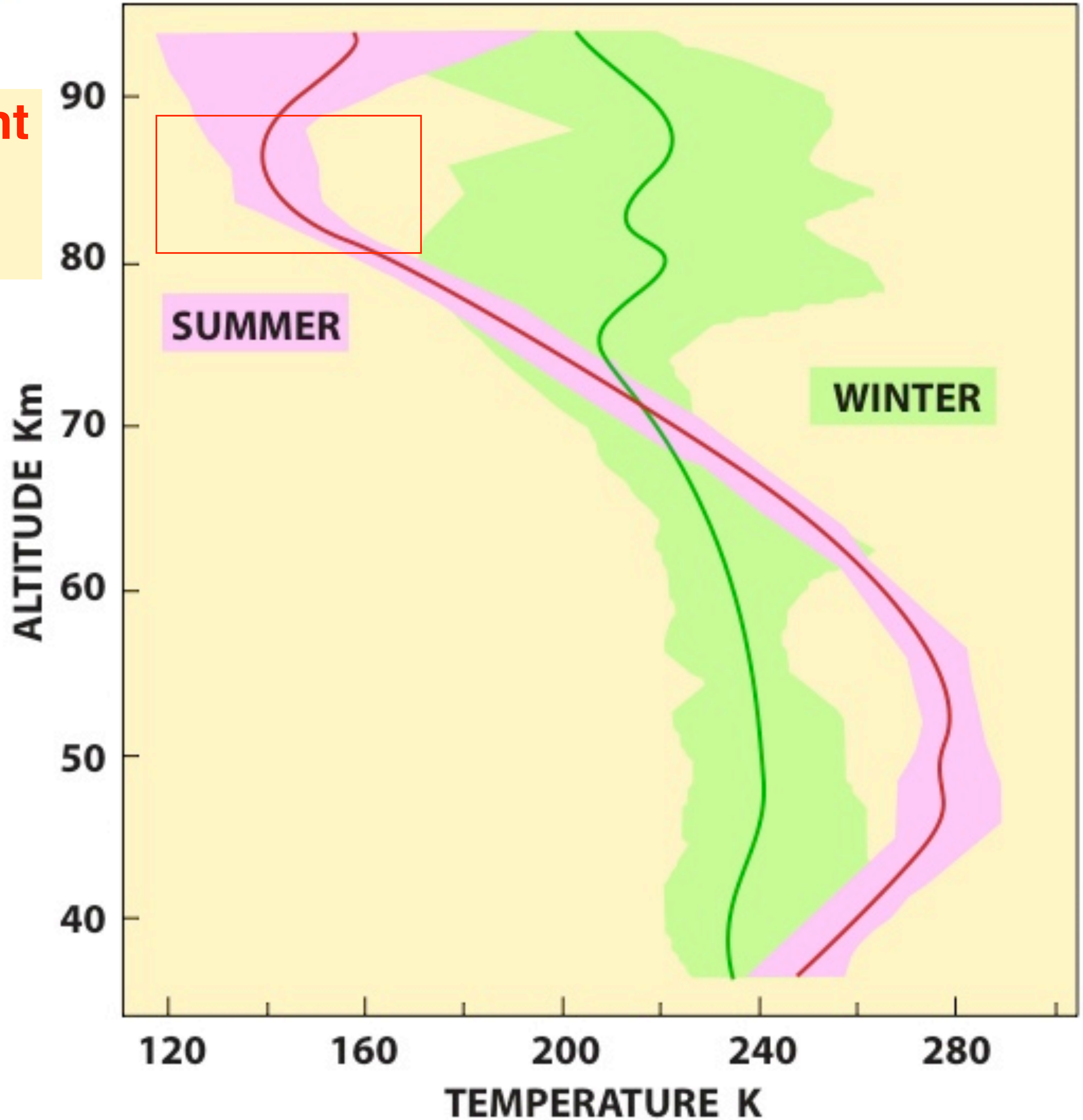

Small Ice Particles

Noctilucent Cloud – 27 Jul 1989 – Turku, Finland

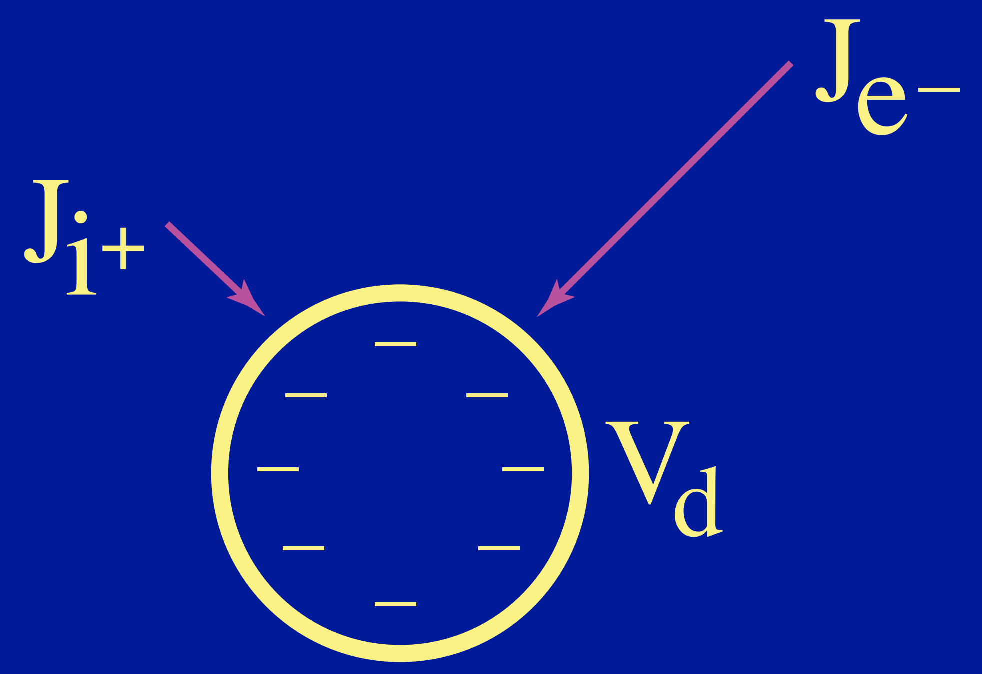

$$J = n\, v_{thermal}$$

$$v_e \gg v_i$$
$$n_e = n_i$$

$$J_e \gg J_i$$

$$J_{i^+} + J_{e^-} = 0 \Rightarrow V_d \neq 0$$

The mesosphere has free electrons and ions:
thermal current equilibrium results in negative charge on the dust particles

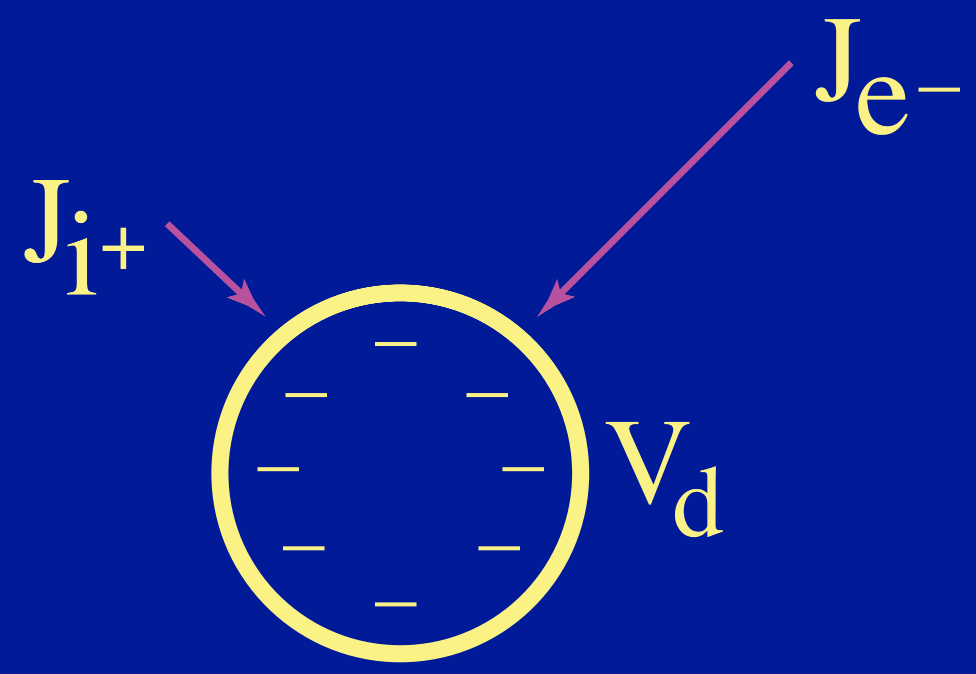

$$J = n\, v_{thermal} \qquad \begin{matrix} v_e \gg v_i \\ n_e = n_i \end{matrix} \qquad J_e \gg J_i$$

$$J_{i^+} + J_{e^-} = 0 \Rightarrow V_d \neq 0$$

The mesosphere has free electrons and ions:
thermal current equilibrium results in negative charge on the dust particles

---

Electrons diffuse with the mass of the dust due to Coulomb force

PMSE Doppler spectra: velocity variance

Electron velocity fluctuations can be induced by air turbulence

EISCAT VHF 13 July 2004

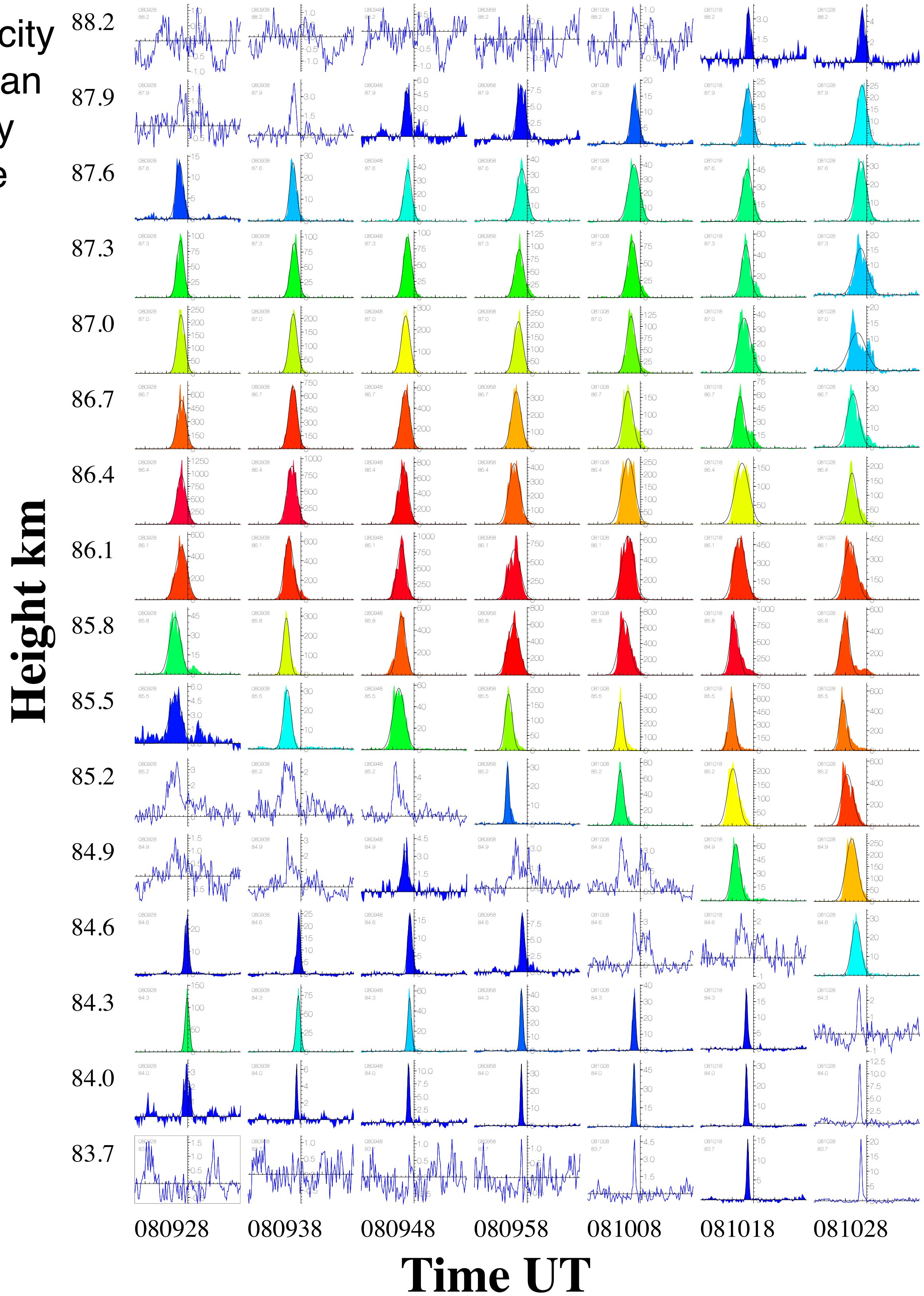

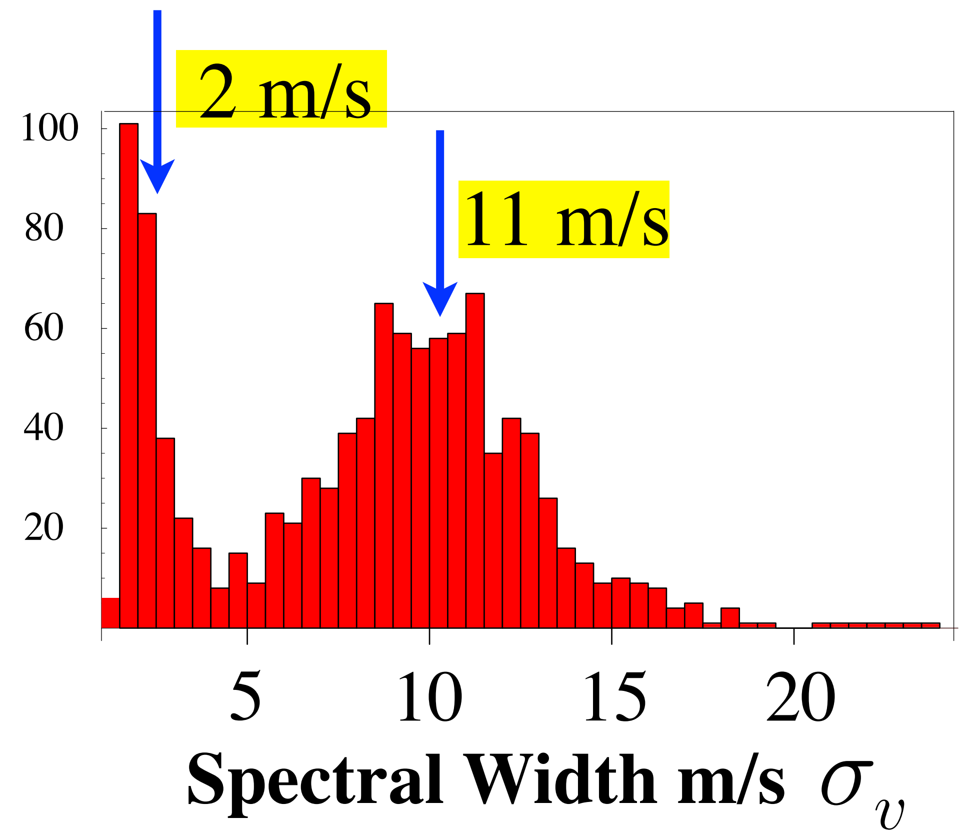

PMSE Doppler spectra: velocity variance

Electron velocity fluctuations can be induced by air turbulence

EISCAT VHF 13 July 2004

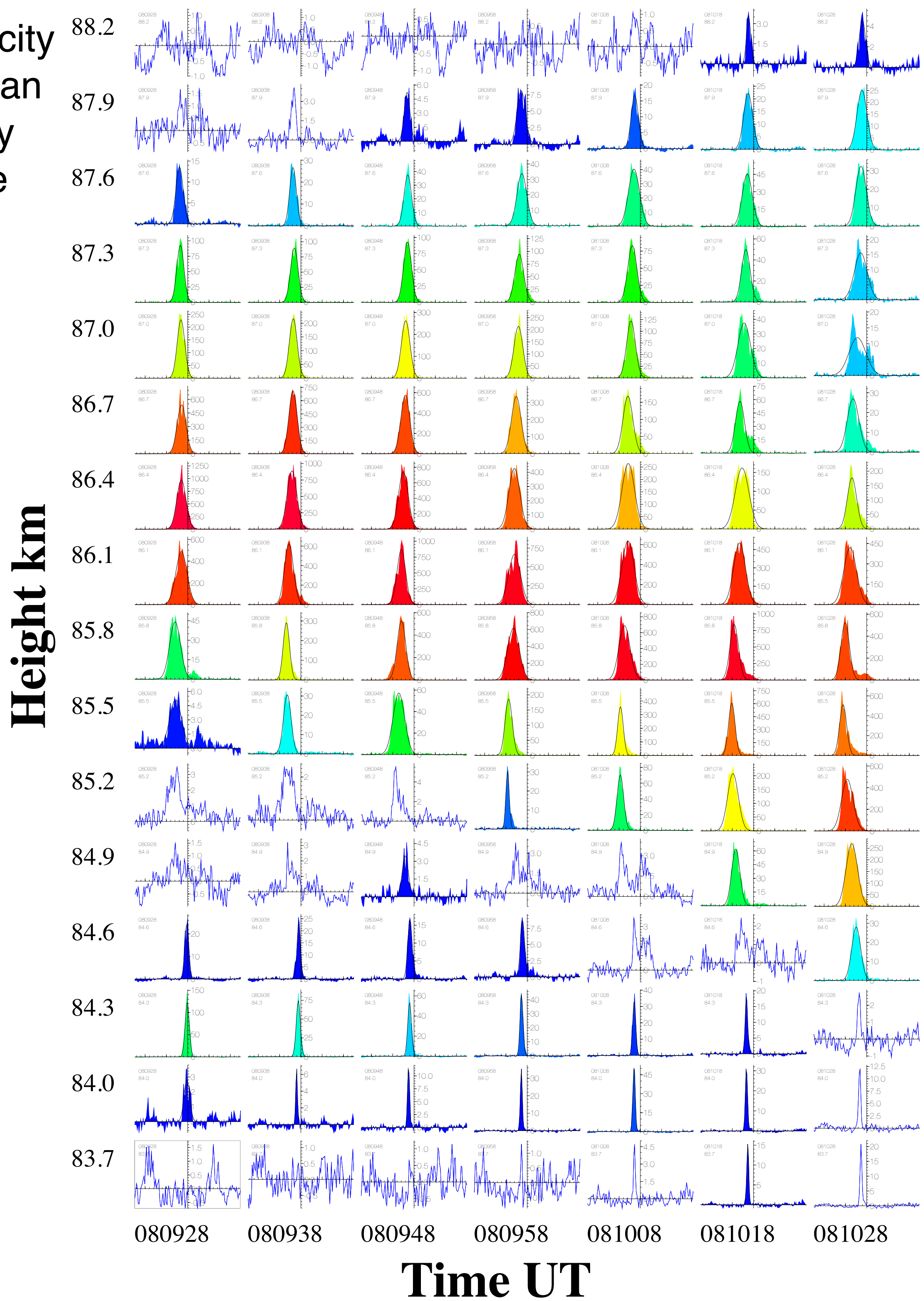

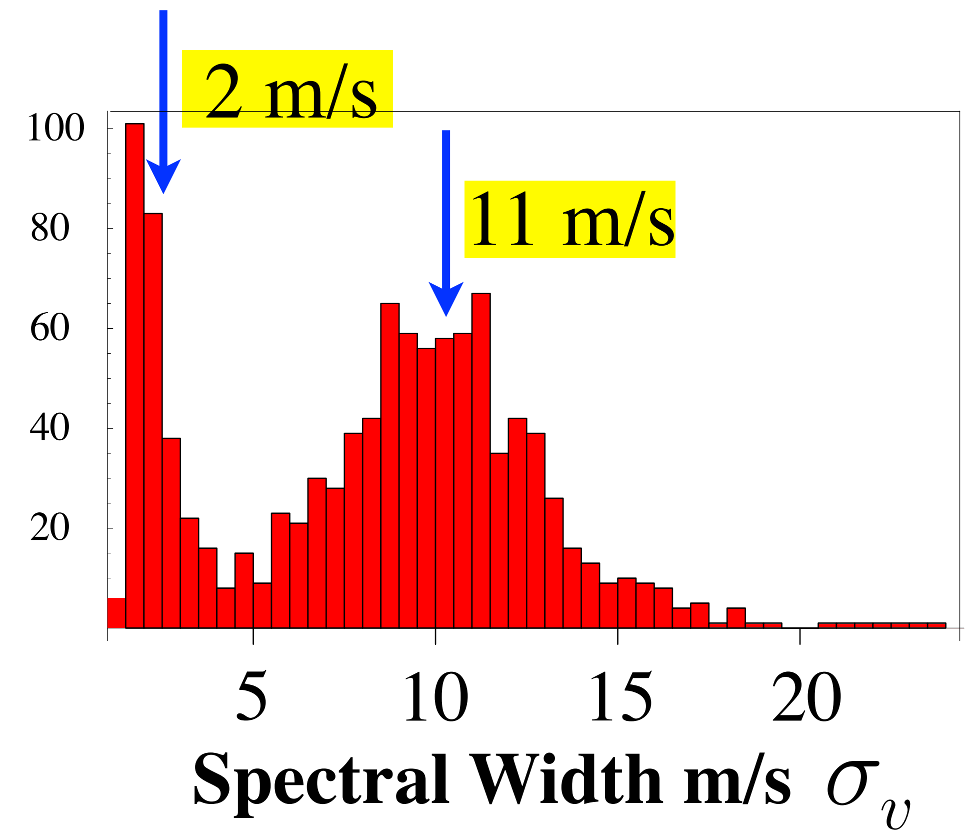

Energy Dissipation Rate of Turbulence

$$\epsilon = \alpha\, \sigma_v^2$$

PMSE Doppler spectra: velocity variance

Electron velocity fluctuations can be induced by air turbulence

EISCAT VHF 13 July 2004

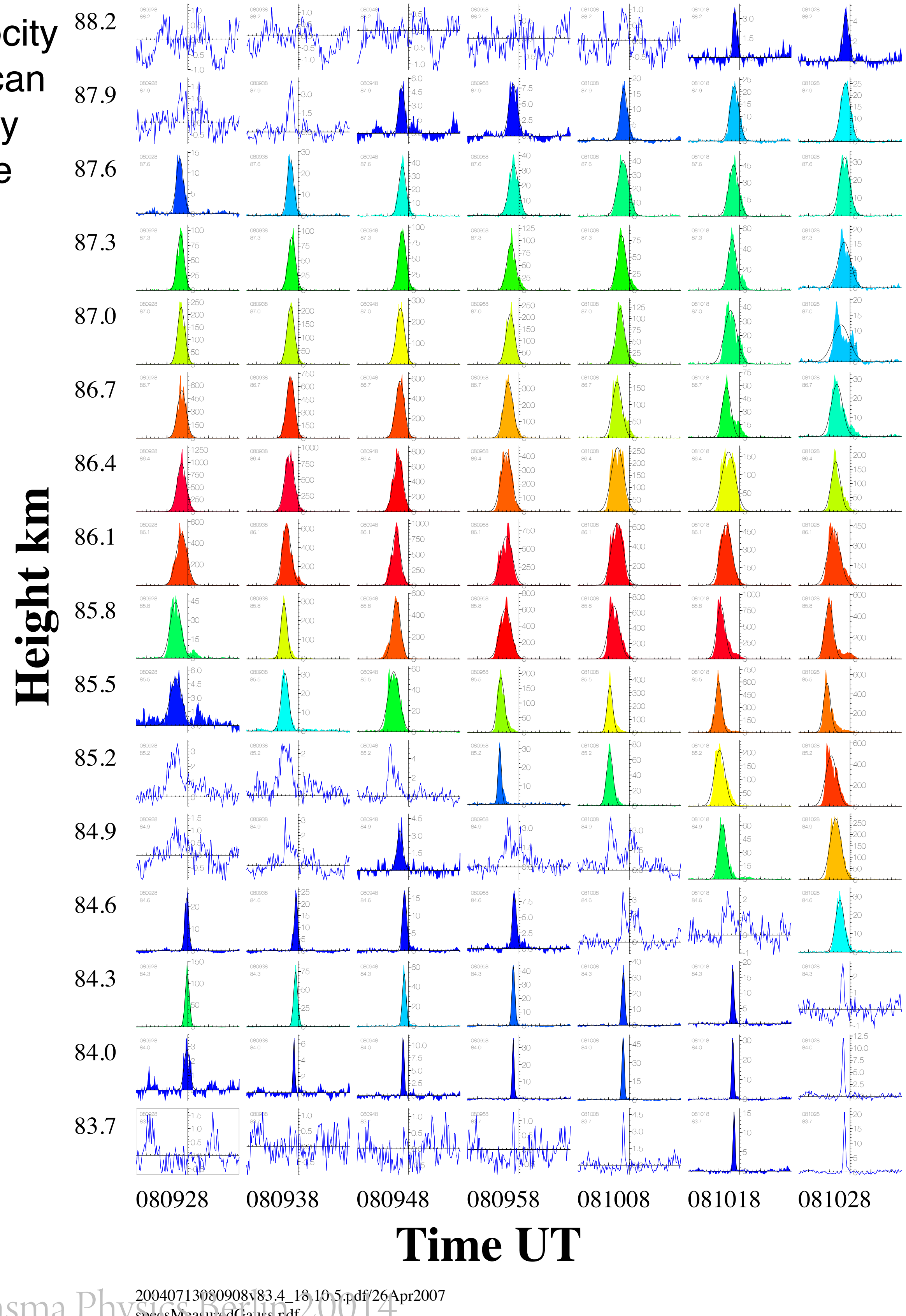

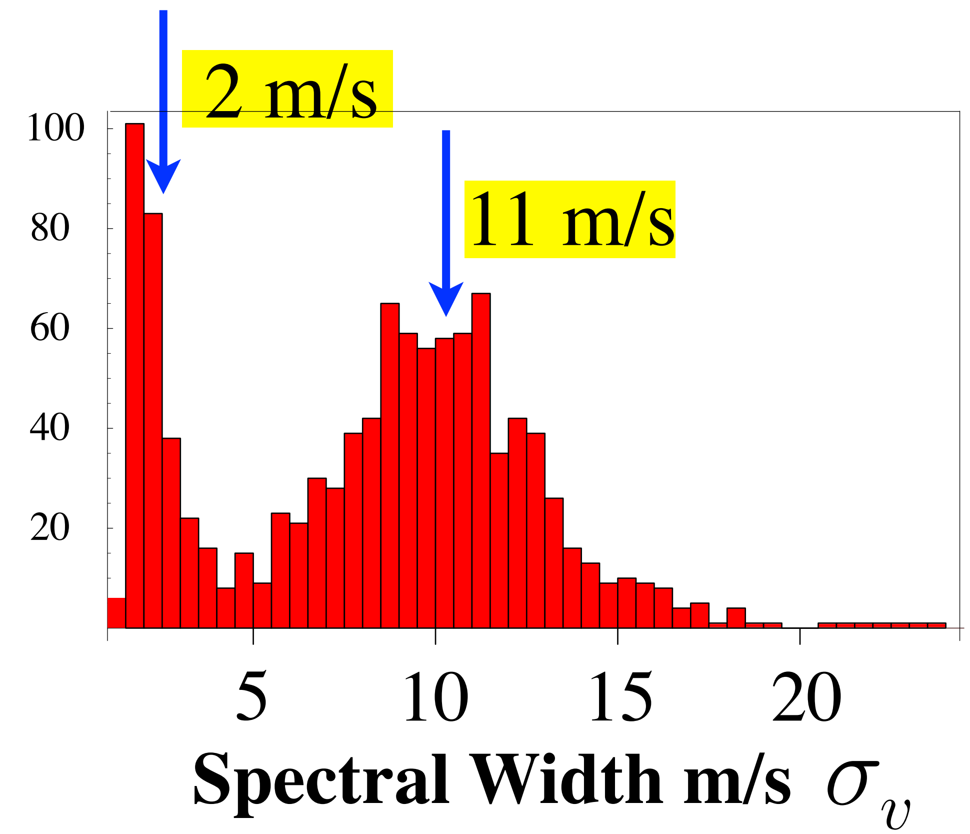

Energy Dissipation Rate of Turbulence

$$\epsilon = \alpha\, \sigma_v^2$$

Kolmogorov turbulence spectrum

Possible scattering with enhanced Schmidt number

Kolmogorov scale $\eta = \left(\frac{\nu_a^3}{\epsilon}\right)^{1/4}$ $\qquad$ $\mathrm{Sc} = \frac{\nu_a}{D_e}$

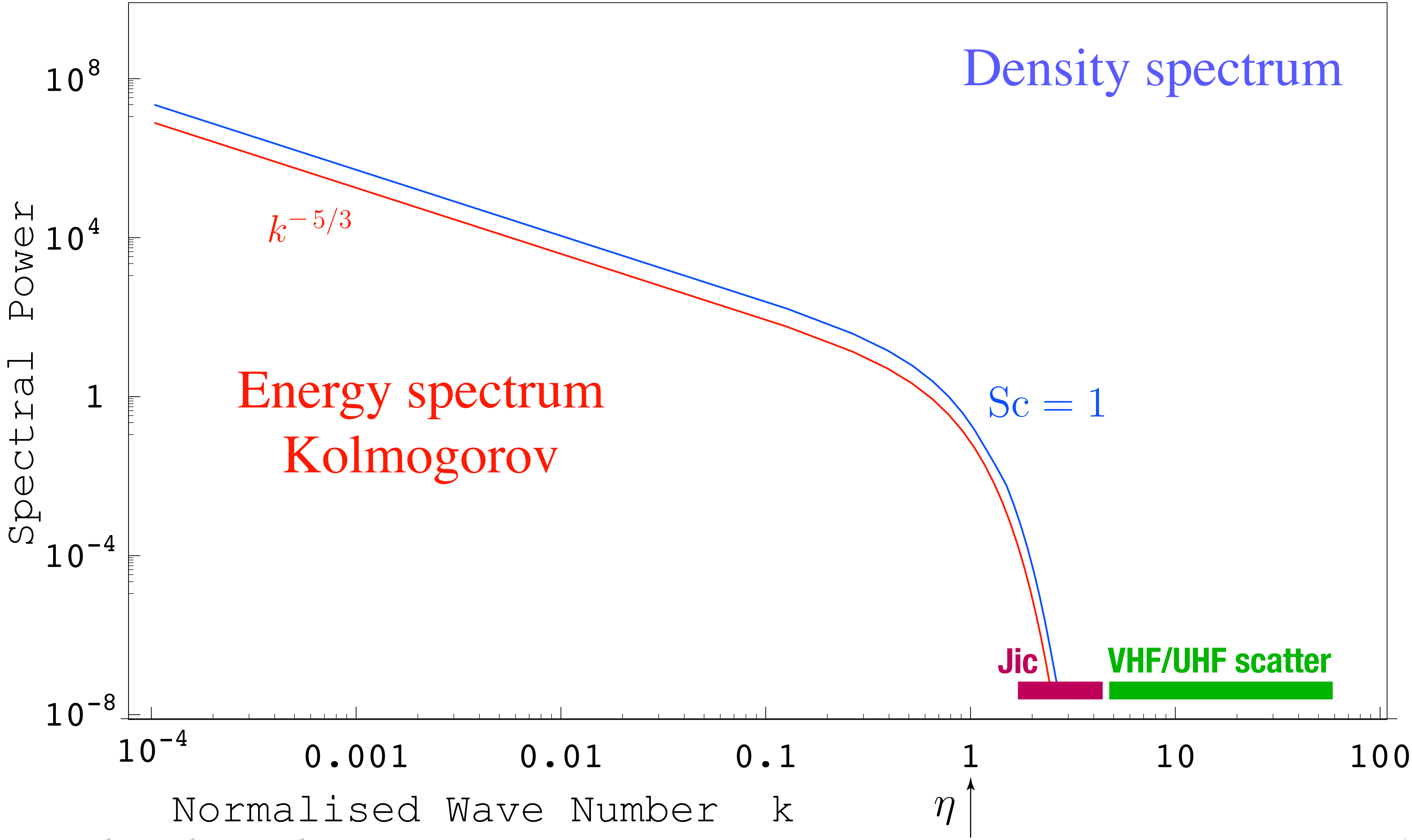

Possible scattering with enhanced Schmidt number

Kolmogorov scale $\eta = \left(\frac{\nu_a^3}{\epsilon}\right)^{1/4}$ $\quad \mathrm{Sc} = \frac{\nu_a}{D_e}$ $\quad \eta_B = \left(\frac{\nu_a D_e^2}{\epsilon}\right)^{1/4}$ Batchelor scale

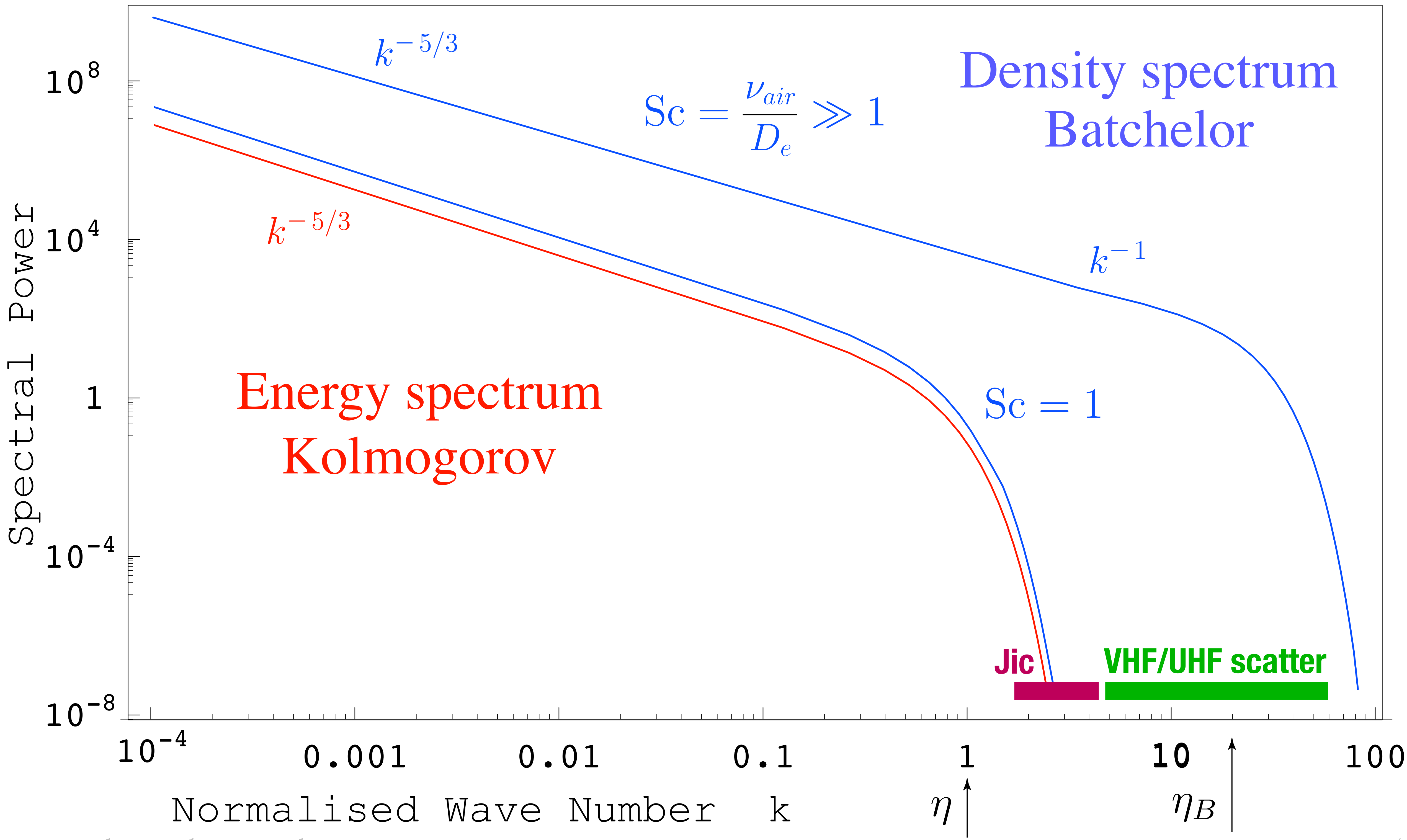

Possible scattering with enhanced Schmidt number

Kolmogorov scale $\eta = \left(\frac{\nu_a^3}{\epsilon}\right)^{1/4}$ $\mathrm{Sc} = \frac{\nu_a}{D_e}$ $\eta_B = \left(\frac{\nu_a D_e^2}{\epsilon}\right)^{1/4}$ Batchelor scale

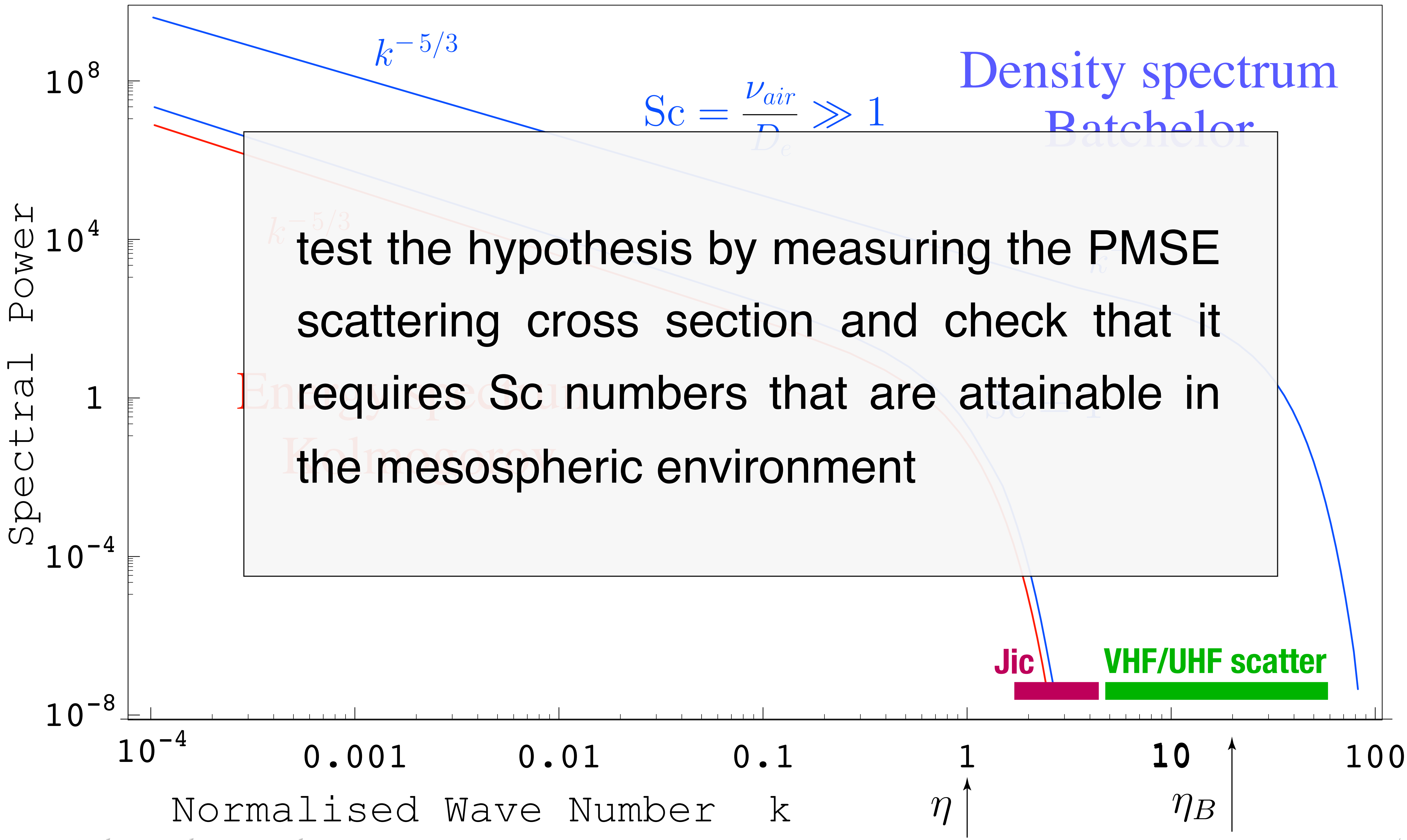

test the hypothesis by measuring the PMSE scattering cross section and check that it requires Sc numbers that are attainable in the mesospheric environment

Scattering cross section with Sc number

Measured:

$$\eta_{rad}(\mathrm{VHF}) = 5250 \times 10^{-18}\ \mathrm{m}^{-1}$$

$$\eta_{rad}(\mathrm{UHF}) = 3.5 \times 10^{-18}$$

Fitted:

$$Sc = 894\ (4470)$$

$$\chi_{ne} = 7.9 \times 10^{14}\ m^{-6} s^{-1}$$

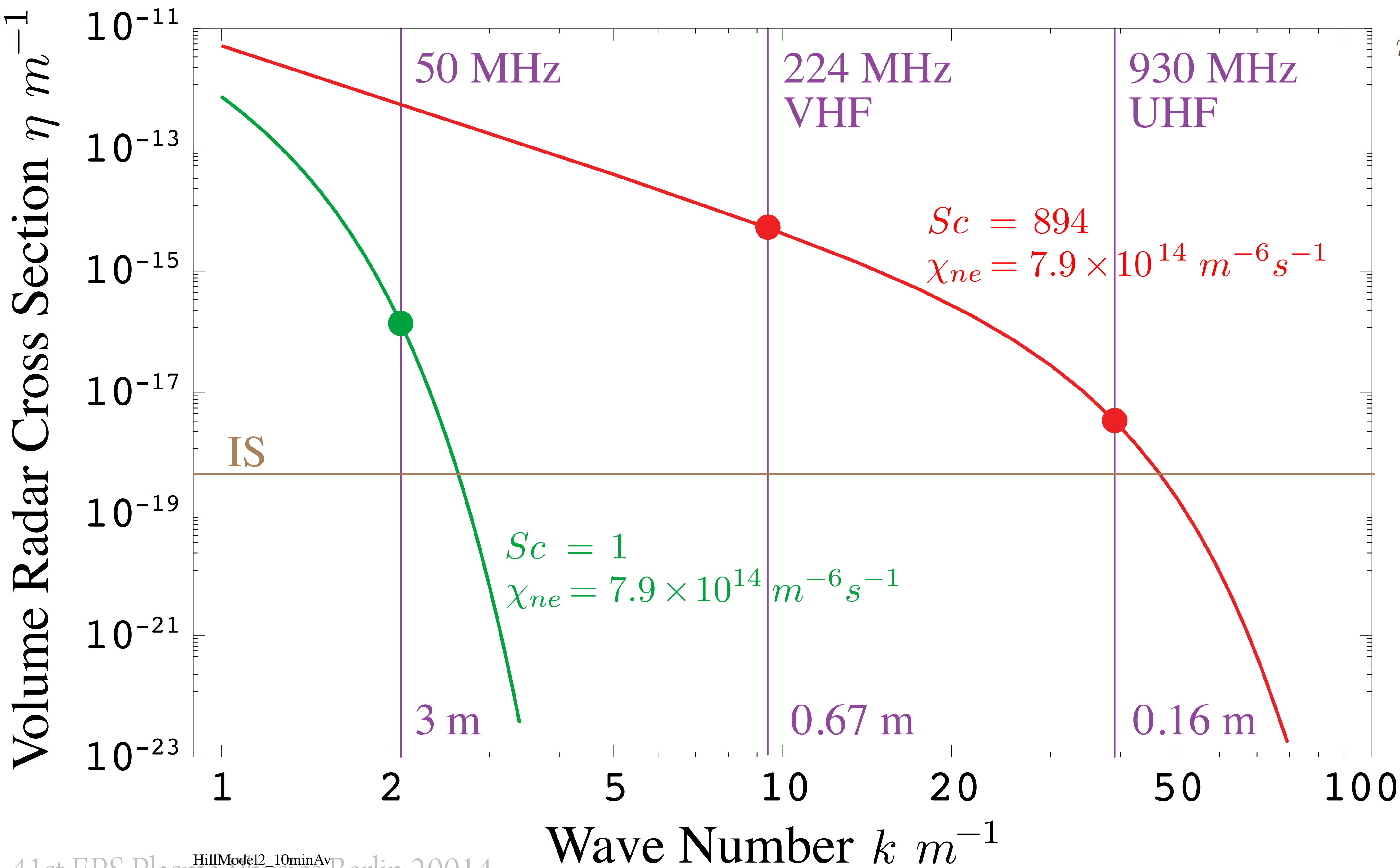

$n_{eo} = 9 \times 10^{9}\ m^{-3}$

$\sigma_v = 10\ ms^{-1}$ (2)

$\nu = 0.567\ m^2 s^{-1}$

$\epsilon = 840\ mW\ kg^{-1}$

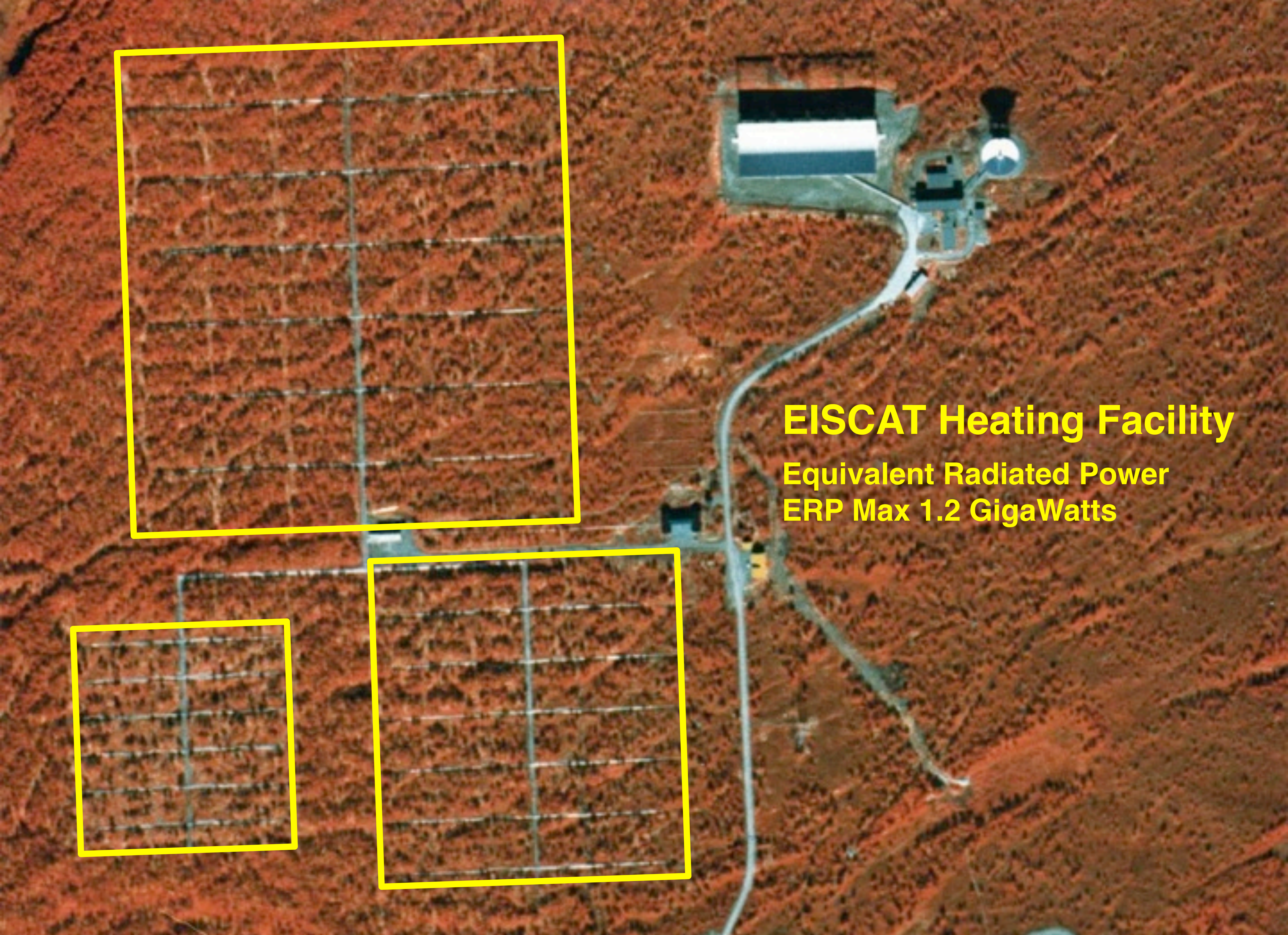
EISCAT Heating Facility
Equivalent Radiated Power
ERP Max 1.2 GigaWatts

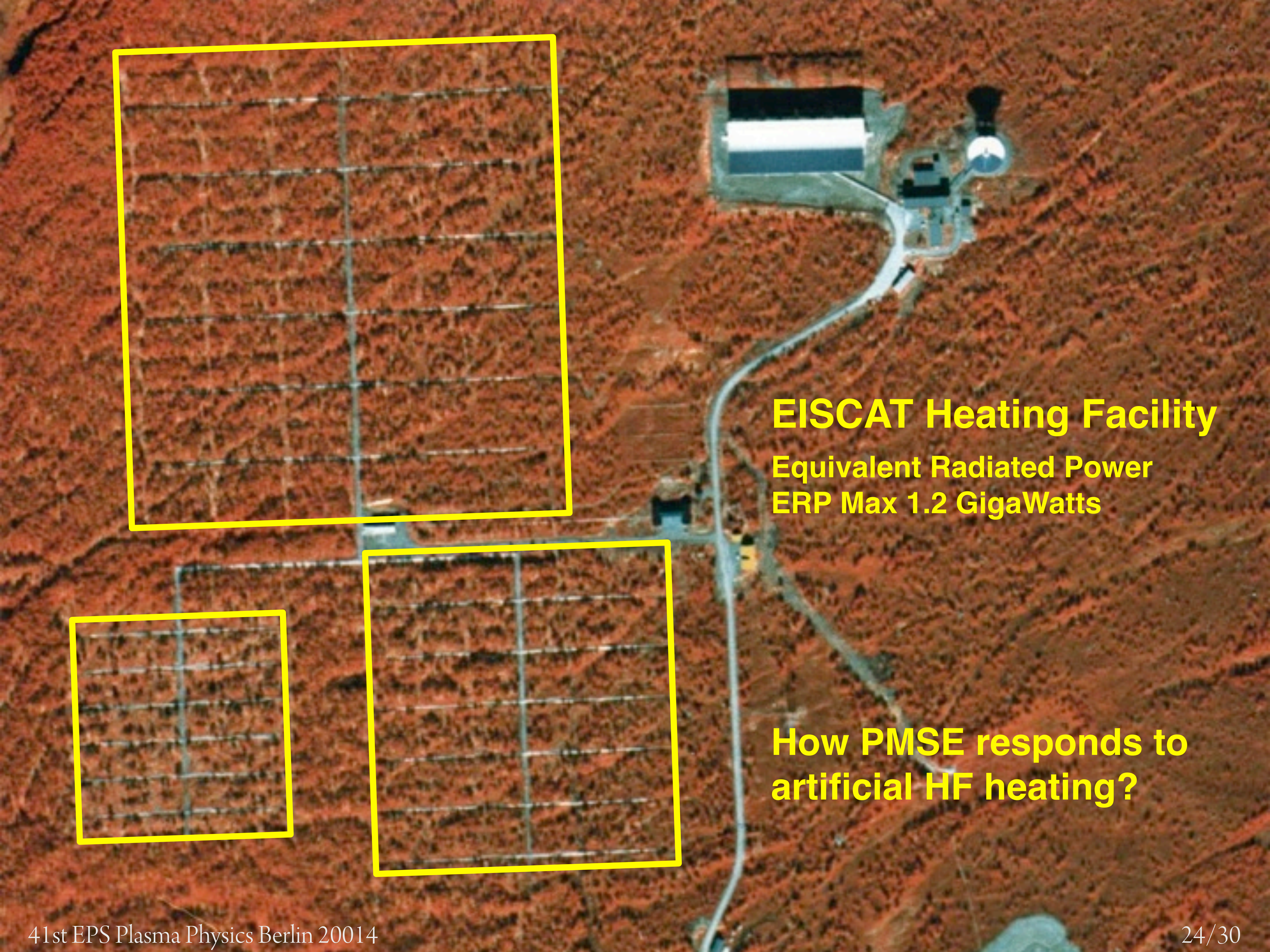
EISCAT Heating Facility
Equivalent Radiated Power
ERP Max 1.2 GigaWatts
How PMSE responds to
artificial HF heating?

Ove Havnes (2001) predicted the Overshoot effect

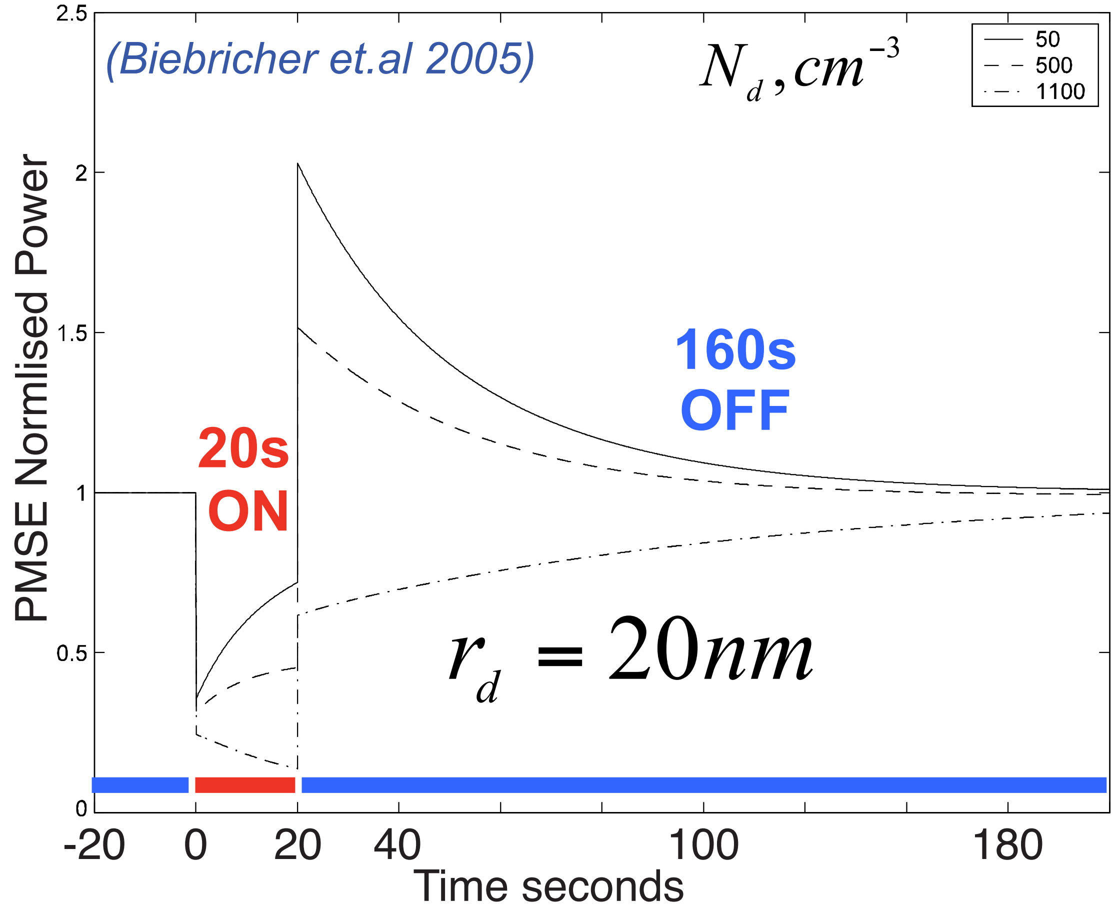

Ove Havnes (2001) predicted the Overshoot effect

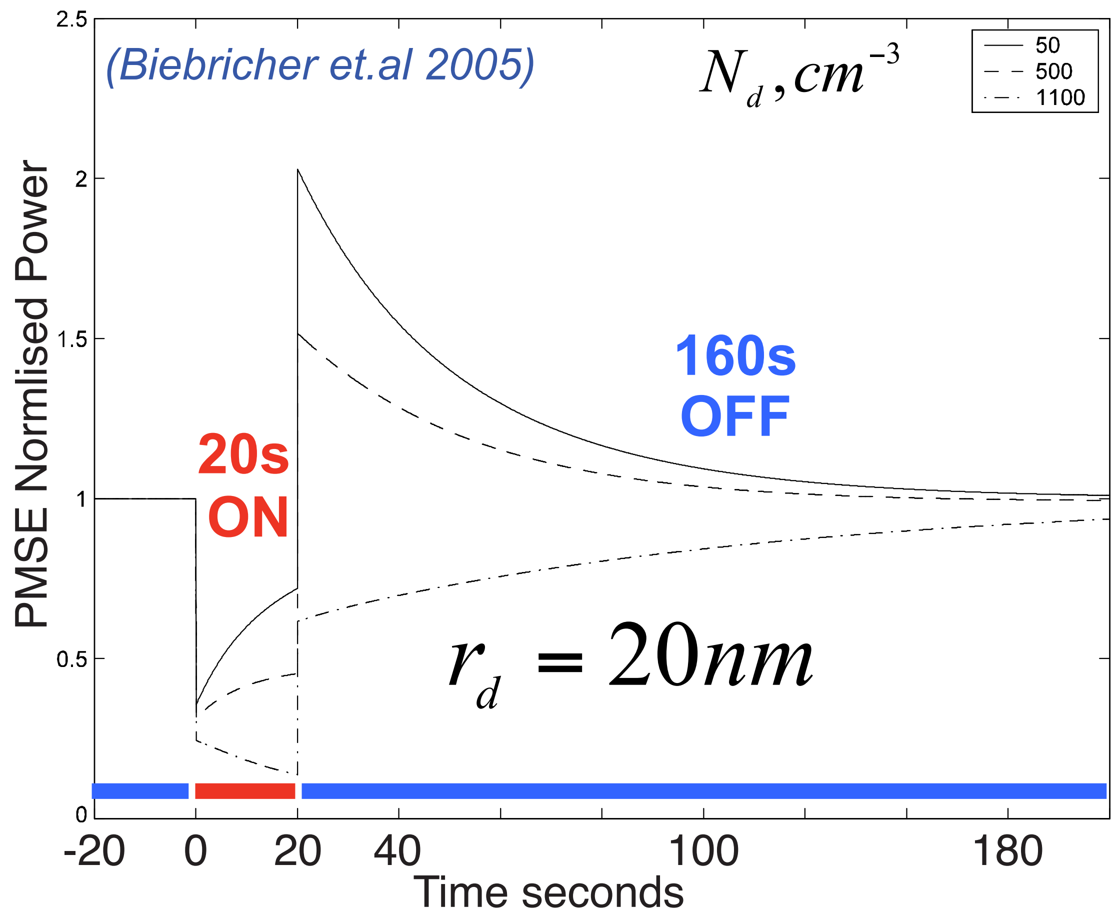

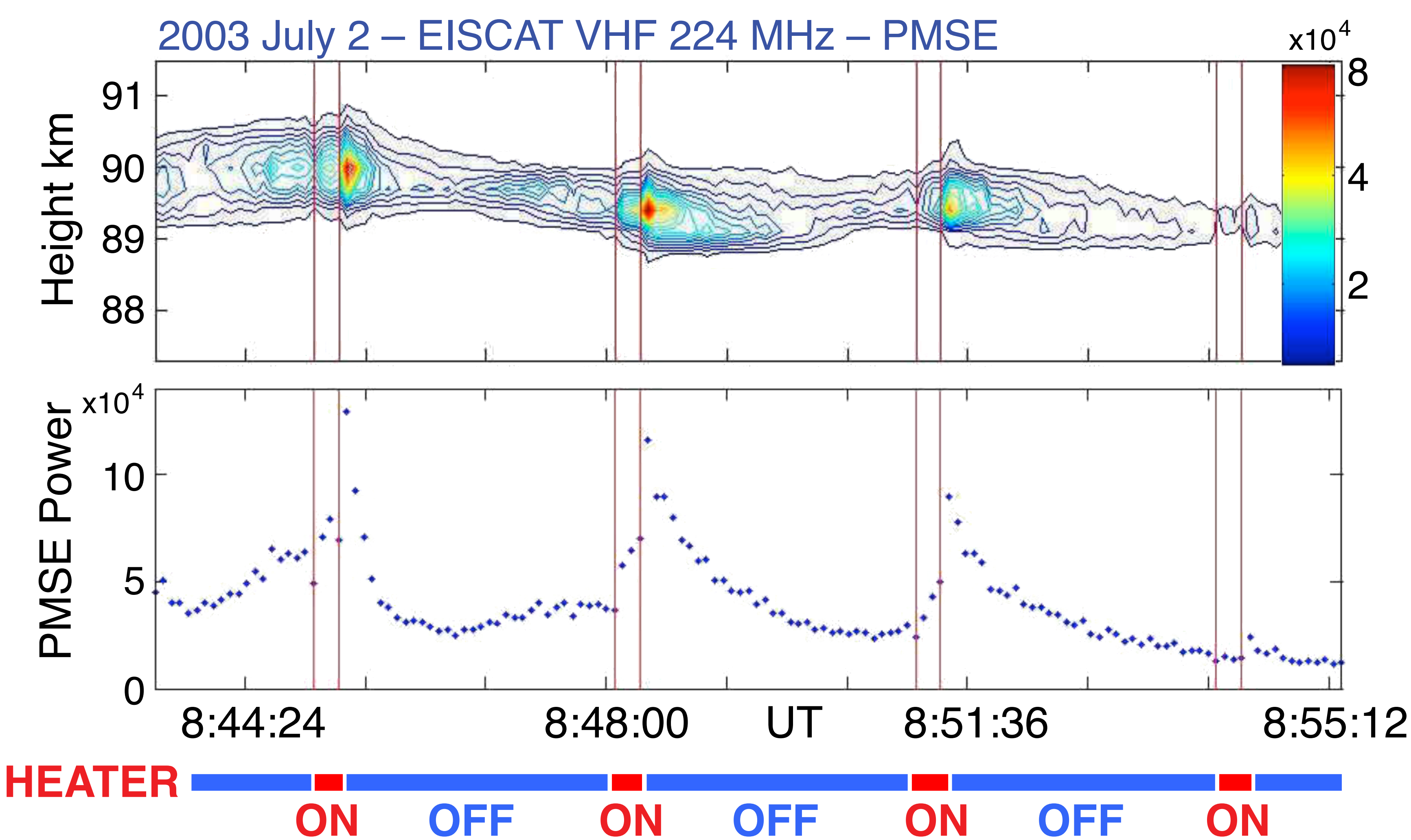

Ove Havnes (2001) predicted the Overshoot effect

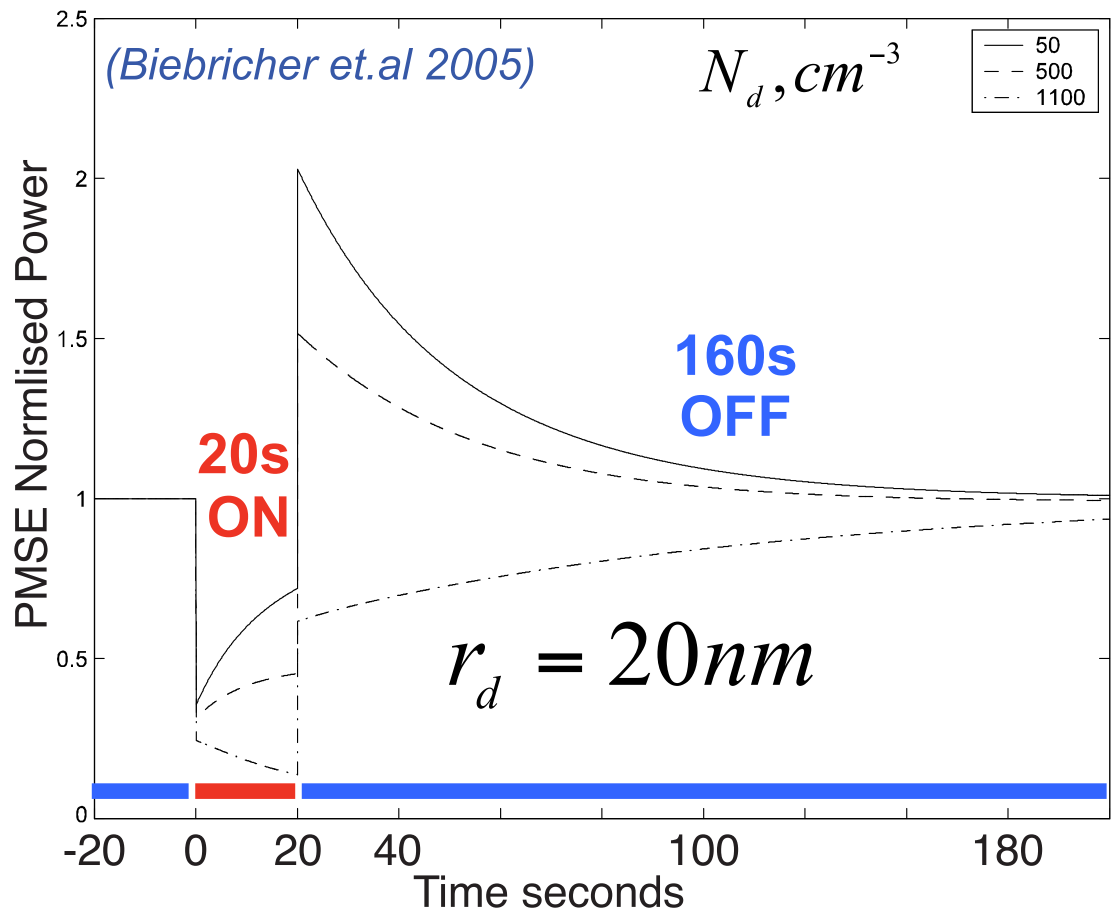

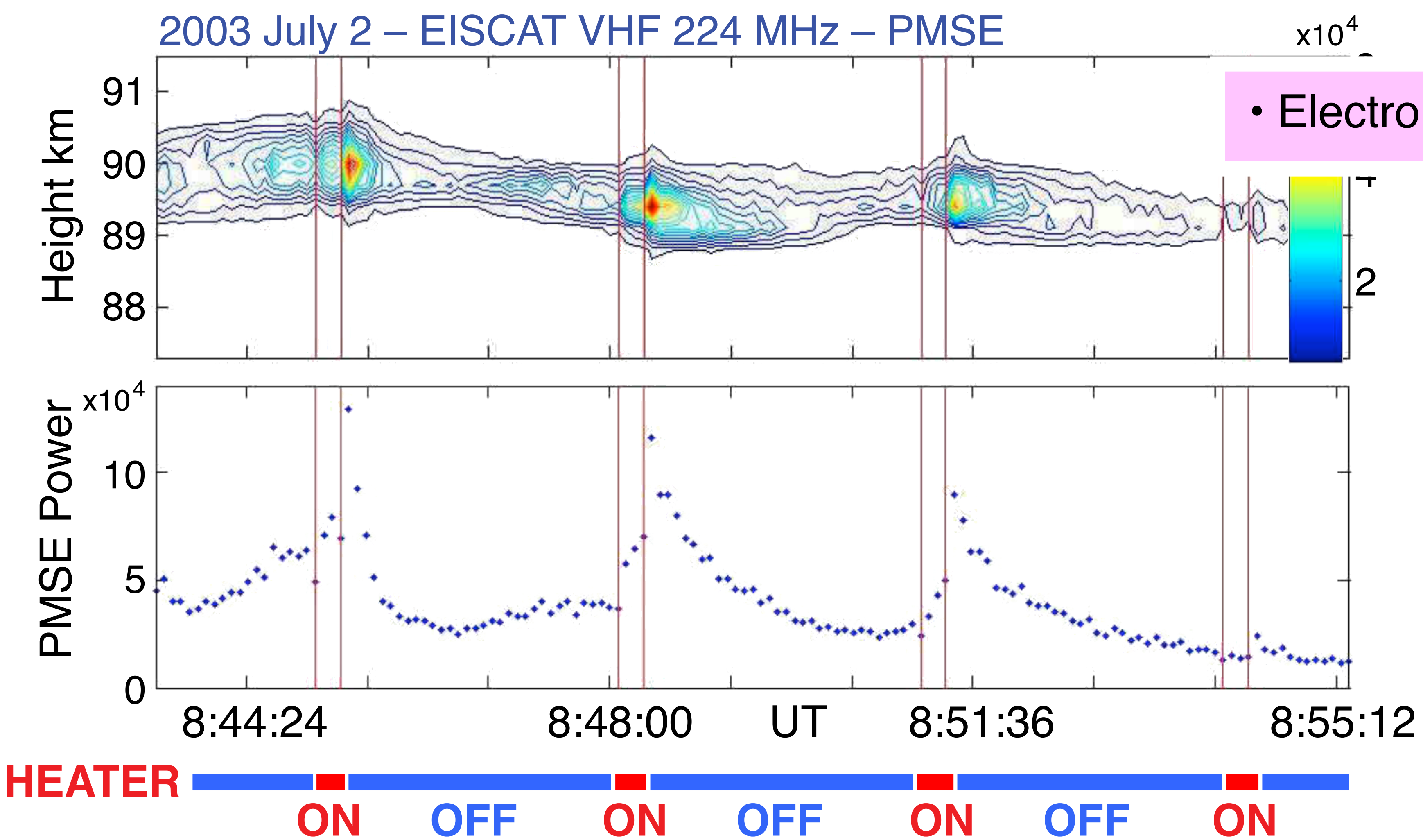

- Electron temperature Te increases

Ove Havnes (2001) predicted the Overshoot effect

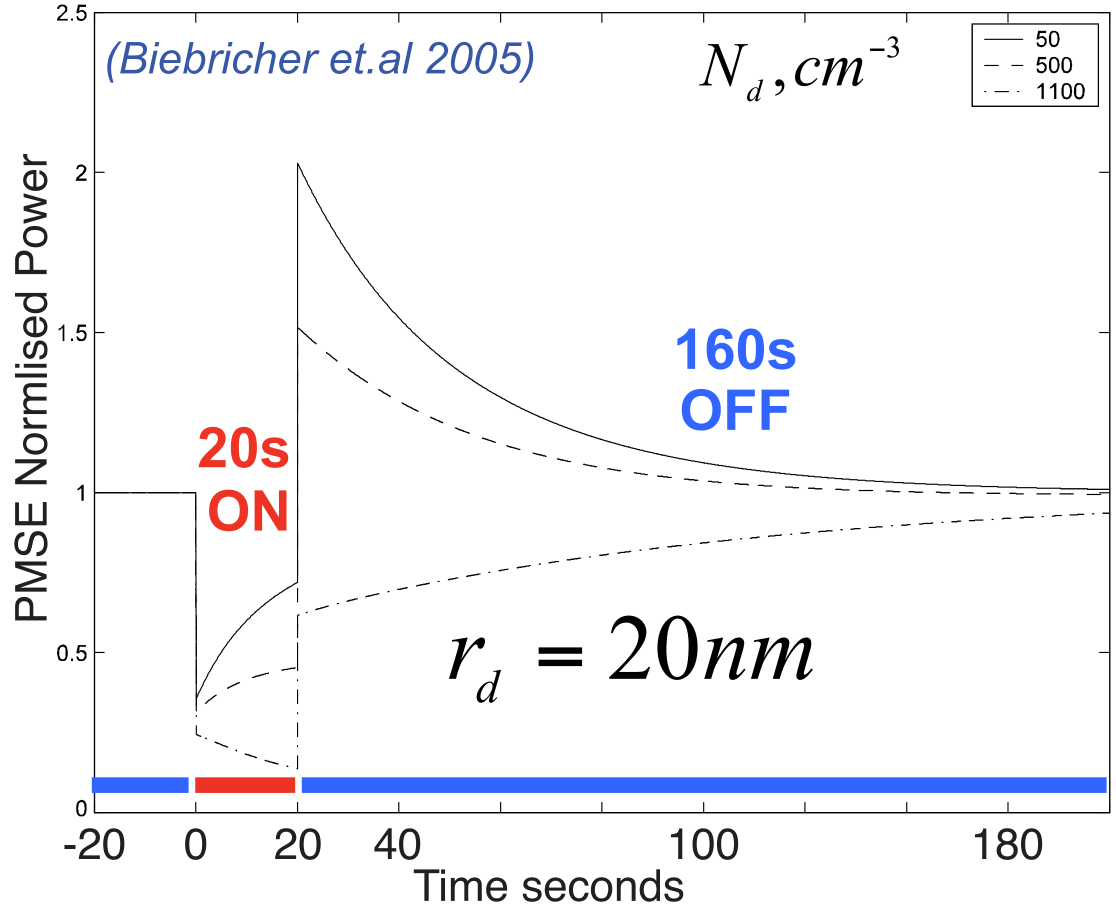

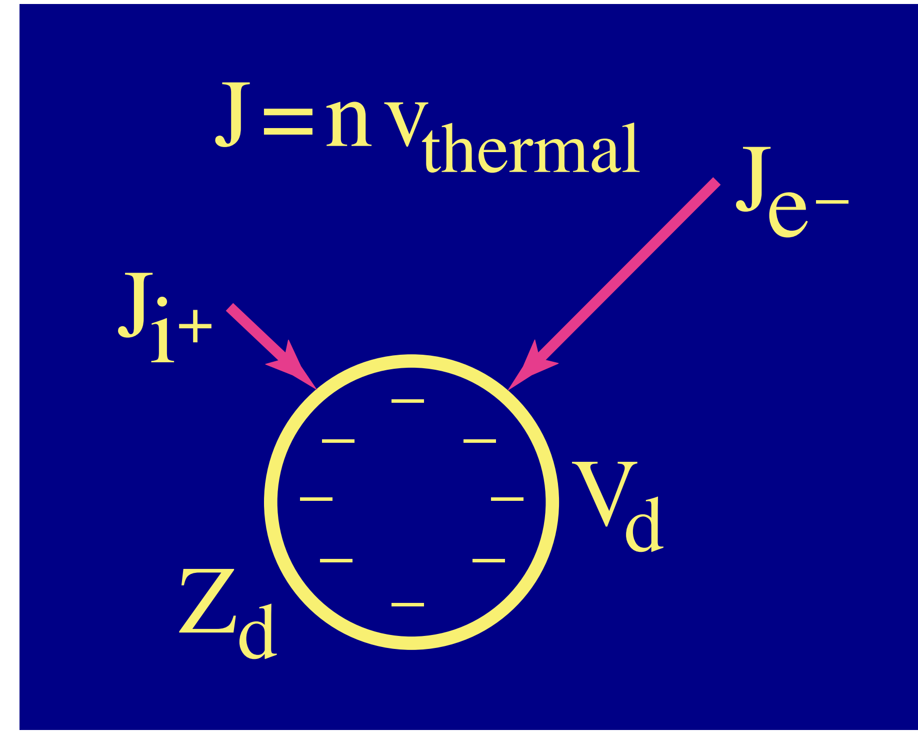

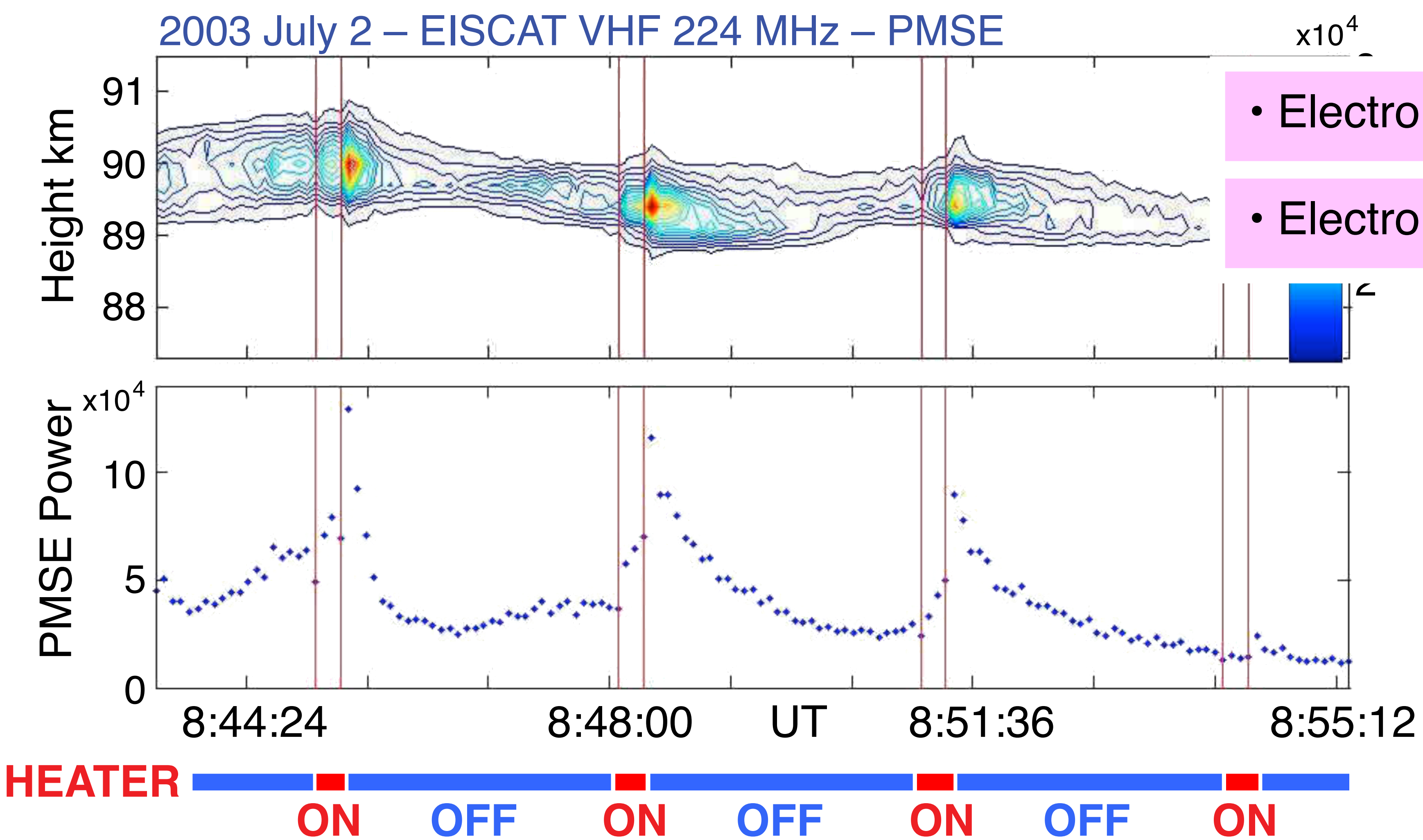

- Electron temperature Te increases
- Electron thermal velocity increases

Ove Havnes (2001) predicted the Overshoot effect

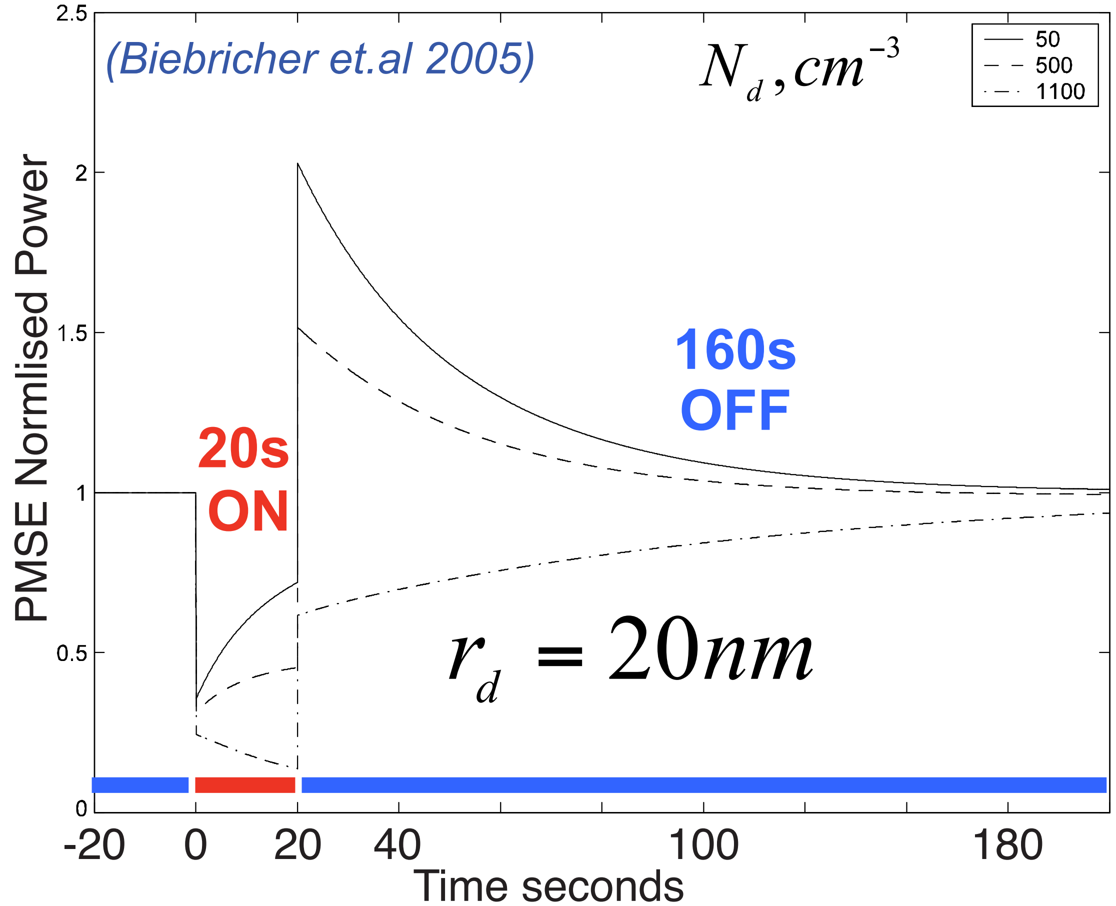

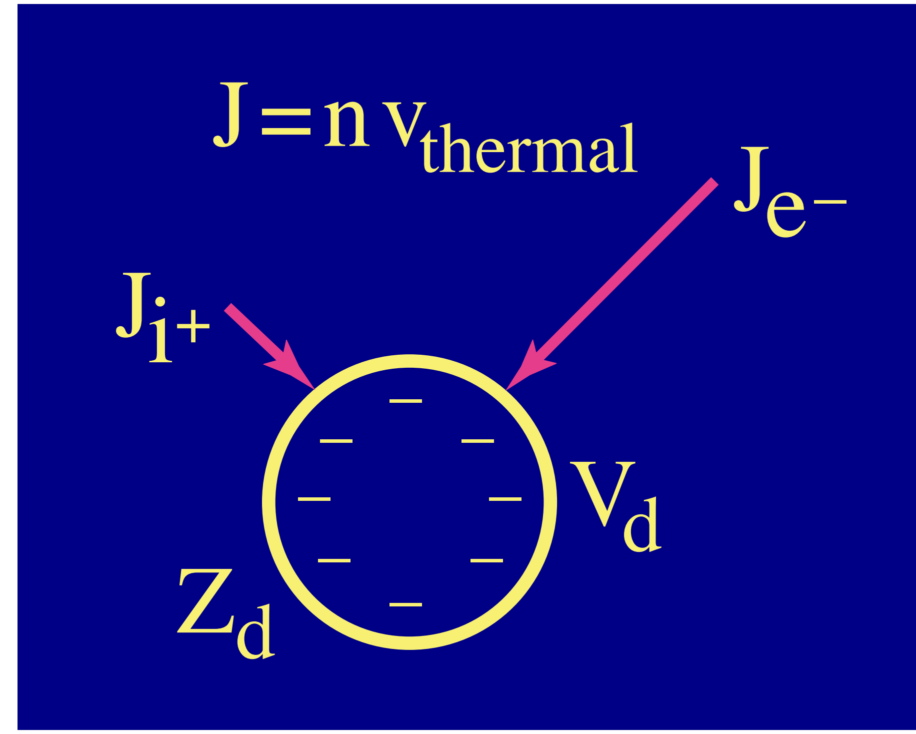

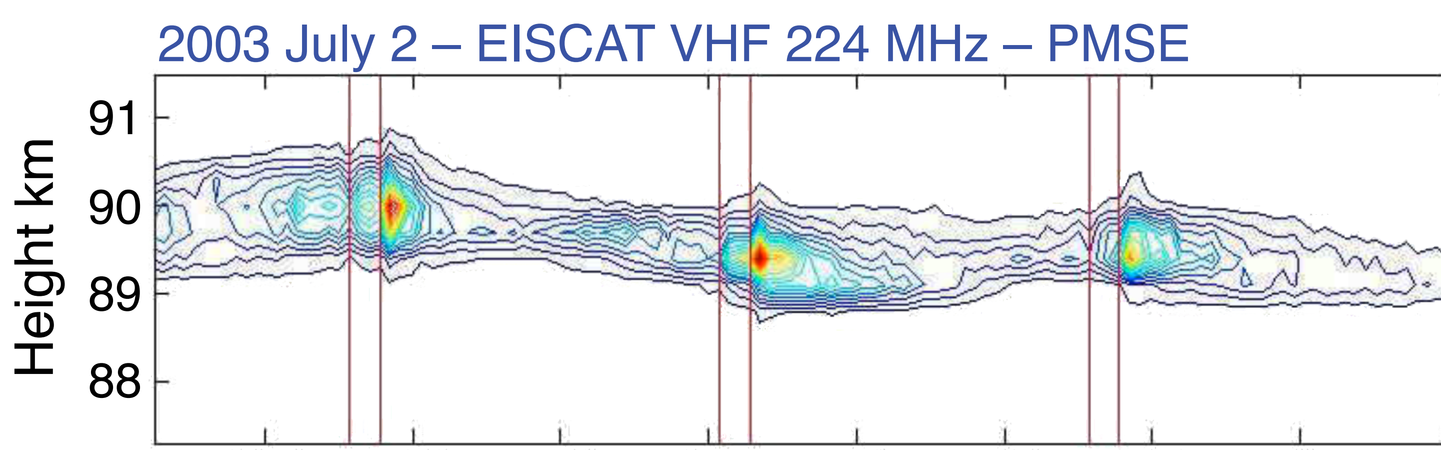

- Electron temperature Te increases
- Electron thermal velocity increases
- Electron current density Je increases

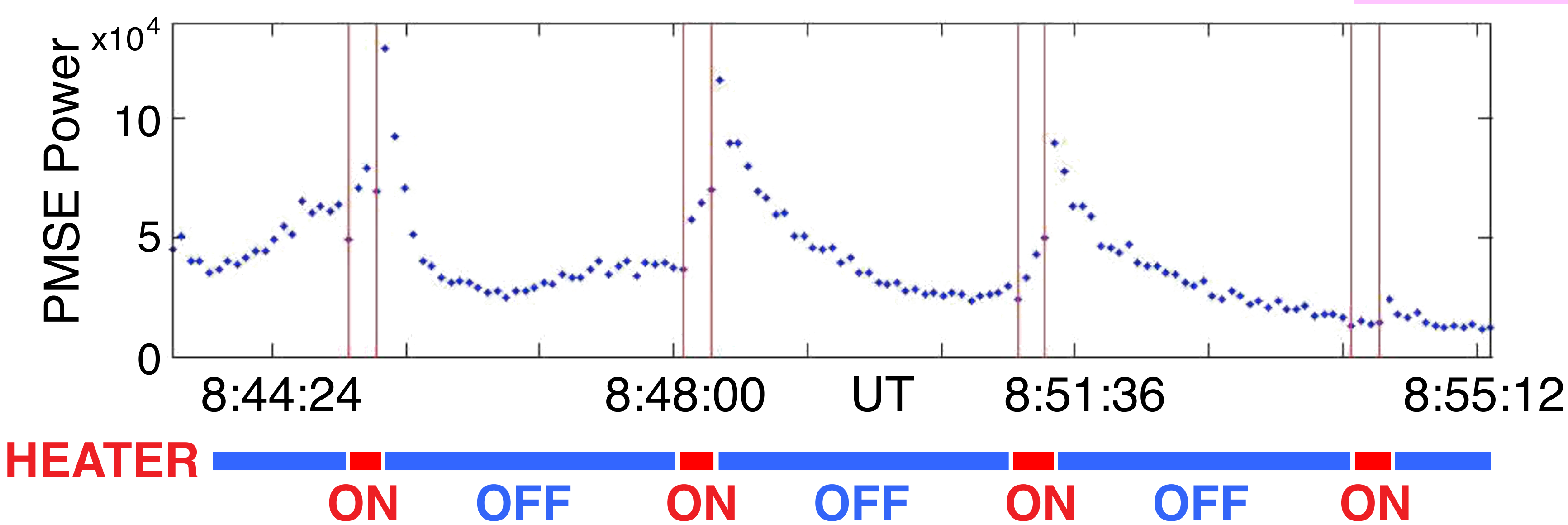

Ove Havnes (2001) predicted the Overshoot effect

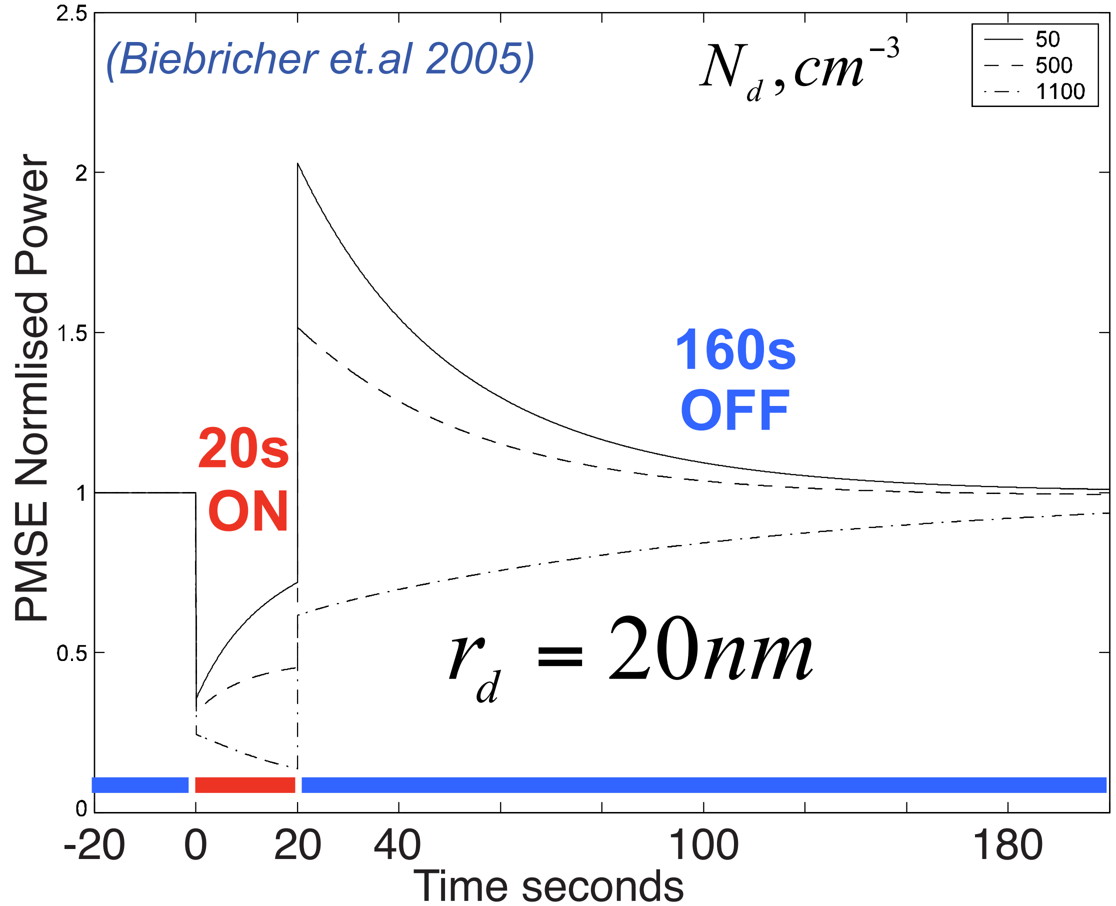

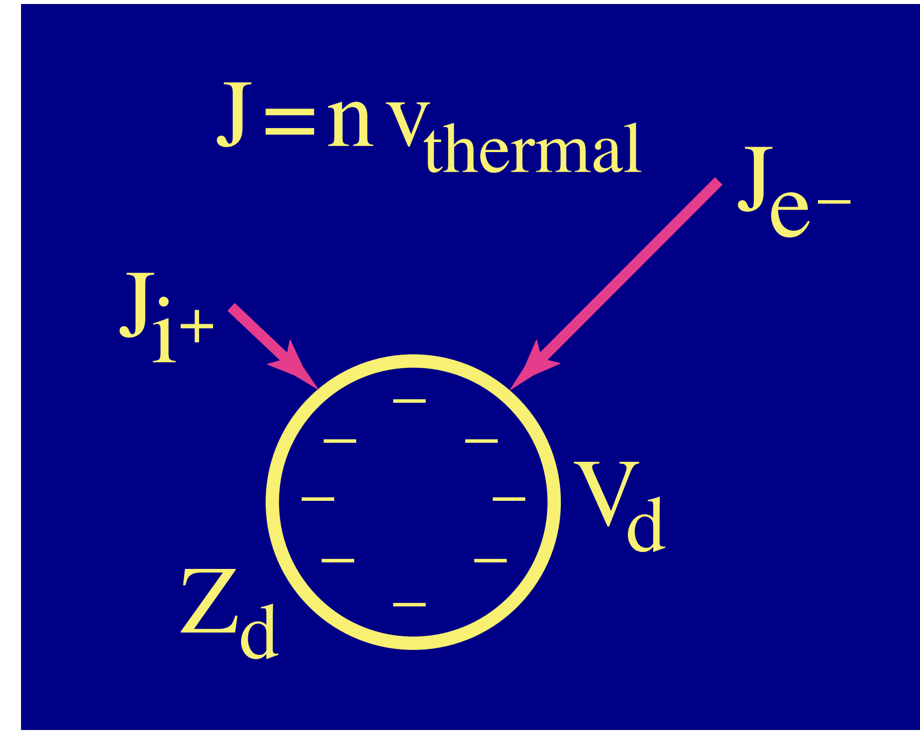

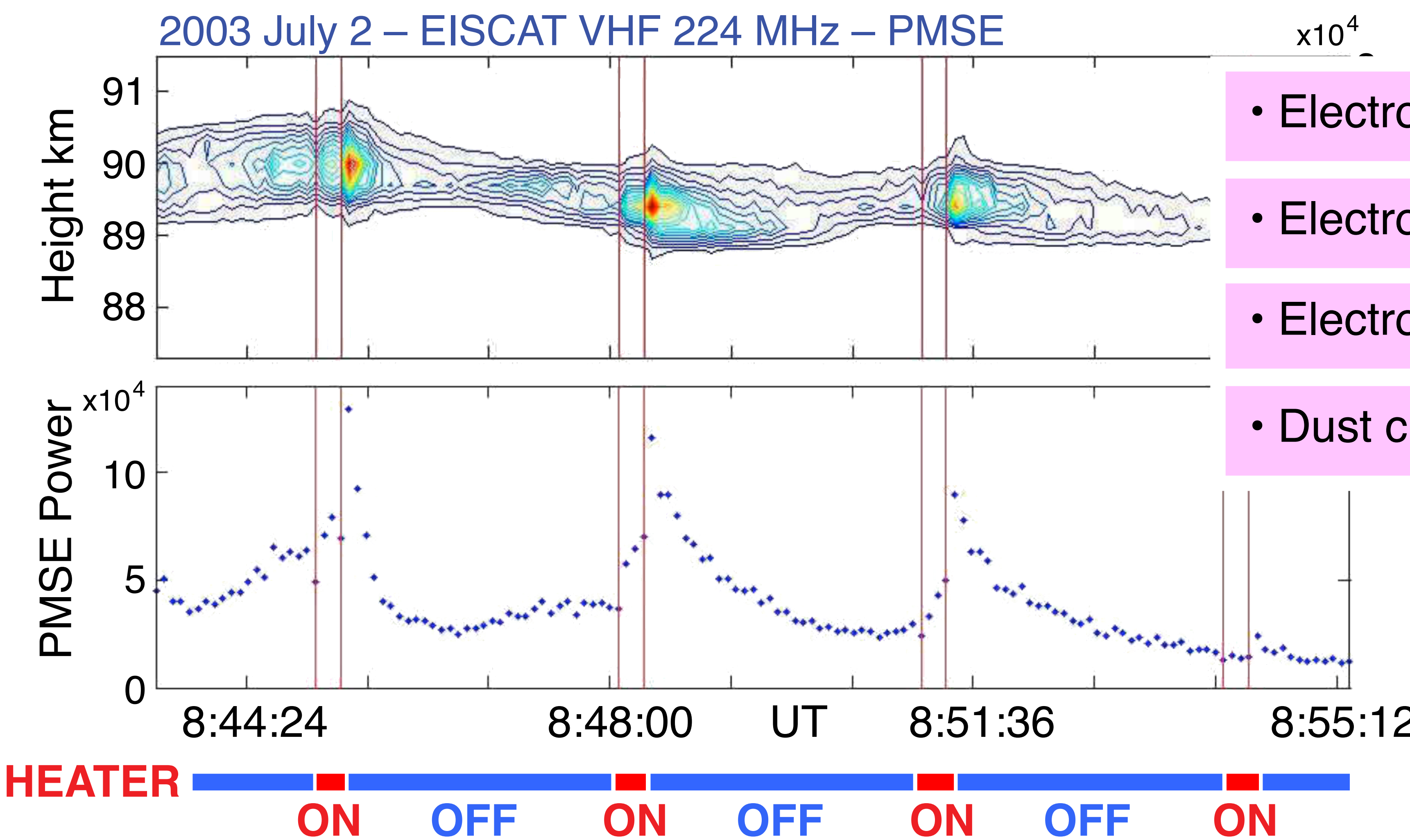

- Electron temperature Te increases
- Electron thermal velocity increases
- Electron current density Je increases
- Dust charge Zd increases

Ove Havnes (2001) predicted the Overshoot effect

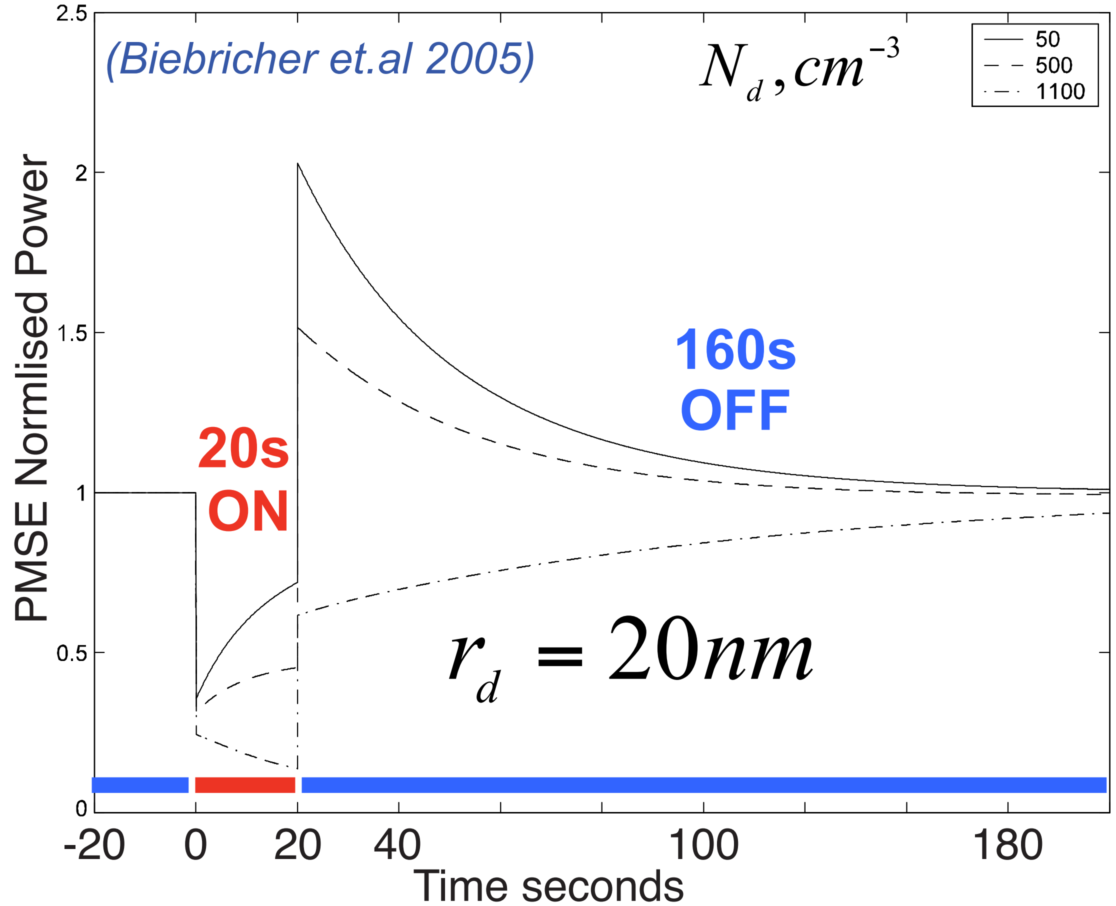

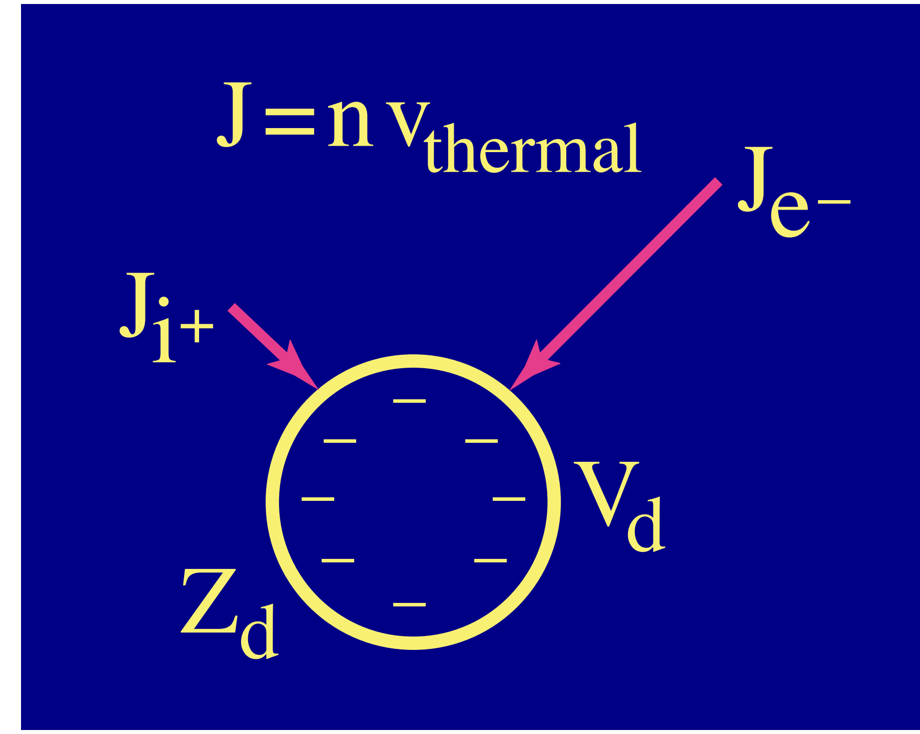

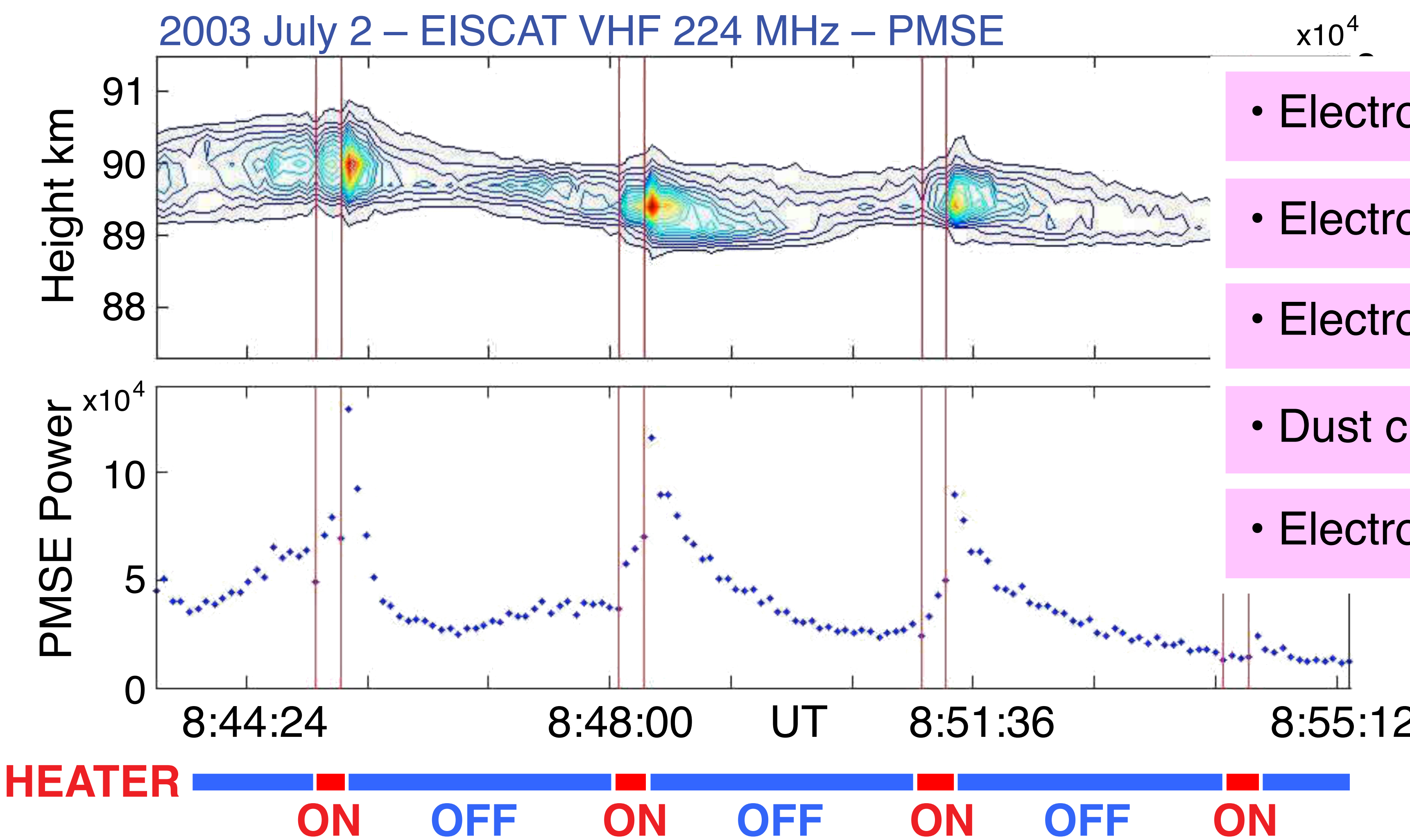

- Electron temperature Te increases
- Electron thermal velocity increases
- Electron current density Je increases
- Dust charge Zd increases
- Electron density gradients increase

Ove Havnes (2001) predicted the Overshoot effect

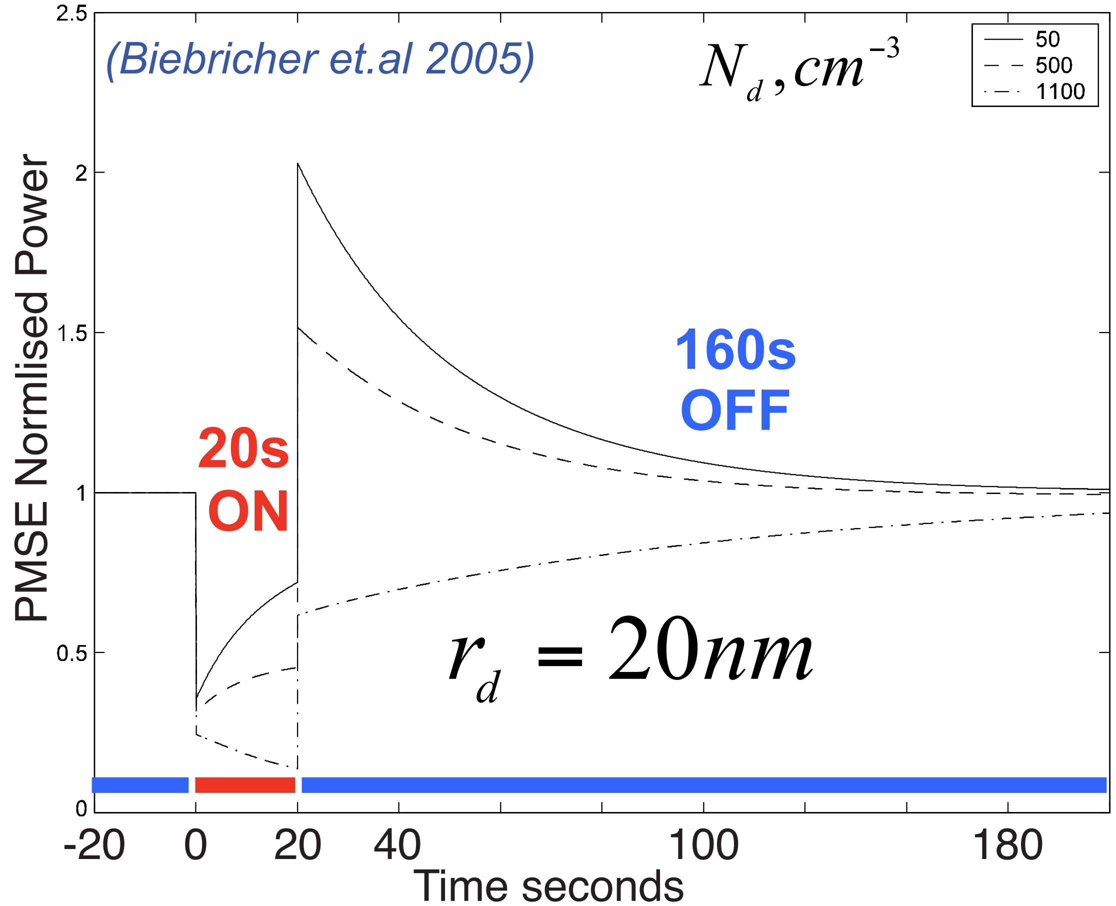

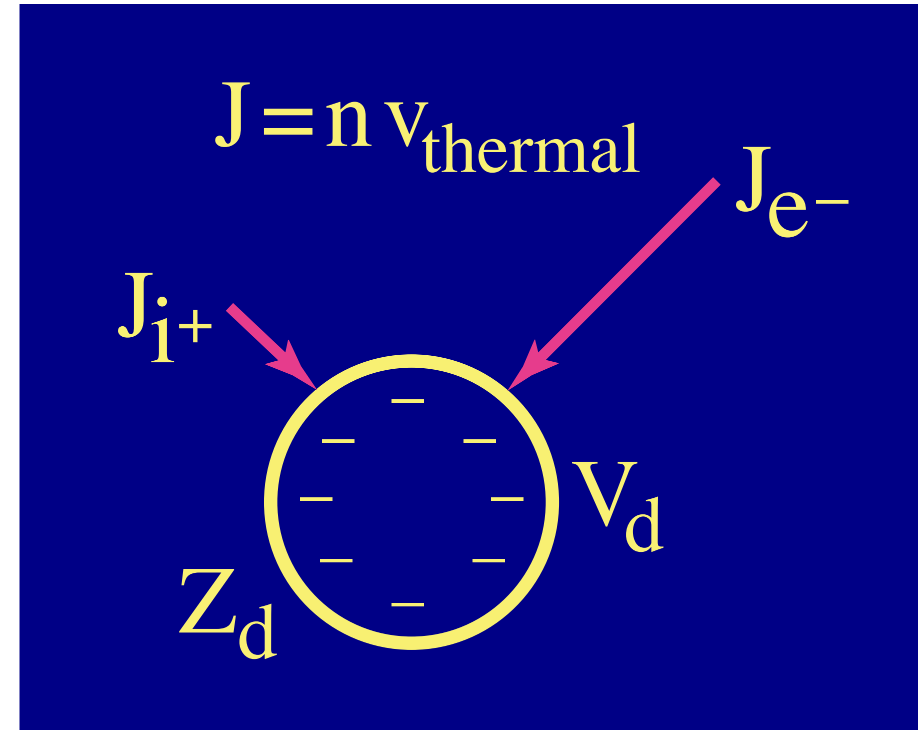

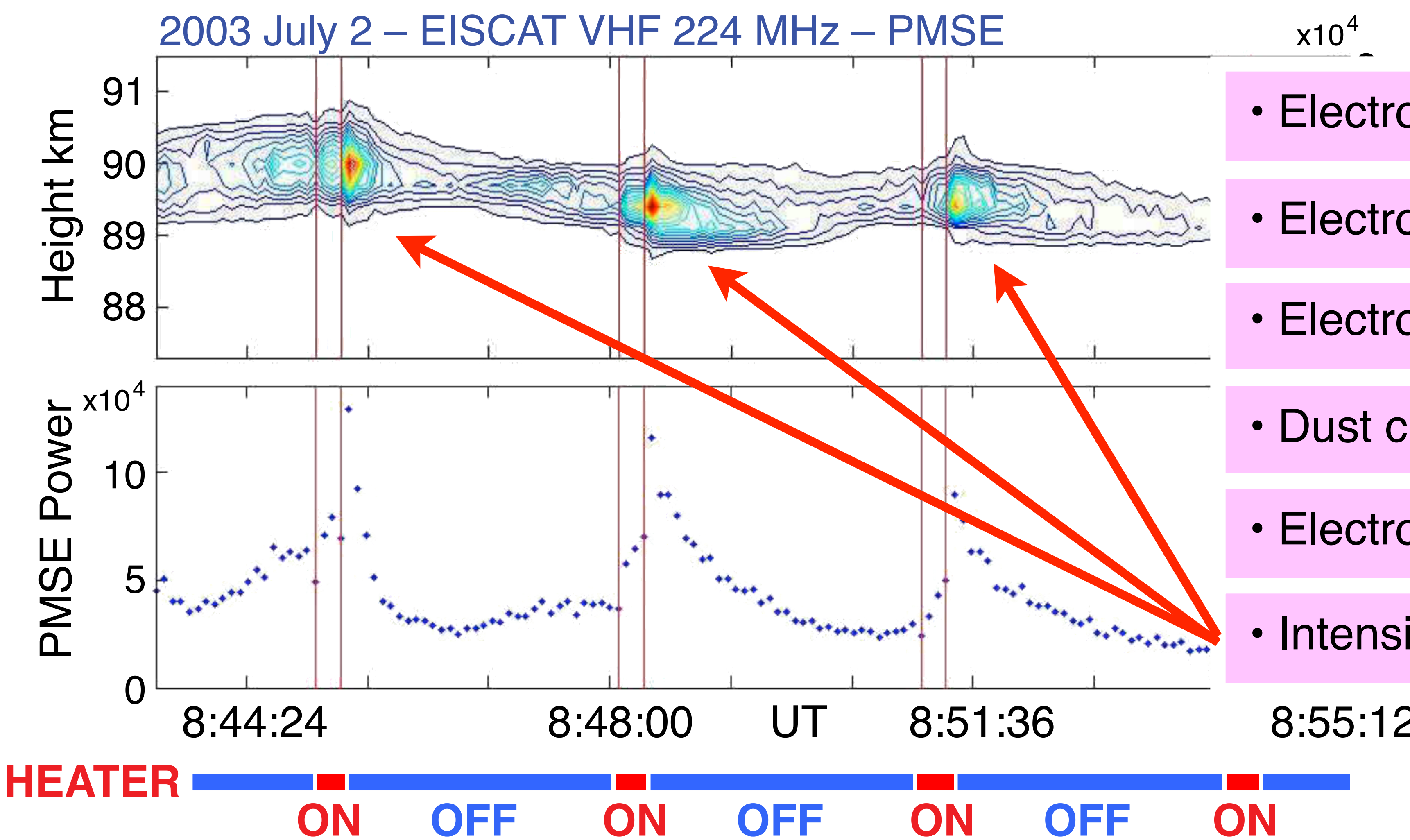

- Electron temperature Te increases
- Electron thermal velocity increases
- Electron current density Je increases
- Dust charge Zd increases
- Electron density gradients increase
- Intensification of radar scattering

Painting the sky with the EISCAT Heater:
The world's first
EURORA

Painting the sky with the EISCAT Heater: The world's first

***EURO*RA**

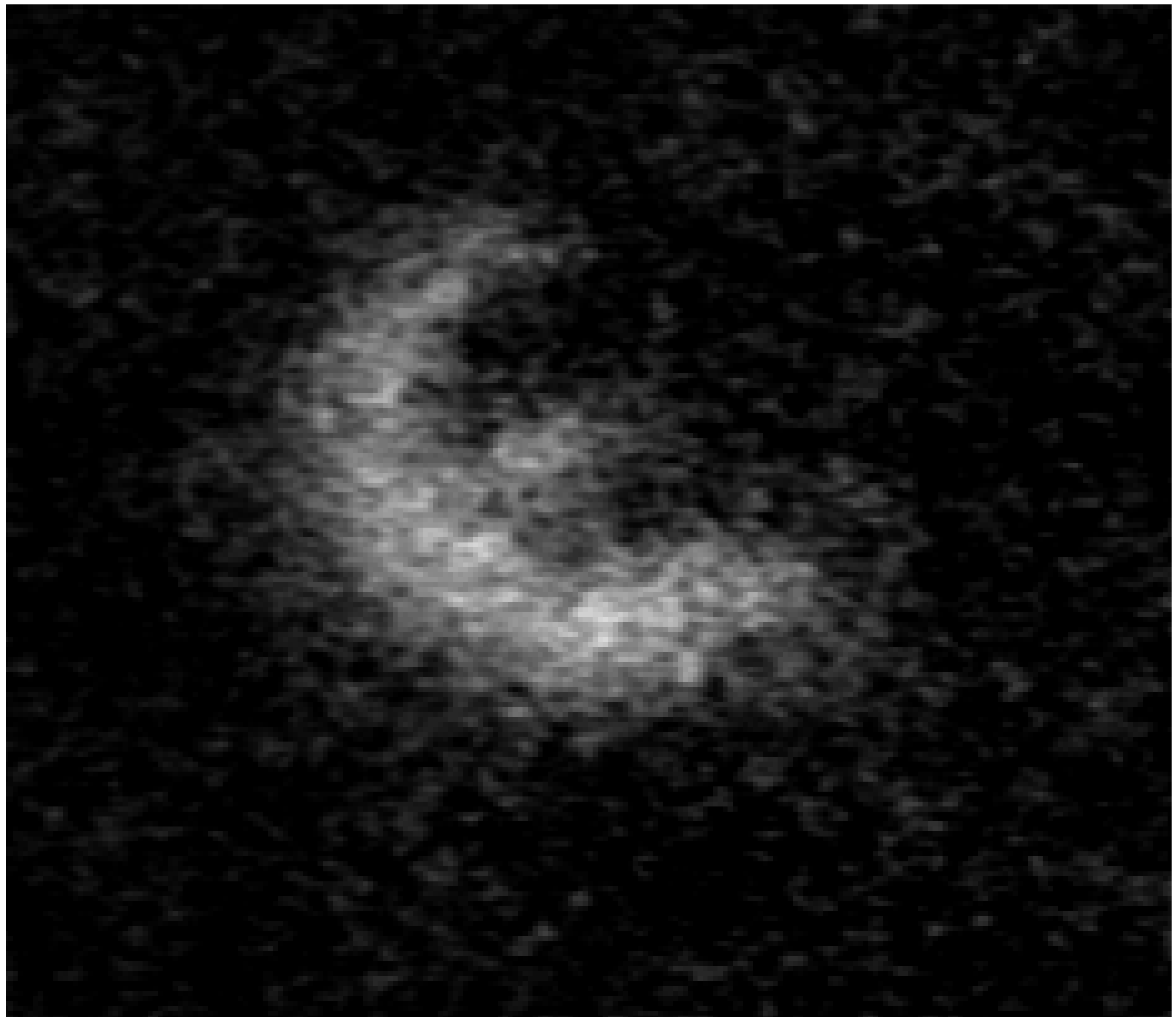

This unique artificial aurora formation was unexpectedly generated by the super-Heater, operating at 630 MW, on 12 November 2001 at 16:41:20 UT with the beam tilted 9^o South. The wavelength is 557.7 nm and the image integration is 5 sec.

4. Langmuir Turbulence

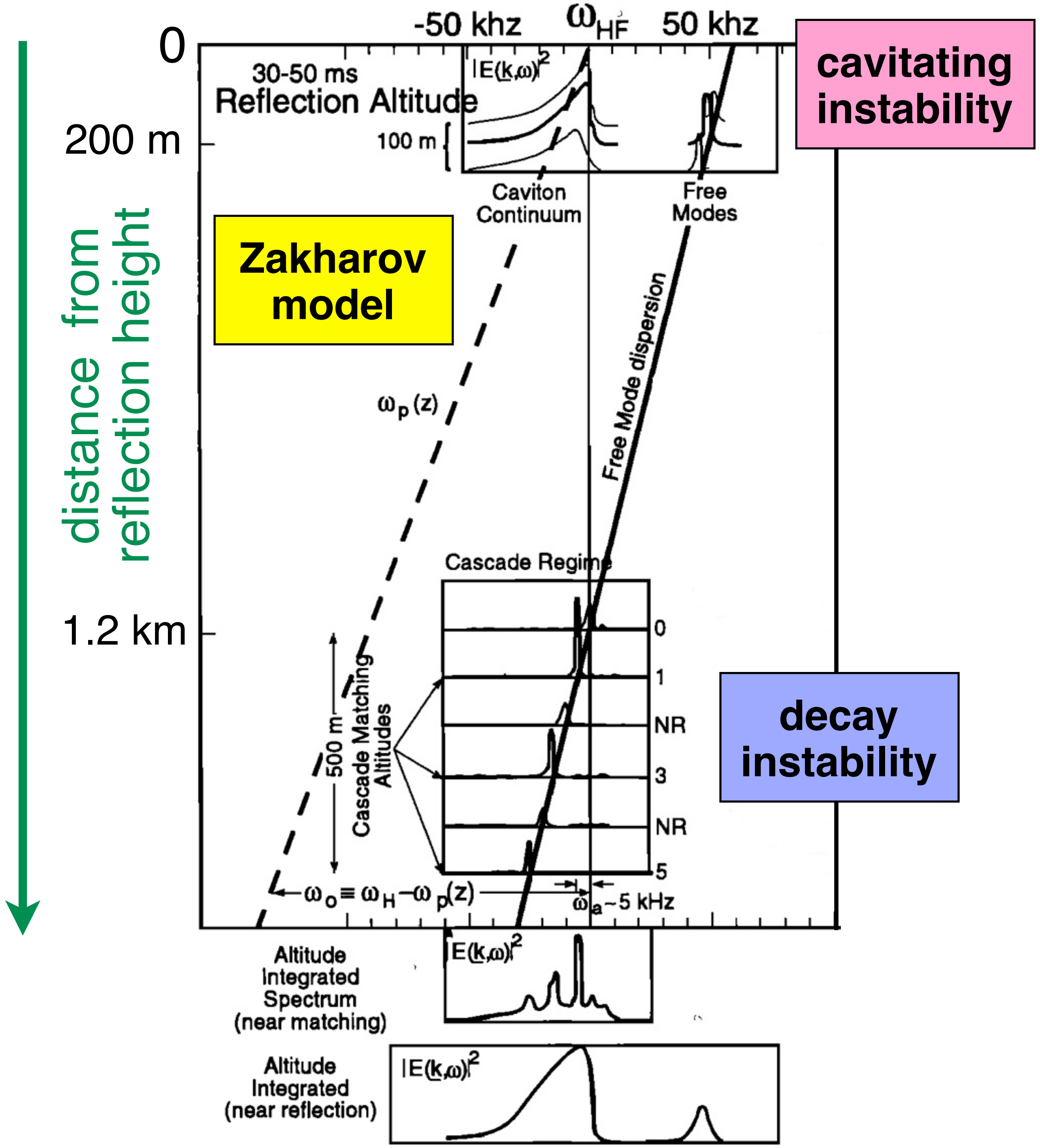

4. Langmuir Turbulence

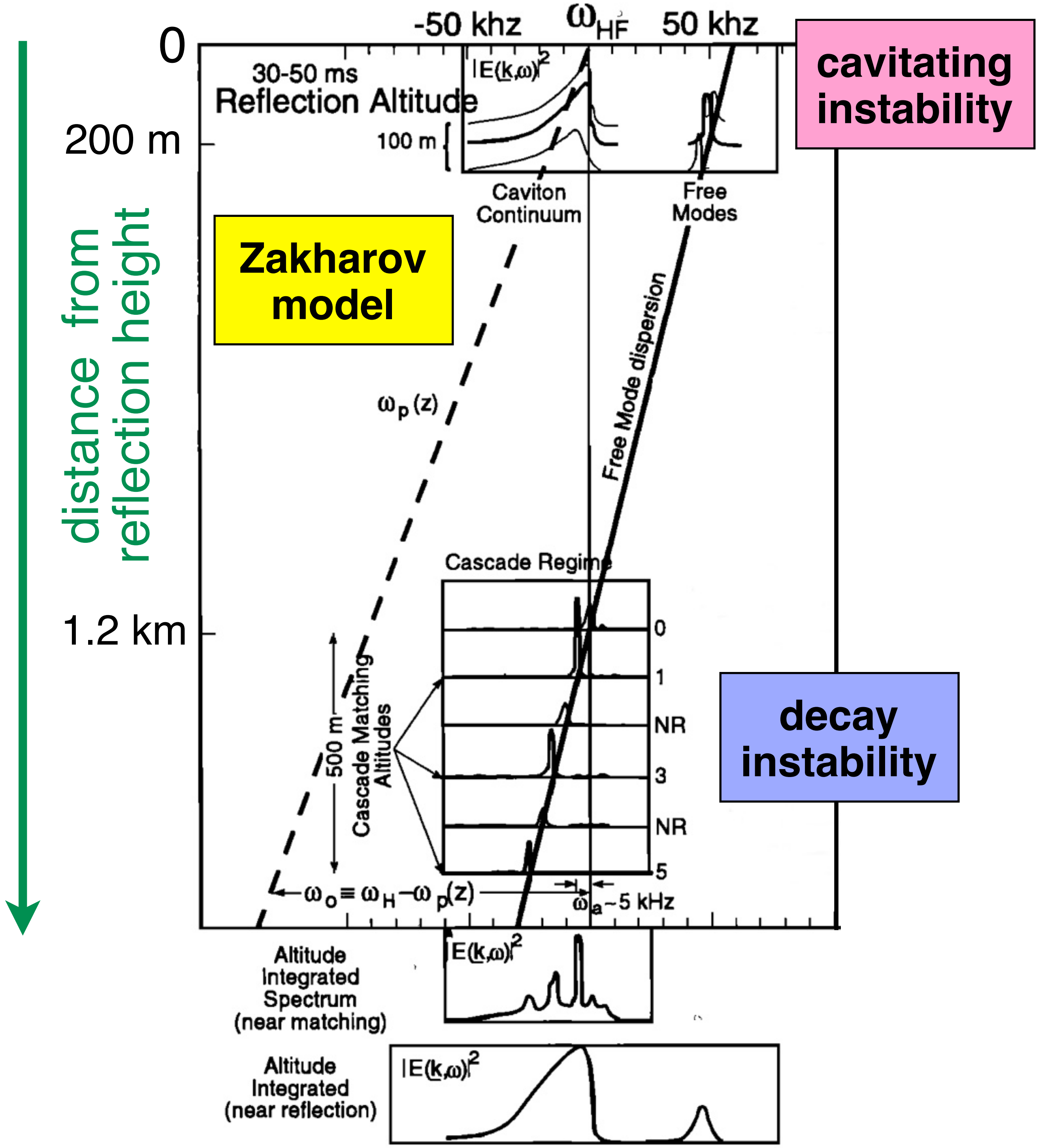

$$\omega_{pe}^2 = \frac{n_e e^2}{\epsilon_o^2 m_e}$$

4. Langmuir Turbulence

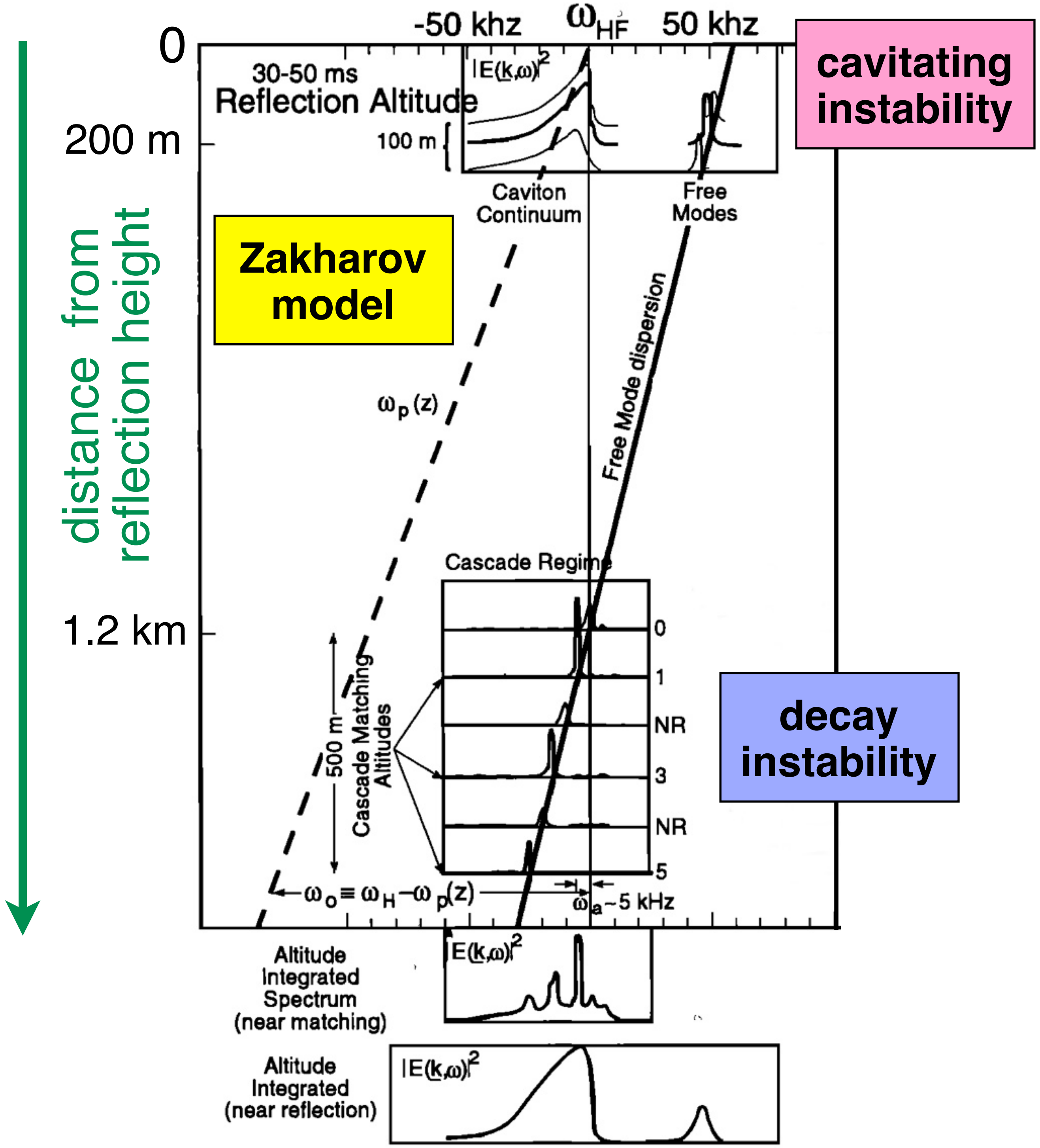

$$\omega_{pe}^2 = \frac{n_e e^2}{\epsilon_o^2 m_e}$$

$$\omega_L^2 = \omega_{pe}^2 + 3k_2 v_{e,th}^2$$

4. Langmuir Turbulence

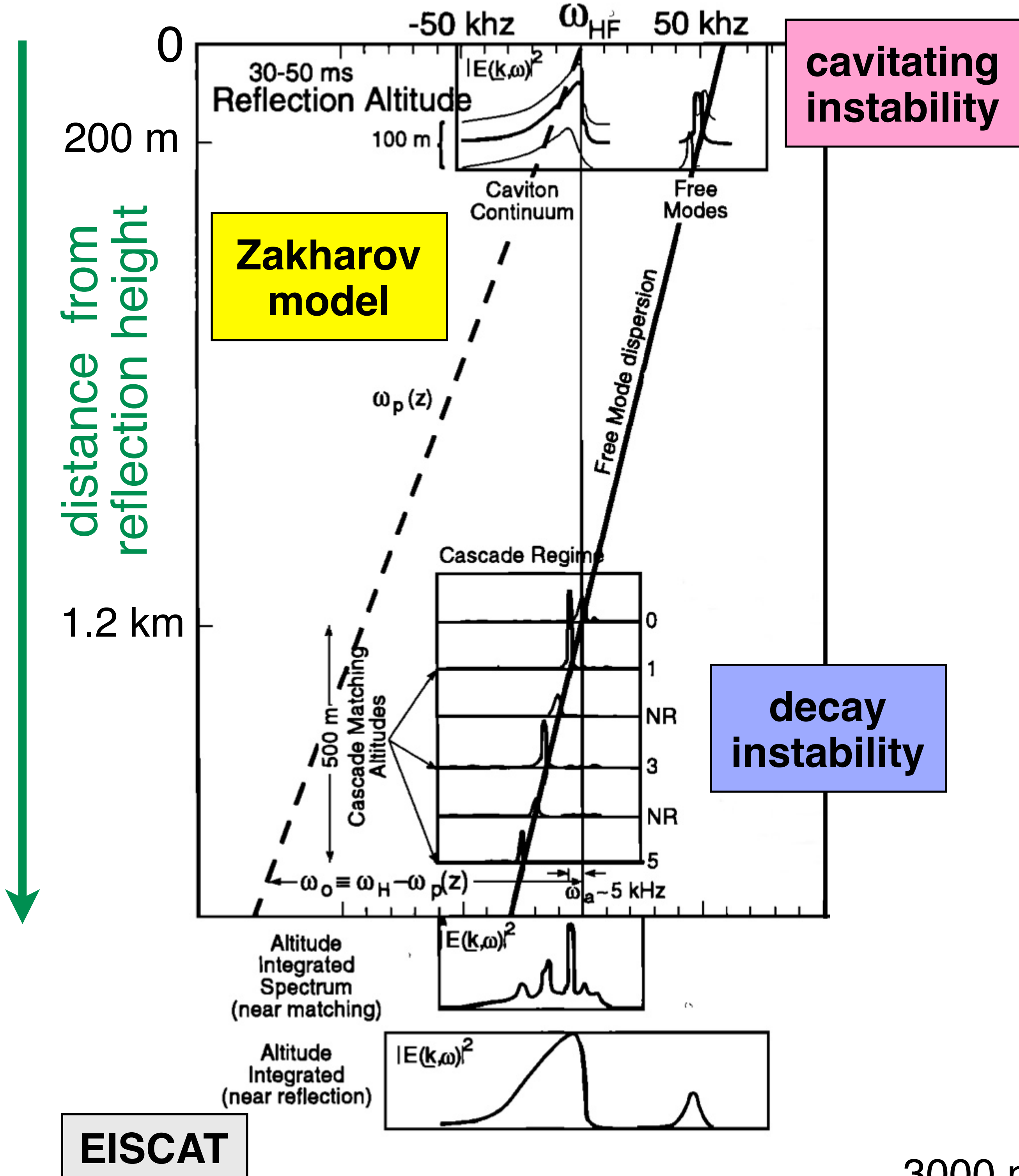

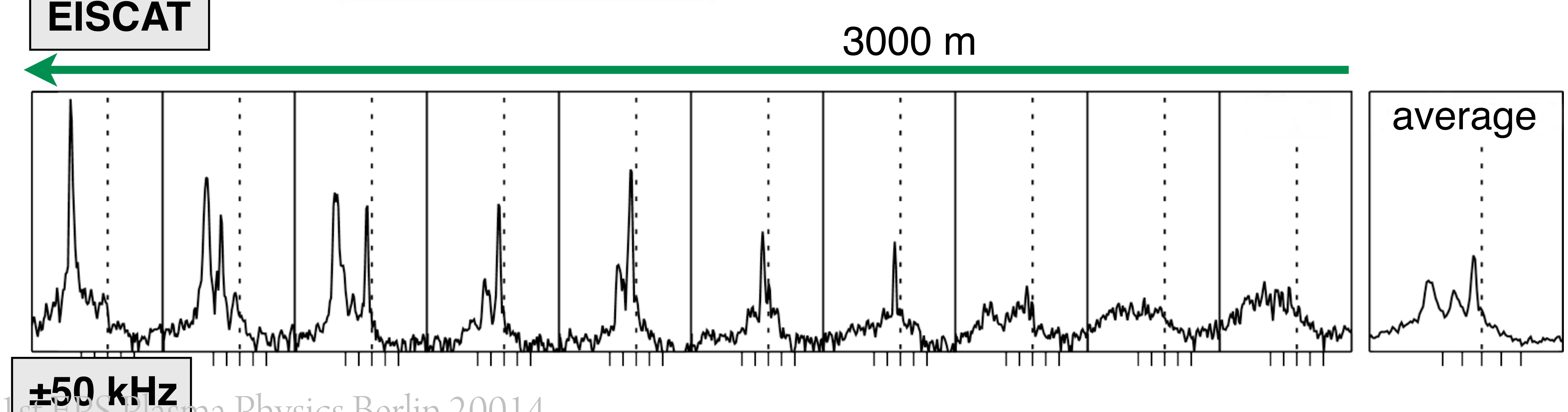

$$\omega_{pe}^2 = \frac{n_e e^2}{\epsilon_o^2 m_e}$$

$$\omega_L^2 = \omega_{pe}^2 + 3k_2 v_{e,th}^2$$

4. Langmuir Turbulence

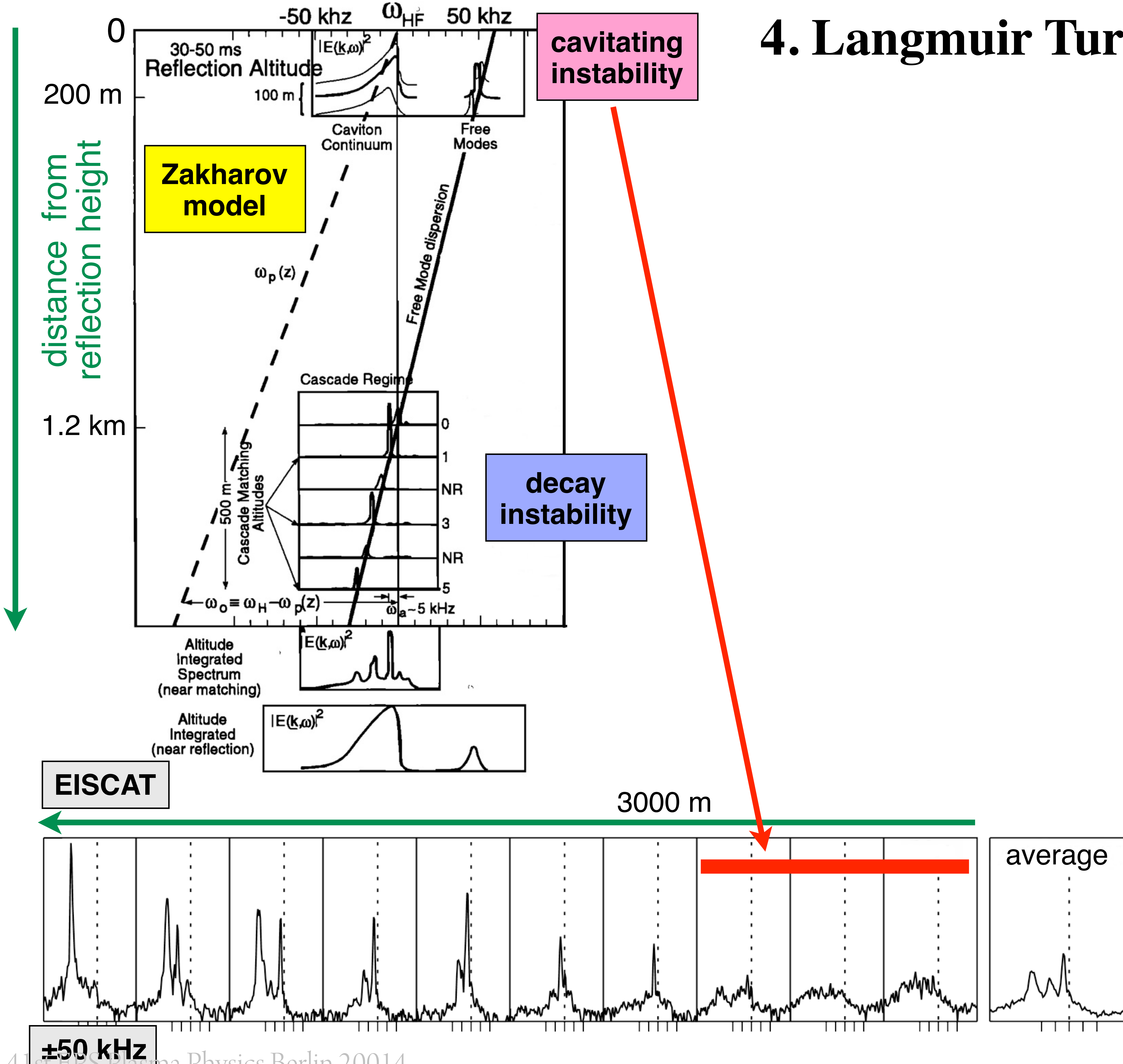

$$\omega_{pe}^2 = \frac{n_e e^2}{\epsilon_o^2 m_e}$$

$$\omega_L^2 = \omega_{pe}^2 + 3k_2 v_{e,th}^2$$

4. Langmuir Turbulence

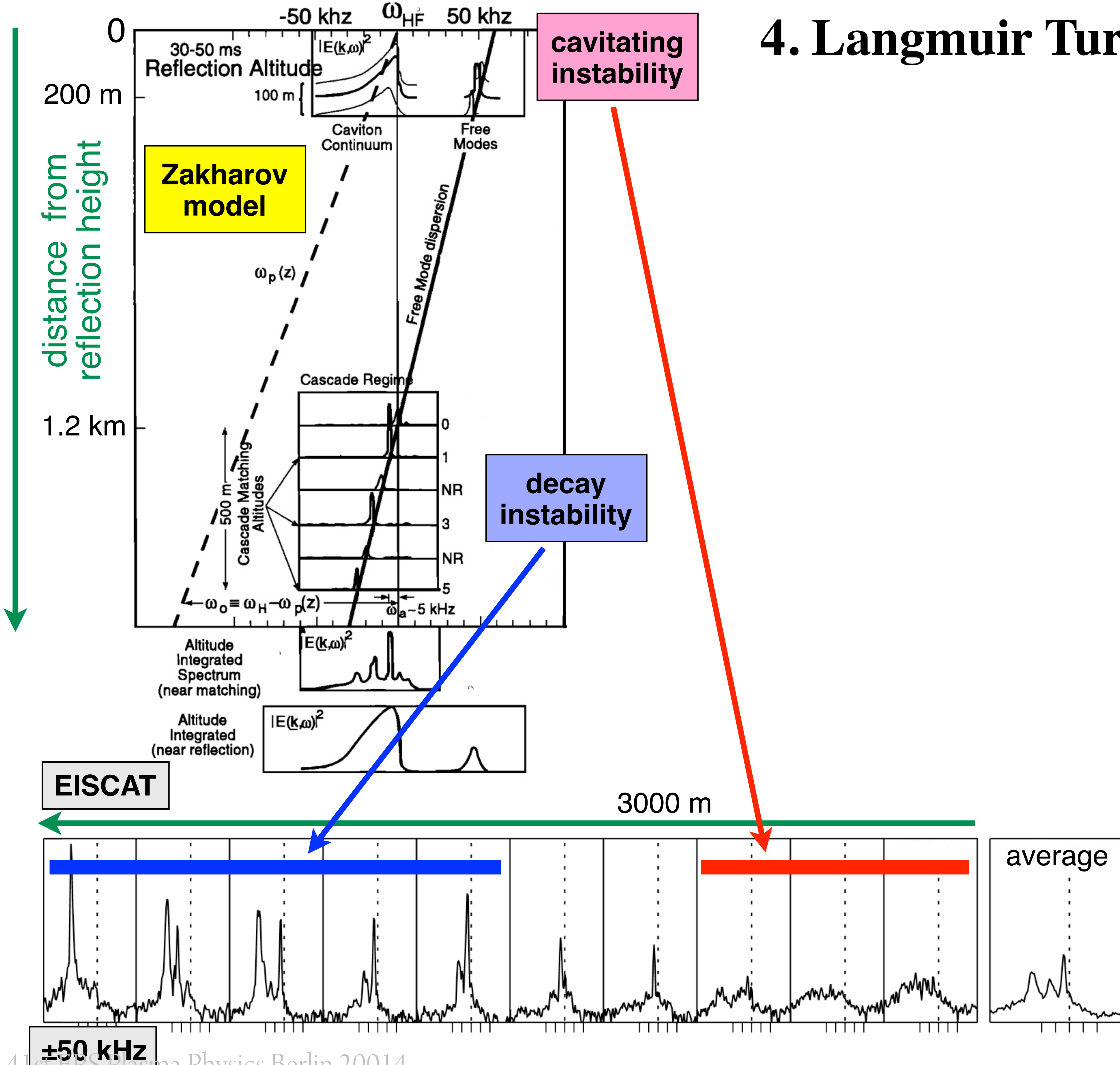

$$\omega_{pe}^2 = \frac{n_e e^2}{\epsilon_o^2 m_e}$$

$$\omega_L^2 = \omega_{pe}^2 + 3k_2 v_{e,th}^2$$

4. Langmuir Turbulence

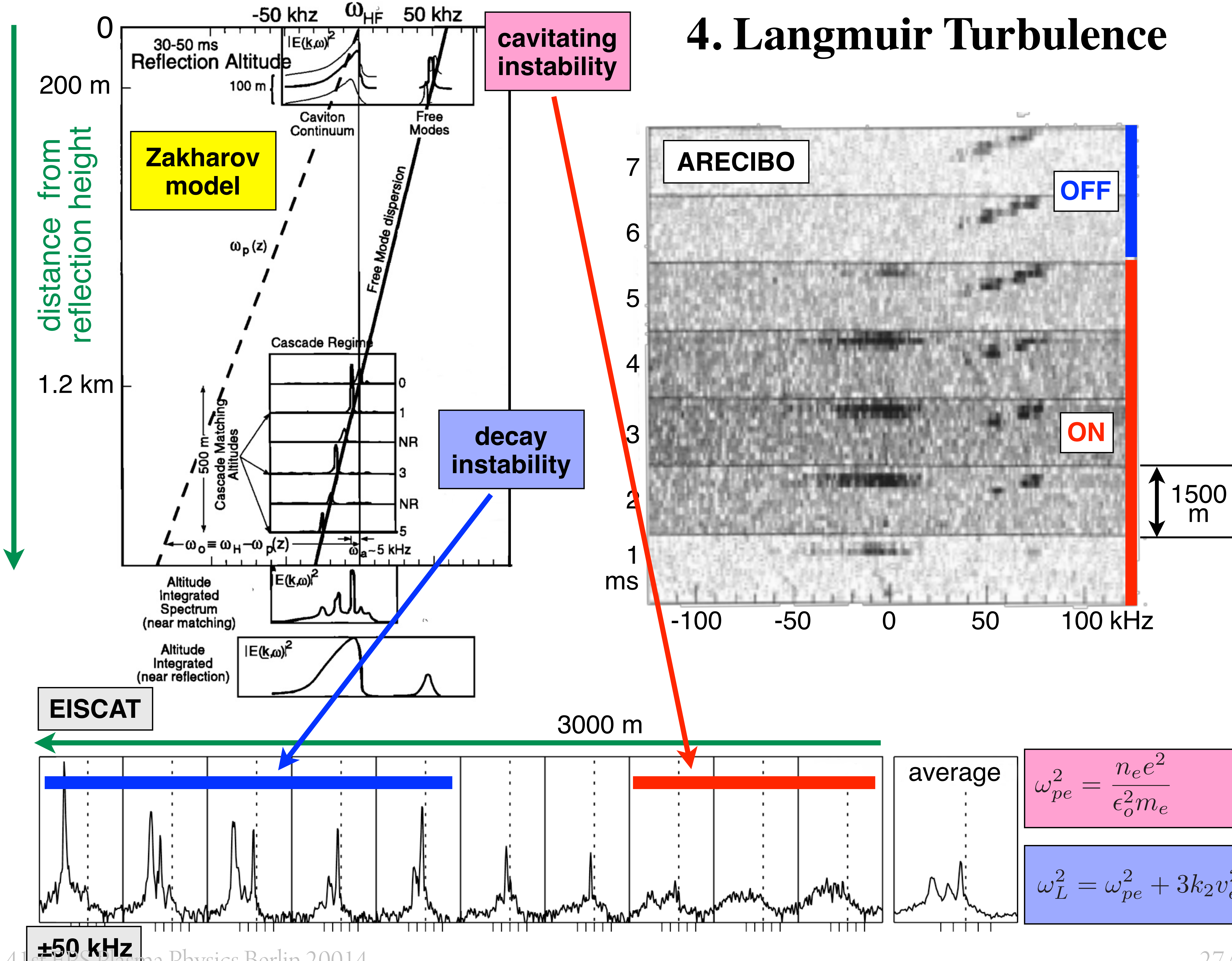

$$\omega_{pe}^2 = \frac{n_e e^2}{\epsilon_o^2 m_e}$$

$$\omega_L^2 = \omega_{pe}^2 + 3k_2 v_{e,th}^2$$

4. Langmuir Turbulence

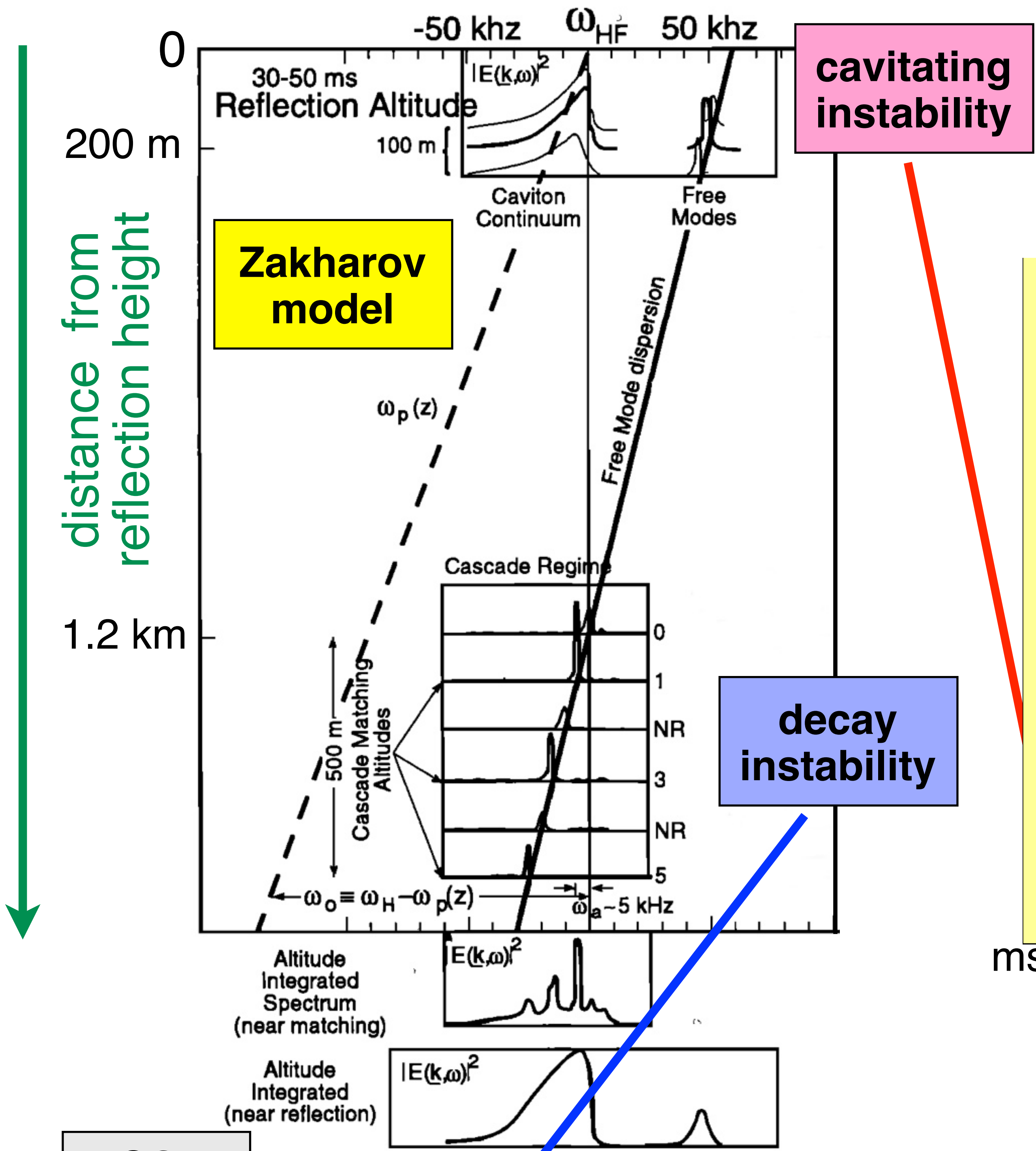

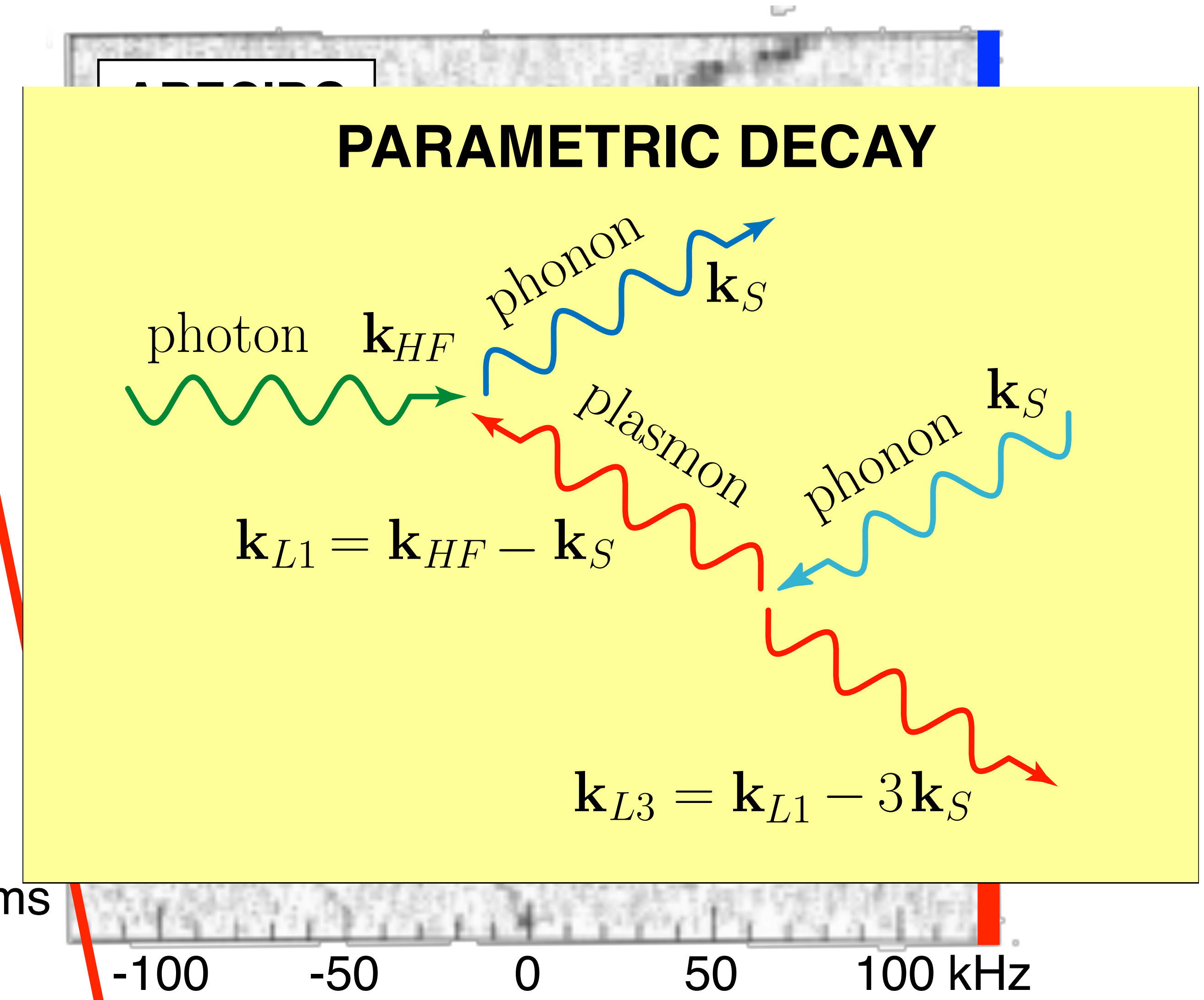

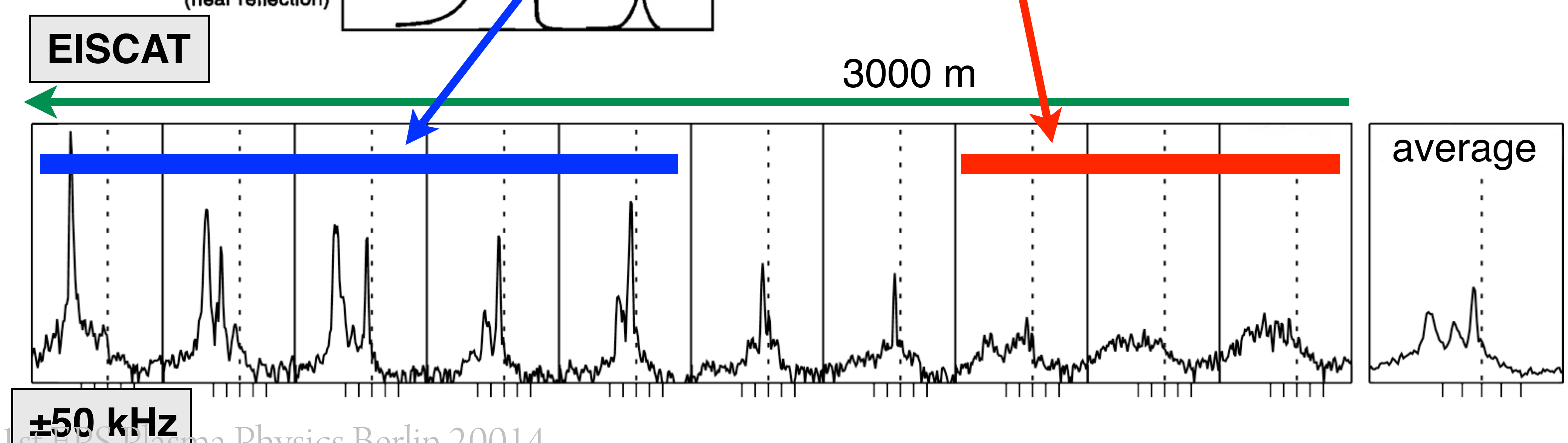

$$\omega_{pe}^2 = \frac{n_e e^2}{\epsilon_o^2 m_e}$$

$$\omega_L^2 = \omega_{pe}^2 + 3k_2 v_{e,th}^2$$

4. Langmuir Turbulence

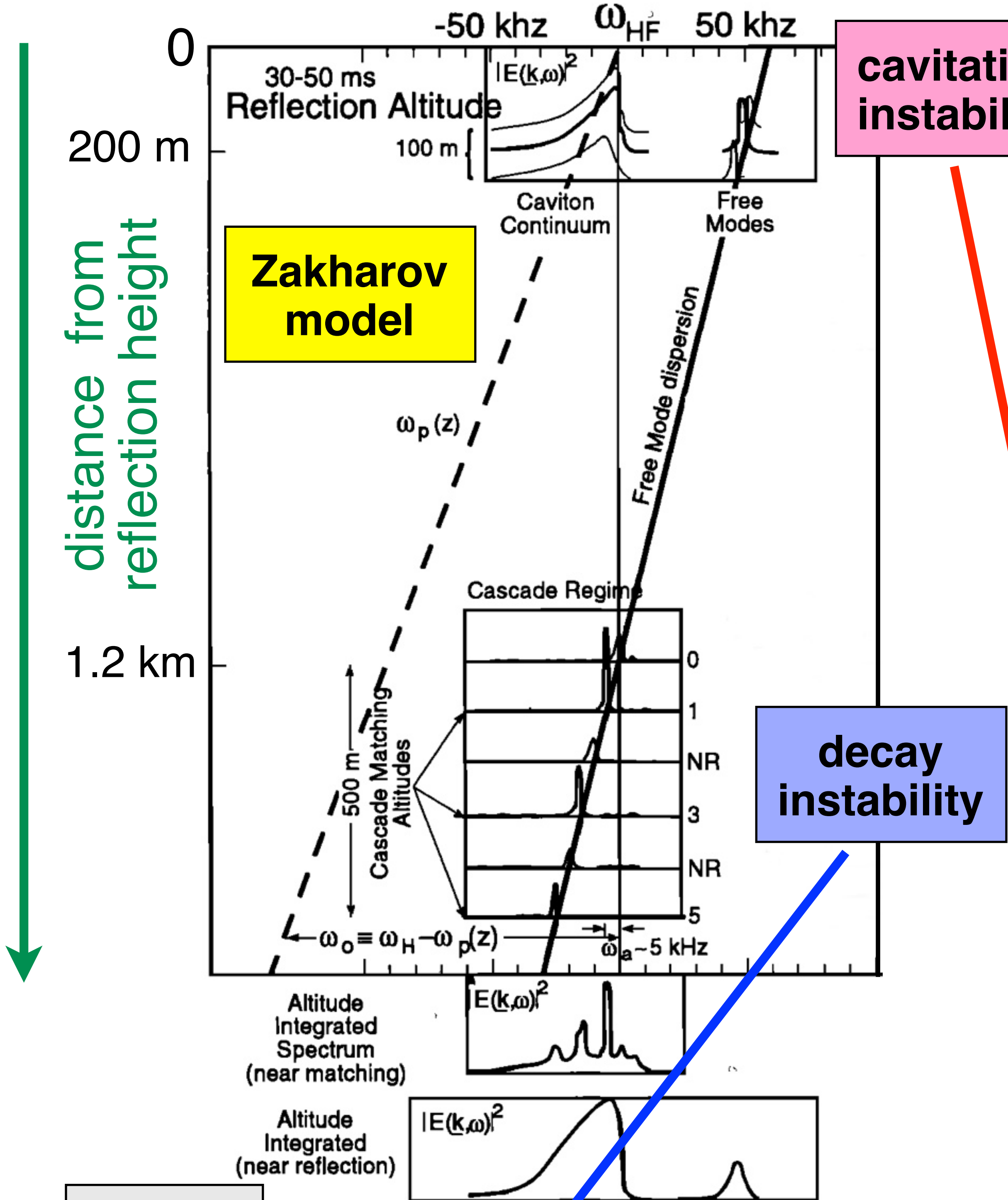

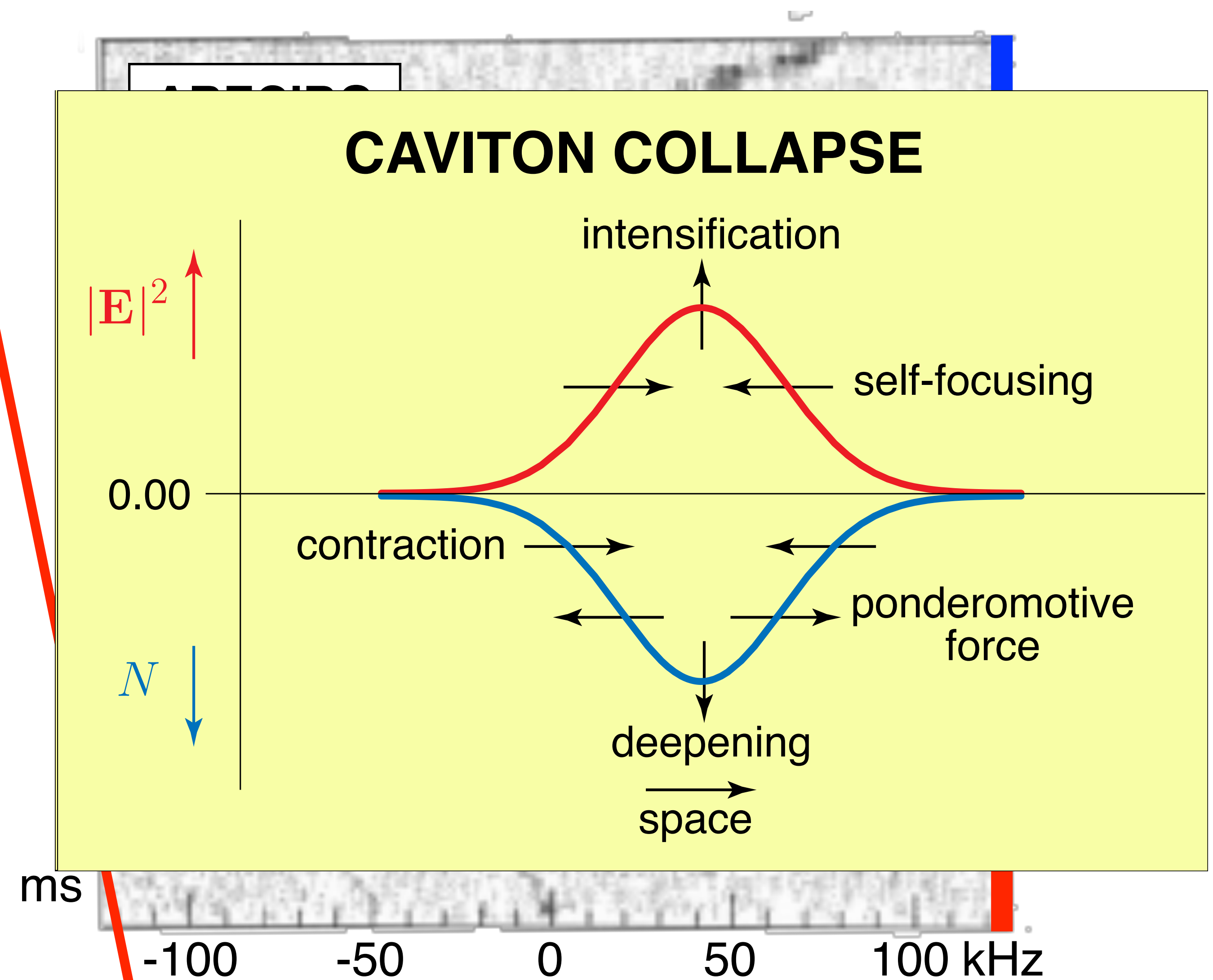

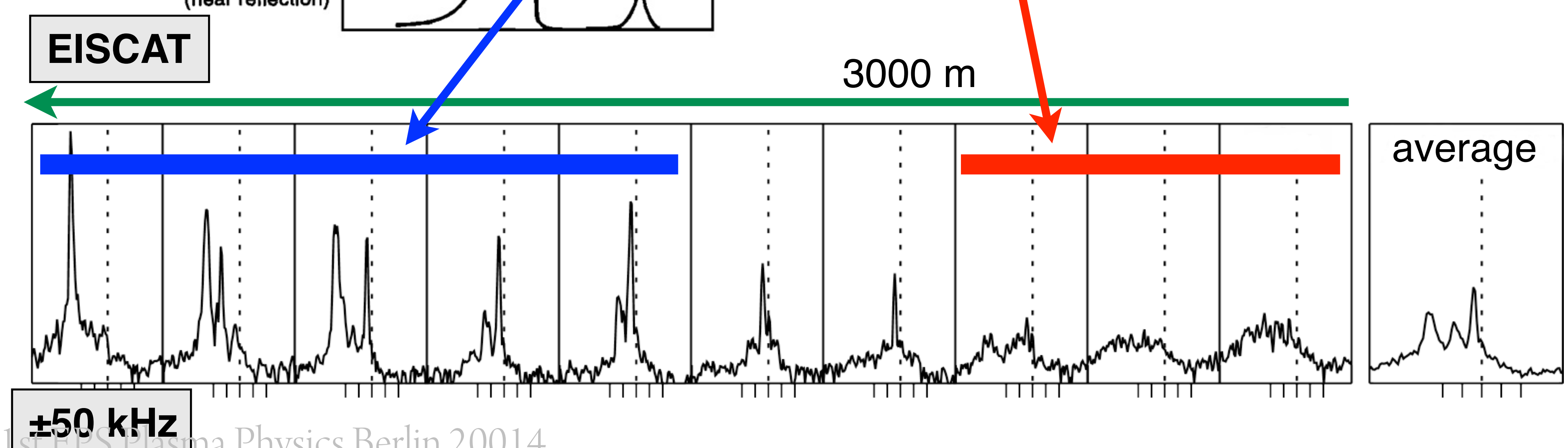

$$\omega_{pe}^2 = \frac{n_e e^2}{\epsilon_o^2 m_e}$$

$$\omega_L^2 = \omega_{pe}^2 + 3k_2 v_{e,th}^2$$

4. Langmuir Turbulence

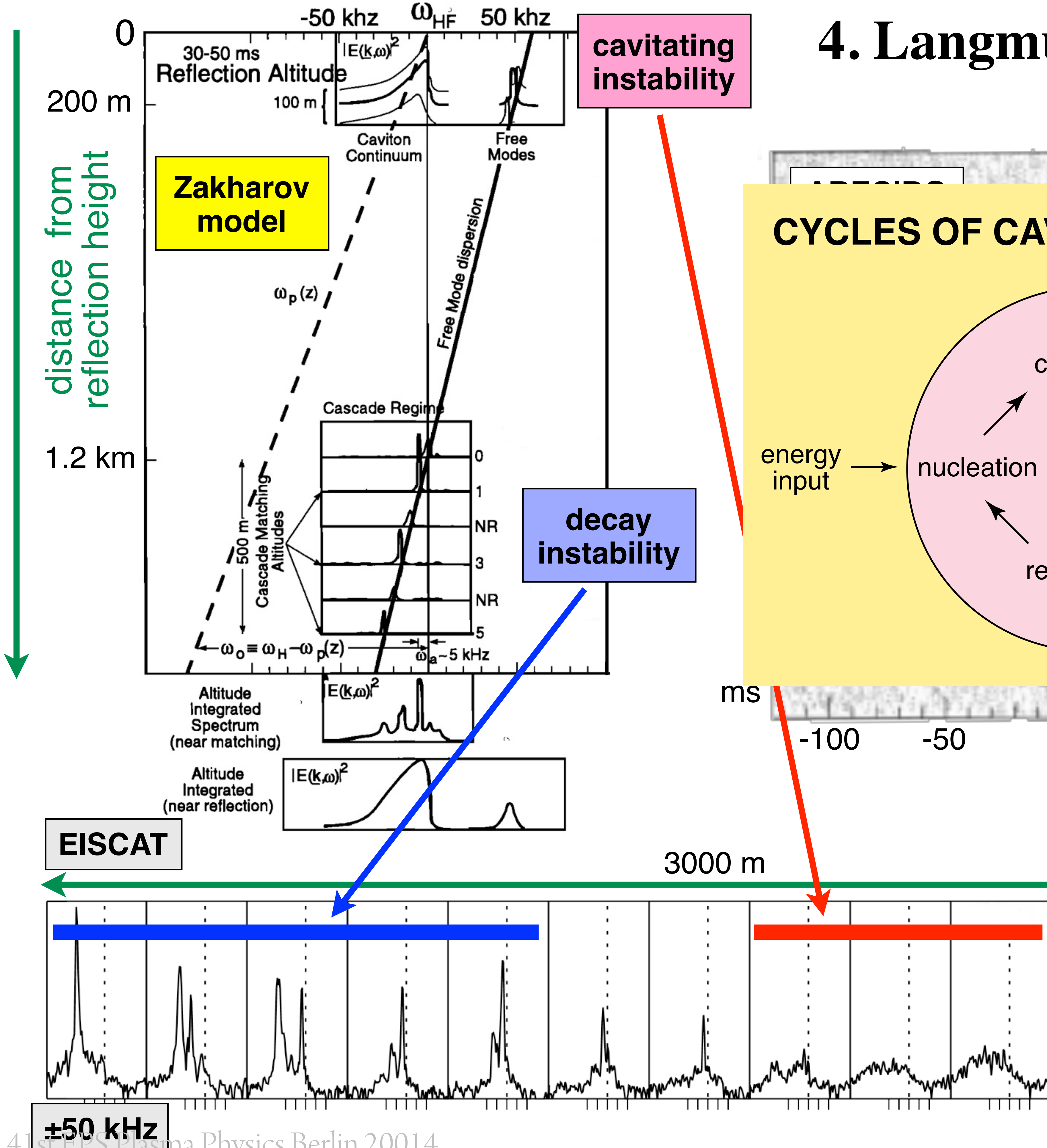

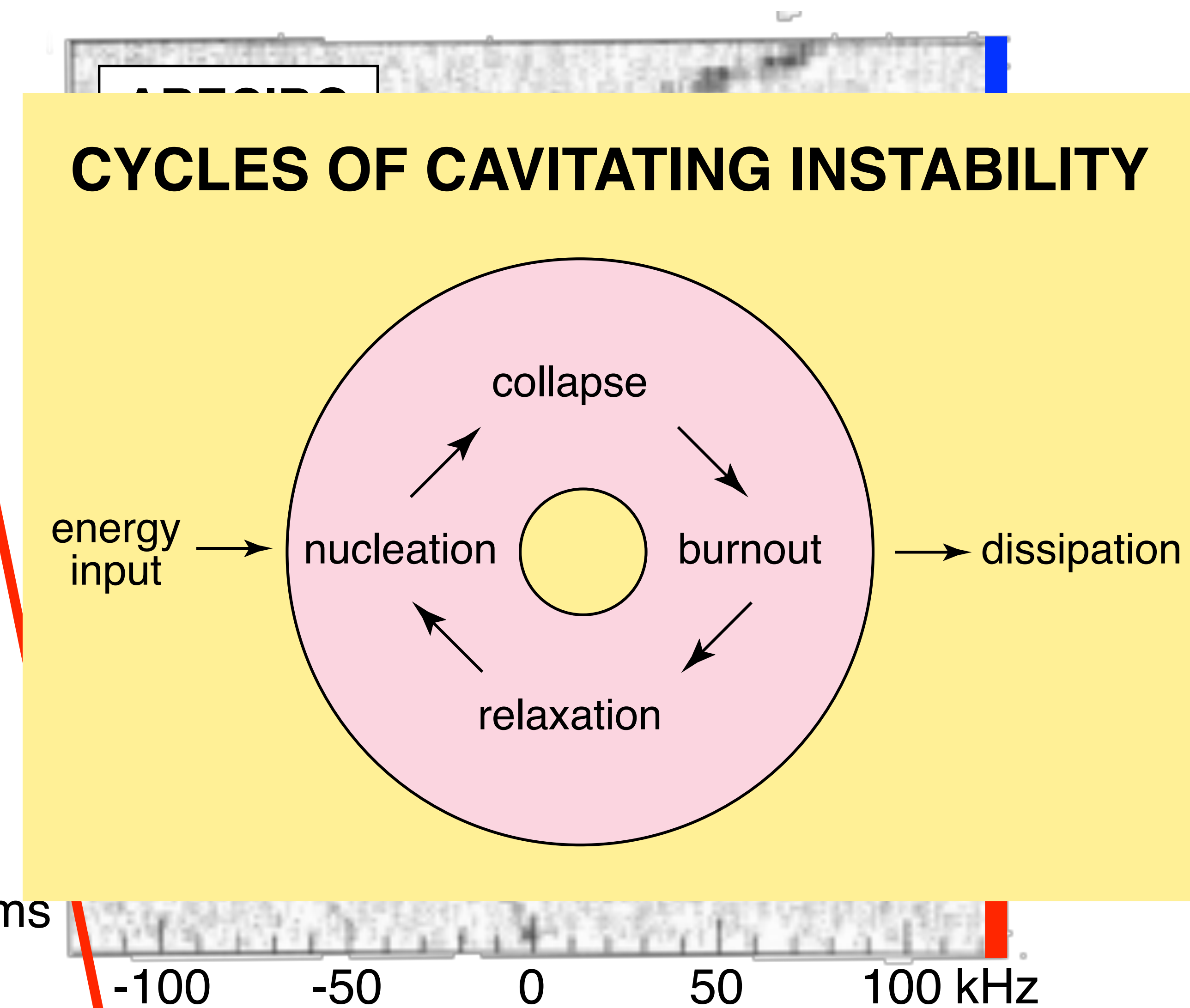

$$\omega_{pe}^2 = \frac{n_e e^2}{\epsilon_o^2 m_e}$$

$$\omega_L^2 = \omega_{pe}^2 + 3k_2 v_{e,th}^2$$

ARTIFICIAL AURORA

16 Feb 1999 4.04 MHz ERP = 75 MW O-mode

17:40 HF ON

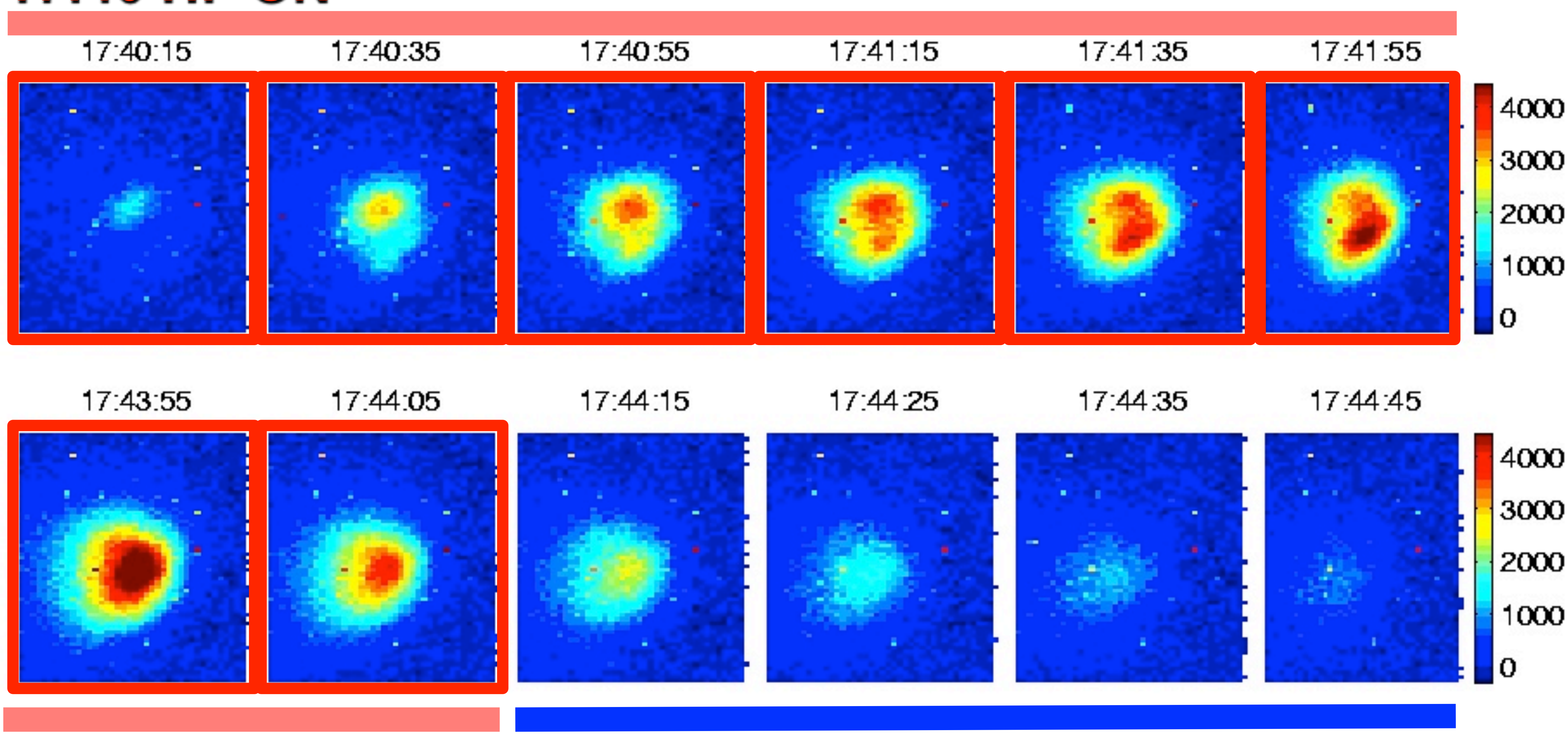

17:44 HF OFF

Brandstrom et al., GRL, 1999

advertisement

the future: EISCAT_3D

artist concept

advertisement

the future: EISCAT_3D

artist concept

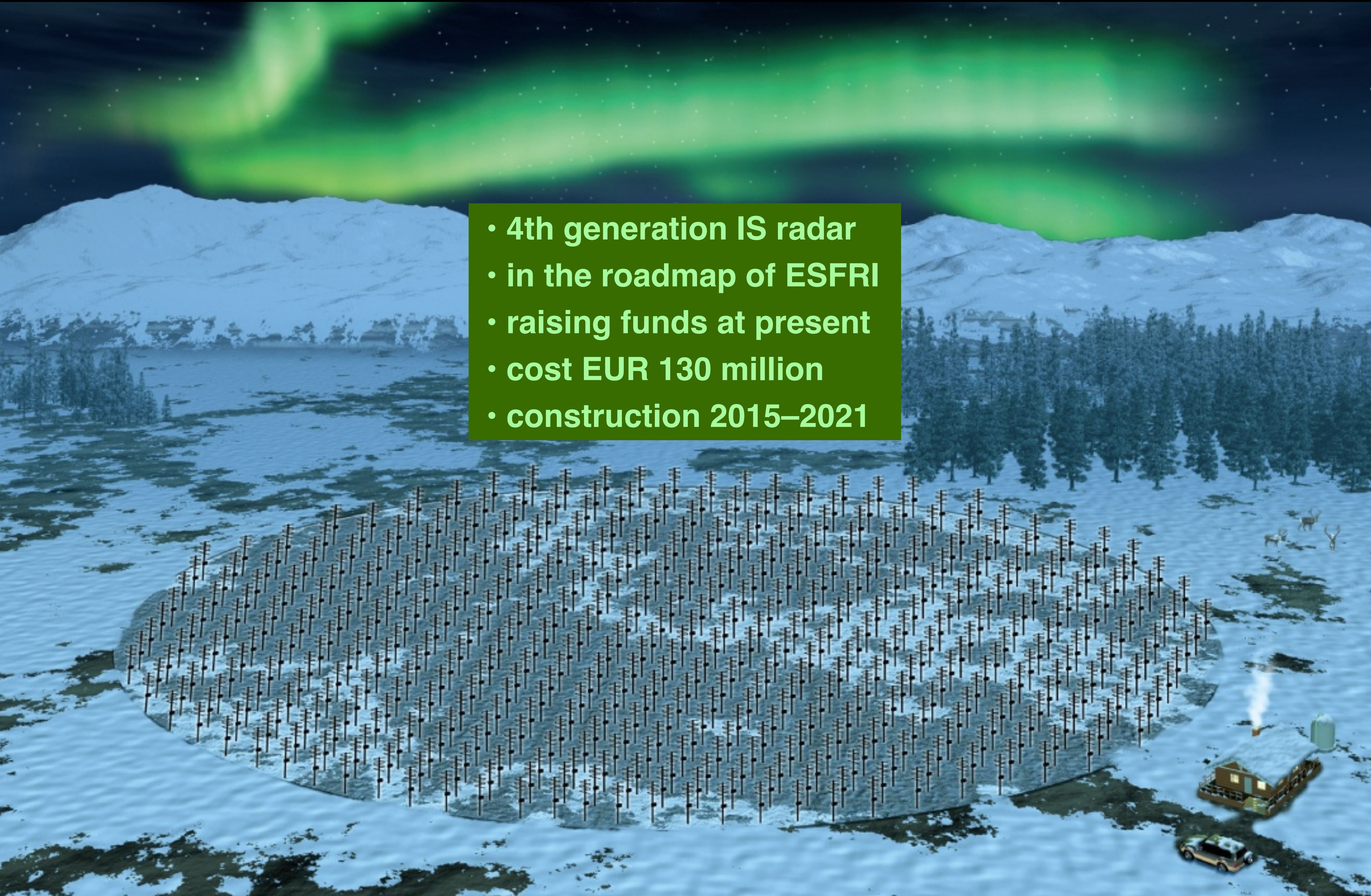

- 4th generation IS radar
- in the roadmap of ESFRI
- raising funds at present
- cost EUR 130 million
- construction 2015–2021

incoherent scatter theory is one of the first and most compelling successes of linear plasma physics theory.

Don Farley

… the predictions of the 2-D Langmuir turbulence theory in [ionospheric heating] are now well verified. It is one of the best verified regimes of plasma turbulence.

Don DuBois

thank you !

Radar Sounding of the Auroral Plasma

by

Cesar La Hoz

cesar.la.hoz@uit.no

with contributions by my friends

Brett Isham, Mike Kosch and Mike Rietveld

The Arctic University of Norway

Cornell University

STRONG LANGMUIR TURBULENCE
CAVITON COLLAPSE

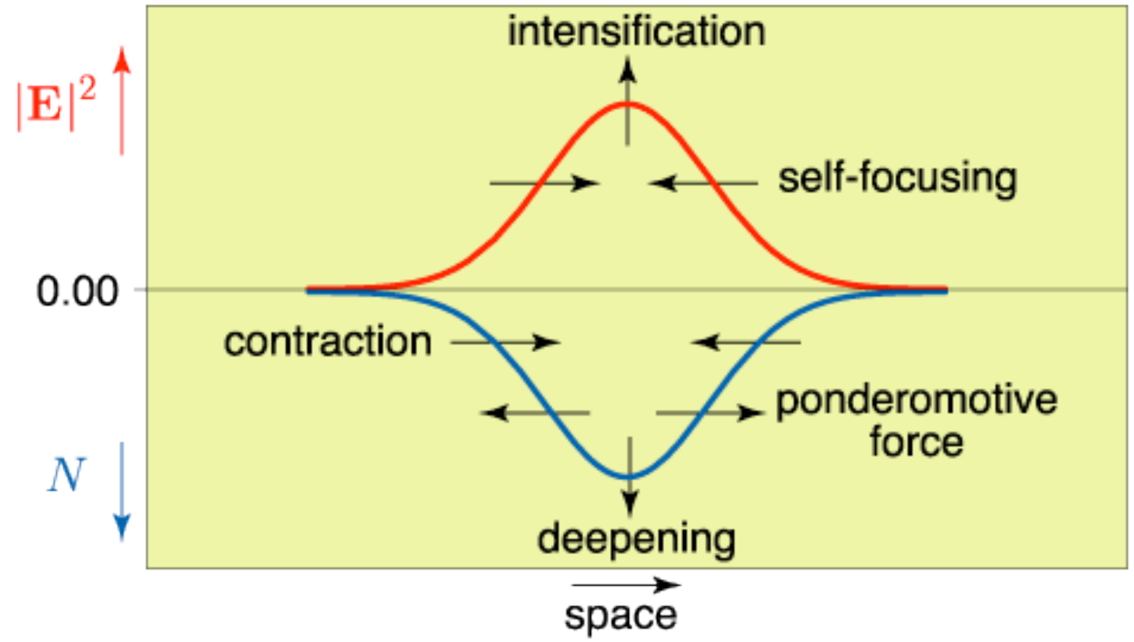

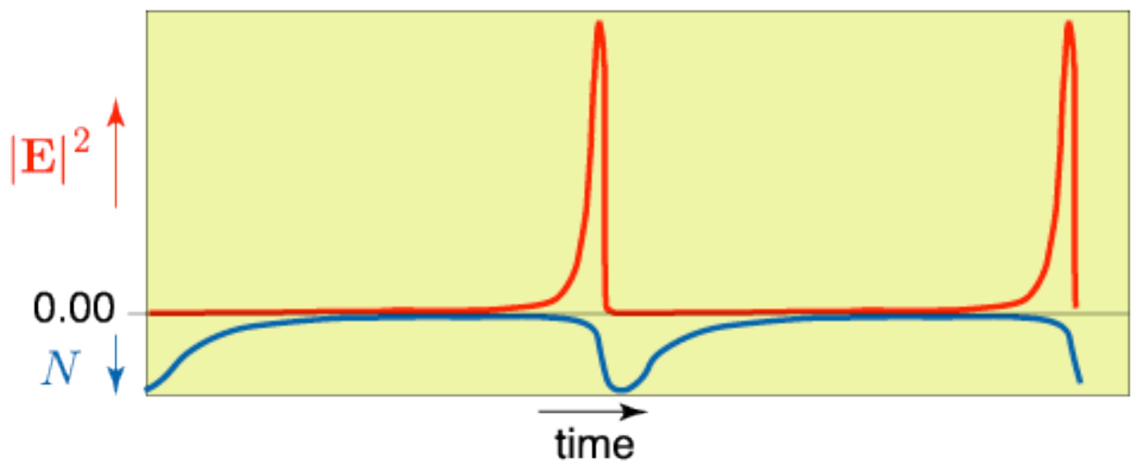

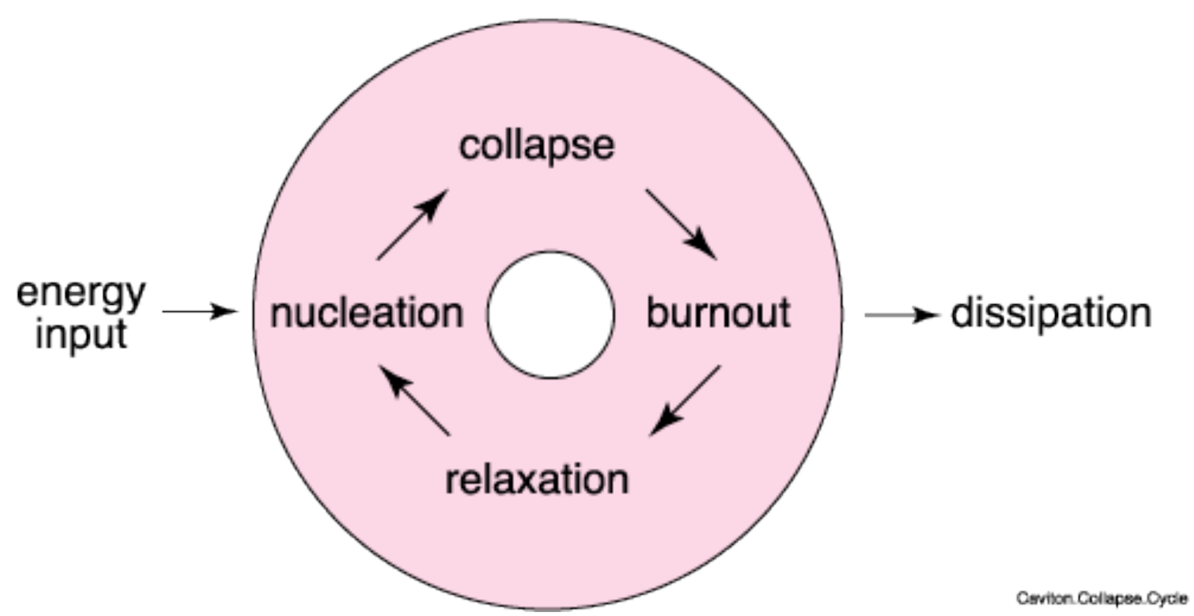

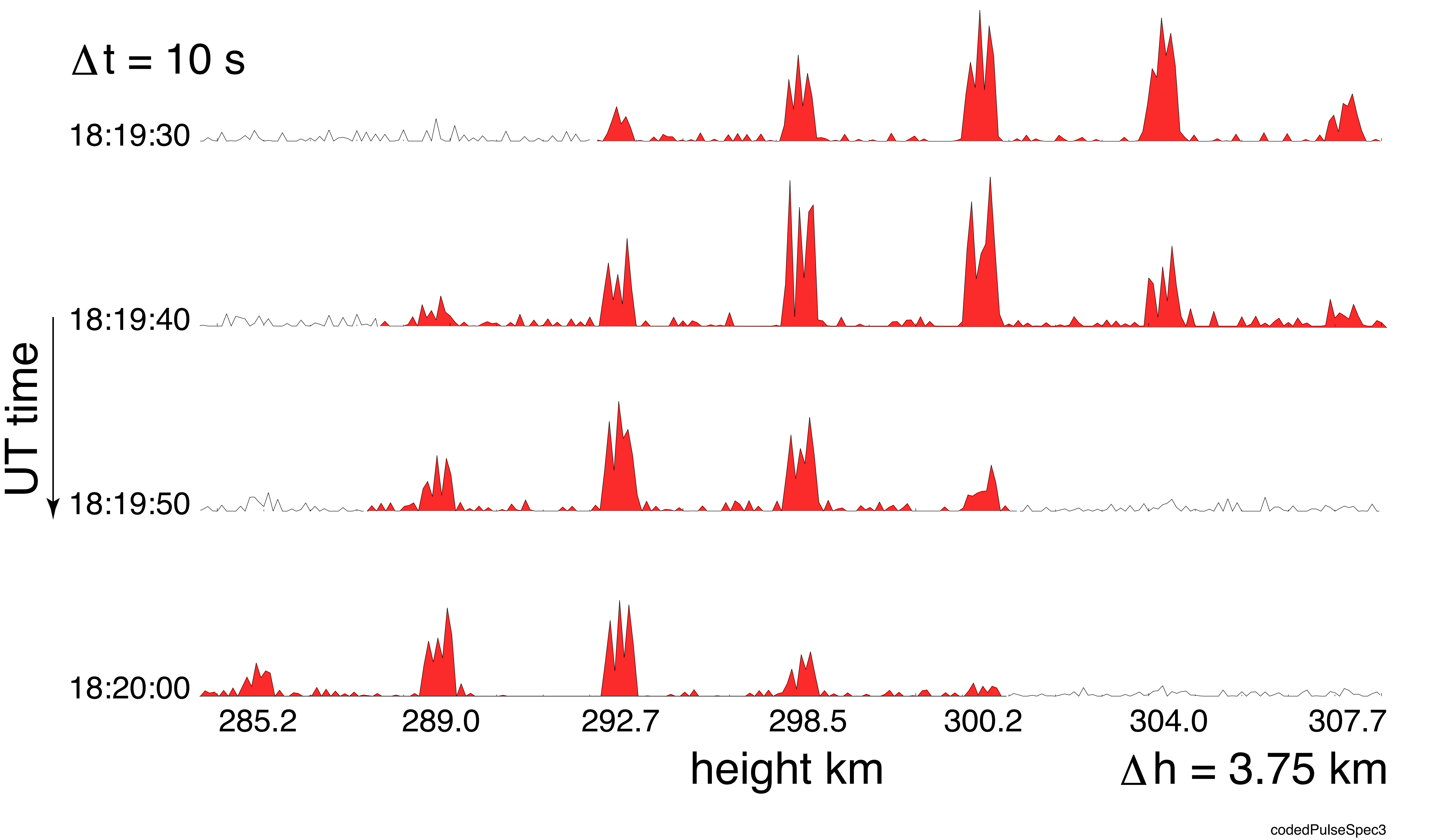

Δt = 10 s
18:19:30
18:19:40
18:19:50
18:20:00
UT time
285.2
289.0
292.7
298.5
300.2
304.0
307.7
height km
Δh = 3.75 km
codedPulseSpec3

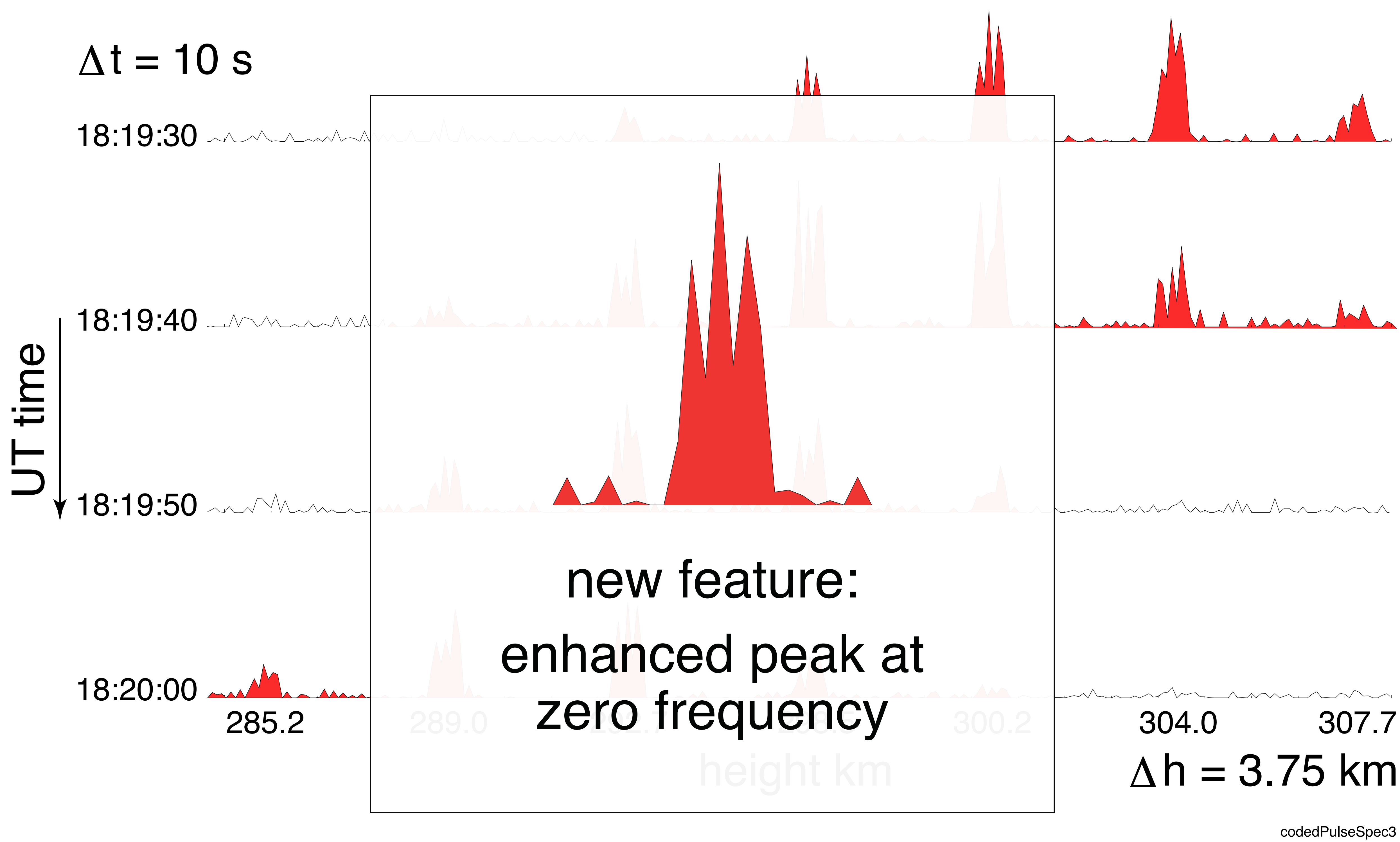

Δt = 10 s
18:19:30
18:19:40
18:19:50
18:20:00
UT time
285.2
304.0
307.7
Δh = 3.75 km
new feature:
enhanced peak at
zero frequency
codedPulseSpec3

$$S_e(\mathbf{k},\omega) = N_e \left| 1 - \frac{\chi_e(\mathbf{k},\omega)}{\epsilon(\mathbf{k},\omega)} \right|^2 \int f_e(\mathbf{v})\delta(\omega - \mathbf{k}\cdot\mathbf{v})d^3\mathbf{v} + \sum_i N_i \left| \frac{\chi_e(\mathbf{k},\omega)}{\epsilon(\mathbf{k},\omega)} \right|^2 \int f_i(\mathbf{v})\delta(\omega - \mathbf{k}\cdot\mathbf{v})d^3\mathbf{v}$$

$$S_e(\mathbf{k},\omega) = N_e\left|1 - \frac{\chi_e(\mathbf{k},\omega)}{\epsilon(\mathbf{k},\omega)}\right|^2 \int f_e(\mathbf{v})\delta(\omega - \mathbf{k}\cdot\mathbf{v})d^3\mathbf{v} + \sum_i N_i \left|\frac{\chi_e(\mathbf{k},\omega)}{\epsilon(\mathbf{k},\omega)}\right|^2 \int f_i(\mathbf{v})\delta(\omega - \mathbf{k}\cdot\mathbf{v})d^3\mathbf{v}$$

$$S_e(\mathbf{k},\omega) = N_e\left|1 - \frac{\chi_e(\mathbf{k},\omega)}{\epsilon(\mathbf{k},\omega)}\right|^2 \int f_e(\mathbf{v})\delta(\omega - \mathbf{k}\cdot\mathbf{v})d^3\mathbf{v} + \sum_i N_i\left|\frac{\chi_e(\mathbf{k},\omega)}{\epsilon(\mathbf{k},\omega)}\right|^2 \int f_i(\mathbf{v})\delta(\omega - \mathbf{k}\cdot\mathbf{v})d^3\mathbf{v}$$

$$\epsilon(\mathbf{k},\omega) = \mathbf{0}$$

Ion Line $S_{IL}(\mathbf{k},\omega)$

$$S_e(\mathbf{k},\omega) = N_e \left| 1 - \frac{\chi_e(\mathbf{k},\omega)}{\epsilon(\mathbf{k},\omega)} \right|^2 \int f_e(\mathbf{v}) \delta(\omega - \mathbf{k}\cdot\mathbf{v}) d^3\mathbf{v} + \sum_i N_i \left| \frac{\chi_e(\mathbf{k},\omega)}{\epsilon(\mathbf{k},\omega)} \right|^2 \int f_i(\mathbf{v}) \delta(\omega - \mathbf{k}\cdot\mathbf{v}) d^3\mathbf{v}$$

$$\epsilon(\mathbf{k},\omega) = \mathbf{0}$$

$$\omega_{ia}(k) \approx k\sqrt{\frac{T_e + 3\,T_i}{m_i}}$$

IS.SpecFormula4.ai6

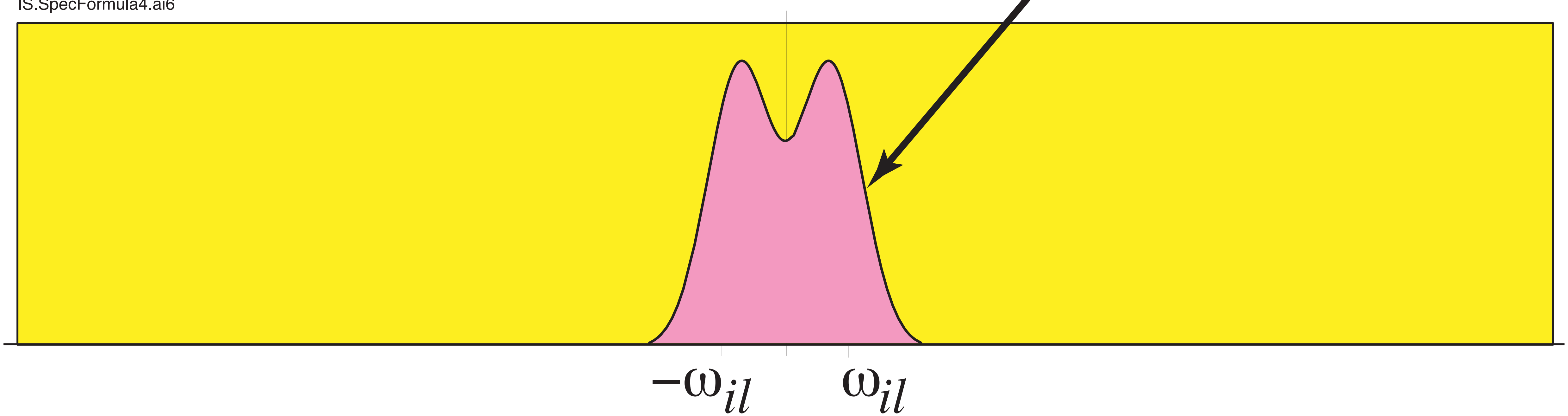

Ion Line

Plasma Line $S_{PL}(\mathbf{k},\omega)$ **Ion Line** $S_{IL}(\mathbf{k},\omega)$

$$S_e(\mathbf{k},\omega) = N_e \left| 1 - \frac{\chi_e(\mathbf{k},\omega)}{\epsilon(\mathbf{k},\omega)} \right|^2 \int f_e(\mathbf{v})\delta(\omega - \mathbf{k}\cdot\mathbf{v})d^3\mathbf{v} + \sum_i N_i \left| \frac{\chi_e(\mathbf{k},\omega)}{\epsilon(\mathbf{k},\omega)} \right|^2 \int f_i(\mathbf{v})\delta(\omega - \mathbf{k}\cdot\mathbf{v})d^3\mathbf{v}$$

$$\epsilon(\mathbf{k},\omega) = \mathbf{0}$$

$$\omega_{pl}(k) \approx \omega_{pe}(1+3\ \lambda_D^2 k^2)$$

$$\omega_{ia}(k) \approx k\sqrt{\frac{T_e + 3\,T_i}{m_i}}$$

IS.SpecFormula4.ai6

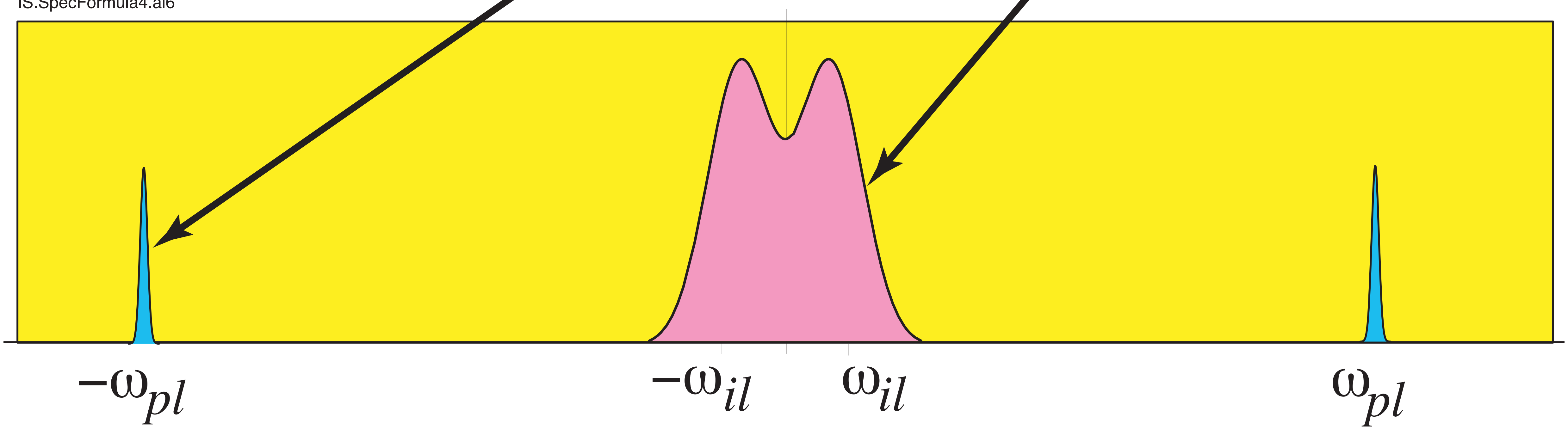

downshifted Plasma Line **Ion Line** **upshifted Plasma Line**

Plasma Line $S_{PL}(\mathbf{k},\omega)$ **Ion Line** $S_{IL}(\mathbf{k},\omega)$

$$S_e(\mathbf{k},\omega) = N_e \left| 1 - \frac{\chi_e(\mathbf{k},\omega)}{\epsilon(\mathbf{k},\omega)} \right|^2 \int f_e(\mathbf{v}) \delta(\omega - \mathbf{k}\cdot\mathbf{v}) d^3\mathbf{v} + \sum_i N_i \left| \frac{\chi_e(\mathbf{k},\omega)}{\epsilon(\mathbf{k},\omega)} \right|^2 \int f_i(\mathbf{v}) \delta(\omega - \mathbf{k}\cdot\mathbf{v}) d^3\mathbf{v}$$

Plasma Line $S_{PL}(\mathbf{k},\omega)$ **Ion Line** $S_{IL}(\mathbf{k},\omega)$

$$S_e(\mathbf{k},\omega) = N_e \left|1 - \frac{\chi_e(\mathbf{k},\omega)}{\epsilon(\mathbf{k},\omega)}\right|^2 \int f_e(\mathbf{v})\delta(\omega-\mathbf{k}\cdot\mathbf{v})d^3\mathbf{v} + \sum_i N_i \left|\frac{\chi_e(\mathbf{k},\omega)}{\epsilon(\mathbf{k},\omega)}\right|^2 \int f_i(\mathbf{v})\delta(\omega-\mathbf{k}\cdot\mathbf{v})d^3\mathbf{v}$$

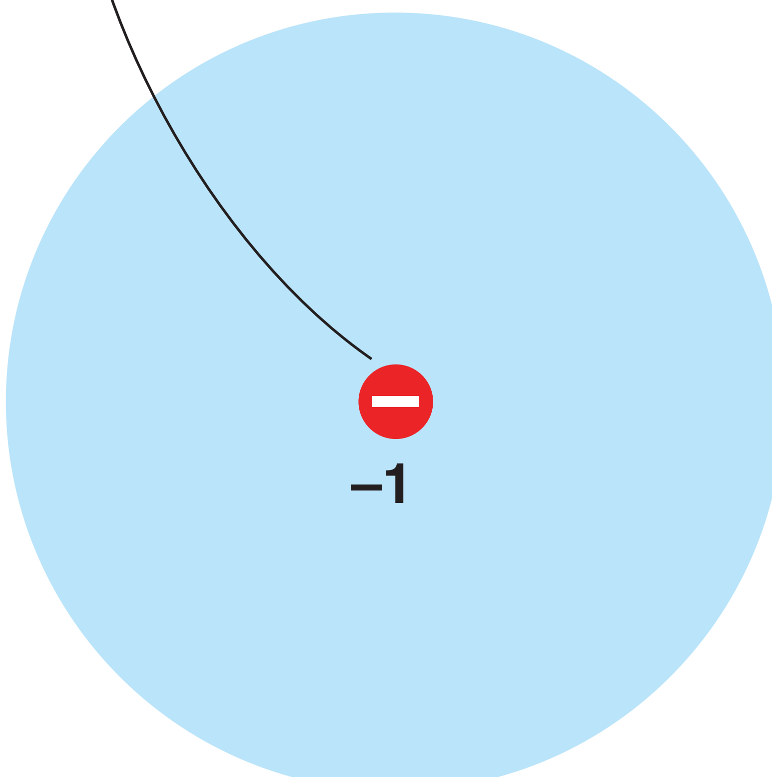

Plasma Line $S_{PL}(\mathbf{k},\omega)$ **Ion Line** $S_{IL}(\mathbf{k},\omega)$

$$S_e(\mathbf{k},\omega) = N_e\left|1 - \frac{\chi_e(\mathbf{k},\omega)}{\epsilon(\mathbf{k},\omega)}\right|^2 \int f_e(\mathbf{v})\delta(\omega - \mathbf{k}\cdot\mathbf{v})d^3\mathbf{v} + \sum_i N_i\left|\frac{\chi_e(\mathbf{k},\omega)}{\epsilon(\mathbf{k},\omega)}\right|^2 \int f_i(\mathbf{v})\delta(\omega - \mathbf{k}\cdot\mathbf{v})d^3\mathbf{v}$$

electron with cloud

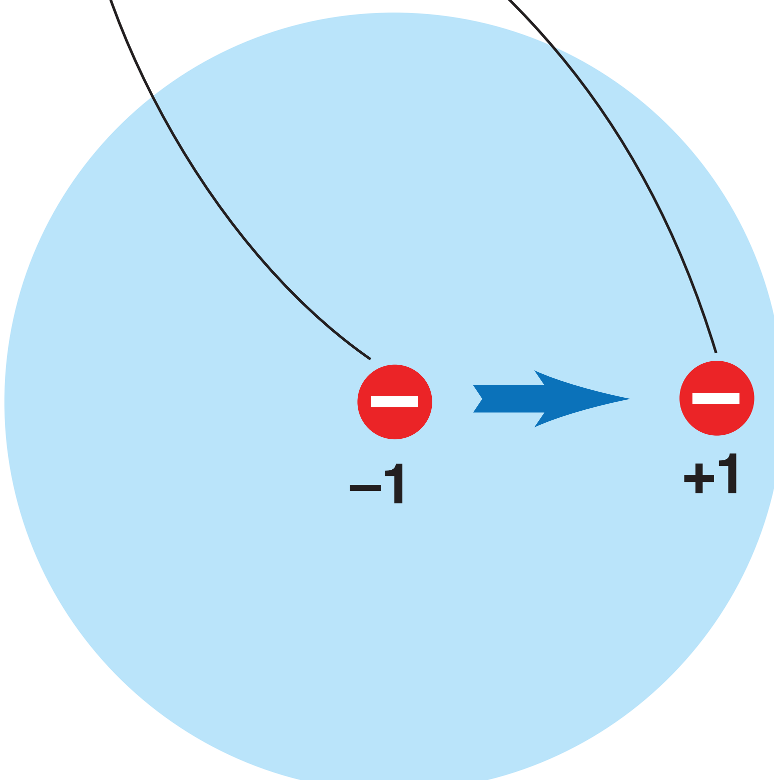

Plasma Line $S_{PL}(\mathbf{k},\omega)$ **Ion Line** $S_{IL}(\mathbf{k},\omega)$

$$S_e(\mathbf{k},\omega) = N_e\left|1 - \frac{\chi_e(\mathbf{k},\omega)}{\epsilon(\mathbf{k},\omega)}\right|^2 \int f_e(\mathbf{v})\delta(\omega - \mathbf{k}\cdot\mathbf{v})d^3\mathbf{v} + \sum_i N_i\left|\frac{\chi_e(\mathbf{k},\omega)}{\epsilon(\mathbf{k},\omega)}\right|^2 \int f_i(\mathbf{v})\delta(\omega - \mathbf{k}\cdot\mathbf{v})d^3\mathbf{v}$$

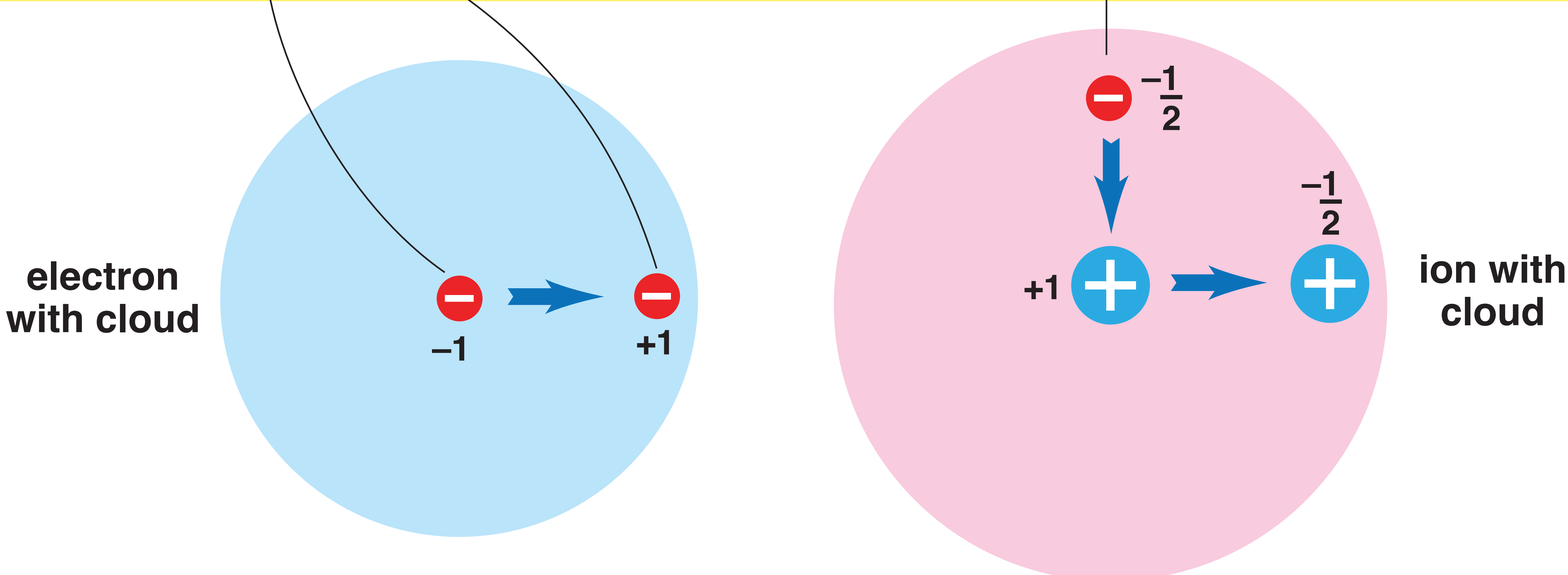

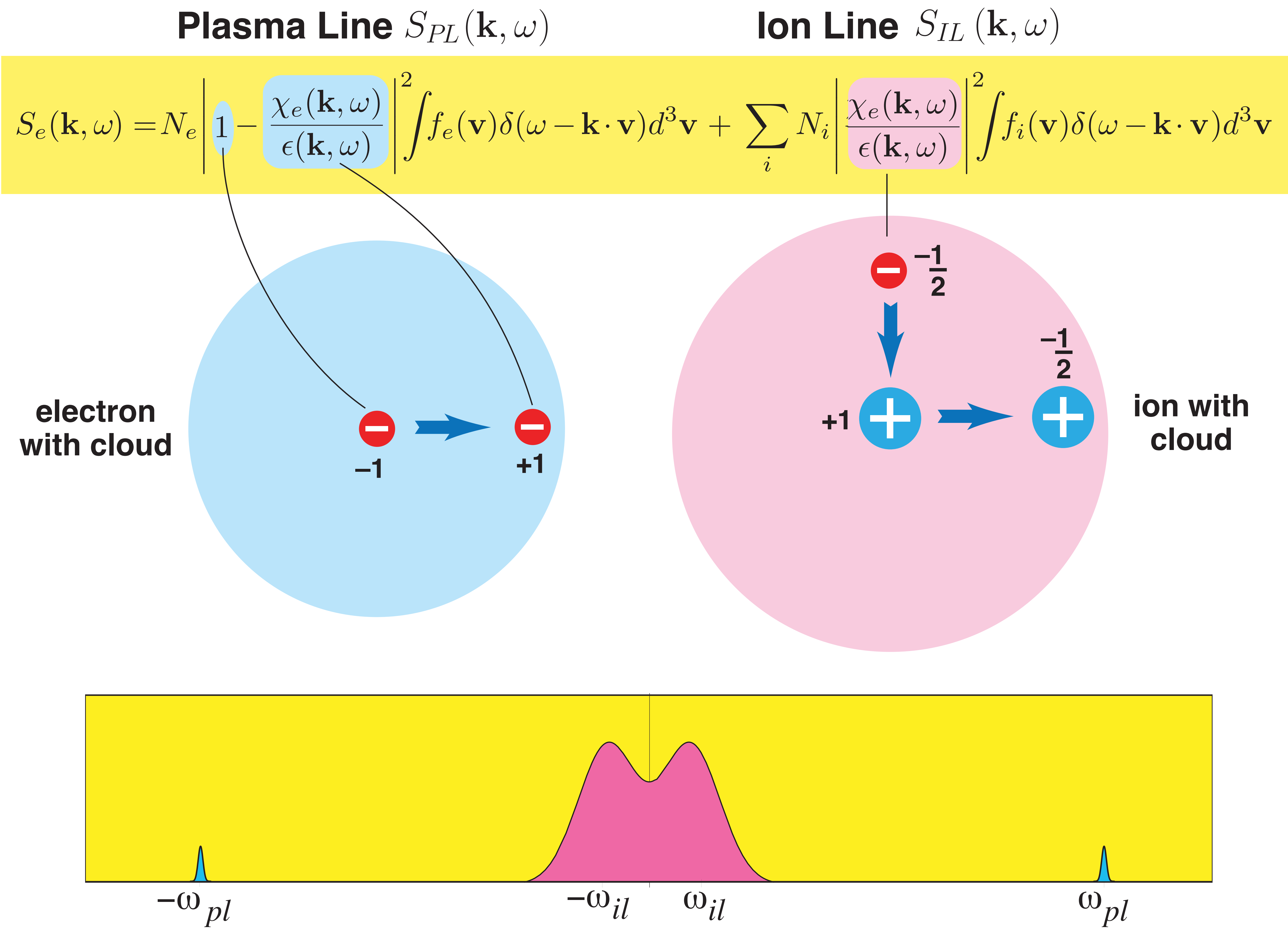
Plasma Line $S_{PL}(\mathbf{k},\omega)$
Ion Line $S_{IL}(\mathbf{k},\omega)$
$S_e(\mathbf{k},\omega) = N_e \left| 1 - \frac{\chi_e(\mathbf{k},\omega)}{\epsilon(\mathbf{k},\omega)} \right|^2 \int f_e(\mathbf{v}) \delta(\omega - \mathbf{k}\cdot\mathbf{v}) d^3\mathbf{v} + \sum_i N_i \left| \frac{\chi_e(\mathbf{k},\omega)}{\epsilon(\mathbf{k},\omega)} \right|^2 \int f_i(\mathbf{v}) \delta(\omega - \mathbf{k}\cdot\mathbf{v}) d^3\mathbf{v}$
electron with cloud
−1
+1
$-\frac{1}{2}$
+1
$-\frac{1}{2}$
ion with cloud
$-\omega_{pl}$
$-\omega_{il}$
ω_{il}
ω_{pl}

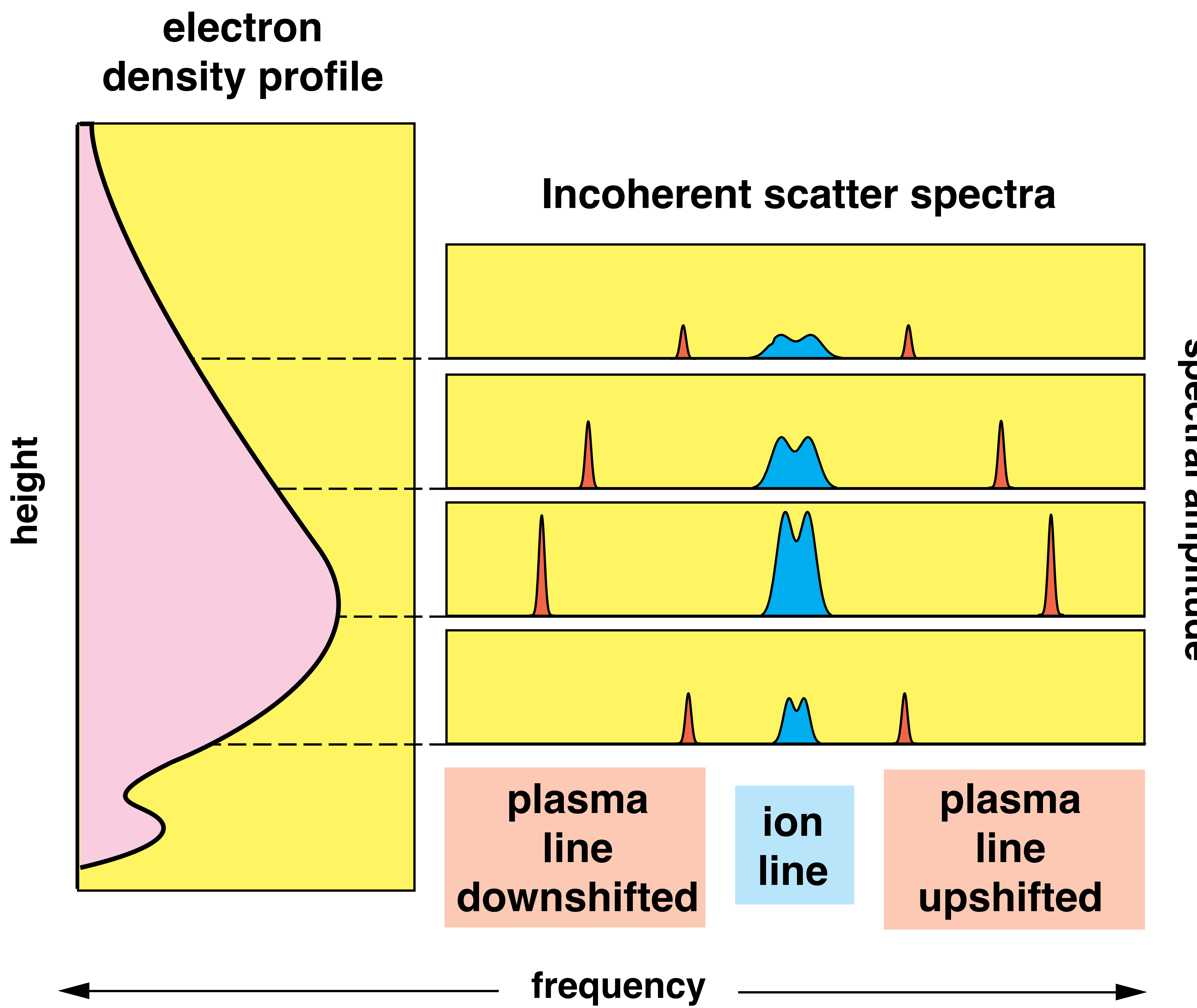
electron
density profile
Incoherent scatter spectra
height
spectral amplitude
plasma
line
downshifted
ion
line
plasma
line
upshifted
frequency

The Polar Mesosphere is Colder in Summer than in Winter

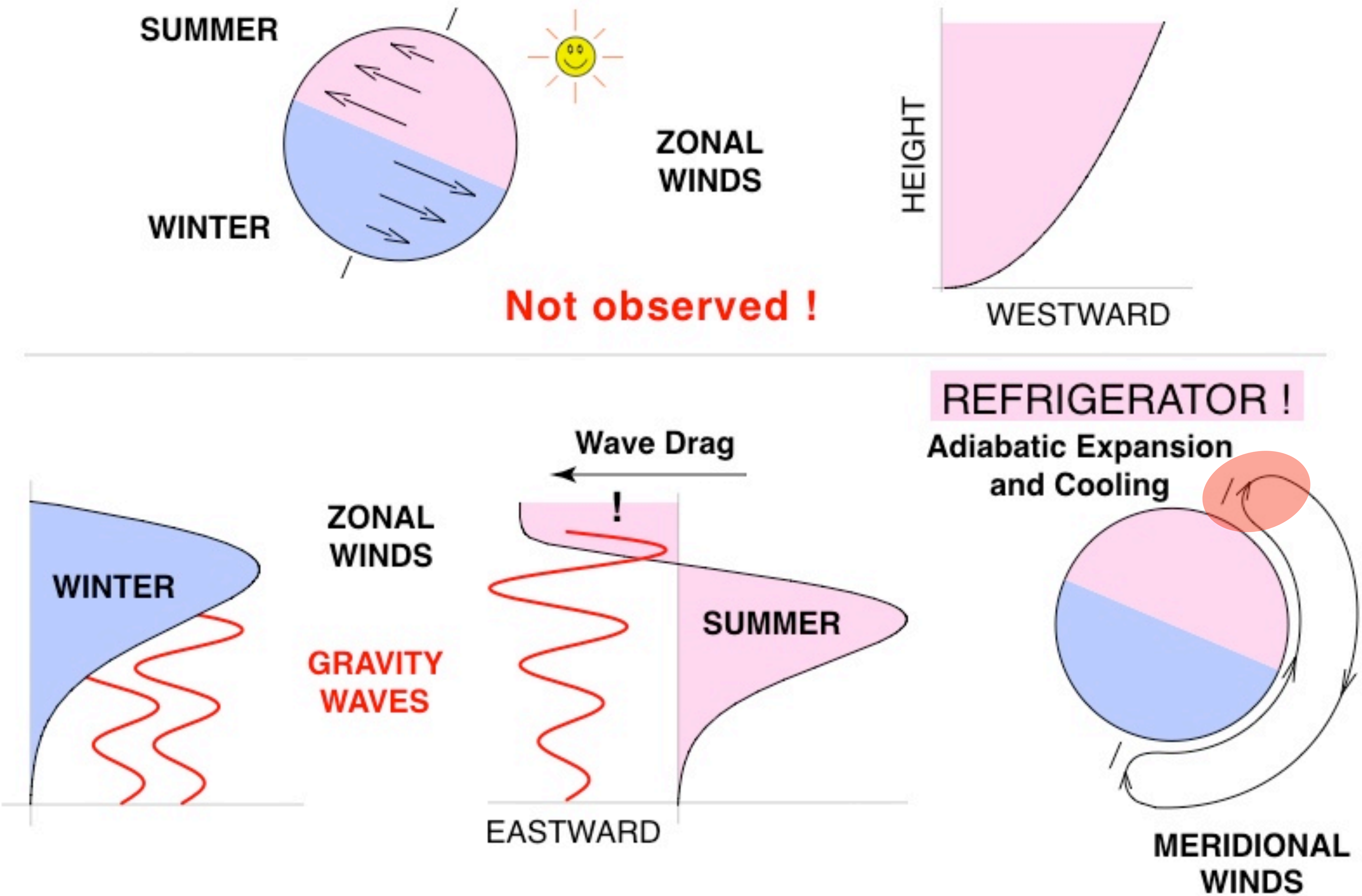

The Polar Mesosphere is Colder in Summer than in Winter

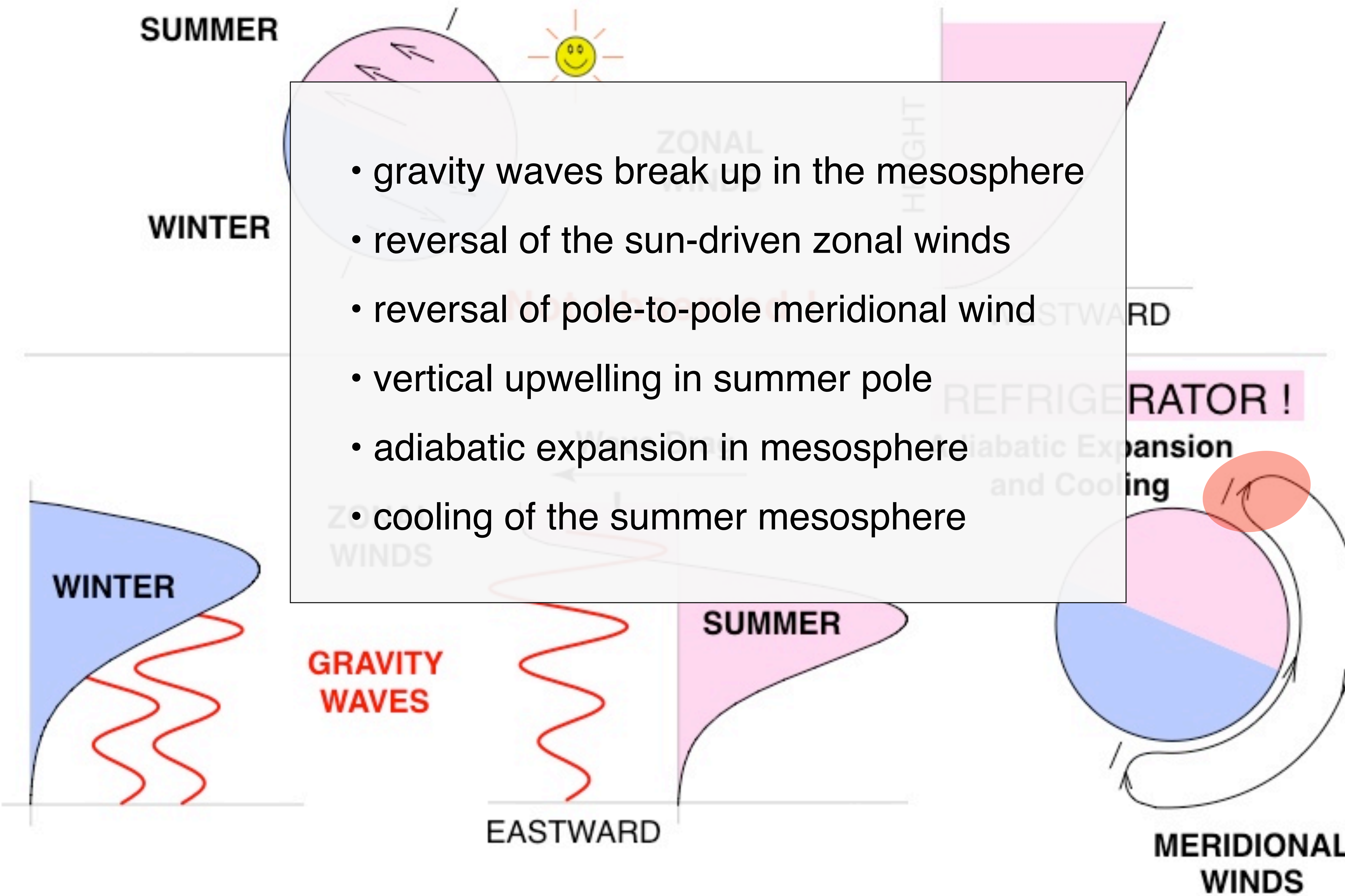

- gravity waves break up in the mesosphere
- reversal of the sun-driven zonal winds
- reversal of pole-to-pole meridional wind
- vertical upwelling in summer pole
- adiabatic expansion in mesosphere
- cooling of the summer mesosphere